4

PICTURE GALLERY

4.1 SHOCK AND PERCUSSION IN NATURE – Lunar Surface, a Result of Meteorite Impacts

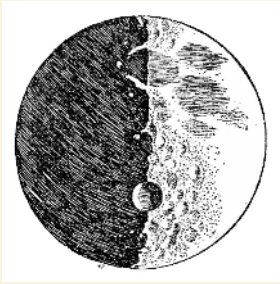

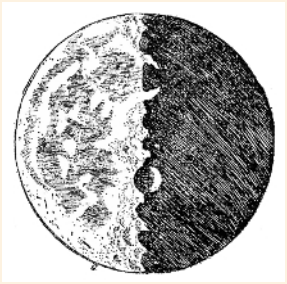

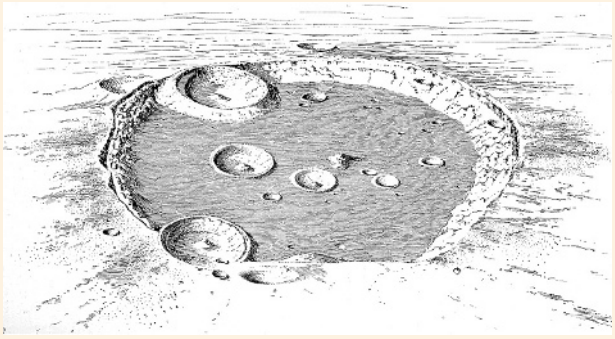

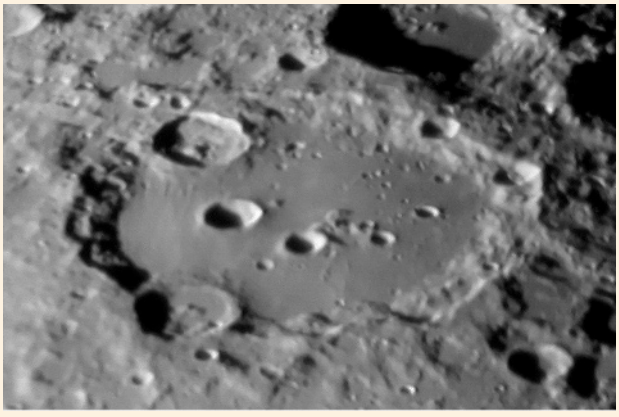

4.1–A ***Top:*** Galileo GALILEI, inspired in 1609 by the account of a Dutch invention of a telescope, built his own instrument. Using the telescope to observe the surface of the Moon, Galileo discovered new spots in addition to those already visible to the naked eye. From their change of light at different phases he concluded that the surface of the Moon must be rough with deep depressions and high mountains, contrary to the opinions of the ancients who assumed a smooth and polished surface. Those parts which remained or became brilliant he inferred were land, while those which remained obscure – the permanent spots – were water. These sketches are from his memoir *Sidereus Nuncius* (1610). [*G. GALILEI. Opere*. R. Ricciardi, Milano (1953)] ***Center:*** Pen-and-ink drawing of lunar crater Clavius (diameter c.225 km, depth c.3.5 km) by U.S. geologist Grove Karl GILBERT showing a grouping of craters. He used this crater as an example to illustrate that younger and typically smaller craters occurred on and within larger craters. [Bull. Phil. Soc. Wash. **12**, 241 (1893)] ***Bottom, left:*** This is a more recent photo of Clavius. [Photo taken on Feb. 2, 2003. © 2007 Markus WEBER, Verein Sternwarte Trier e.V.] ***Bottom, right:*** In 1893, GILBERT gave cogent argument for the impact origin of craters on the Moon. He concluded that "all features of the typical lunar crater and of its varieties may be explained as the result of impact." His hypothesis has been the basis of all subsequent thinking along these lines. [Reprinted from Bull. Phil. Soc. Wash. **12**, 241 (1893)]

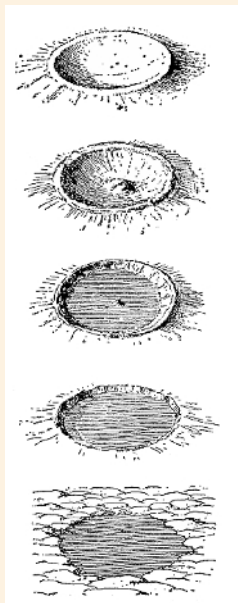

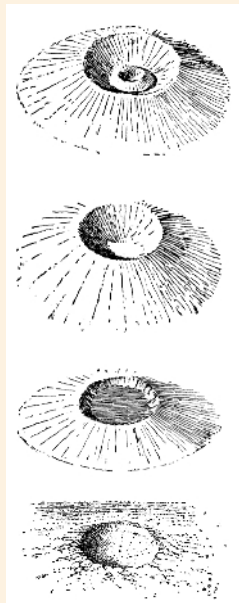

→

Left: Classifying lunar crater structures according to size, GILBERT noticed that the smallest craters have a simple concave geometry (*uppermost sketch*), while with increasing size a central hill in the inner plain becomes typical, which, again, does not exist in craters of the largest diameters (*lowermost*). ***Right:*** He also studied terrestrial crater forms like craters of the Vesuvius type with central hills (*uppermost*) and without such hills, craters of the Hawaiian type, and craters of the mare type (*lowermost*).

4.1 **SHOCK AND PERCUSSION IN NATURE** – Meteor Crater and Shock Metamorphism

4.1–B ***Top:*** Aerial view of Meteor Crater (dia. 1.2 km, depth 200 m) – now officially called "Barringer Crater" – that is about 50,000 years old. In 1905, the U.S. mining engineer Daniel M. BARRINGER first suggested its extraterrestrial origin. U.S. geologist Harvey H. NININGER, following him along these lines, proposed in 1956 the natural occurrence of coesite in Coconino sandstone at the crater bottom. [Photo by David J. RODDY and Karl ZELLER, courtesy USGS; http://www.lpi.usra.edu/publications/slidesets/craters/slide_10.html] ***Bottom:*** Using X-ray diffraction (*left*), U.S. geologist Edward C.T. CHAO and collaborators demonstrated that the polymorphic transformation from quartz to coesite, a high-pressure modification of quartz, may have occurred under shocks generated from meteorite impact, thus providing a reliable criterion for the recognition of other impact sites on Earth and other planets. [In the public domain. Reprinted from Science **132**, 220 (July 22, 1960)] Schematics of crystal models of natural quartz (*center*) and coesite (*right*). The difference in crystal structure cannot be seen under a microscope but requires X-ray diffraction analysis. [Courtesy Prof. Caroline RÖHR, Dept. of Chemistry and Pharmacy, Univ. of Freiburg]

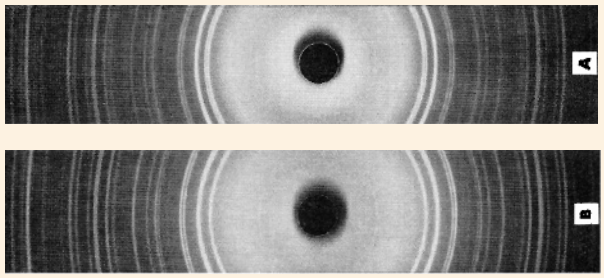

↑ X-ray powder diffraction patterns: Pattern of natural coesite with minor amounts of quartz (*A*) from sheared Coconino sandstone. It is identical to the X-ray powder diffraction pattern (*B*) of coesite synthesized by Francis R. BOYD at the Geophysical Laboratory, Carnegie Institute, Washington, DC.

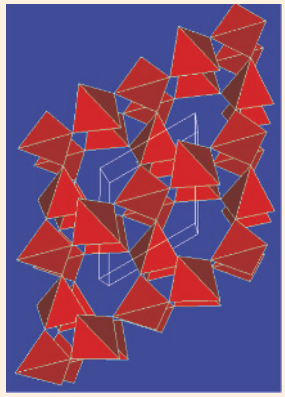

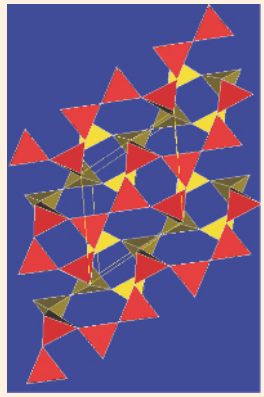

4.1 SHOCK AND PERCUSSION IN NATURE – Asteroid Impact: Ries Basin and Steinheim Basin

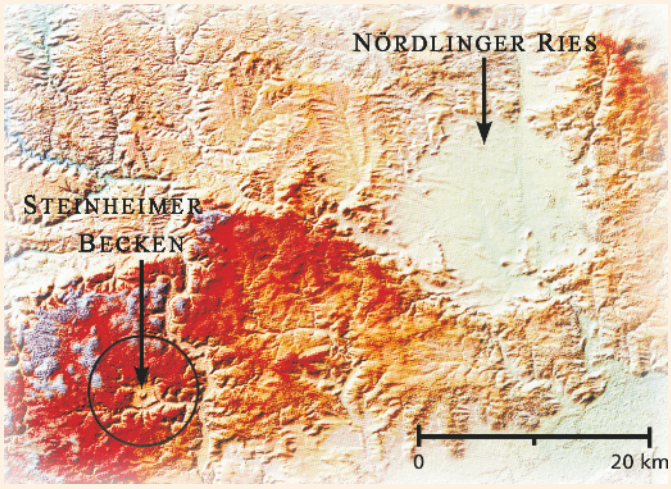

4.1–C ***Left, top:*** This is a satellite radar image taken from the area of the *Nördlinger Ries* (Ries Basin) and the *Steinheimer Becken* (Steinheim Basin) in Bavaria. Both structures are only about 30 km apart and were produced by a meteorite impact about 15 million years ago – most probably by the same asteroid that broke apart during its passage through the atmosphere. [ESA, ERS-1 and ERS-2 data. Courtesy DLR, Oberpfaffenhofen; M. GOTTWALD: Sterne und Weltraum **10**, 832 (2000)] ***Left, center:*** Aerial view of Ries Basin. Note that the crater (diameter 20–24 km) has a plain structure at its bottom. [Courtesy Rieskrater-Museum, Nördlingen, Germany] ***Left, bottom:*** An aerial view of the Steinheim Basin (diameter 3.5 km, depth 120 m) clearly reveals a central hill. ***Right:*** The findings of *Schwabenstein* or suevite (*top* and *center*) and of coesite in the Ries Crater as well as of so-called "shatter cones" *(bottom)* in the Steinheim Basin gave clear evidence that these geological structures were indeed generated by a meteorite impact. [Courtesy Prof. Eberhard STABENOW, Heidenheim]

4.1 SHOCK AND PERCUSSION IN NATURE – Two Famous Meteorites: Ensisheim and Murchison

4.1–D ***Top, left:*** On November 7, 1492, after a very loud explosion, a 127-kg meteorite fell in a wheat field near the German village of Ensisheim, in the province of Alsace (now France), where it produced an approx. 1-m-deep crater. An old woodcut depicting the scene shows the fall watched by two people emerging from a forest. In fact, the event was only witnessed by a young boy who led the townsfolk to the impact site. [From leaflet by Sébastien BRANT (1492); http://www.educnet.education.fr/planeto/pedago/systsol/astero.htm] ***Top, right:*** The Ensisheim meteorite is perhaps the most famous of all historic falls because it is the oldest witnessed fall in the Western Hemisphere from which specimens are preserved in many museums around the world. An approx. 55-kg residue, almost without fusion crust, is preserved and displayed at the Regency Museum in the Town Hall of Ensisheim. [Photo by Bernd GRÜNEWALD, EMI, Freiburg; with kind permission of Regency Museum, Ensisheim] ***Bottom, left:*** The Murchison meteorite fall occurred on September 28, 1969 over Murchison, a town in the state of Victoria, Australia. Over 100 kg of this meteorite have been found. Classified as a carbonaceous chondrite, type II (CM2), this meteorite is of possible cometary origin, based on its high water content of 12%. An abundance of amino acids found within this meteorite has led to intense study by researchers as to its origins. More than 92 different amino acids have been identified within the Murchison meteorite to date; nineteen of these are found on Earth. The remaining amino acids have no apparent terrestrial source. This picture shows a 5.28-g fragment which has a size of about 16×15 mm^2. [Photo courtesy Pierre-Marie PELÉ, France; http://www.meteor-center.com/collection/chondrites.asp] ***Bottom, right:*** In 1997, Richard B. HOOVER, a scientist at NASA's Marshall Space Flight Center, announced that he had seen and photographed in the Murchison meteorite microfossils that resembled microorganisms. The fossils were seen in freshly broken pieces of the meteorite, so the chance that they were earthly contaminants was low. The chemical evidence around the microfossils was most readily explained as the result of biological activity. The most interesting and unusual form, seen in many examples, curls to a tapered end. [Courtesy R.B. HOOVER, NASA/MSFC/NSSTC; Proc. SPIE **3111**, 115 (1997)]

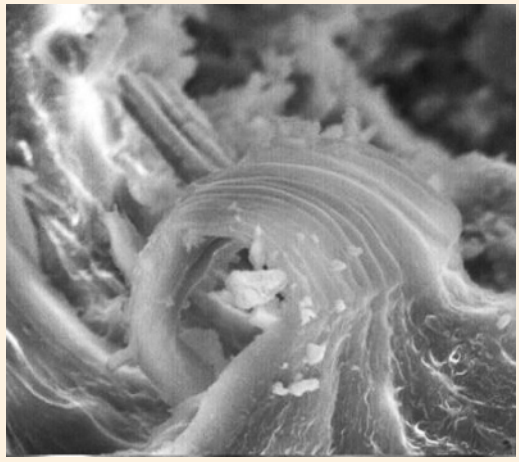

4.1 SHOCK AND PERCUSSION IN NATURE – Great Earthquakes: Lisbon (1755)

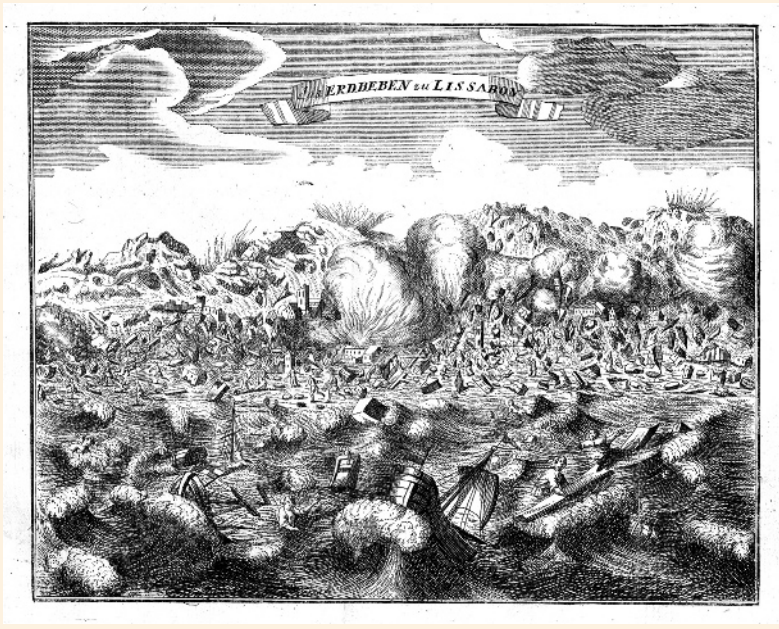

4.1–E These two contemporary pen-and-ink drawings illustrate the terrible Lisbon Earthquake that occurred on the morning of November 1 (All Saints' Day), 1755 and largely destroyed the Royal Portuguese residential town (*bottom*). Thousands of Portuguese who survived the earthquake were killed by a tsunami that followed a few minutes later. Before the great wave hit, the harbor waters retreated, revealing lost cargo and forgotten shipwrecks. The disaster, which in Lisbon killed about 10,000 people and injured 40,000 to 50,000, challenged the well-established Baroque philosophy that hitherto regarded the Universe as a perfect creation. It was this catastrophe that is said to have caused VOLTAIRE, one of the greatest French authors and philosophers, to abandon religion. However, the disaster also stimulated the scientific community to investigate its possible causes. [*Kurz-verfaste Beschreibung der vortrefflichen, mächtigen und reichen Haupt- und Residenzstadt Lissabon im Königreiche Portugall (1756).* Courtesy Bayerische Staatsbibliothek, Munich]

4.1 SHOCK AND PERCUSSION IN NATURE – Great Earthquakes *(cont'd)*: Lisbon (1755)

Interrogatorios para a organização
do «Diccionario Geographico» do P.e Luis Cardoso

(Mandados pelo Govêrno aos parochos depois do terremoto de 1755)

O QUE SE PROCURA SABER D'ESSA TERRA É O SEGUINTE

Venha tudo escrito em lettra legivel, e sem breves

1. Em que provincia fica, a que bispado, comarca, termo e freguesia pertence?
2. Se é d'el-rei, ou de donatario, e quem o é ao presente?
3. Quantos vizinhos tem [*e o numero das pessoas*]?
4. Se está situada em campina, valle, ou monte, e que povoações se descobrem d'ella, e quanto dista?
5. Se tem termo seu, que lugares, ou aldeias comprehende, como se chamam, e quantos vizinhos tem?
6. Se a parochia está fóra do lugar, ou dentro d'elle, e quantos lugares, ou aldeias tem a freguesia, todos pelos seus nomes?
7. Qual é o seu orago, quantos altares tem, e de que santos, quantas naves tem; se tem irmandades, quantas, e de que santos?
8. Se o parocho é cura, vigario, ou reitor, ou prior, ou abbade, e de que apresentação é, e que renda tem?
9. Se tem beneficiados, quantos, e que renda tem, e quem os apresenta?
10. Se tem conventos, e de que religiosos, ou religiosas, e quem são os seus padroeiros?
11. Se tem hospital, quem o administra, e que renda tem?
12. Se tem casa de misericordia, e qual foi a sua origem, e que renda tem; e o que houver notavel em qualquer d'estas cousas?
13. Se tem algumas ermidas, e de que santos, e se estão dentro, ou fóra do lugar, e a quem pertencem?
14. Se acode a ellas romagem, sempre, ou em alguns dias do anno, e quaes são estes?
15. Quaes são os fructos da terra, que os moradores recolhem em maior abundancia?
16. Se tem juiz ordinario, etc., camara, ou se está sujeita ao governo das justiças de outra terra, e qual é esta?
17. Se é couto, cabeça de concelho, honra, ou behetria?
18. Se ha memoria de que florecessem, ou d'ella sahissem, alguns homens insignes por virtudes, lettras, ou armas?
19. Se tem feira, e em que dias, e quantos dura, se é franca ou cativa?
20. Se tem correio, e em que dias da semana chega, e parte; e, se o não tem, de que correio se serve, e quanto dista a terra aonde elle chega?
21. Quanto dista da cidade capital do bispado, e quanto de Lisboa, capital do reino?
22. Se tem alguns privilegios, antiguidades, ou outras cousas dignas de memoria?
23. Se ha na terra, ou perto d'ella alguma fonte, ou lagoa celebre, e se as suas aguas tem alguma especial qualidade?
24. Se for porto de mar, descreva-se o sitio que tem por arte ou por natureza, as embarcações que o frequentam e que póde admittir?
25. Se a terra for murada, diga-se a qualidade de seus muros; se for praça de armas, descreva-se a sua fortificação. Se ha nella, ou no seu districto algum castello, ou torre antiga, e em que estado se acha ao presente?
26. Se padeceu alguma ruina no terremoto de 1755, e em que, e se está reparada?
27. E tudo o mais, que houver digno de memoria, de que não faça menção o presente interrogatorio.

4.1–E *(cont'd)* ***Left:*** POMBAL's questionnaire, entitled *Interrogatórios enviados aos párocos depois do Terramoto de 1755* ("Interrogations Sent to the Parishes After the Earthquake of 1755"), was divided into three parts: questions regarding information about the land (27 questions, *left*), about the mountains (13 questions), and about the rivers (20 questions). For example, his questionnaire asked whether dogs or other animals behaved strangely prior to the earthquake. Was there a noticeable difference in the rise or fall of the water level in wells? How many buildings were destroyed and what kind of destruction occurred? Their answers – today kept in the Arquivos Nacionais, Torre do Tombo, Alameda da Universidade, Lisboa – enabled modern seismologists to precisely reconstruct the course of the earthquake and its severity at different localities. The response of the Portuguese authorities to the earthquake represents one of the first historic examples of integrated post-disaster recovery planning. Under the direction of king JOSEPH's first minister, Sebastião José DE CARVALHO E MELO (later Count of Oeiras and Marquês DE POMBAL), data were collected in written form and in the form of city plans and maps. [Archeólogo Português (Lisboa) **1**, 268 (1895)] ***Right:*** Oil painting showing the Marquis DE POMBAL (1699–1782). He commissioned the military engineers General Manuel DA MAIA, Captain Eugénio DOS SANTOS, and Lieutenant Colonel Carlos MARDEL not only to remap the city but also to make a complete inventory of damage. This provided a worthwhile database for earth scientists and hazard analysts prior to the advent of the seismograph in the late 19th century. [Portrait of Sebastião José DE CARVALHO E MELO – oil on canvas. Unknown artist, middle of XVIII century. Courtesy Lisbon City Museum]

4.1 SHOCK AND PERCUSSION IN NATURE − Great Earthquakes *(cont'd)*: San Francisco (1906)

4.1–E *(cont'd):* On April 18, 1906, at 5:13 A.M., San Francisco was wrecked by a series of heavy earthquake shocks of magnitude 8.3 on the Richter scale. Many buildings immediately caught fire, and trapped victims could not be rescued. A major aftershock struck at 8:14 A.M. causing the collapse of many damaged buildings (the death toll was more than 3,000 from all causes). The earthquake destroyed 3,000 acres (ca. 12 km^2) in the heart of the city. ***Top, left:*** The steel skeleton of the City Hall of San Francisco was stripped of masonry by the seismic shocks. ***Top, right:*** The San Andreas fault ruptured 430 km from San Juan Bautista to the Cape Mendocino triple junction (with San Francisco in between). [Courtesy Zpub, San Francisco; http://www.zpub.com/sf/history/1906earth.html] ***Bottom:*** In the largest maritime rescue in U.S. history more than 30,000 people were taken from the shoreline between Fort Mason and the foot of Lombard Street. The painting by William Alexander COULTER (1849–1936) depicts the flotilla of rescue vessels ferrying survivors from the burning city to Sausalito. [Courtesy Virtual Museum of the City of San Francisco; http://www.sfmuseum.org]

4.1 **SHOCK AND PERCUSSION IN NATURE** – Explosive Volcanic Eruption: Krakatau (1883)

← Map of present Krakatau Island and vicinity. The volcano is still active and formed Anak Krakatau, a small island in the middle of the ocean-filled caldera. [By Lyn TOPINKA, USGS/Cascades Volcano Observatory, Vancouver, WA. Modified from T. SIMKIN and R.S. FISKE: *Krakatau 1883: the volcanic eruption and its effects*. Smithsonian Institution Press, Wash., DC (1983)]

4.1–F The famous Krakatau (or Krakatoa) eruption was one of the largest in history (with an Volcanic Explosivity Index of *VEI* = 6). ***Top, left:*** View of Krakatau during modest, early stage of eruption taken on May 27, 1883. [G.J. SYMONS (ed.): *The eruption of Krakatoa and subsequent phenomena*. Trübner, London (1888)] ***Top, right:*** The Krakatau volcano lies in the Sunda Strait between Java and Sumatra (*top*). Since 1927, small but frequent eruptions have constructed a new island, Anak Krakatau (*bottom*), shown here with a column of ash rising above it. Remnants of the northern part of Krakatau are visible in the background. [Reprinted with permission from J. Geophys. Res. **66**, 3497 (1961)] ***Bottom:*** Drawing of northern remnants of Krakatau island made 2 months after the final, most violent outbursts, which occurred on August 26 and 27 of the same year. They destroyed a large northern portion of the basaltic cone of the former Rakata Peak (2,623 ft) and formed a nearly vertical cliff, thus giving rise to a magnificent section that afforded a perfect view of the interior structure of the volcano. [R.D.M. VERBEEK: *Krakatau*, *Album van Straat Soenda*. Landsdrukkerij, Batavia (1885/1886)]

4.1 SHOCK AND PERCUSSION IN NATURE – Explosive Volcanic Eruptions: Krakatau (1883) *(cont'd)*

Examples of accounts of observed sound phenomena given in English miles at the following locations:

1 – Merak (Java; 38 miles from Krakatau) "heavy detonations and violent shocks, but no earthquake."

2 – Batavia (Java; 94 miles) "a series of detonations, towards night they grew louder, till in the early morning (August 27, 1883) the reports and concussions were simply deafening."

3 – Brig *Airlie* at sea (390 miles; Lat. 0° 30' S, Lon. 105° 54' E) "sounds like those of heavy artillery… The last report made the ship tremble all over."

4 – Hambantota (Ceylon; 1,866 miles) "a steady sequence of reports, and then a rapid succession of them, ending, very often, in a loud burst of two or three, or half a dozen, almost together, which was generally followed by a lull. The intensity of the sounds greatly varied."

5 – Alice Springs (Central Australia; 2,233 miles) "two distinct reports, similar to the discharge of a rifle."

6 – Rodriguez (island near Mauritius, Indian Ocean; 2968 miles) the most distant location at which sounds originating from the eruption were perceived, "reports like the distant roars of heavy guns."

4.1–F *(cont'd)* The illustrated map, with Krakatau at its center, shows the places at which the sounds of the explosive eruptions were heard on August 26–27, 1883. The large number of accounts of observed sound phenomena were carefully collected and analyzed by the Krakatoa Committee established in 1884 by The Royal Society of London. The *red line* indicates the approximate area over which the sounds were heard; the most distant locations were more than 4,000 km away. It is remarkable that at many places in the more immediate neighborhood of the volcano the sounds ceased to be heard. Very probably this peculiar phenomenon was caused by the large amount of solid matter that, emitted into the atmosphere by the volcano, formed in the lower strata of the air a screen of sufficient density to prevent the sound waves from penetrating to those places over which it was more immediately suspended. The eruptions caused atmospheric fluctuations that were also recorded in Europe. Furthermore, the tremendous eruptions caused tsunamis that reached heights of 40 m, killing tens of thousands of people on the low shores of Java and Sumatra. [After G.J. SYMONS (ed.): *The eruption of Krakatoa and subsequent phenomena*. Trübner, London (1888)]

4.1 SHOCK AND PERCUSSION IN NATURE – Explosive Volcanic Eruption: Mount St. Helens (1980)

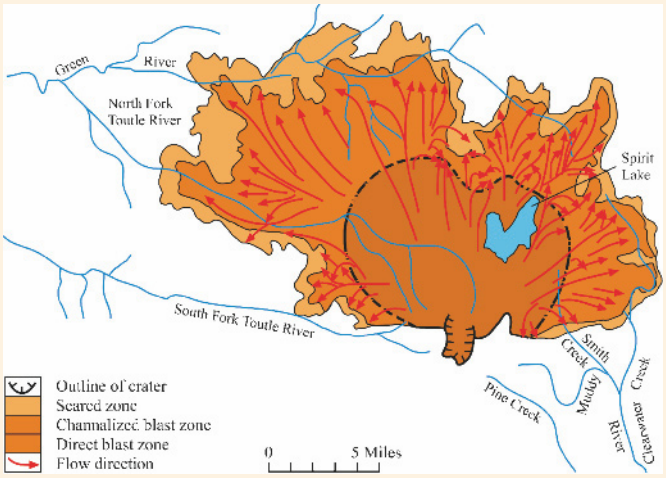

↑ The inner zone – the *direct blast zone* – averaged about 8 miles in radius in which virtually everything, natural or manmade, was obliterated or carried away. For this reason, this innermost zone has also been called the "tree-removal zone." The flow of the material carried by the blast was not deflected by topographic features in this zone. The *channelized blast zone*, an intermediate zone, extended out to distances as far as 19 miles from the volcano, an area in which the flow flattened everything in its path and was channeled to some extent by topography. In this zone, the force and direction of the blast are strikingly demonstrated by the parallel alignment of toppled large trees, broken off at the base of the trunk like blades of grass mown by a scythe. This zone was also known as the "tree-down zone." The *seared zone*, also called the "standing dead zone," is the outermost fringe of the impacted area, a zone in which trees remained standing but were singed brown by the hot gases of the blast.

4.1–G On May 18, 1980, a magnitude 5.1 earthquake shook Mount St. Helens in the State of Washington, and the volcano erupted explosively. ***Right:*** View of eruption taken on this day. The bulge and surrounding area slid away in a gigantic rockslide and debris avalanche, releasing pressure, and triggering a major pumice and ash eruption of the volcano. The eruptive cloud rose to an altitude of more than 12 miles in 10 min. The swirling ash particles in the eruptive cloud generated lightning, which in turn started forest fires. Other fires were ignited by the initial blasts and later pyroclastic flows. Nearly 550 million tons of ash fell over an area of approx. 60,000 km^2. Note the erosional "furrows" below the mouth of the volcano. [Courtesy USGS; photo by Austin POST.] ***Left, top:*** The area affected by the blast from the explosive eruption can be subdivided into three roughly concentric zones. [USGS, http://pubs.usgs.gov/publications/msh/lateral.html] ***Left, bottom:*** Oblique aerial view of a devastated area in Skamania and Cowlitz Counties, showing uprooted trees blown down by the blast wave. Note how the blast followed the contours of the mountainside. [Courtesy USGS, Branch of Exhibits]

4.1 SHOCK AND PERCUSSION IN NATURE – Plate Tectonics

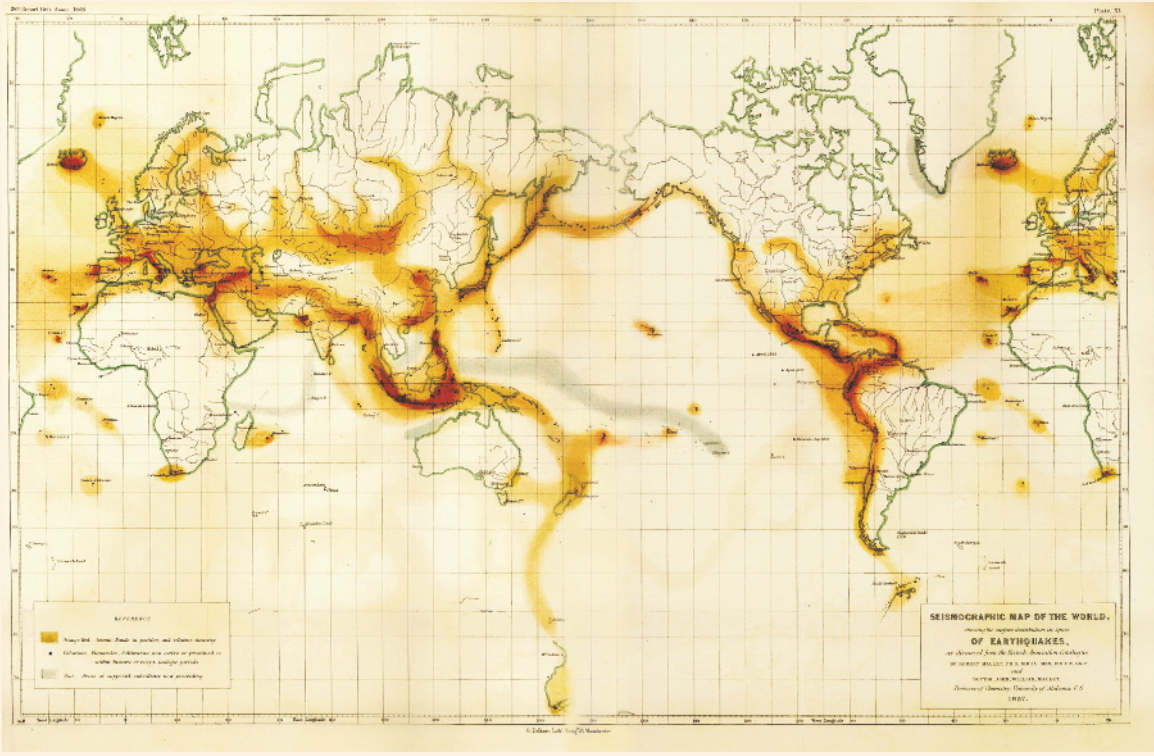

4.1–H The Irish engineer Robert MALLET compiled a "Seismographic Map" (1857) of the world for the British Association for the Advancement of Science using his great "Earthquake Catalogue" (1852–1854), which contains 6,831 earthquakes reported between 1606 B.C. and A.D. 1858. In addition, he used data from previous attempts such as the "Physikalischer Atlas" (1845) of the German geographer Heinrich BERGHAUS and the "Physical Atlas" (1848) of the Scottish cartographer and geographer royal Alexander Keith JOHNSTON. By mapping earthquakes in terms of disturbed areas rather than of epicenters (the modern and more accurate method), MALLET divided earthquakes into three classes – great, mean, and minor. His map (original size 75×48 in.^{2}) is not only a very attractive piece of early color-printed cartography, but also illustrates the importance of seismic bands, their color varying according to the intensity of the shocks experienced, the volcanoes active in historic times, and the areas of supposed oceanic subsidence. These seismic bands generally follow the lines of elevation that divide the great oceanic or terr-oceanic basin of the earth's surface; insofar as these are frequently the lines of mountain-chains, and these latter of volcanic vents, so the seismic bands are found to follow them as well. The regions of least or no disturbance are the central areas of great oceanic or terr-oceanic basins and the greater islands existing in shallow seas. The great seismic band, running from the Aleutian and Kurile Islands through Japan and the Philippines to the East Indies, is clearly marked. By delimiting the lithosphere plates, MALLET unconsciously anticipated the development of plate tectonic theory in the 1960s; *see also* C. DAVISON: *The Founders of Seismology.* New York, pp. 73–75 (1978). [Rept. Meet. Brit. Assoc. **28**, 1 (1858); plate 11]

4.1 SHOCK AND PERCUSSION IN NATURE – Plate Tectonics *(cont'd)*

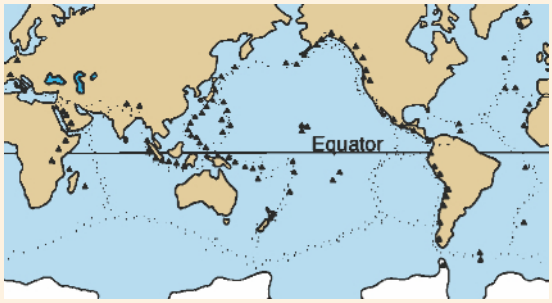

4.1–I ***Left, top & center:*** The location of plate boundaries coincides in most cases with the loci of volcanoes and the epicenters of earth- and seaquakes (*top*), *i.e.*, with the loci of naturally generated discontinuities such as seismic shocks and lateral blasts. Global distribution of volcanoes (▲) and earth- and seaquakes (· . · . ·). Major tectonic plates of the world are separated by faults (——), major fractures of the Earth's crust (*bottom*). Geologists define 7 large plates and 20 smaller plates. Most of the plates consist of both oceanic and continental lithosphere. [Courtesy Dept. of Space Studies, University of North Dakota; http://volcano.und.nodak.edu/vwdocs/vwlessons/plate_tectonics/part12.html] ***Right, top:*** The San Andreas fault zone, which is about 1,300 km long and in places tens of kilometers wide, slices through two thirds of the length of California. Aerial view of the San Andreas fault, slicing through the Carrizo Plain in the Temblor Range east of the city of San Luis Obispo (about 320 km south of San Francisco). [Photo by Robert E. WALLACE, USGS; http://pubs.usgs.gov/publications/text/San_Andreas.html] ***Left, bottom:*** Example of a left-lateral strike-slip fault, generated during the 1976 Guatemala Earthquake in the cultivated field west of El Progreso (Dept. Jutiapa). The thick, saturated, unconsolidated deposits have yielded by plastic deformation rather than rupture along the fault. [Courtesy NGDC, NOAA; http://www.ngdc.noaa.gov/seg/hazard/slideset/10/10_slides.shtml] ***Right, bottom:*** Fault trace northwest of Olema, generated during the 1906 San Francisco Earthquake. The greatest displacement was 21 ft (6.4 m) about 30 miles (48 km) northwest of San Francisco. [Courtesy J.B. Macelwane Archives, Saint Louis University, St. Louis, MO; http://www.eas.slu.edu/Earthquake_Center/1906EQ/olema/m40A.html]

4.1 SHOCK AND PERCUSSION IN NATURE – Lightning and Thunder

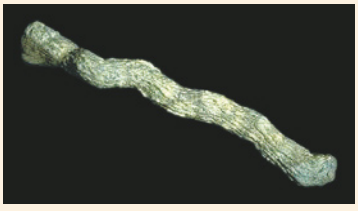

Left, bottom: Damage by lightning strikes includes explosion and melting effects; the best known examples are split tree trunks, damaged brickwork buildings, and destroyed electrical equipment by induced short-circuits. This rare snapshot of a lightning strike was taken in 1996 in Alabama by Johnny AUTERY from his pickup truck. A 65-foot-tall sycamore tree is lit from top to bottom by a direct lightning strike. Lightning often damages or destroys trees. [A. FALLOW: *Powers of nature: lightning*. National Geographic World No. 250 (June 1996)]

4.1–J In ancient times, the hammer and mallet – the basic tools to produce percussion and shock phenomena – were considered to be of divine origin and to possess marvelous, supernatural abilities. ***Left, top:*** View of a small, 6.4-cm bronze statuette of THOR (ca. A.D. 1000), the god of thunder, which he produced with his short-handed hammer *Mjolnir* (meaning "The Destroyer"). The hammer, here shown on THOR's knees, had the marvelous quality of returning to the thrower like a boomerang. THOR was a deity common to all early Germanic peoples. [Thor (Natmus #10880), photo by Ivar BRYNJOLFSSON. Courtesy National Museum of Iceland, Reykjavik] ***Right, top:*** Corinthian bronze statuette (ca. 470 B.C.) found at Dodōna in the ancient Epirus (now Dodoni, Albania). It shows the god ZEUS hurling a thunderbolt. He was regarded as the sender of lightning, thunder, rain, and winds. His most prominent symbol was the thunderbolt, resembling a mallet. In Teutonic mythology, thunderbolts were ascribed to THOR, in Germany called DONAR, while in the Hindu cosmology, SHIVA, one of the great trinity of Hindu deities, was represented with a bow, a thunderbolt, and an axe. [Photo by Bildarchiv Preußischer Kulturbesitz. Berlin] ***Right, center:*** Some lightning phenomena are known as "lightning tubes" ore "fulgurites," which are branched, irregular tubular bodies with a glassy structure. They are produced by lightning in loose, unconsolidated sand (mostly quartz). The interior is normally very smooth or lined with fine bubbles. [From P. MENZEL, National Geographic World No. 250 (June 1996)] ***Right, bottom:*** Obviously, the expanding shock wave, generated during a lightning strike, pushed and compressed the sand grains into a thin shell of compacted sand. The silicate fulgurites shown below were found in Egypt. Although of very narrow cross-section and short length, some specimens have been found to exceed several centimeters in diameter and 20 m in length. [Courtesy Mineralogical Research Company, San Jose, CA; http://www.minresco.com/]

4.1 SHOCK AND PERCUSSION IN NATURE – The Riddle of Ball Lightning



4.1–K ***Left:*** A 19th-century French wood engraving showing the propagation of ball lightning in a barn. Since antiquity this curious but rare phenomenon, which can end in a violent explosion, has often been observed and described, but it remains an enigma to modern science. Note that the size of ball lightning, ranging in diameter between a golf ball and a beach ball as reconfirmed also by numerous more recent accounts, has been reproduced correctly. [Courtesy Bildarchiv Preußischer Kulturbesitz (bpk), Berlin, image no. 20.031.187] ***Center:*** Although about 1% of the population reports having seen ball lightning, clear photographs of this phenomena are extremely rare. This picture was taken by D. KUHN in Germany at Ludwigshafen/Rhein during a heavy thunderstorm. According to his account, the phenomenon had a diameter of about 50 cm and passed by silently. [Die Naturwissenschaften **38**, 518 (1951)] ***Right:*** This spectacular example of a fireball, which may be the rare phenomenon of ball lightning, was taken by Werner BURGER on a summer night in 1978 at St. Gallenkirch in Vorarlberg, western Austria. It had a whitish center with a blue surround and a luminous tail. [Courtesy Fortean Picture Library, Ruthin, U.K.]

4.1 SHOCK AND PERCUSSION IN NATURE – Tidal Bores

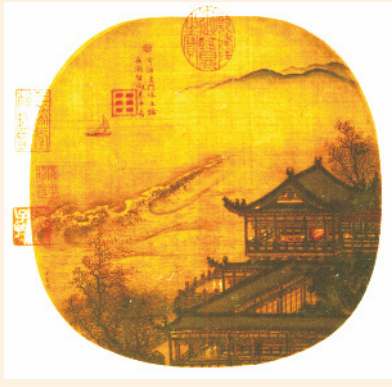


4.1–L Tidal bores are hydraulic jumps propagating upstream and frequently can be observed in shallow estuaries. ***Left:*** In China tidal-bore watching at the Qiantang River has a history of over 2,000 years. This picturesque scene of a bore propagating up the Qiantang River was recorded by the Chinese artist Li SUNG (1166–1243). [Collection of the National Palace Museum. Taiwan, Republic of China] ***Right:*** The tidal bore of the Qiantang River, the greatest such bore in the world reaching heights of up to almost 9 m, is caused by the horn-shaped topography of the Hangzhou Bay, which concentrates the bore's energy. [Photographer unknown. Linden Software, North Ferriby, U.K.; http://www.linden-software.com/china.html]

4.1 **SHOCK AND PERCUSSION IN NATURE** – Hydraulic Jumps

← The flowing water, when hitting the floor of the sink, spreads out at a speed that is higher than the local wave speed, forming a disk of shallow, rapidly diverging flow. ▪ A ring-shaped discontinuity can also be observed in space: it arises when the supersonic solar wind, interacting with the interstellar medium, has slowed down to subsonic velocity. Compression and heating effects produce a ring-shaped "termination shock" surrounding the Sun at a distance of about 75–90 AU (*c*.11–13 billion km).

4.1–M Hydraulic jumps are a curious flow phenomenon. They are characterized by sudden changes in depth and velocity, separated by an intermediate region of turbulence, and can occur both as stationary and traveling discontinuities. ***Top, left:*** This illustrious example of a stationary hydraulic jump can easily be observed in a kitchen sink when the tap is left running, which produces a ring-shaped discontinuity. A bore, which in nature is a traveling discontinuous phenomenon and is called a "hydraulic jump," can be demonstrated by turning off the faucet. Then the front moves inward. [Courtesy Prof. Philippe BELLEUDY, Laboratoire d'études des Transferts en Hydrologie et Environnement (LTHE), Grenoble, France; http://www.eng.vt.edu/fluids/msc/gallery/waves/sink.htm] ***Top, left:*** View of a shooting flow in a narrow channel, a so-called "hydraulic jump" that can be generated, for example, by suddenly opening a water reservoir at the other end of the channel. [E. PREISWERK: *Anwendungen gasdynamischer Methoden auf Wasserströmungen mit freier Oberfläche*. Ph.D. thesis, ETH Zurich (1938), p. 65] ***Bottom:*** Mach reflection can also be seen in nature. The British scientist Vaughan CORNISH first photographed the interaction of two hydraulic jumps approaching each other in very shallow water: regular reflection (*left*) and Mach reflection (*right*). Unfortunately, CORNISH didn't report on the scale of his observed interaction phenomena. The pictures might suggest aerial views, *i.e.*, that the interactions took place on a rather large scale. However, it is more probable that the photos are close-ups. On a small scale, say in a field of about 1×1 m^2, Mach reflection can be observed on a shallow beach quite frequently, particularly when the angle between the incident wave front and the beach is large. [V. CORNISH: *Waves of the sea and other water waves*. Fisher Unwin, London (1910), frontispiece and p. 173]

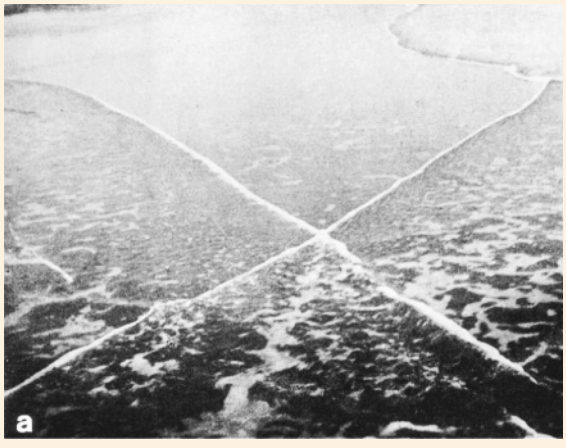

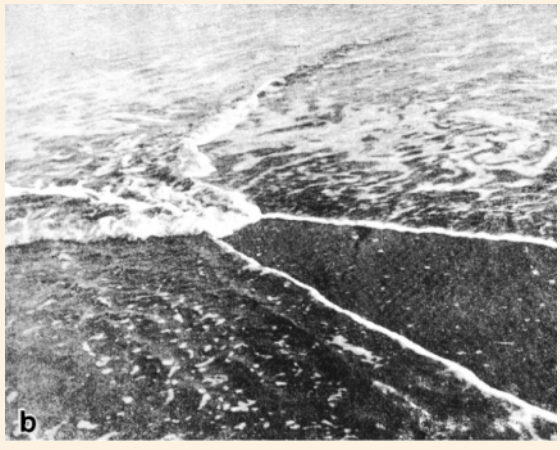

4.1 SHOCK AND PERCUSSION IN NATURE – Tsunami Caused by Submarine Volcanic Eruption

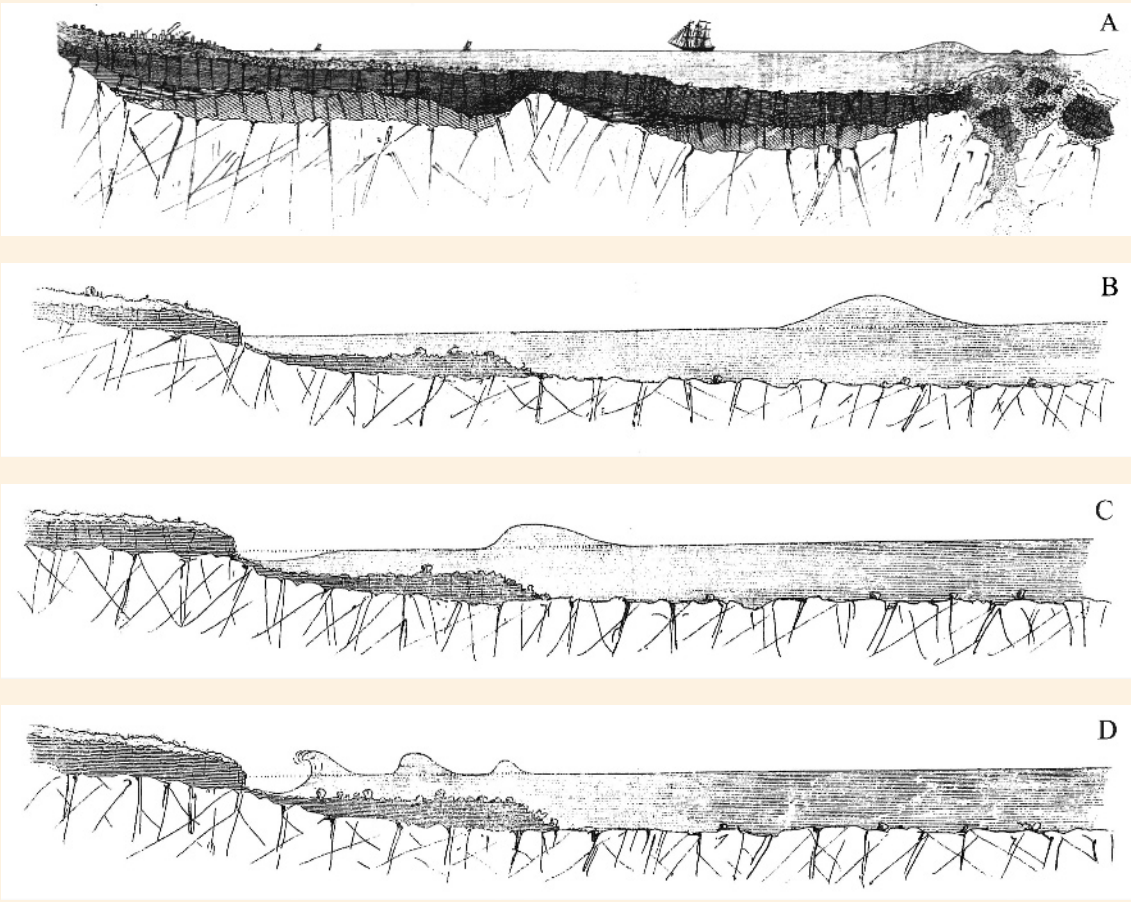

4.1–N The Irish engineer Robert MALLET considered an earthquake to be "the transit of a wave of elastic compression in any direction, from vertically (as shown here) to horizontally, through the surface and crust of the Earth…" The causes of tsunamis – or great sea waves as they were still called in the 19th century – are very complex and were a puzzle to early seismologists. Particularly the Lisbon Earthquake (1755) had clearly demonstrated a correlation between earthquakes and tsunamis. Although the origin of seismic waves by earth- and seaquakes was already recognized by the German natural philosopher Immanuel KANT (1756) and the British geologist Reverend John MICHELL (1760), the origin of these vertical displacements of the sea floor was disputed, and most contemporary naturalists favored the hypothesis of submarine explosions. In his memoir *On the Dynamics of Earthquakes* (1846), MALLET illustrated earthquake motion in the Earth's crust and the seismic origin of sea waves. His schematics illustrate the general relation of earthquake phenomena in their successive occurrence. ***(A)*** Following a submarine eruption, the fast Earth wave, prior to the great sea wave, after passing the ship at sea, has arrived at land, marked by a tower falling upon the shore (*left*). The great sea wave and its minor successors are still on their way toward land. This sequence of the following three schematics shows the effects upon the great sea wave of its arrival from deep water upon a shore, which suddenly shelves by steep escarpments. ***(B)*** The great sea wave advances as a solitary mass with equal front and rear slopes over the deep sea. ***(C)*** After reaching the sounding edge, the front face of the wave becomes steep while the rearward slope flattens and the water at the beach is in the process of receding. ***(D)*** Shortly thereafter, the solitary wave is broken into several smaller ones, at heights bearing relation to the shallow water beneath, and the leading wave is about to form a great "breaker" upon the shore, no longer having any depth to remain unbroken. [Trans. Roy. Irish Acad. **21**, 51 (1846)]

4.1 SHOCK AND PERCUSSION IN NATURE – Tsunami Caused by Subduction

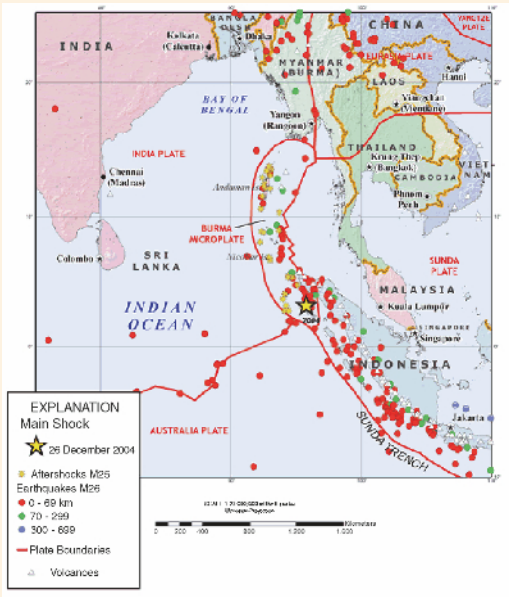

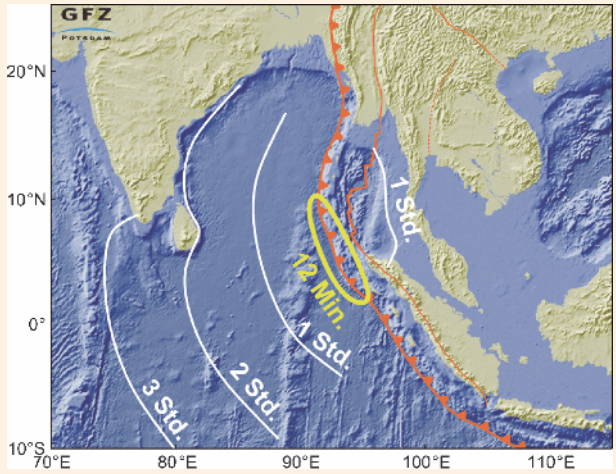

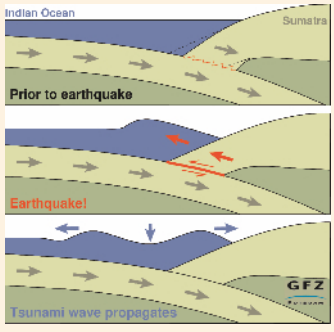

The velocity of an ocean wave v_O whose length L is sufficiently large compared to the still water depth H (*i.e.*, for $L > 25\ H$) can be approximated by $v_O = (gH)^{½}$, where g is the acceleration of gravity. Thus, the velocity of such "shallow-water waves" is independent of wavelength L. As the wave approaches the coast, the wavelength decreases and the wave height increases. The rupture, triggered by frictional instability and initially affecting only a relatively small area, propagated outside the hypocenter northwestward about 1,200 km along the fault with the shear-wave velocity v_S (presumably ranging between 2 and 4 km/s). The required time for the rupture is then of the order of only 5 to 10 minutes. Even in deep water ($L >> H$) v_O is much smaller (about 5%) than the rupture velocity, and the fault displacement was quasi-instantaneous. ▪ Theoretical, numerical, observational and experimental research indicates that shear ruptures can propagate faster than the shear wave speed {ROSAKIS ET AL. ⇨1999}. The rupture velocities v_R of some fault segments in recent large strike-slip earthquakes have been interpreted as propagating at transonic ($v_S < v_R < v_L$) or even supersonic ($v_R > v_L$) velocities (in respect of the longitudinal velocity v_L).

4.1–N *(cont'd)* ***Left, top:*** On December 26, 2004, the world's largest earthquake in 40 years hit southern Asia (about 230,000 casualties). Known as the "2004 Sumatra-Andaman Earthquake" it occurred at the interface between the India and Burma plates and was caused by the release of stresses that develop as the India plate subducts beneath the overriding Burma plate. [Courtesy USGS] ***Right:*** The magnitude 9 quake, which occurred under the sea floor at a depth of more than 10 km and had its epicenter about 200 km off the west coast of northern Sumatra, produced a destructive tsunami that traveled at speeds of up to 800 km/s and arrived at all coasts along the Indian Ocean. Countries in the vicinity of the quake such as Indonesia, Thailand, Malaysia, Sri Lanka, and the Maldives were particularly affected by the tsunami. Note that the tsunami arrived at the west coast of Sumatra only 13 min after the quake but needed about 1 h to reach the west coast of Thailand and 2 h to reach the east coast of Sri Lanka. Many lives could have been saved by a tsunami warning system, which, however, did not exist. Just three months apart, in March 2005, another earthquake happened along the Sunda megathrust and produced a smaller but still considerable tsunami. ***Left, bottom:*** Schematic illustrating the tsunami wave development mechanism by the sudden release of strain that shifted the Burma plate upward by ca. 10 m, thus causing the overlying water to move up and down and generating the tsunami. [Courtesy Geoforschungszentrum Potsdam; http://www.gfz-potsdam.de/news/recent/archive/20041226/Downloads/index.html]

4.1 SHOCK AND PERCUSSION IN NATURE – Examples of Early Tsunami Research

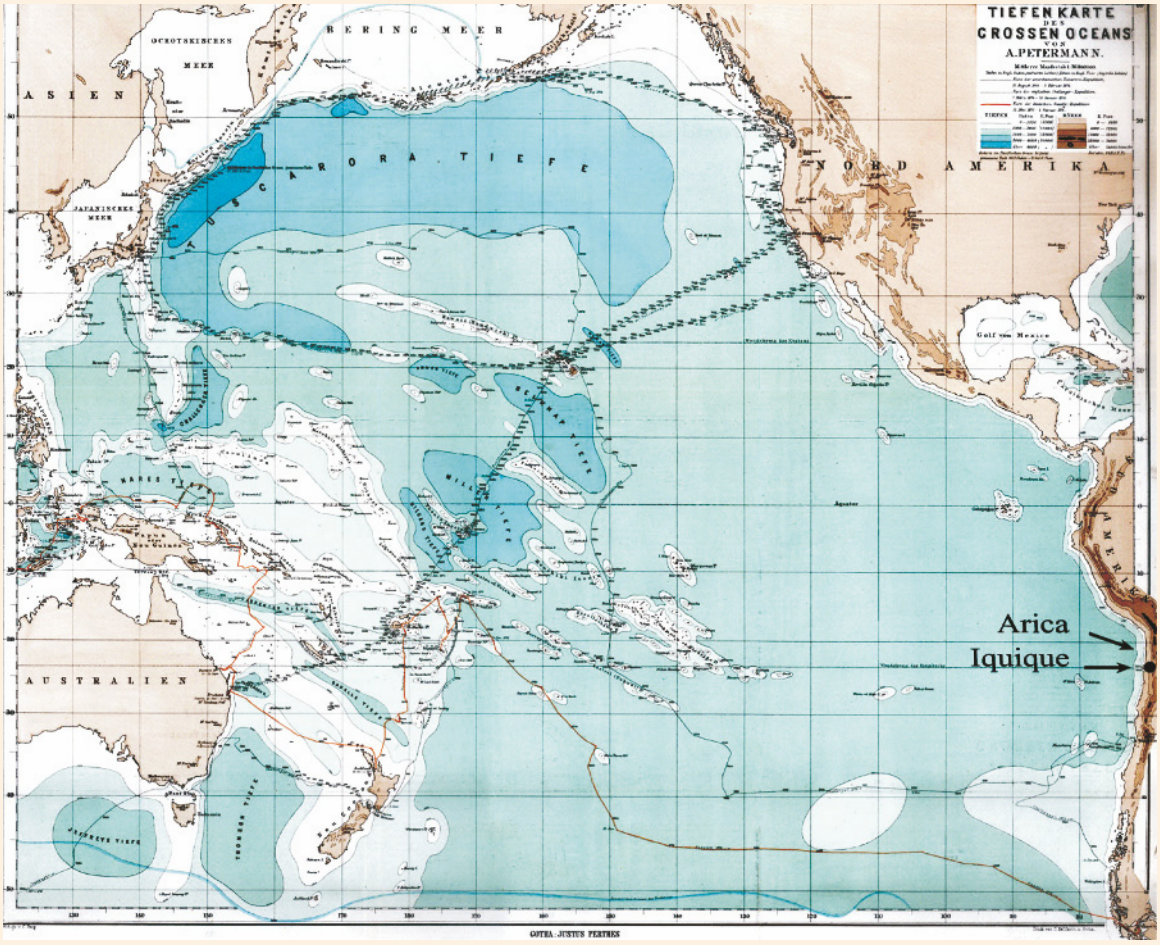

4.1–O The German geographer August PETERMANN published in 1877 the first chart of bathymetric data of the Pacific Ocean, based on 738 deep-sea soundings performed during the expeditions of the HMS *Challenger* (1872), the USS *Tuscarora* (1873–1876), and the German SMS *Gazelle* (1874–1876). It first revealed the existence of submarine ridges of considerable depth, later identified as sources of submarine landslides causing dangerous tsunami effects at remote coasts. However, as shown in the map, the ridge west of the South American coast, a seismically active region, was not yet fully known. Inspired by the Arica Earthquake (1868), which created destructive tsunami effects at remote coasts of the Pacific Ocean, German geologist Ferdinand VON HOCHSTETTER proposed to calculate the average velocity of the seismic sea wave v_{AV} by the formula $v_{AV} = (h_{AV} g)^{½}$ and to compare the result with an average velocity $w_{AV} = s/(t_2 - t_1)$. Here h_{AV} is an average depth calculated from bathymetric data, g the gravitational acceleration, t_1 the time at which the earthquake started, and t_2 the arrival time of the seismic sea wave at remote distance s. He found reasonable agreement for waves traveling freely between Arica and remote coasts ($v_{AV} \approx w_{AV}$). His hypothesis was also confirmed by his colleague F. Eugen GEINITZ on the occasion of the Iquique Earthquake (1877), which caused tsunami effects as destructive as the Arica Earthquake. [Mitth. aus Justus Perthes' Geograph. Anstalt **23**, 125 (1877)]

4.1 SHOCK AND PERCUSSION IN NATURE – Examples of Early Tsunami Research *(cont'd)*

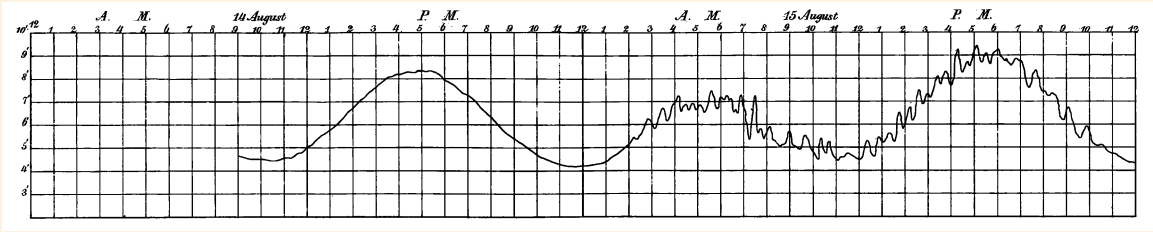

4.1–P ***Top:*** At remote coasts a water-depth gauge records a tsunami as a number of spikes superimposed on the daily fluctuations caused by the tides. This record of a self-registering gauge was taken in August 1868 at Sydney harbor after the violent Arica Earthquake (1868) with its epicenter near the coastal town of Arica, Chile. A similar record was obtained at South Georgia (an island in the South Atlantic Ocean) after the explosive eruption of Krakatau volcano. It first showed that, despite different causes, similar tsunami effects are generated at remote coasts of the Pacific Ocean. [Sitzungsber. Akad. Wiss. Wien **60** (II), 818 (1869)] ***Bottom:*** This map shows schematically epicenters of earthquakes that occurred in Japan during the period 684–1960 and were accompanied by tsunamis. [Proc. Tsunami Meetings at the10th Pacific Science Congr., University of Hawaii, Honolulu (1961). Institut Géographique National, Paris (1963), p. 260]

Year	Location	Grade of Tsunami	Magnitude of Earthquake
684	E	III	8.4
869	B	IV	8.6
887	DE	III	6.5
1361	E	III	7.0
1498	D	III	8.6
1605	DE	III	7.9
1611	B	IV	8.1
1703	C	III	8.2
1707	DE	IV	8.4
1741	F	III	6.9
1771	G	III	7.4
1854	D	III	8.4
1854	E	III	8.4
1896	B	IV	7.6
1933	B	III	8.5
1944	D	III	8.3
1946	E	III	8.1
1952	A	II	8.2
1960	(Chile)		(8.7)

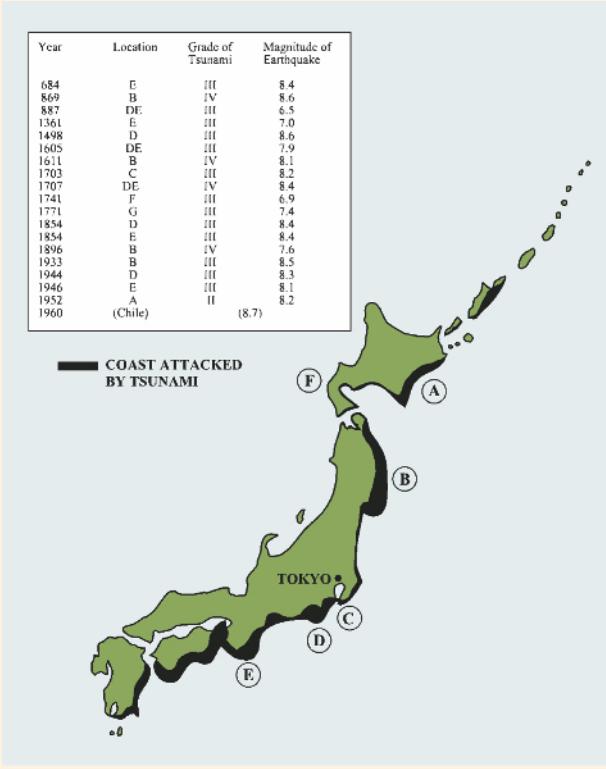

← Japan has frequently been pounded by tsunamis that caused tremendous loss of life and damage on the coast. Since tsunami waves follow an earthquake within a few minutes, it was recognized early that a causal connection must exist between earthquakes and tsunamis. However, the complex mechanism of tsunami generation has been a subject of debate among scholars that has continued to this day. Historical tsunami research may prove helpful in analyzing the frequency of occurrence of tsunamis and their relationship to large earthquakes.

The islands of Japan lie along the circum-Pacific seismic zone. This figure shows the locations and magnitudes of large earthquakes that had their epicenters on the sea bottom very close to the coasts along which the great tsunamis were generated. In the table the magnitudes of earthquakes are given in terms of the Richter-Gutenberg scale and the grades of tsunamis in terms of total energy:

Grade II: 4×10^{22} ergs;
Grade III: 16×10^{22} ergs, and
Grade IV: 64×10^{22} ergs.

The most powerful tsunamis over the last 100 years were the Sanriku tsunamis (location B), which occurred in 1896 (Grade IV) and 1933 (Grade III). On the Sanriku Coast many tsunami monuments have been erected bearing the warning "Expect a tsunami if you feel an earthquake!" However, dangerous tsunamis generated off the coast at very remote distances – so-called "teletsunamis," such as those resulting from the Chilean Earthquake (1960), topographically diametrically opposite Japan – also proved most destructive to Japan's coasts.

4.1 SHOCK AND PERCUSSION IN NATURE – The Tsunami in Indian Mythology

4.1–Q Rockslides in the Lituya Bay (southern Alaska) can transform into dangerous tsunamis. ***Left, top:*** In July 1958, a rockslide, triggered by an earthquake, occurred along the eastern wall of the Gilbert Inlet. The mass of rock striking the surface of the bay created a giant splash, which sent water surging to a height of 1,720 ft (524 m) across the point opposite the inlet. The giant local tsunami sweeping across the bay inundated approx. 5 square miles (15.5 km^2) of land along the shores of Lituya Bay, sending water as far as 3,600 ft (1,027 m) inland. This map shows a close-up of Lituya Bay. [Tsunami Research Group, University of Southern California; http://www.usc.edu/dept/tsunamis/alaska/1958/webpages/lituyacloseup.html] ***Center:*** This aerial photo was taken in August 1958, one month after the earthquake. [Courtesy USGS Photographic Library] ***Bottom, left:*** A unique example of illustrating wave discontinuities is kept at the Museum of the National American Indian, Heye Foundation, New York. [Courtesy National Museum of the American Indian, Smithsonian Institution. NMAI photo no. T009205] ***Bottom, right:*** Reproduction of a carving on an about 500-year-old wooden box excavated from an archaeological site on Kodiak Island, Alaska – the oldest known illustration of a volcanic eruption and volcanic tsunami in the Western Hemisphere. [Courtesy Prof. James E. BEGÉT, Alaska Volcano Observatory; *Encyclopedia of volcanoes*. Academic Press, San Diego (2000), p. 1007]

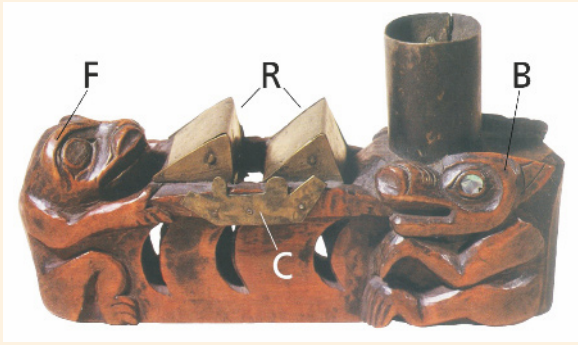

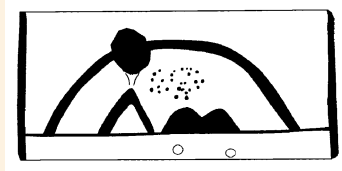

← According to an old Indian legend and illustrated on this beautiful Tlingit Indian pipe, a froglike monster *F* – today identified as a large geological fault running across the mouth of the bay – sits opposite a bearlike demon *B* who dwells in the underwater caverns close to the bay entrance. Note the two enormous ridges *R* created by the froglike monster swamping a two-man canoe, shown here in the form of a brass plate *C*.

4.1 SHOCK AND PERCUSSION IN NATURE – Destructive Tsunami Effects

4.1–R ***Top:*** On April 1, 1946, a magnitude 8.0 earthquake with the source about 145 km south of Unimak Island and a focal depth of 25 km occurred in the Aleutian Islands of Alaska. It triggered a Pacific-wide tsunami which had a surface-wave magnitude of 7.8. The tsunami, then bounding 3,800 km to the Hawaiian Island, stroke its coasts 4.9 hours later, in some areas producing waves over 6 meters high. [USC Tsunami Research Center, Los Angeles, CA]. ***Bottom:*** Destructive effects on Unimak Island by the tsunami [National Geophysical Data Center (NGDC)/USGS; http://www.ngdc.noaa.gov/nndc/struts/results?eq_1=25&t=101634&s=0&d=4&d=44]

←← Scotch Cap Lighthouse on Unimak Island, Alaska as it looked before the earthquake and tsunami. The structure was built in 1940. It was located 9.8 m above sea level and five stories high.

← Remains of Scotch Cap Lighthouse after the tsunami. All five occupants were killed. Only the foundation and part of the concrete sea wall remained. The tsunami also wiped out the 31-m high radio antenna.

4.1–S On 26 December 2004, at 8 a.m. local time, a magnitude 9.1 earthquake happened off the coast of Sumatra which triggered a huge tsunami. Because of the fault geometry, the waves propagating to the East (towards Thailand and Myanmar) began with a receding wave which explains why the sea started to retreat minutes before flooding the coast. On the opposite, to the West (towards India and Sri Lanka) a large wave suddenly hit the coast without warning. ***Left:*** View of the tsunami in the moment of hitting the famous Hat Railay Beach near Krabi in southern Thailand, a tourist resort located about 860 km distant from the epicenter of the quake. The woman in the foreground, running toward the wave, is a Swedish mother attempting to save her three children. They somehow managed to survive. Also the other tourists, running for their lives and rushing to safety, reportedly survived. The water had receded before the first of six tsunami waves struck the beach. About 200 people died in this area. [© Getty Images Deutschland GmbH; Photo by Agence France Presse (AFP), Paris]

4.1 SHOCK AND PERCUSSION IN NATURE – Destructive Tsunami Effects *(cont'd)*

Aftershocks, defined as earthquakes that follow the largest earthquake of an earthquake sequence, are smaller than the main shock and within 1–2 fault lengths distance from the main shock fault. They can continue over a period of weeks, months, or years. In general, the larger the main shock, the larger and more numerous the aftershocks, and the longer they will continue.

4.1–S *(cont'd)* The 26 December 2004 Earthquake – actually a seaquake – happened on the interface of the India and Burma plates and extended along the subduction zone from western Sumatra to the Andaman Islands {⇨Fig. 4.1–N} – thus named "Sumatra-Andaman Islands Earthquake". Resulting from thrust-faulting in a shallow depth of about 30 km, it produced a destructive tsunami causing more casualties (estimated 230,000) than any other in recorded history. But also remote coasts of other nations bordering the Indian Ocean were affected such as in India, Sri Lanka, Thailand, Malaysia, Kenya, Somalia, Tanzania and on Mauritius, Madagascar, the Nicobar Islands and Andaman Islands, and the Maldives. ***Left:*** Map showing the epicenters of the 26 December 2004 Earthquake (moment magnitude 9.1) which produced a large tsunami and of the 28 March 2005 Earthquake (moment magnitude 8.7) which, probably a result of stress placed on the fault by the first quake, only produced a small tsunami. Both earthquakes happened along the same Sunda trench fault line and at about the same focal depth of about 30 km. [Courtesy USGS] ***Right:*** The epicenter of the 26 December 2004 was off the west coast of western Sumatra, only about 250 km apart from Banda Aceh, capital of the Indonesian Province of Aceh. Banda Aceh, located at the northernmost part of Sumatra, was the closest major city to the earthquake's epicenter. The two satellite photos taken with QuickBird show a shore detail of Banda Aceh on June 23, 2004 (*top*) and on December 28, 2004 (*bottom*), only two days after being struck by the tsunami. [© Getty Images Deutschland GmbH; Satellite Photography, reproduced with permission from DigitalGlobe] This comparison illustrates the enormous destructive power which the tsunami caused in coastal regions of western Sumatra. A considerable portion of the town of Banda Aceh was totally destroyed, but much of downtown, the airport and roads from outside survived so that recovery supplies could get in more systematically than in other parts of the province. According to the U.S. Agency for International Development (fiscal year 2005) over 104,000 people were killed, over 10,000 were missing and over 650,000 were displaced in Indonesia alone.

4.1 SHOCK AND PERCUSSION IN NATURE – Rogue or Freak Waves

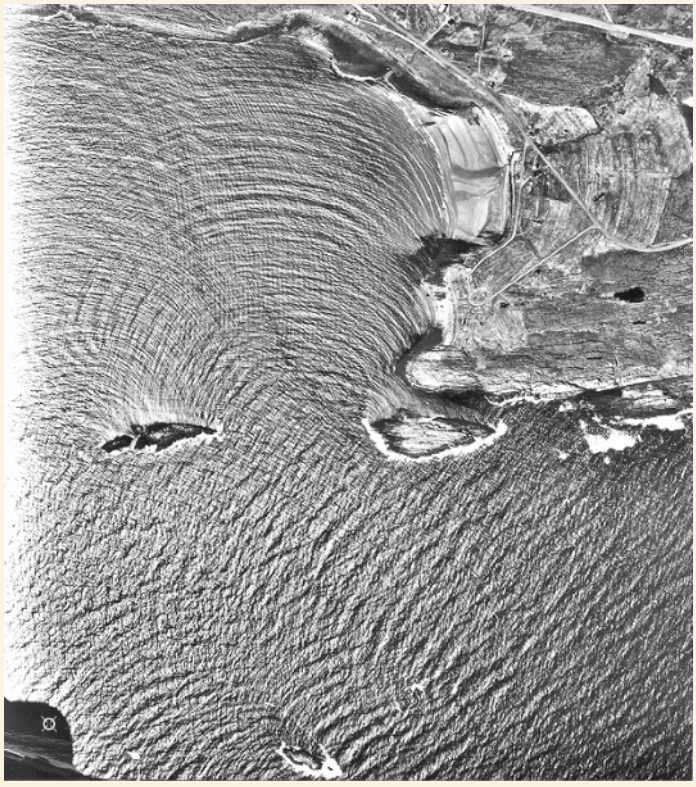

4.1–T Rogue waves, also known as "freak waves," are giant sea waves. Presently, there is no consensus about whether they are "normal" extremes of a superposition of waves or the result of totally different generation mechanisms, such as nonlinear interaction and phase locking of wave trains. ***Top:*** Aerial view of an area near Kiberg on the coast of Finmark, a county in the extreme northeast of Norway, taken on June 12, 1976. Aerial photography allows one to localize dangerous areas where in shallow waters refraction and diffraction of surface waves can cause focusing of wave energy, resulting in waves of unusual amplitudes. In addition, radar images taken by satellites allow one to measure the wave length, crest height, and direction of propagation of ocean surface waves. [Courtesy Vardø Kommune, Norway. Photo by Fjellanger Widerøe Foto AS, Trondheim & Oslo, Norway] ***Bottom, left:*** The unusual record of an extreme wave was measured on January 1, 1995 with a depth gauge under an oil platform in the North Sea, proving that such waves do indeed exist. [http://www.math.uio.no/~karstent/waves/index_en.html] For centuries sailors have blamed mysterious surges of water for unexplainable sinkings or damage, but the claims have always attracted plenty of skepticism. ***Bottom, right:*** View of a giant wave shortly before striking a cargo ship with huge force. Extreme waves are studied jointly by Norwegian researchers at the Universities of Oslo and Bergen and at Norges Teknisk-Naturvitenskapelige Universitet (NTNU). [Courtesy BBC, London http://news.bbc.co.uk/1/hi/sci /tech/2450407.stm]

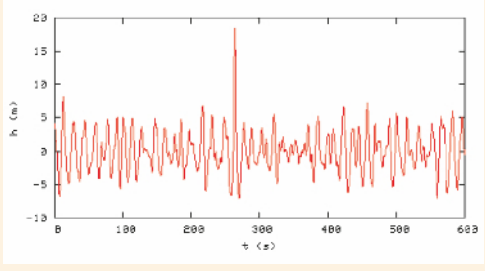

↑ The maximum amplitude of 18.5 m is more than three times the significant amplitude for the wave train. This wave is known in the international scientific community as the "New Year Wave." [Courtesy Prof. Karsten TRULSEN, University of Oslo. Data provided by Drs. Ove T. GUDMESTAD and Sverre HAVER at Statoil, Stavanger, Norway]

4.1 SHOCK AND PERCUSSION IN NATURE – Sunspots, Solar Flares, and Prominences

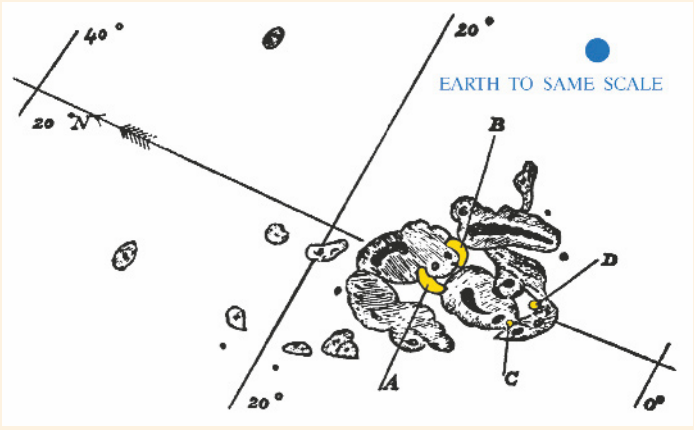

← CARRINGTON observed near a large sunspot (an area of cooler gas on the Sun's surface) two patches of intensely bright light, *A* and *B*, which moved within 5 min to positions *C* and *D*, respectively. Corresponding to a distance of 35,000 miles (about 56,000 km), this indicated an average lateral velocity of about 116 miles/s (187 km/s). The diminished size of spots *C* and *D* clearly shows one of the characteristic features of a solar flare, *i.e.*, that its intensity strongly decreases within a short time. His famous discovery first revealed the enormous dimensions and velocities of solar-surface phenomena. The techniques of CARRINGTON and his contemporaries gave birth to the new science of solar physics, which played a key role in the evolution of modern astrophysics.

4.1–U ***Top:*** In 1860, the English astronomer Richard C. CARRINGTON customarily observed sunspots using a telescope that projected the image of the Sun's disk onto a plate of glass coated with distemper of a pale straw color. He witnessed unusual violent eruptions, so-called "flares." At the same time, similar observations were made independently by his countryman Richard HODGSON. [Month. Not. Astron. Soc. **20**, 14 (1860)] ***Bottom, left:*** Prominences are beautiful solar phenomena with enormous horizontal and vertical dimensions attaining in some cases some 100,000 km. They can be active or quiescent and encompass different types of structures. These prominences were observed by the French artist and amateur astronomer E. Leopold TROUVELOT on April 15, 1872 (*top*) and April 29, 1872 (*bottom*). [*Meyers Konversations-Lexikon*. Bibliographisches Institut, Leipzig (1897), vol. 16, plate II] ***Bottom, right:*** This ultraviolet photograph was acquired from NASA's Skylab space station on December 19, 1973. It shows one of the most spectacular solar flares ever recorded that, propelled by magnetic forces emitted by the Sun, spans more than 588,000 km of its surface. [Courtesy NASA-GSFC]

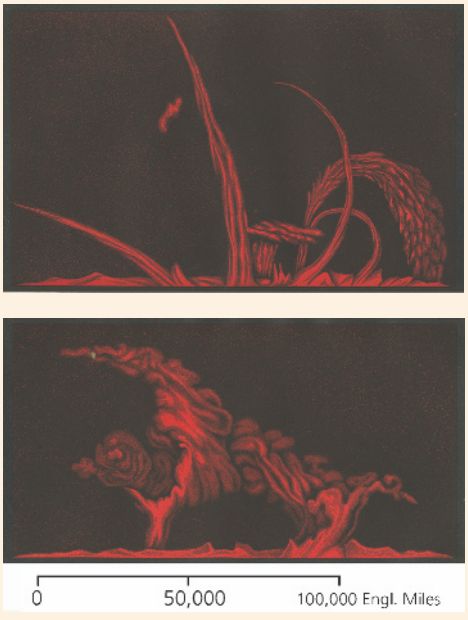

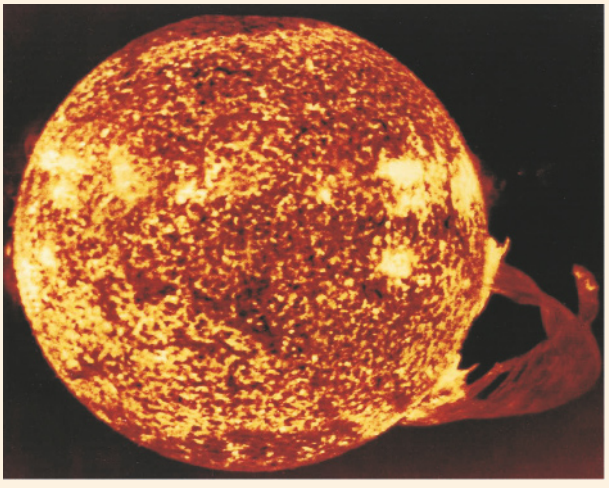

← In 1876, TROUVELOT's pictures were issued as lithographic color prints by Harvard College Observatory and became widely known. Not only are they aesthetic, but they also give a vivid impression of the enormous dimensions of surface phenomena which happen on the Sun, our closest star.

4.1 SHOCK AND PERCUSSION IN NATURE – Solar Flares and Solar Quakes

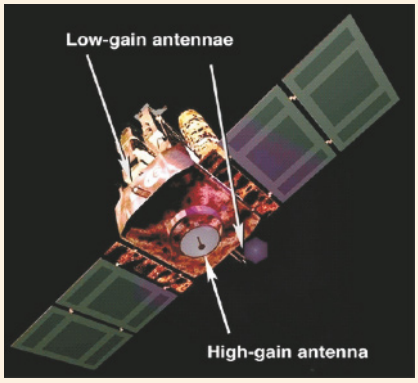

← ***Left, top:*** The 1,850-kg ESA/NASA Solar and Heliospheric Observatory (SOHO), built by the European space industry and launched in 1995, is stationed 1.5 million km from Earth on the sunward side of the Earth, which allows an uninterrupted view of the Sun. It carries both European and American instruments. The Michelson Doppler Imager is a key instrument for measuring magnetic fields and vibrations on the surface of the Sun (*right*). Pictures of solar flares (*bottom*) were obtained with the Extreme Ultraviolet Imaging Telescope. [© ESA/NASA]

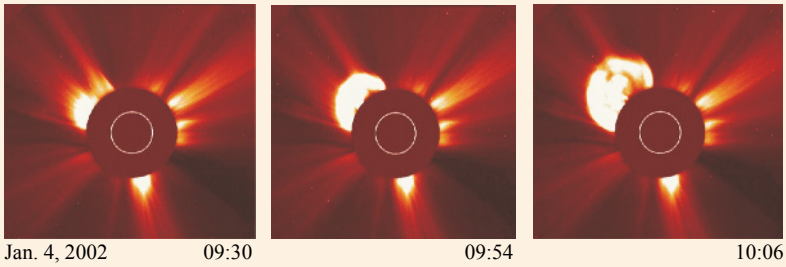

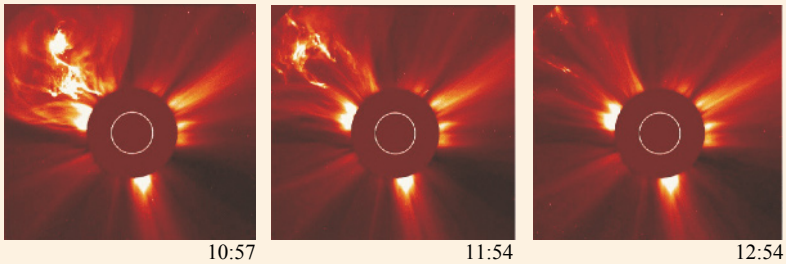

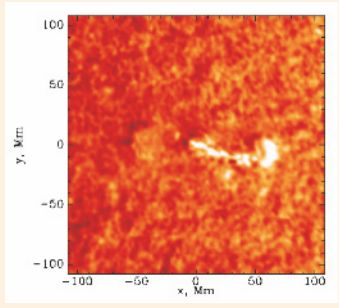

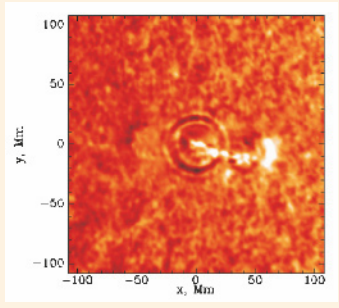

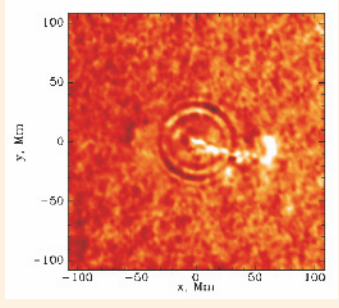

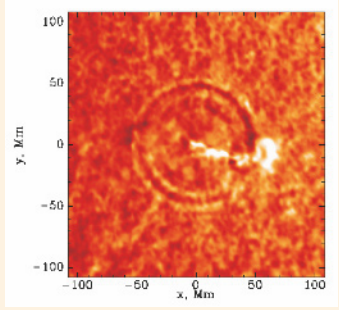

4.1–V ***Left, bottom*****:** A spectacular coronal mass ejection took off from the Sun on January 4, 2002, starting off as a filament eruption seen by the LASCO coronagraph of ESA/NASA's spacecraft SOHO [LASCO C2 team, © NASA/ESA] ***Right*****:** A sequence of images taken of the July 9, 1996 solar quake; the images were created from SOHO/MDI dopplergrams. The solar flare that initiated the shock wave is shown in the first picture (*top, left*). The following three pictures cover a time from 30 min to 1 h 30 min after the X-ray flare onset. The solar quake generated ripples on the Sun's surface 3 km high, growing larger and larger in the following pictures. The ridges began at 09:32, 20 min or so after the flare, at about 18,000 km from the flare and reached 120,000 km at 10:02. The velocity of the wave packet increased from about 30 km/s to about 100 km/s as the wave moved from 20,000 to 120,000 km from the epicenter. The flare of July 9, 1996 was of moderate size, containing, for example, "only" 40,000 times the energy released in the great earthquake that devastated San Francisco in 1906. [Courtesy Dr. Alexander G. KOSOVICHEV, Stanford University, CA]

4.1 SHOCK AND PERCUSSION IN NATURE – Big Bang Portrait

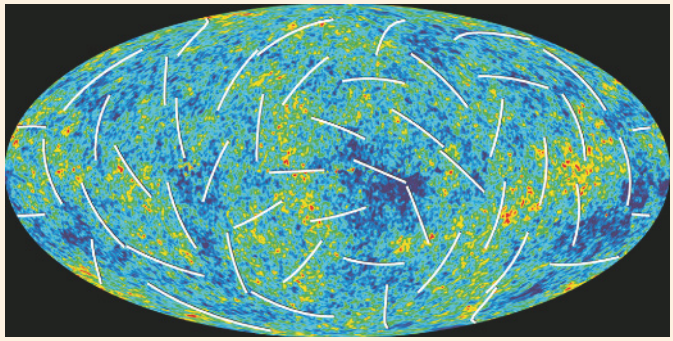

↑ Colors indicate "warmer" (*red*) and "cooler" (*blue*) spots. The *white bars* show the "polarization" direction of the oldest light

4.1–W Cosmic portrait showing afterglow – so-called "cosmic microwave background" – of the Big Bang that occurred over 13 billion years ago. It was captured using NASA's Wilkinson Microwave Anisotropy Probe (WMAP) during a sweeping 12-month observation of the entire sky. This is a full-sky map of the oldest light in the Universe released by NASA-GSFC on Feb. 11, 2003. The microwave light captured in this picture is from 379,000 years after the Hot Big Bang, so to speak a "baby" picture of the Universe in galactic coordinates. The oval shape is a projection to display the whole sky, similar to the way the globe of the Earth can be represented as an oval. [Courtesy NASA/WMAP Science Team, NASA-GSFC; *see* http://map.gsfc.nasa.gov/m_mm.html]

4.1 SHOCK AND PERCUSSION IN NATURE – Earth's Bow Shock

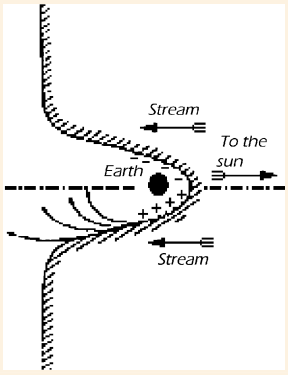

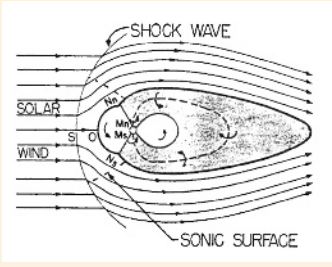

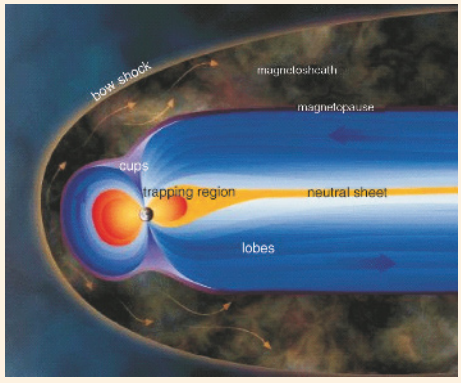

4.1–X ***Left:*** In 1931, the British astrophysicists Sydney CHAPMAN and Vincent FERRARO proposed that the Sun sent out huge clouds of electrically neutral plasma and that magnetic storms arose when those clouds enveloped the Earth. Many magnetic storms were observed to begin with a small steplike jump in the magnetic field, taking just a minute or so. CHAPMAN and FERRARO also proposed that such jumps marked the cloud's arrival. They realized that the strong field of the Earth would hold off the cloud, carving a cavity in the cloud in which the Earth and its magnetic field would be confined. Their theory proved to be prophetic, except for one important detail: the flow of plasma from the Sun was not confined to isolated clouds, but went on all the time, in the form of the solar wind. [Terr. Magnet. Atmos. Electric. **36**, 171 (1931). *See also* D.P. STERN and M. PEREDO: *The magnetopause – history*; http://www-spof.gsfc.nasa.gov/Education/whmpause.html] ***Center:*** In 1962, the astrophysicists William I. AXFORD and Paul J. KELLOG predicted independently of each other that a shock wave must exist in the interplanetary medium a short distance upstream of the Earth's magnetosphere. This discontinuity is created when the supersonic solar wind ($M = 3–20$) encounters the magnetic field of the Earth. [J. Geophys. Res. **67**, 3791, 3805 (1962) © American Geophysical Union (AGU). Reproduced by permission of AGU] ***Right:*** Based on an increasing amount of data obtained by various satellite missions the schematic of the magnetosphere underwent numerous refinements. The solar wind, a stream of charged particles continuously being ejected by the Sun, flowing past the Earth, and interacting with the Earth's magnetic field, generates a bow shock similar to an object exposed to a supersonic flow. [Courtesy NASA-GSFC; http://www.eng.vt.edu/fluids/msc/gallery/shoks/earth.htm]

4.1 SHOCK AND PERCUSSION IN NATURE – Cosmic Jets, Shock Waves, and Mach Cones

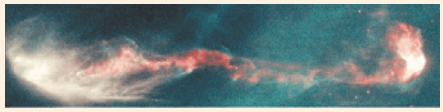

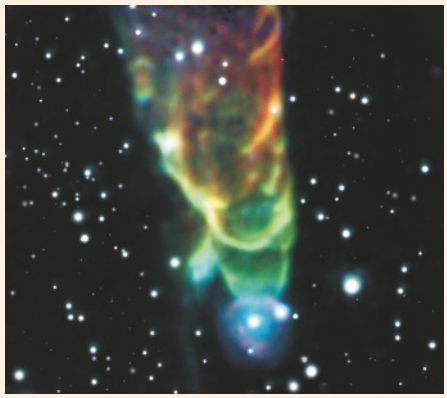

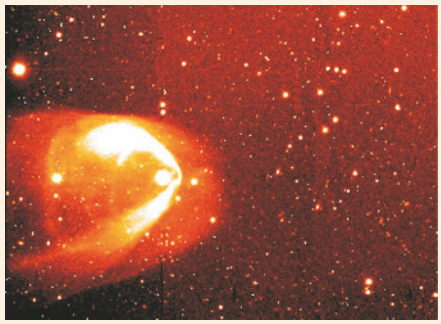

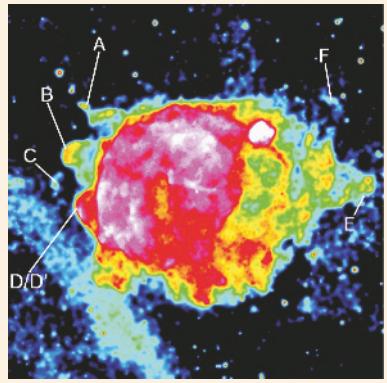

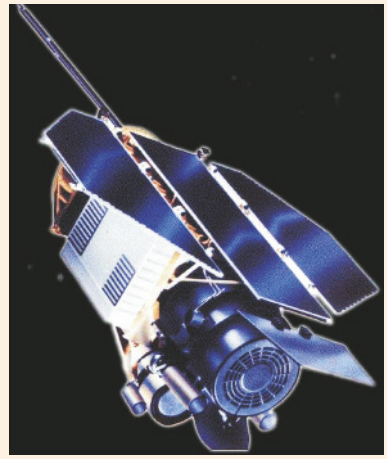

4.1–Y ***Left, top:*** Astrophysical jets are highly collimated beams of matter and energy that are ejected from some astronomical objects. The Herbig-Haro object HH 47, a small bright nebula in a star-forming region, expels an energetic beam of charged particles into interstellar space. The jet, here moving from left to right, moves at a velocity of nearly 300 km/s. [Courtesy NASA-GSFC; http://antwrp.gsfc.nasa.gov/apod/ap951012.html] ***Left, center:*** Cosmic tornadoes – here shown using the example of HH 49/50 – are mysterious astrophysical jets with a spiral structure. They are energetic outflows associated with the formation of young stars. [J. BALLY (Univ. of Colorado) ET AL., JPL-CalTech, NASA; http://www.astronet.ru/db/xware/msg/1211349] ***Left, bottom:*** Astrophysical shock waves can arise in a number of different situations. For example, an explosive event may generate supersonic flows that, impacting the surrounding gas, generates a cosmic bow shock. BZ Cam is a binary star system that contains an accreting white dwarf and a 0.3 to 0.4 solar mass main-sequence donor. It lies about 2,500 light-years away toward *Camelopardalis* ("The Giraffe," a constellation of the Northern Hemisphere) and expels an unusually large wind of particles that creates a large bow shock as the system moves through the surrounding interstellar gas. [R. CASALEGNO, C. CONSELICE ET AL.; WIYN, NOAO, MURST, NSF; http://antwrp.gsfc.nasa.gov/apod/ap001128.html] ***Right:*** Based on X-ray images taken by the Roentgen satellite ROSAT in the spectral range 0.1 to 2.4 keV, astrophysicists at the MPE (Garching, Bavaria) discovered explosion fragments (labeled *A*–*F*) well outside the *Vela* supernova remnant shock-wave boundary. The area containing feature *D* shows evidence for the superposition of two bow-shaped objects. They suggested that X-ray emission associated with the protruding objects was produced by shock-heating of the ambient medium by supersonic motion of the objects. For the protruding objects *A*–*E*, which they interpreted as Mach cones, they calculated Mach numbers ranging from 4 (for object *A*) to 2.4 (for object *E*). [Nature **373**, 587 (1995); Reprinted with permission of Dr. Bernd ASCHENBACH, MPI für extraterrestrische Physik (MPE), Garching]

4.1 SHOCK AND PERCUSSION IN NATURE – Animal World

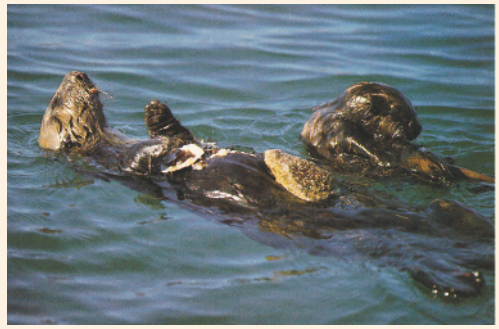

4.1–Z Only a few animal species use the principle of percussion as a tool. ***Top, left:*** The Egyptian vulture [*Neophron percnopterus*] uses a stone, ranging in weight from 100 to 300 g, as a tool to fracture the shell of an ostrich-egg. He picks the stone in his beak and hammers or throws it against the shell. [Photo by H. VAN LAWICK and J. VAN LAWICK-GOODALL. Reprinted with permission from Nat. Geographic Mag. **133**, No. 5, 631 (1968). ©2007, National Geograhic Image Collection] ***Top, right:*** Tool-using is also practiced by the California sea otter [*Enhydra lutris nereis*]. It applies small stones to detach and open shellfish, particularly abalones which are often tightly attached to the rocks. It usually eats while floating on its back as shown here. If it cannot get at the fleshy animal inside the shell, it will hold the shell against its chest with one paw and pound it with a stone. It often tucks a good stone under an armpit as it swims or dives. [Photo by W.F. BRYAN, reprinted from D.R. GRIFFIN, Am. Scient. **72**, 456 (1984)]

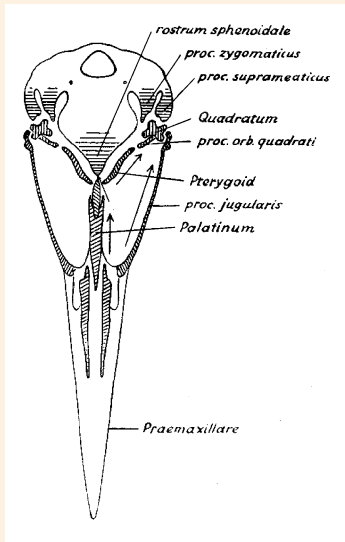

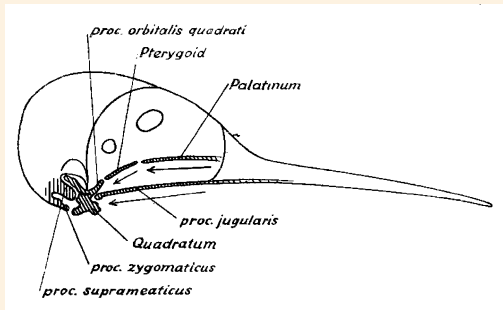

Bottom, left & center: Woodpeckers hammer their lives away for feeding, nest construction and drumming, up to 20 times a second. Their thick bony skulls with relatively spongy bones partially cushion the incessant blows, thus protecting the brain. In the early 1950s, the German neurologist Fritz BECHER studied the skull and beak anatomy, and how the impact force is transmitted and absorbed. In his schematic of the skull of a woodpecker the arrows indicate the direction of the impact force which splits into several branches, thus favorably bypassing the shock-sensitive brain. The hatched zones indicate those parts of the skull which are most stressed during hammering action. Inside the skull there is almost no cerebrospinal fluid which further prevents shock transmission to the brain. [Reprinted from Z. Naturforschung **8B**, 192-203 (1953)] ***Bottom, right:*** Woodpeckers [family *Picidae*] are found worldwide including over 200 species. View of the German "Buntspecht" [*Dendrocopos mayor*] which lives in central Europe. [Reprinted from J.F. NAUMANN: *Naturgeschichte der Vögel Mitteleuropas.* Köhler, Gera (1901), Bd. IV, Tafel 31]

4.1 SHOCK & PERCUSSION IN NATURE – Animal World *(cont'd)*

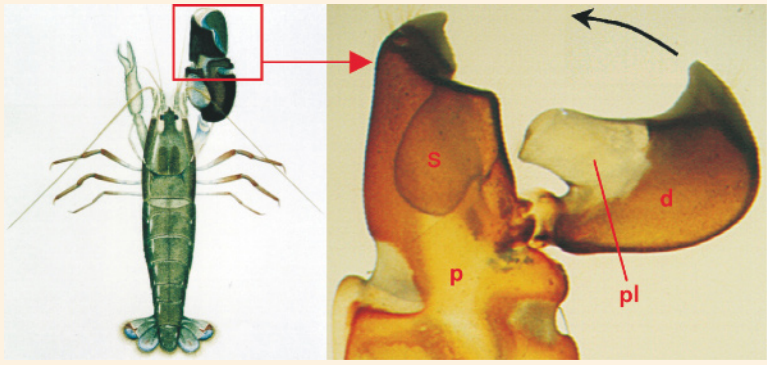

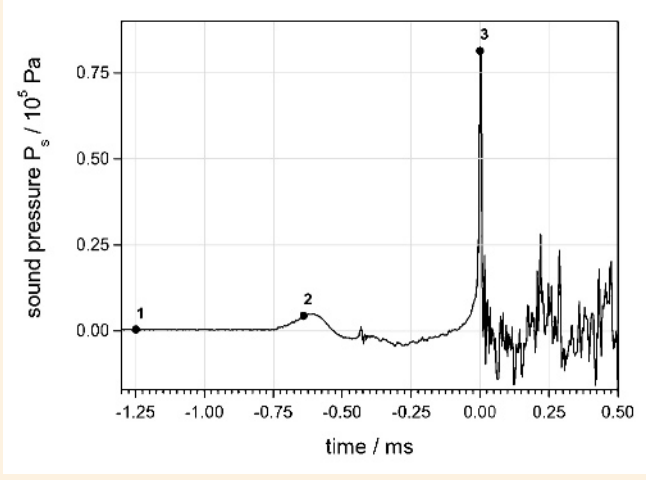

4.1–Z *(cont'd)* ***Top:*** The little snapping shrimp [*Alpheus heterochaelis*] which lives in warm, shallow seawater belongs apparently to the only species which produces shock waves. It has a protruding plunger *pl* on the dactyl *d* and a matching socket *s* in the immobile propus *p*. During the extremely rapid closure of the snapper claw, a high-velocity water jet is formed when the plunger displaces the water from the propus socket. ***Center:*** Using hydrophone diagnostics and high-speed videography, Michel VERSLUIS and collaborators at the University of Twente and Barbara SCHMITZ at TU Munich observed that the rapid claw closure generates a fast water jet, causing a cavitation bubble. Its collapse which results in a weak shock wave and produces a peak pressure of about 80 bars in a distance of 4 cm can stun nearby prey. ***Bottom:*** High-speed videography was used to resolve the rapid closure of the snapper claw. As an example this series shows four selected images, interframe time is 222 µs, frame size 17×17 mm^2. An analysis of the images reveals that the cavitation bubble is non-spherical and elongated in the direction of the water jet, reaching in the third frame a maximum length of more than one millimeter. [Courtesy M. VERSLUIS and B. SEIBEL, TU Munich. Reprinted from Science **289**, 2020 and 2114 (2000)]

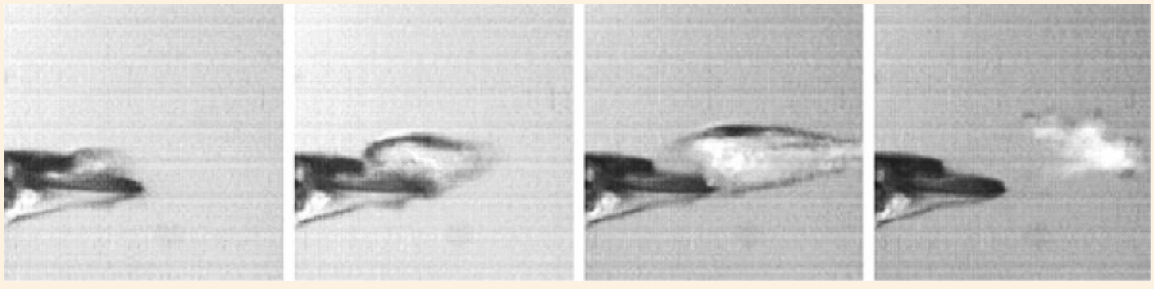

4.2 PERCUSSION IN THE EVOLUTION OF TECHNOLOGY – Basic Tool of Civilization

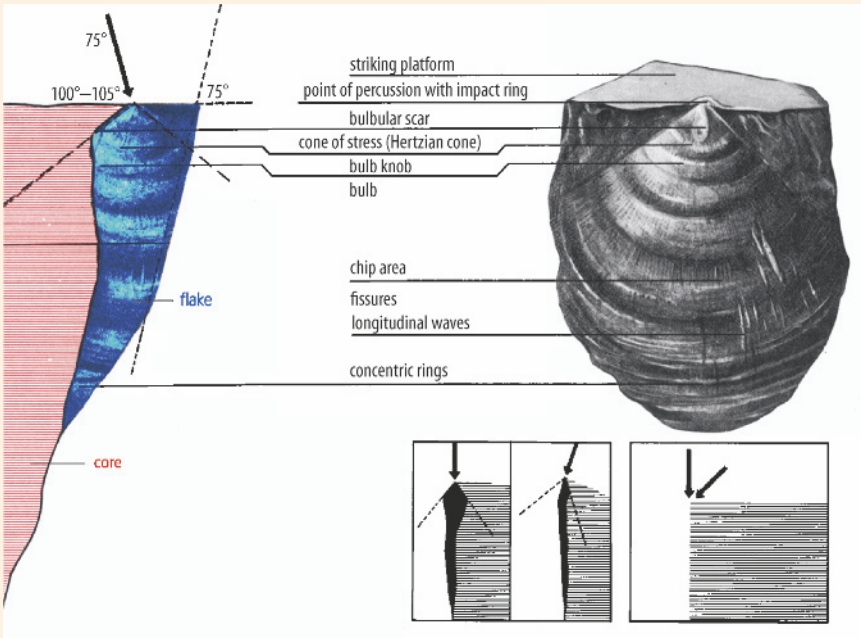

← The flake (*left*) was processed into a handaxe, a knife, a saw, an arrow point, a scraper, a bore, *etc.* The core (*right*) was discarded, processed into further flakes, or used as a heavy-duty chopping tool. [After L. PFEIFFER: *Die steinzeitliche Technik*. Fischer, Jena (1912); and P. HONORÉ: *Es begann mit der Technik*. Deutsche Verlagsanstalt, Stuttgart (1969)]

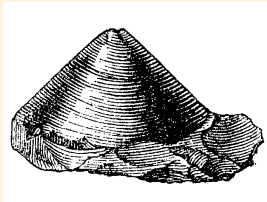

4.2–A ***Left:*** The basic method of stone fracture and disintegration, used by primitive humans throughout a period of at least 2 million years, is based on the generation of a *percussion bulb* extending from the point of percussion into the stone. This allowed the user to manufacture crude, but very effective, stone tools and weapons of great diversity. ***Right:*** Drawing of an artificial cone of flint produced by a single blow of a hammer. [J. EVANS: *The ancient stone implements.* Longman & Green, London (1872), p. 247] The term "bulb of percussion" was apparently coined in the middle of the 19th century by the Scottish palaeontologist Hugh FALCONER (1808–1865).

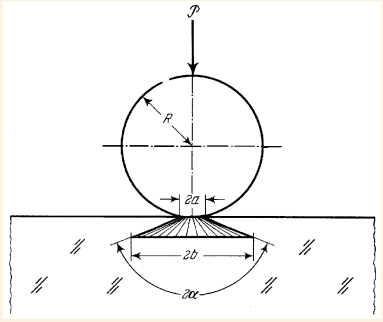

← Schematic of the formation of *Hertzian cone* with apex angle 2α when a glass cube is loaded by a steel sphere under pressure P, such as by a static load or dynamically by impact. The circular contact area between sphere and glass cube has the diameter $2a$

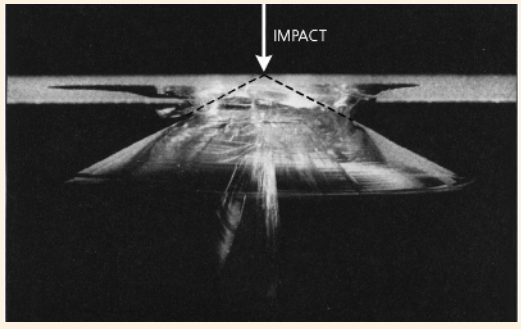

4.2–B Frank KERKHOF, a German applied physics professor and expert on fracture mechanics at EMI, Freiburg, and Hans Jürgen MÜLLER-BECK, a prehistorian at the University of Tübingen, first recorded cinematographically the growth of the "bulb of percussion" – a fracture residue of the "Hertzian cone," which they generated by impacting a glass cube at the top with a 30-mm-dia., 3.25-kg semispherical steel anvil dropped from a height of 23 cm. ***Left:*** Schematic illustrating the generation of the Hertzian cone. ***Right:*** This photo was taken in reflected light and shows the fully grown Hertzian cone. Its surface represents the fracture area that, from the point of impact, extends into the interior at an angle of $2\alpha \approx 135°$. [Glastech. Berichte **42**, 439 (1969)]

4.2 PERCUSSION IN THE EVOLUTION OF TECHNOLOGY – Basic Tool of Civilization *(cont'd)*

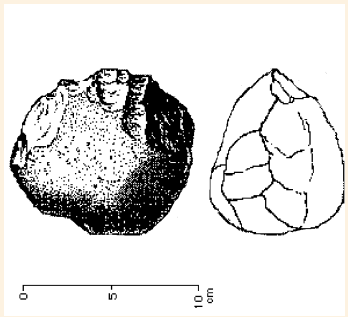

↑ Schematic of side chopper found at Olduvai Gorge. Flakes, provided with razor-sharp edges, were most effective at slicing through animal hide, cutting up and defleshing carcasses. Cores were most suited to removing dried flesh and smashing bones to get access to brain and bone marrow.

4.2–C ***Left:*** The first stone tools appearing in the fossil record around 2.6 million years ago were discovered in East Africa in 1959 by the British archeologists Mary and Louis LEAKEY at Olduvai Gorge, northern Tanzania. They have been taken as a key indicator of an early human species that anthropologists have called "australopithecines." [Photo by Guston SONDIN-KLAUSNER taken in 2006; http://commons.wikimedia.org/wiki/Image:Olduvai_Gorge.jpg] ***Right:*** Typically, these hominoids applied lava cobbles (cores) with flakes chipped away simply by hitting with another stone, the so-called "direct percussion technique" (Oldowan stone tools, 2.6 to 1.5 million years ago). [Dept. of Anthropology, UC Santa Barbara; http://www.mc.maricopa.edu/dept/d10/asb/anthro2003/archy/lithictech/lithictech5.html]

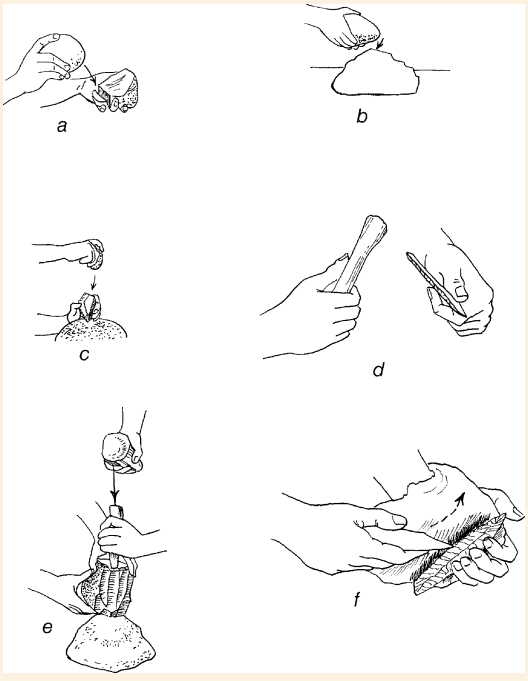

4.2–D Schematics of basic examples of major dynamic and static high-pressure techniques as practiced in the Old Stone Age (about 2,500,000–10,000 years ago) for the manufacture of stone tools and weapons. The various dynamic techniques, using percussion in a direct or indirect manner, are the oldest ones and probably all originated in East Africa.

(1) In the "direct percussion method," the core was held in the hand and struck with a hammer of stone, wood, or bone. ***(a)*** hard-hammer, free-hand percussion; ***(b)*** anvil technique; ***(c)*** bipolar technique; and ***(d)*** soft-hammer percussion.

(2) In the "indirect percussion method," ***(e)*** the core was placed on a large stone on the ground and the flake detached with a hammer and punch. Or the core was placed on a pointed anvil stone and struck at the top with a hammer (not shown here). This indirect percussion method was refined in the Late Pleistocene (100,000–35,000 years ago) and produced very delicate and fine blades.

(3) Blades could also be detached by generating the Hertzian cone statically, for example ***(f)*** by exerting a static pressure on the core with a pointed tool such as a sharpened piece of antler or bone, a technique known as "pressure flaking." [I. TATTERSALL ET AL. (eds.): *Encyclopedia of human evolution and prehistory*. Garland, New York (1988), p. 545]

4.2 PERCUSSION IN THE EVOLUTION OF TECHNOLOGY – Basic Tool of Civilization *(cont'd)*

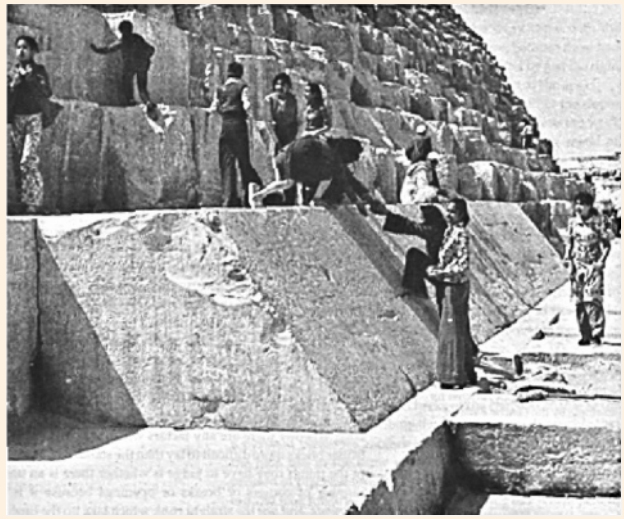

4.2–E ***Left, top:*** The handaxe, based on the "direct percussion method" and developed from the crude pebble chopper, was one of the principal tools in ancient Egypt for working stone surfaces. Many were made of dolerite, a very hard volcanic stone, and have been found at Giza, closely to the great pyramids. Another important tool based on the principle of direct percussion was the adze with a short handle, made with a metal blade of bronze or copper and used in the quarries of ancient Egypt. ***Left, bottom:*** An example of a tool based on the "indirect percussion method" is the chisel, which was applied together with a wooden mallet. It was the basic tool for most crude and fine masonry of ancient cultures. Typically, mallets have short handles, and the amplitude of swing is small, allowing a succession of rapid blows without undue operator fatigue. To provide energy and momentum, the mallet head is heavy. Being of wood, it does not rebound in the same manner as a metal head but stays on the chisel, which transmits the blow to the cutting edge that focuses it into a small area of stone to be spalled off. Ancient Egyptian chisels consisted of copper, arsenical copper, tin bronze, and leaded tin bronze. In the 26th Dynasty (664–525 B.C.), iron became as common as bronze. The tools shown here were used by the pyramid builders and found in the quarries north of the great pyramids at Giza. [Courtesy Dr. Rosemarie KLEMM, Univ. of Munich; *see also* her book *Steine und Steinbrüche im alten Ägypten.* Springer, Berlin (1993)] ***Right, top:*** Reconstruction of a scene of a man dressing a limestone block with chisel and mallet. The painting is from the Theban tomb of the Vizier REKHMIRA serving under Pharaoh THUTMOSE III who ruled from 1504–1450 B.C. [Courtesy W. MARTINI, EMI, Freiburg] ***Right, bottom:*** The Great Pyramid at Giza, on which construction began at about 2,590 years B.C., was built in a relative short period of less than 25 years. It consists of about 2.3 million blocks of white limestone. These blocks, which have an average weight of about 2.5 tons, were essentially produced using only simple tools based on the principle of percussion. [http://www-lib.Haifa.ac.il/www/art/construction_lower-closer.gif]

4.2 PERCUSSION IN THE EVOLUTION OF TECHNOLOGY – Early War Machines

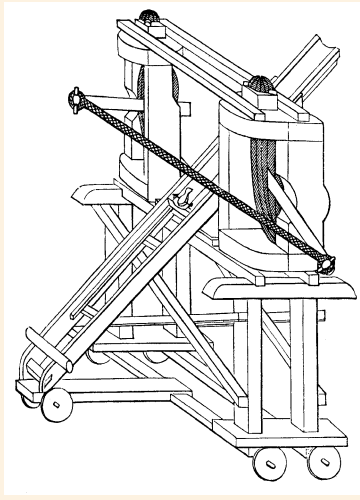

4.2–F ***Left:*** Illustration on an Attic drinking bowl (about 540 B.C.) showing a war galley (*right*) that is going to attack a trading vessel with reefed sail (*left*). Note the ram at the galley's bow, which was commonly fortified by metal. [Courtesy British Museum, London] ***Right:*** The catapult or *ballista* was used on a large scale in the Punic Wars (246–146 B.C.). Being a Greek invention, it was capable of bestowing the projectile with a considerable kinetic energy that upon impact was transformed via percussion into destructive power. [*Meyers Konversationslexikon.* Bibliogrphisches Institut, Leipzig (1894), vol. 2, p. 291]

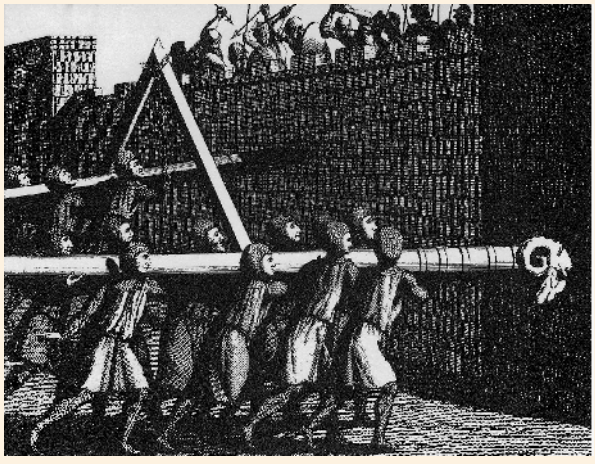

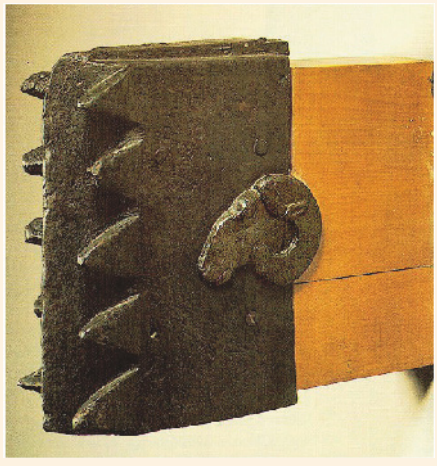

4.2–G ***Left:*** The "battering ram" (Lat. *aries*), a wooden pole or plank usually tipped with a bronze or iron ram, is based on the principle of percussion and was used in Antiquity until the Middle Ages to break down walls and gates. It was up to 30 m long and was operated by a crew of up to 100 men. To better protect from battlement attacks, a transportable shelter was applied, the ram being suspended from its roof on chains. [F. GROSE: *Military antiquities respecting a history of the English army.* S. Hooper, London (1786)] ***Right:*** This bronze battering ram is the only surviving besieging instrument of its kind from Antiquity (5th century B.C.). On both sides are symbolic depictions of ram heads, whence its name. [Courtesy Archaeological Museum, Olympia, Greece]

4.2 PERCUSSION IN THE EVOLUTION OF TECHNOLOGY – Devices Based on Rapid Expansion

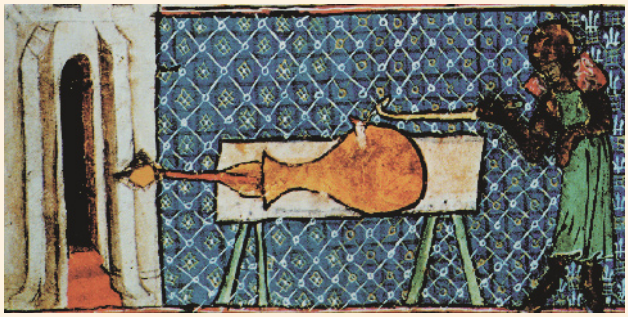

4.2–H ***Left:*** This is the oldest known illustration (A.D. 1320) of a cannon shot, found in a miniature of the English cleric Walter DE MILIMETE. It shows a subcaliber incendiary dart projectile at the moment of issue from the muzzle. [Courtesy Library of Christ Church College, Oxford] ***Right:*** In 1861, a bronze cannon was found in the south Swedish town of Loshult. Dating back to the early 14th century, it is the oldest known firearm. Note that its vaselike combustion chamber is similar to the geometry shown in the left picture. [Courtesy Statens Historiska Museum, Stockholm]

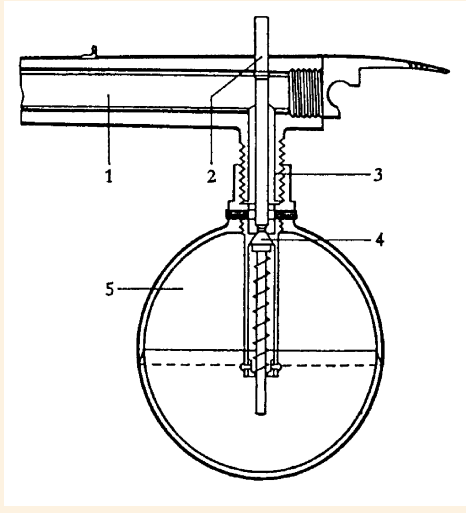

←
1 – Barrel
2 – Tappet and trigger
3 – Joint
4 – Spring-loaded cone valve
5 – Air pressure reservoir

4.2–I ***Left:*** The "blowgun" was apparently invented by Malaysians and already in pre-Columbian times imported to America and Europe. Applying the human breath to propel a projectile, it is a high-tech pneumatic tubular weapon still in use by some primitives. Veterinarians in zoos and elsewhere also use the blowgun to narcotize wild and large animals before treatment. Blowguns vary in length from 0.45 to 7 m and allow surprisingly precise aiming. The picture shows an Indian from the Amapá Territory, northern Brazil, while loading his approx. 2-m-long blowgun with a thin, pointed arrow. [Orion **12**, 423 (1957)] ***Right:*** The "wind-gun" or "air-gun," a derivative of the blowgun, was invented in Germany in the 15th century. This schematic shows the construction of a wind-gun dated A.D. 1606. Provided with an attached spherical reservoir of compressed air, it was capable of firing only a single shot, but more advanced gun constructions allowed one to fire a number of shots without recharging. Since the muzzle blast is modest compared to common firearms, it was favorably used by poachers and political assassins and, therefore, outlawed in numerous countries. Modern commercially available wind-guns reach muzzle velocities of up to 280 m/s. [H. MÜLLER: *Gewehre, Pistolen, Revolver*. Kohlhammer, Stuttgart (1979)]

4.2 PERCUSSION IN THE EVOLUTION OF TECHNOLOGY – Devices Based on Rapid Expansion *(cont'd)*

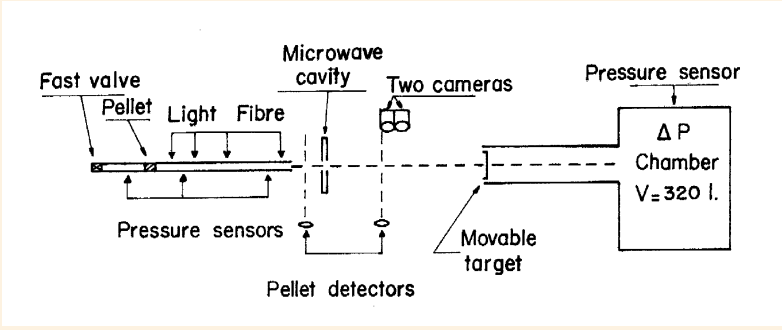

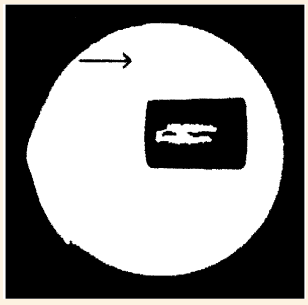

4.2–J The principle of the "pneumatic gun" is very versatile. ***Left:*** It was resumed in the 1980s in France at the Centre d'Etudes Nucléaires de Grenoble in order to accelerate deuterium pellets for possibly refueling fusion plasmas in a tokamak reactor. ***Right:*** The shadowgraph shows a 6-mm-dia. solid deuterium pellet at a velocity of 1,390 m/s that, before firing, was produced in a cryostat from deuterium gas frozen to 14 K. [Proc. 14th Symp. on Fusion Technology, Avignon, France (1986). Euratom Publ. 10936 EN, Pergamon, Oxford (1986)]

4.2 PERCUSSION IN THE EVOLUTION OF TECHNOLOGY – Devices Based on Rapid Compression

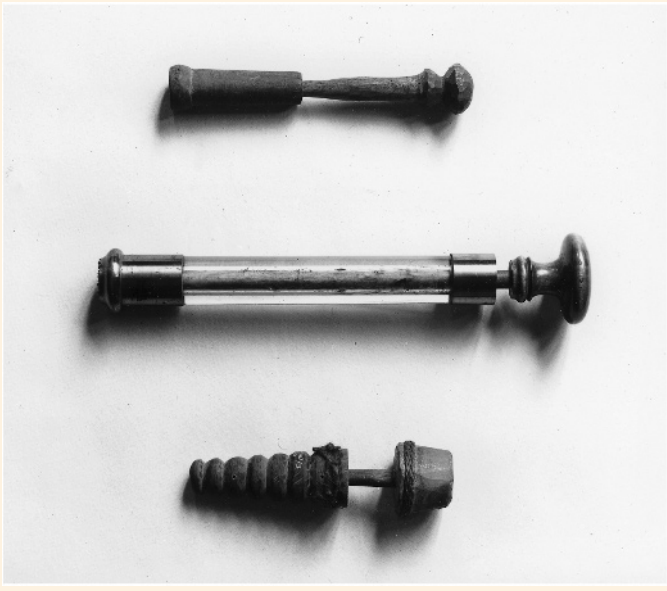

4.2–K In the 16th century, the adiabatic nature of the rapid compression of air was well known and apparently has been used for a long time in southeast Asia – from Burma to Flores and Sumatra to Mindanao – in daily life in so-called "pneumatic lighters," also known as "compression lighters" or "fire pumps." In the early 19th century, the device was reinvented almost simultaneously in England and France. The application of the device was very simple: a small piece of dry tinder was fixed on a little hook attached to the bottom of the piston, which was rapidly pushed into the cylinder. After compression the piston was immediately pulled out to provide the ignited tinder with fresh air. ***Top:*** An early pneumatic lighter from the Isle of Luzon, the Philippines. The cylinder and the piston were made from natural material such as wood and buff horn. ***Center:*** Advanced European model as used in the 19th century, consisting of a glass cylinder and a metal piston. ***Bottom:*** Pneumatic lighter from China. [Courtesy Technisches Museum, Vienna]

4.2 PERCUSSION IN THE EVOLUTION OF TECHNOLOGY – Periodically Operating Devices

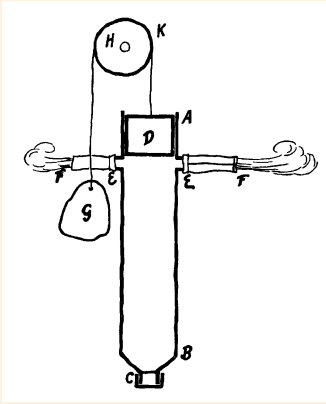

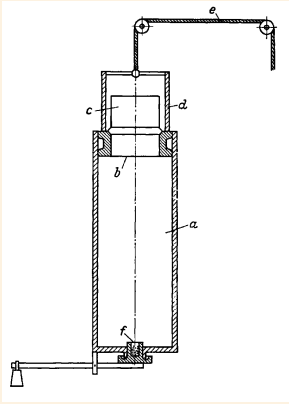

4.2–L ***Left:*** Christiaan HUYGENS' sketch of his "ballistic pump," dated September 22, 1673. Gunpowder, placed in a cylinder and ignited at the bottom, moves a piston *P* upward. The explosive products leave the cylinder at valves arranged at the top. This creates a vacuum that moves the piston down, thus creating work by atmospheric pressure such as for lifting a weight. [*Œuvres Complètes de C. HUYGENS.* Martinus Nijhoff, La Haye (1897), vol. 7: *Correspondance*, p. 357; Deutsches Museum München] ***Right:*** Denis PAPIN, a French-born English physicist, incorporated the outlet valves in the piston head and facilitated refueling by using a lever arrangement at the piston bottom. He proposed steam instead of gunpowder, thus anticipating Thomas NEWCOMEN's atmospheric steam engine. [E. GERLAND: *LEIBNIZens und HUYGENS' Briefwechsel mit PAPIN, nebst der Biographie Papin's*. Verlag der Königl. Akad. Wiss., Berlin (1881), p. 44]

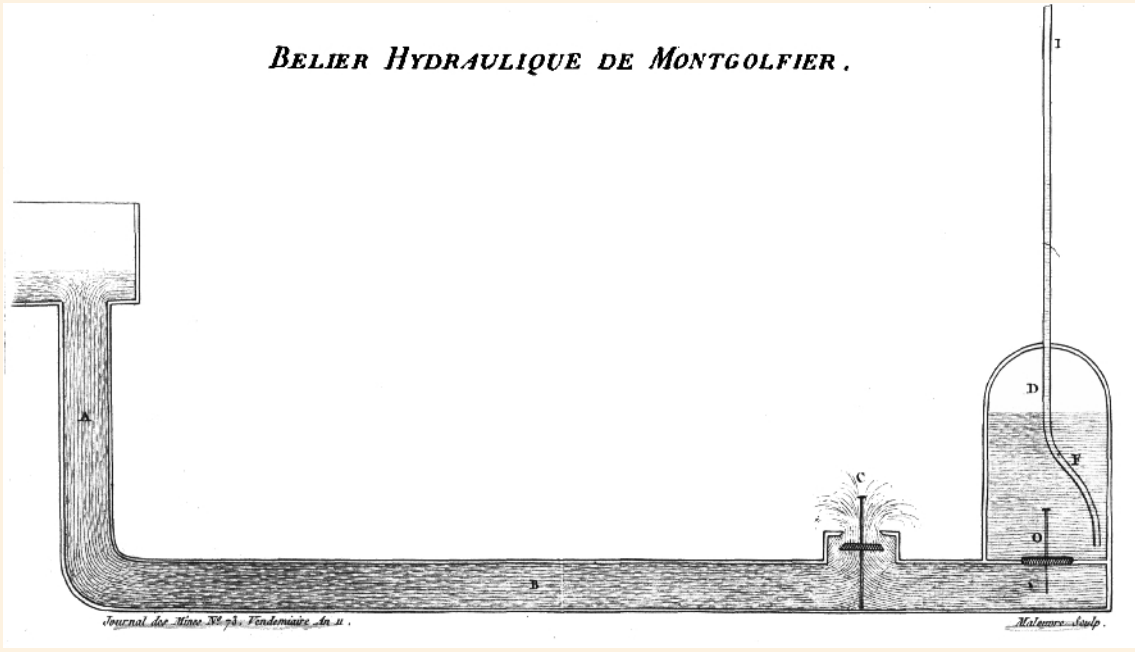

4.2–M In the late 1790s, the French manufacturer Joseph Michel MONTGOLFIER, today widely known for his hot-air balloon rides, devised the first "hydraulic ram," a simple water pump. It uses a copious flow of water to drive running water to a higher level that, emerging from an elevated water source *A* and propagating in a pipe *B*, leaves at an escape valve *C*. When *C* is suddenly closed, the resulting pressure increase forces the water through a delivery valve *O* into a chamber *D*, which compresses the air that partially fills that chamber. After valve *C* shuts, the air pressure pushes water up the vertical outlet pipe *F* to a height *I*. When the escape valve *C* drops open, the cycle begins to repeat. Because of its simplicity, the hydraulic ram is still in use today. [J. des Mines **XIII**, 42 (1802/1803)]

4.2 PERCUSSION IN THE EVOLUTION OF TECHNOLOGY – Pile Driver

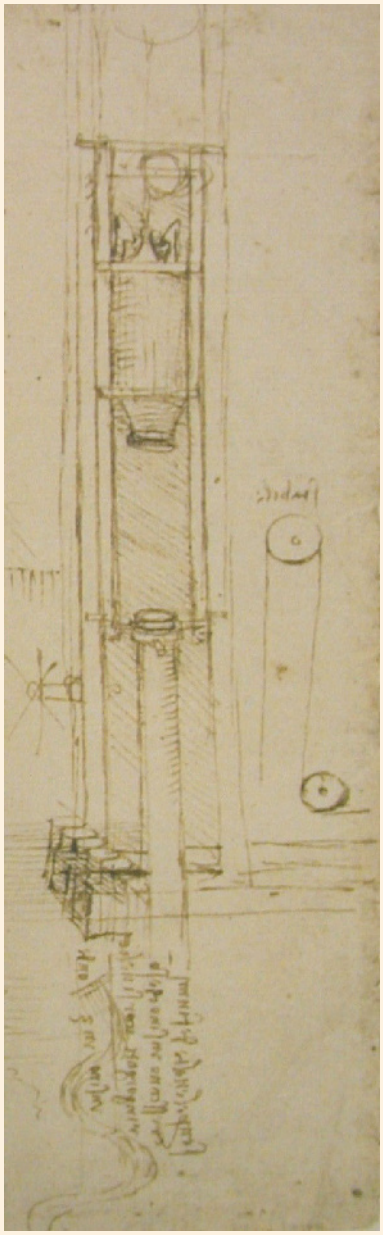

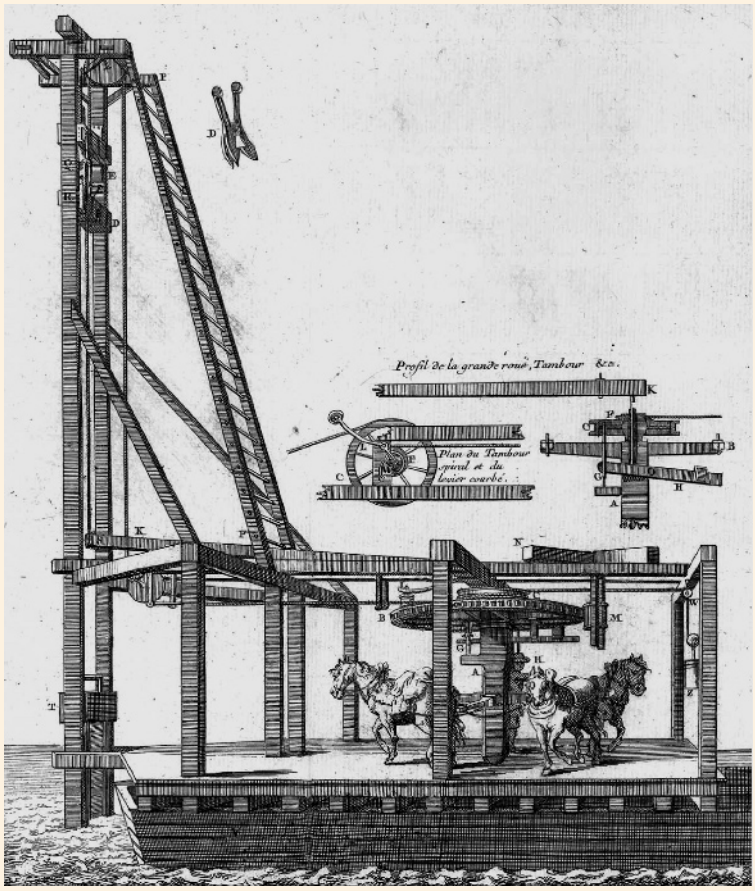

4.2–N Piles are large stakes or beams, sharpened at the end to be driven into the ground, for a foundation to build upon in marshy places. The effect of the blow is proportional to the height fallen by the hammer or ram, to the head of the pile, and the weight of the hammer or ram. ***Left:*** Pencil drawing of a so-called "pile engine" made by Leonardo DA VINCI around 1490. Such machines were then used for changing the course of the Arno River. [Il *codice atlantico di Leonardo di Vinci*. Giunti-Barbera, Florence (1975), vol. IX, p. 785] ***Right:*** In the 1750s, the most advanced machine for driving piles was based on an invention made by the watchmaker James VAULOUE: it consisted of a high frame with appliances for raising and dropping the pile hammer, a heavy weight that was lifted by horsepower. The whole engine was installed on a pontoon and used, for example, in driving piles in the foundations of Westminster Bridge in London. [J.T. DESAGULIERS: *A course of experimental philosophy*. W. Innys et al., London (1745), vol. 2, plate 26]

4.2 PERCUSSION IN THE EVOLUTION OF TECHNOLOGY – Forge Steam Ram and Explosion Ram

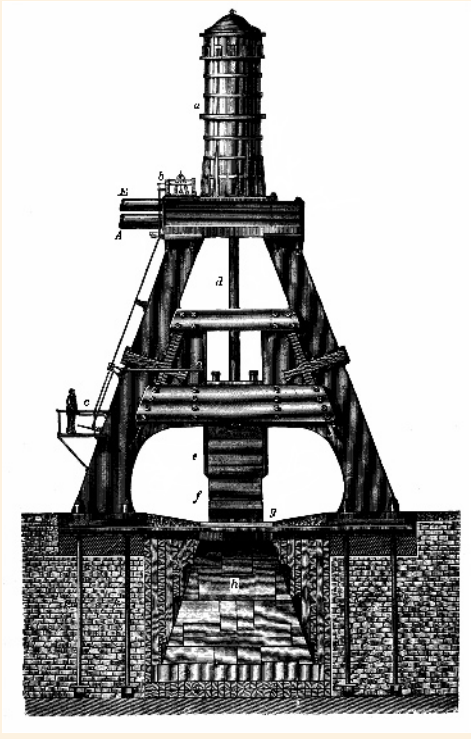

4.2–O ***Left:*** With the invention of the steam engine in the latter part of the 18th century, forces of men and horses were increasingly replaced by steam engines, and bigger pile engines could be constructed. This huge, single-action steam hammer was used for forging operations in the late 1880s at the Schneider & Co. ironworks in Le Creusot, France. The hammer weighed 80 tons and was dropped from a height of 5 m. [*Brockhaus' Konversations-Lexikon*, Brockhaus, Leipzig (1908), vol. 4, p. 666] ***Right:*** Example of a handheld explosion ram, first built in 1926 by the Deutsche Elektromaschinen- und Motoren-Bau AG (DELMAG Co.). The main parts of an explosion ram are: *a* – fuel chamber, *b* – air intake, *c* – carburetor, *d* – piston, *e* – cylinder, *f* – exhaust slot, *g* – free piston shaft, *h* – cylinder head, *i* – hand lever, *k* – main valve, *l* – spark plug, and *m* – piston spring. The machine was used mainly for paving but also for pile driving. [Z. VDI **73**, 1273 (1929)]

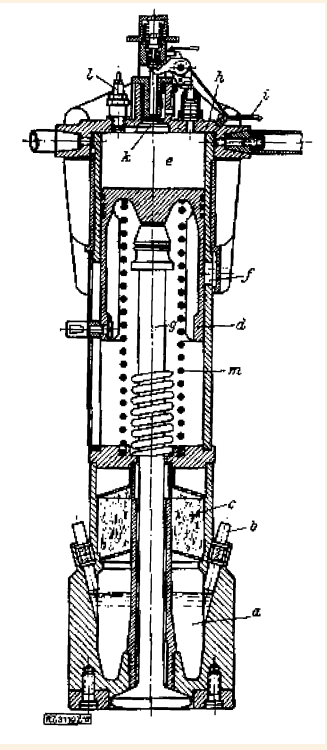

4.2 PERCUSSION IN THE EVOLUTION OF TECHNOLOGY – Explosion Tamper and Wrecking Ball

4.2–P ***Left:*** This 2.5-ton DELMAG explosion thumper, popularly known as the "frog tamper" [Germ. *Froschstampfer*] was built in 1939 for soil condensation purposes. A large explosive percussion force is generated by igniting a diesel fuel/air mixture in a cylinder that drives a piston connected with the ram. The machine was widely used in the construction of the German Autobahn. [Courtesy S.A. MEWES, DELMAG, Esslingen, Germany]

Right: View of a 2-ton wrecking ball for building demolition purposes. [Courtesy LST, Herrsching, Germany]

4.2 PERCUSSION IN THE EVOLUTION OF TECHNOLOGY – Percussion Boring

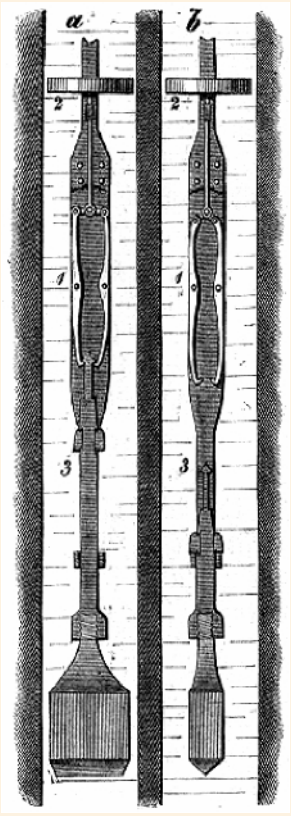

←
In early mining operations, manual percussion drilling performed by two men was the common method until the advent of pneumatic drilling machines: one man turns the drill while the second swings the hammer. The blows are applied successively, and with each blow the tool is rotated slightly so that a new portion of the face is attached at each blow. The origin of this method is unknown, but since it requires a metal chisel, it could have been invented at the earliest in the Bronze Age (in Europe ca. 2000–700 B.C.).

4.2–Q ***Left:*** In 1834, the German mining engineer Karl G. KIND invented "percussion boring," the first effective technique for drilling deep holes. It uses a gliding jar *1* that is connected to the end of the bore rod and centered in the bore hole by a disk *2*. A heavy tool *3* that is connected to the jar *1* is repeatedly dropped on the same spot from a suitable height, thereby pulverizing the rock by percussion and gradually penetrating the spot. Illustration *a* shows the apparatus in the starting position when the percussion tool *3* is lifted. Illustration *b* shows the triggered jar after provoking the dropping of tool *3*. Then the bore hole is flushed by water, which not only washes away the pulverized rock but also triggers *3* via *1* by suddenly shifting the bore rod. [E. BOBRIK (ed.): *Das neue Buch der Erfindungen, Gewerbe und Industrien. III. Die Gewinnung der Rohstoffe*. Spamer, Leipzig (1864), vol. 3] ***Right:*** This 19th-century pen-and-ink drawing illustrates the "two-men percussion drilling method" which occasionally is still in use because of its simplicity.

4.2 PERCUSSION IN THE EVOLUTION OF TECHNOLOGY – Ricocheting

4.2–R When a moving body obliquely strikes the surface of a solid or a liquid at a slight angle, it rebounds in a succession of skips. This unique phenomenon, called "ricochet" and invented in the 17th century by the French military engineer Marshal Sébastien LE PRESTRE DE VAUBAN, is a complex process of gliding and percussion that generates finite-amplitude waves in the struck body. In the 1920s, it attracted renewed interest with the advent of hydroplanes. Ricochet fire was delivered by guns, howitzers, and sometimes mortars, using small charges of powder. This particular artillery technique also allows projectiles to be skipped over the surface of the water to better ensure a hull hit. However, ricochet firing requires a perfectly smooth sea. The picture shows a "ricochet fire" of a 16-in. (40.64-cm) projectile in water. [J. Appl. Phys. **15**, 264 (1944)]

4.2 PERCUSSION IN THE EVOLUTION OF TECHNOLOGY – Big Guns of the 19th Century

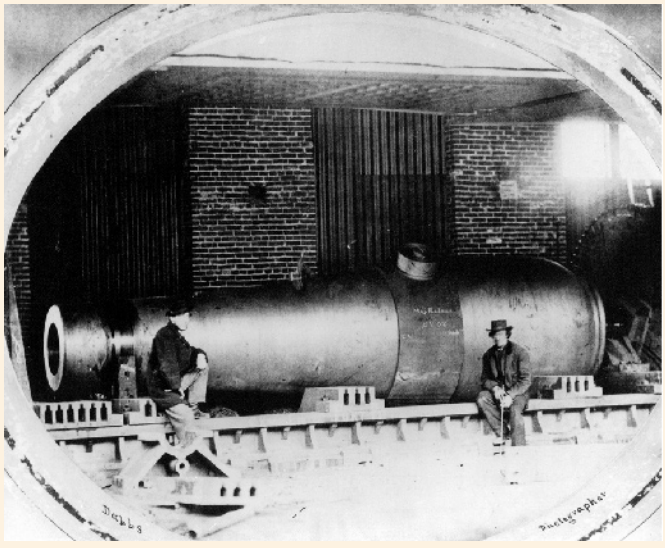

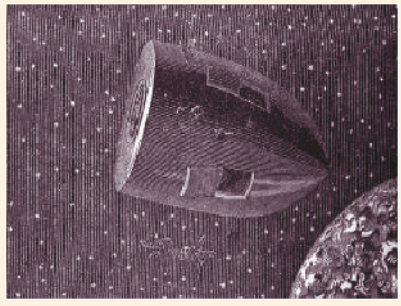

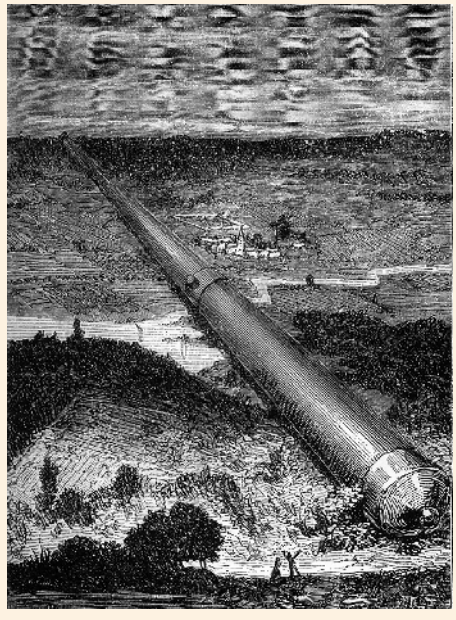

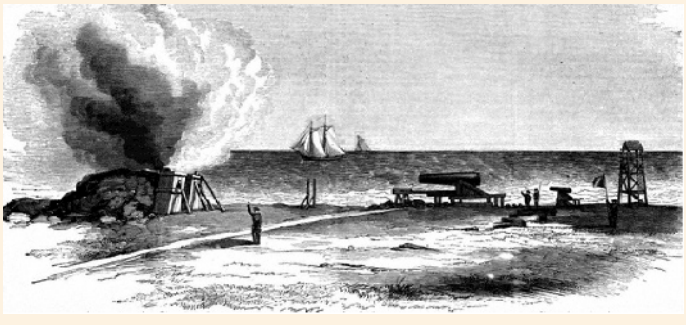

4.2–S In the 1860s, the construction and use of big guns stimulated not only classic ballistics and the invention of new propellants but also aroused the fantasy of science fiction writers. ***Left, top:*** During the American Civil War (1861–1865), Lieut. Thomas J. RODMAN of the Union Artillery initiated the production of huge smooth-bore guns using his method of hollow casting. Cooling occurred from the interior by introducing a stream of water into the core. His guns were cast by Knapp, Rudd & Co. of Pittsburgh, PA. View of a Rodman 20-in. (50.8-cm)-caliber monster gun (1864), then the world's biggest and heaviest gun weighting 80 tons. However, it did not attain military relevance, and the few pieces that were made were fired only a few times. [Collection of the Pennsylvania Dept., The Carnegie Library of Pittsburgh, PA] ***Left, bottom:*** This sketch illustrates the testing of a Rodman 15-in. (38.1-cm) caliber columbiad at Fort Monroe, VA. Slightly smaller than the monster gun shown above, this gun type was installed in large numbers for seacoast defense. Today Fort McHenry near Baltimore has the largest surviving collection of 15-in. Rodman guns. [Harper's Weekly: J. Civilizat. **5**, No. 222 (March 30, 1861)] ***Right:*** RODMAN's huge guns inspired the French science fiction writer Jules VERNE. In his novel *De la terre à la lune* (1865), he discussed the ballistic requirements of a cannon to transport a crew to the Moon. To achieve the necessary velocity to escape from Earth, the so-called "second cosmic velocity" of 11,200 m/s, his 10-ton 108-in. (2.74-m)-dia. aluminum spaceship was fired like a projectile (*top*) from a 270-m-long cast-iron cannon (*bottom*) propelled by 400,000 pounds of gun-cotton. The cannon was positioned vertically and buried in the ground. The crew of VERNE's spacecraft consisted of two Americans, one Frenchman, and two dogs. [J. VERNE: *Von der Erde zum Mond. Reise um den Mond.* Bärmeier & Nikel, Frankfurt/Main (1966)]

4.2 PERCUSSION IN THE EVOLUTION OF TECHNOLOGY – Superguns of the 20th Century

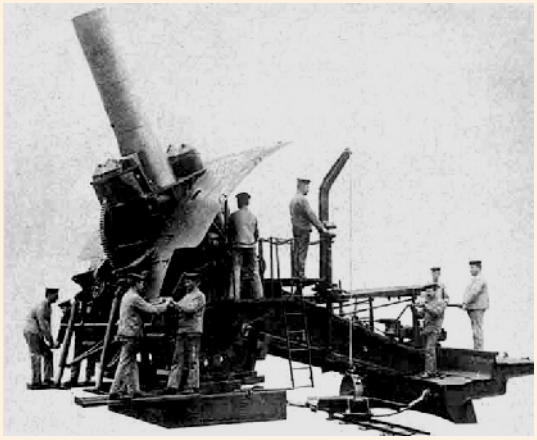

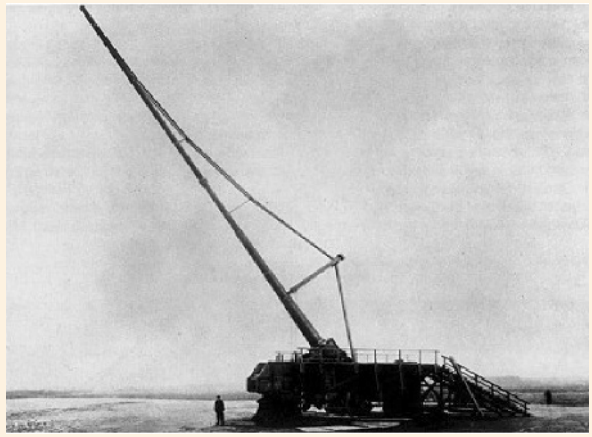

4.2–T The motivation for constructing huge-caliber guns by the German military was the experience from World War I that modern concrete-reinforced fortifications (such as those of Verdun in France) were extremely strong and could not be efficiently destroyed by standard artillery munitions. ***Top, left:*** The German Krupp works built a 42-cm howitzer that was nicknamed *Dicke Bertha* ("Big Bertha") after Mrs. Bertha KRUPP VON BOHLEN UND HALBACH. Capable of shooting a 1-ton shell over a short range (14–15 km) in a high arched trajectory, it was used during World War I against Belgian fortifications. [http://www.waffenhq.de/panzer/dickeberta.html] ***Top, right:*** Another big gun, also used in WW I, was the Krupp "Paris Gun" – officially called "Kaiser-Wilhelm-Geschütz" – a 140-ton, 21-cm caliber gun. It was capable of reaching extraordinarily long distances, up to 122 km. To hold the 33.5-m-long barrel straight, it needed a special support. Four such guns were used in the bombardment of Paris. [http://www.westfront.de/00291.htm] ***Bottom, left:*** During World War II, the German 80-cm railroad gun *Dora* was built and had a weight of 1,350 tons and a barrel length of 32 m. ***Bottom, right:*** *Dora* was capable of firing 7-ton armor piercing shells (*right*) with an initial velocity of 720 m/s ($M = 2.15$) over a distance of up to 38 km. Transportation of this supergun required 5 trains with a total of 99 cars. Being the world's largest artillery gun ever built, it was successfully used in June 1942 for destroying the strong fortifications of Sevastopol. However, further plans for building even larger and heavier guns – *e.g.*, the *Schwerer Gustav* ("Heavy Gustav"), a 80-cm gun with a barrel length of 84 m and an anticipated firing distance of at least 150 km – could only partly be realized. [http://www.waffenhq.de/panzer/dora.htm] Although remarkable high-tech products of the German war industry, all these superguns eventually proved to be faulty developments, from both a military and an economic point of view.

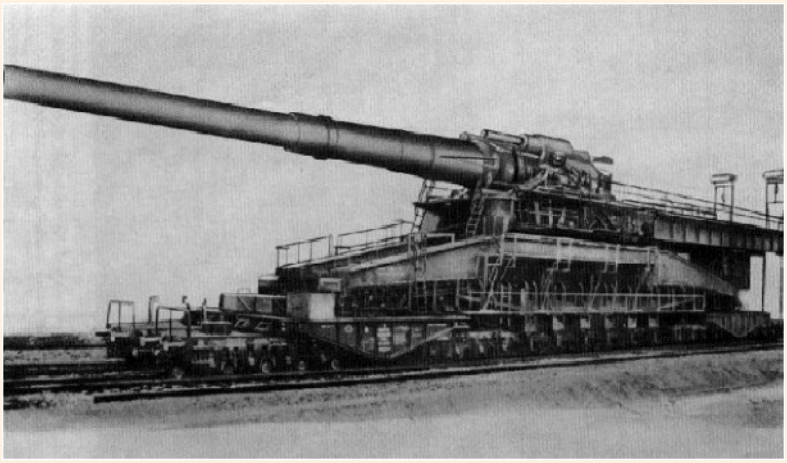

4.3 PERCUSSION STUDIES – 17th Century: The Pioneering Era of Percussion Research

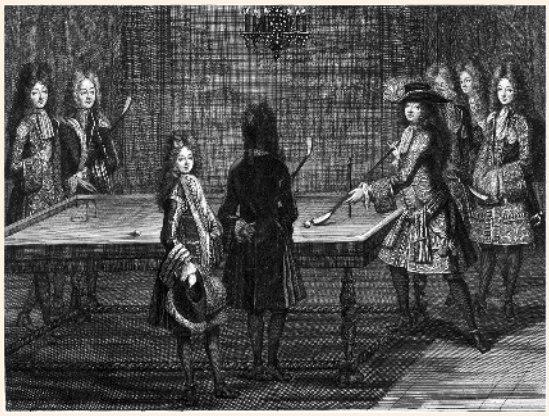

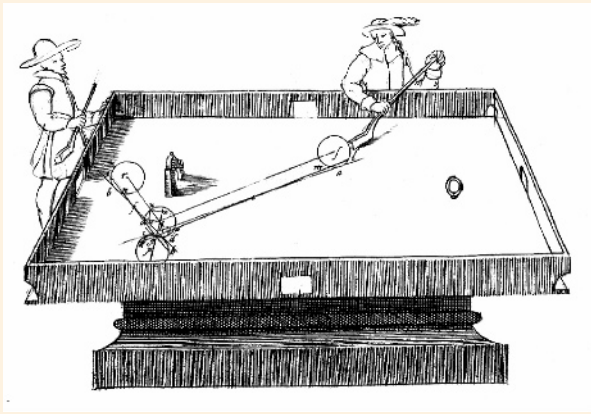

4.3–A Billiards was probably invented in Italy in the 15th century, but reliable references are rare. Well suited to study elastic collision of both centrally and eccentrically hit balls, it has since inspired physicists and mathematicians to uncover the laws of motion and collision of bodies. ***Left:*** Copper engraving by Antoine TROUVAIN (1694) showing king LOUIS XIV playing billiards in his palace at Versailles. [*Grand Larousse encyclopédique*. Larousse, Paris (1960), p. 137] ***Right:*** Marcus MARCI VON KRONLAND, a Bohemian natural philosopher, found that when a ball strikes a plane wall obliquely, the angle of incidence is equal to the angle of reflection. He applied his observation to the game of billiards and attempted to tackle the difficult "carom" problem of French billiards: three balls of equal size and elasticity – *p*, *r*, and *s* – are arranged such that their centers of gravity are not positioned along a straight line. How should the player hit *s* such that after collision with *p, p* is set in motion and hits *r*? The problem, however, was too complex to be solved with available mathematical means. MARCI tried to apply his law of optical reflection, which he derived under the assumption of a plane wall, however, overlooking that the ball's motion is a superposition of translation and rotation. [I.M. MARCI: *De proportione motus*. Typis I. Bilinae, Pragae (1639)]

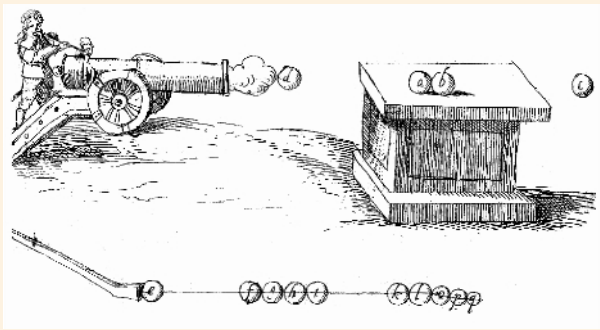

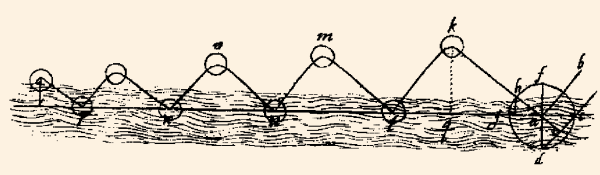

4.3–B Marcus MARCI VON KRONLAND investigated straight collision of elastic bodies and also experimented with stone cannonballs and ivory billiard balls. ***Top:*** In his treatise *De proportione motus* (Prop. XXXVII, Por. I) MARCI stated that a ball *d*, striking a row of two balls *a* and *b* at rest and each having the same mass as *d*, fully transmits its motion to the last ball *b* in the row, which, illustrated here as ball *c*, flies away with the same velocity as that with which ball *d* had initially struck the row of balls *a* and *b*. The principle of NEWTON's cradle is essentially based upon this experiment. ***Bottom:*** MARCI's illustration of a body (*e.g.*, a pebble) impinging under oblique incidence on a water surface. Being reflected along the surface, it jumps from right to left. This phenomenon, explained by MARCI using the simple law of reflection, is actually a complex combination of gliding and percussion. It attracted renewed interest in the 1930s by aeronautical engineers for optimizing the hull geometry of hydroplanes. [I.M. MARCI: *De proportione motus*. Typis I. Bilinae, Pragae (1639)]

4.3 PERCUSSION STUDIES – 17th Century: The Pioneering Era of Percussion Research *(cont'd)*

APROINO: I shall mention the first experiment that our friend essayed in order to get to the heart of this admirable problem of impact: What is sought is the means of finding and measuring its great force, and if possible simultaneously of resolving the essence of impact into its principles and prime causes… It was the Academician's first idea to try to find out what part in the effect and operation of impact belonged, for example, to the weight of a hammer, and what part belonged to the greater or lesser speed with which it was moved. He wanted if possible to find out one measure that would measure both of these, and would assign the energy of each.; and arrive at this knowledge, he imagined what seems to me to be an ingenious experiment.

He took a very sturdy rod, and about three braccia long, pivoted like the beam of a balance, and he suspended at the ends of these balance-arms two equal weights, very heavy. One of these consisted of copper containers; that is, of two buckets, one of which hung at the said extremity of the beam and was filled with water. From the handles of this bucket hung two cords, about two braccia each in length, to which was attached by its handles another like bucket, but empty; this hung plumb beneath the bucket already described as filled with water. The bottom of the upper bucket had been pierced by a hole the size of an egg or a little smaller, which hole could be opened and closed.

Our first conjecture was that when the balance rested in equilibrium, the whole apparatus having been prepared as described, and then the hole in the upper bucket was unstoppered and the water allowed to flow;, this would go swiftly down to strike in the lower bucket; and we conceived that the adjoining of this impact must add to the static moment on that side, sol that in order to restore equilibrium it would be necessary to add more weight to that of the counterpoise on the other arm. This addition would evidently restore and offset the new force of impact of the water, so that we could say that its momentum was equivalent to the weight of the ten or twelve pounds that it would have been necessary as we imagined to add to the counterweight.

SAGREDO: This scheme seems to me really ingenious, and I am eager waiting to hear how the experiment succeeded.

APROINO: The outcome was no less wonderful than it was unexpected by us. For the hole being suddenly opened, and the water commencing to run out, the balance did indeed tilt toward the side with the counterweight; but the water had hardly begun to strike against the bottom of the lower bucket when the counterweight ceased to descend, and commenced to rise with very tranquil motion, restoring itself to equilibrium while water was still flowing; and upon reaching equilibrium it balanced and came to rest without passing a hair-breadth beyond.

SALVIATI: This clever contrivance much pleases me, and it appears to me that without straying from that path, in which some ambiguity is introduced by the difficulty of measuring the amount of this falling water, we might by a not unlike experiment smooth the road to the complete understanding which we desire.

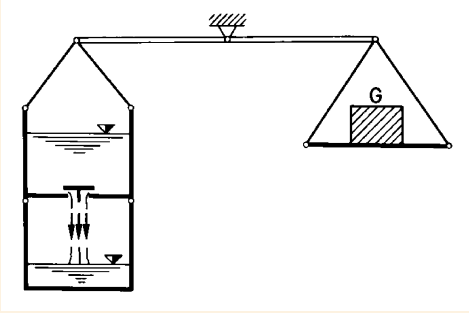

4.3–C ***Top:*** In his *Discorsi e dimostrazioni matematiche* (Leiden 1632), GALILEI pondered on an experiment on how to measure the force of percussion, the first scientific approach to a phenomenon used in stone tools and weapons throughout the evolution of man. He developed his thoughts in a platonic dialog between SALVIATI (a Copernican, representing GALILEI), SAGREDO (an educated layman), and APROINO (an intelligent Aristotelian, his oldest pupil). The experimenters expected some constant effect as long as the flow of water continued, enabling them to reestablish equilibrium by adding weight to the counterpoise. [G. GALILEI: *Two new sciences.* Univ. of Wisconsin Press, Madison, WI (1974), pp. 283-284] The copper engraving made by Stefano DELLA BELLA for the first edition of GALILEI's *Discorsi* shows (from *left* to *right*) the natural philosophers ARISTOTLE, PTOLEMAEUS, and COPERNICUS in a discussion. ***Bottom:*** Schematic of GALILEI's intellectual experiment. [I. SZABÓ: *Geschichte der mechanischen Prinzipien.* Birkhäuser, Basel (1987), p. 428]

4.3 **PERCUSSION STUDIES** – 17th century: The Pioneering Era of Percussion Research *(cont'd)*

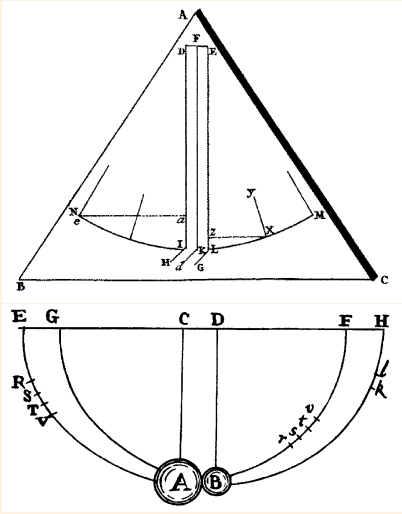

4.3–D Evolution of the percussion machine. ***Top:*** Instead of studying elastic percussion on a plane table like Marcus MARCI (1639) did in his experiments {⇨Fig. 4.3–B}, Edmé MARIOTTE (1676) used a two-sphere percussion pendulum that he applied successfully to experimentally confirm the laws of percussion previously derived by Sir Christopher WREN (1668), John WALLIS (1668), and Christiaan HUYGENS (1669). [*Œuvres de Mariotte,* The Hague (1740), Table I, Fig. 3] ***Bottom, left:*** In 1687, Sir Isaac NEWTON recognized that the ratio e of the relative velocity of two bodies just after a collision to the relative velocity just before the collision is an important quantity to characterize the elasticity in a 1-D collision. To measure the "percussion number," e, of different materials, defined by him as the ratio $(C - c)/(v - V)$, NEWTON used two spheres of two such materials and suspended them on long threads. He determined the velocities of two balls (V, C) before collision and their velocities (v, c) after collision by releasing them from a given height and measuring their heights to which each ball climbed after collision. For example, the big ball A was released at height H_A and after collision climbed to height h_A. The heights are proportional to the square of the velocities V and C, and v and c, before and after collision, respectively. He found that his "percussion number" ranged between 0 for fully inelastic collision and 1 for perfectly elastic collision. [I. NEWTON: *Principia.* S. Pepys, Londini (1687); Corollary VI, p. 22]

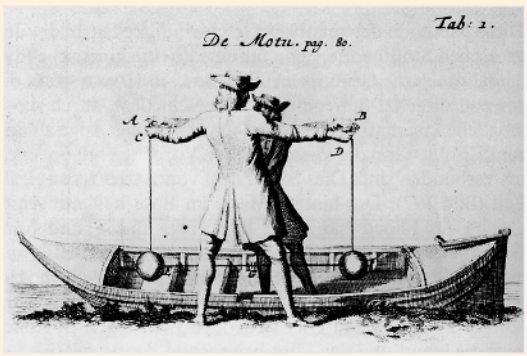

4.3–E Christiaan HUYGENS first pondered the relativity of percussion phenomena in his famous thought experiment. He stated in his first tenet that two equal elastic bodies, impacting with equal velocities, rebound from each other with exactly the same (but opposite) velocities. When this happens in a boat moving with velocity v, he showed that for a spectator in the boat the balls approach with velocities $+v$ and $-v$ and rebound with $-v$ and $+v$. But for a spectator on the shore the velocities of the balls before impact are $2v$ and 0 and after impact 0 and $2v$, respectively. Thus, an elastic body, impinging on another of equal mass at rest, communicates to the latter its entire velocity and remains after the impact itself at rest. [C. HUYGENS: *De motu corporum ex percussione.* Lugduni Batavorum, Leiden (1703)]

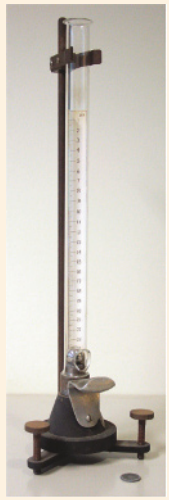

4.3–F NEWTON's percussion number e can be found easily by dropping a small ball on the horizontal surface of a large mass and by comparing the height h to which the ball bounces with the height H from which it is dropped, hence $e = (h/H)^{½}$. In 1879, William THOMSON and Peter G. TAIT called this ratio e the "coefficient of restitution." View of an apparatus for measuring e as used at the University of California at San Diego. [Courtesy Physics Dept., UC San Diego, CA]

4.3 **PERCUSSION STUDIES** – 18th Century: Percussion Machine for Demonstrating Central Percussion

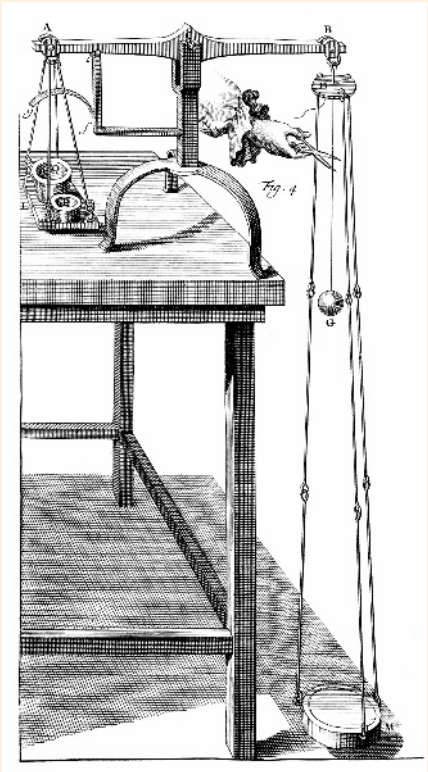

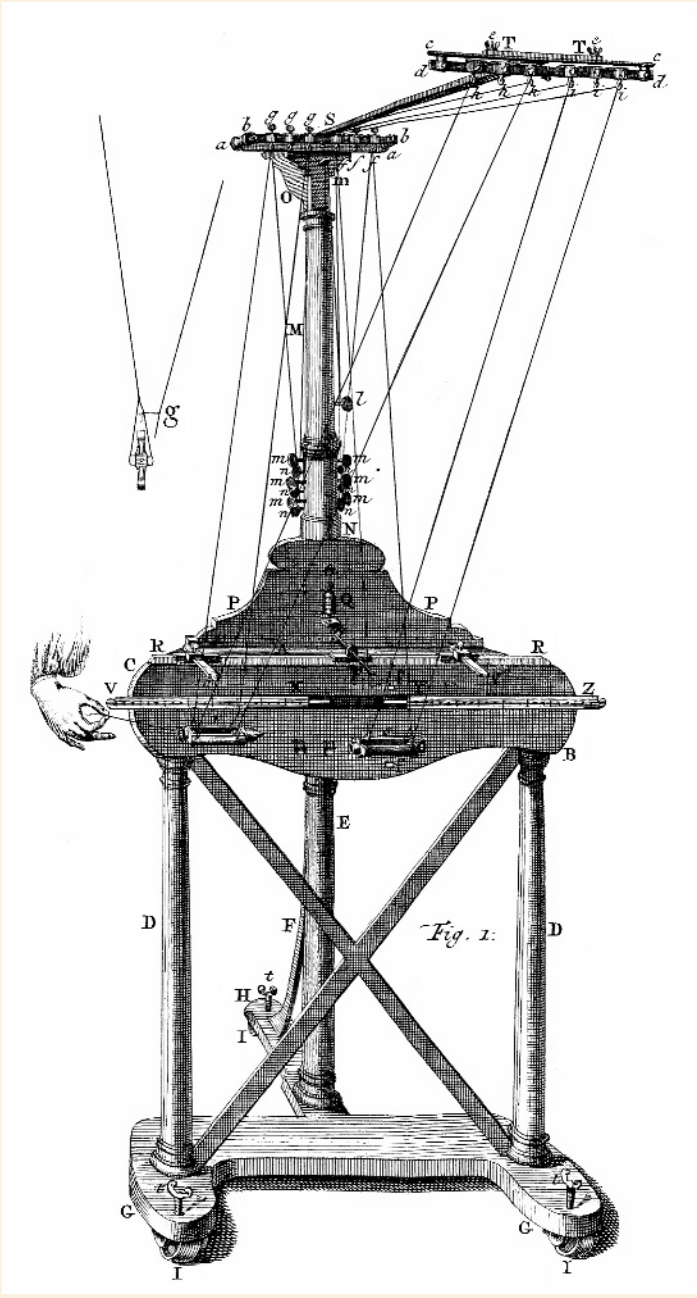

4.3–G The Dutch natural philosopher Willem Jacob's GRAVESANDE constructed throughout his teaching period at the University of Leiden many unique physical apparatus for demonstration purposes. ***Left:*** For example, he modified GALILEI's thought experiment {⇨Fig. 4.3–C} by using a ball pendulum instead of a water jet. The experiment was started by cutting the thread with scissors. ***Right:*** In the early 1720s, GRAVESANDE constructed a percussion machine for quantitatively studying the laws of elastic and inelastic percussion. Note the bifilar suspension of his test bodies, which could be provided at their heads with different materials for studying their elastic properties. It was also possible to mount leaf springs on the heads to simulate a linear chain of mass/spring oscillators. [W.J.'s GRAVESANDE: *Physices elementa mathematica, experimentis confirmata.*. Langerak & Verbeeck, Leiden (1742), plates 27 & 35]

4.3 **PERCUSSION STUDIES** – 18th Century: Percussion Machine for Demonstrating Oblique Percussion

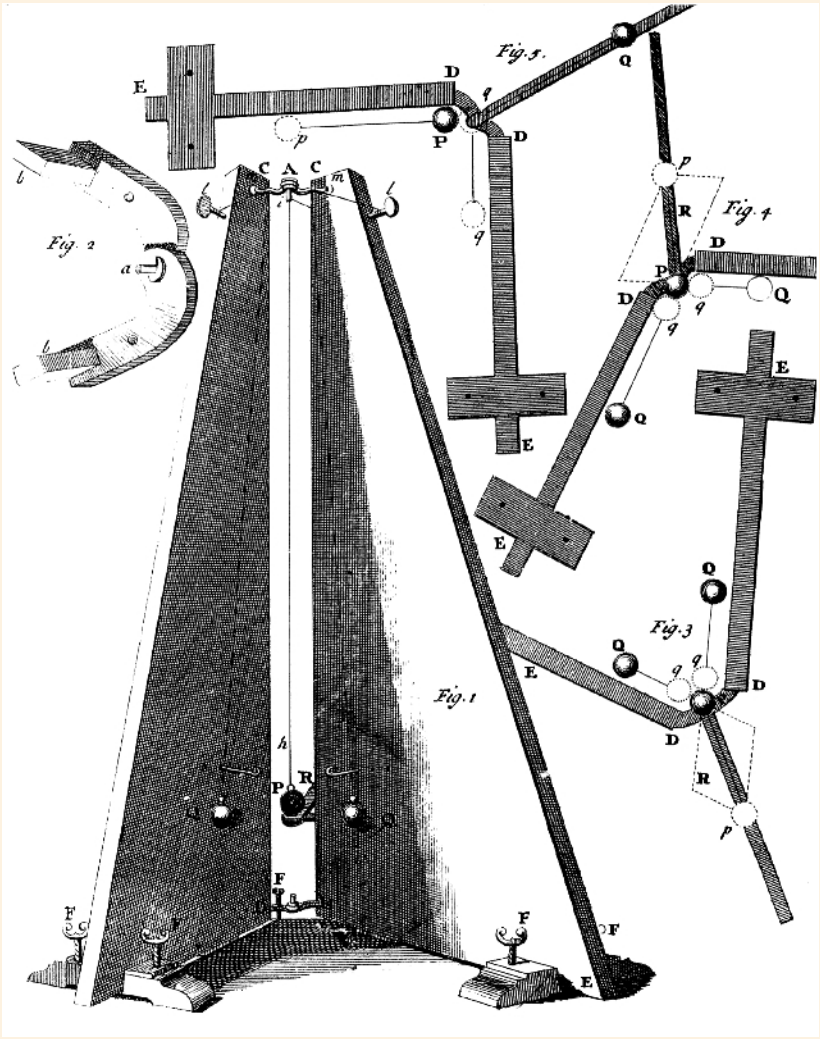

←←← ***Fig. 2:*** "In the Center of the upper Hinge there is a small Cylinder *a*, in whose Case there is a Hole, which meets another in the Side, thro' which the Thread *i h* is to run; at one End of this Thread a Ball, as *P* hangs, and the other End is join'd to the Key *l*. At *m*, *m*, there are two Pins fix'd to the two Planes, from which Pins the Balls *Q*, *Q*, hang, at such a Distance from the Planes, that they may almost touch them; so that if you suppose a Line to pass thro' the Centers of the Balls *P* and *Q*, it shall be parallel to the Plane on that Side: besides, it is required, that, when those Balls hang at the same Height, they touch one another."

←← ***Fig. 5:*** "Let the Ball *Q* and *P* hang; having set the Planes at Right Angles let the Body *Q* with any Direction, and from any Height, come down upon *P*, and strike against it: after the Stroke the Bodies will follow the Directions of the Planes, and rise to Heights, which may be determined by what has been said hitherto."

← ***Figs. 3 and 4:*** "The Body *P* may be driven by either of the Bodies *Q*, with any Direction and Velocity. If the Bodies *Q* and *Q* are let fall at the same time, the Body *P* has two Motions impress'd upon it at the same time, and therefore runs in the Diagonal *Pp* of the Parallelogram, to express those two Motions, and runs up to an Height proportionable to the Length of that Diagonal."

4.3–H In order to quantitatively study oblique percussion phenomena as well, GRAVESANDE constructed a unique machine that he described as follows: "It consists of two Boards, or wooden Planes, *CDE*, *CDE* of the Figure of a right-angled Triangle, whose Side *CD* is in Length about 3 Foot and a half, and the Side *DE* about 1 Foot and a half; these Boards are fixed so as to move in a vertical Situation about the Hinges *A* and *B*. The Experiments upon this Machine are made with Ivory Balls of an Inch and a half Diameter [38.1 mm] … By Help of the Screws *F*, *F*, *F*, *F*, *F*, his Machine is set perpendicular; so as to have the Thread *h i* hang in the Axis of the Machine … Each Ball *Q*, when it swings, moves along the Plane to which it is applied; and the Height, from which it is made to fall, is shewn by an Index fixed to the Plane." [W.J.'s GRAVESANDE: *Mathematical elements of natural philosophy confirmed by experiments, or, an introduction to Sir Isaac NEWTON's philosophy* (Engl. translation by J.T. DESAGULIERS). Senex & Taylor, London (1726), Book I, plate 12]

4.3 **PERCUSSION STUDIES** – 18th Century: First Ballistic Pendulum

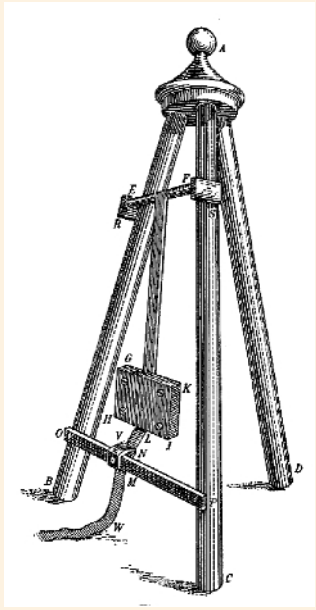

4.3–I In the period 1746–1791, the Englishmen Benjamin ROBINS and Charles HUTTON performed ballistic drag studies that covered velocities up to 2,030 ft/s (626 m/s; $M = 1.85$). ***Top:*** Schematic of ROBINS' so-called "ballistic pendulum," developed by him while at the Royal Military Academy in Woolwich. It essentially consisted of an iron plate, *G–K–H–I,* faced with wood to catch and retain the bullet. The deflection was determined by a thin metal tape *W*, connected at the outer end of the pendulum, *H–I*, and passed through two steel edges, *V–N*, which were pressed lightly together. He derived a formula to estimate the muzzle velocity from the pendulum's swing angle and the mass of the projectile. The device was used by him to measure the muzzle velocity of small shot, like the ball of a musket. By moving the instrument at progressively greater distances from the muzzle, he also studied how aerodynamic drag reduces the velocity of projectiles. [B. ROBINS: *New principles of gunnery*. Nourse, London (1742)] ***Bottom:*** In the 1780s, ROBINS' pendulum was further developed by HUTTON for use of large shot, the so-called "gun pendulum." At Woolwich he combined two similar methods of measuring the velocity of a cannonball: the schematic on the *left* shows a side view of his ballistic pendulum into which the balls were fired. Compared to ROBINS' pendulum, it was reinforced by thick bars of iron. The schematic on the *right* shows a second pendulum for observing the arch of recoil of the gun that was attached to the pendulum. From the deflection angle, measured by this unusual pendulum construction, he could also determine the initial velocity of the cannonball, thus allowing a comparison of both methods. [C. HUTTON: *Tracts on mathematical and philosophical subjects*. T. Davison, London (1812), vol. II, plate VI] Later a pendulum with a 5-ton cannon of 13-in. (33-cm) caliber was installed at Woolwich Arsenal that was described by Fritz HEISE in his book *Sprengstoffe und Zündung der Sprengschüsse, mit besonderer Berücksichtigung der Schlagwetter- und Kohlenstaubgefahr* (Springer, Berlin 1904). [C. HUTTON: *Tracts on mathematical and philosophical subjects*. T. Davison, London (1812), vol. II, plate VI]

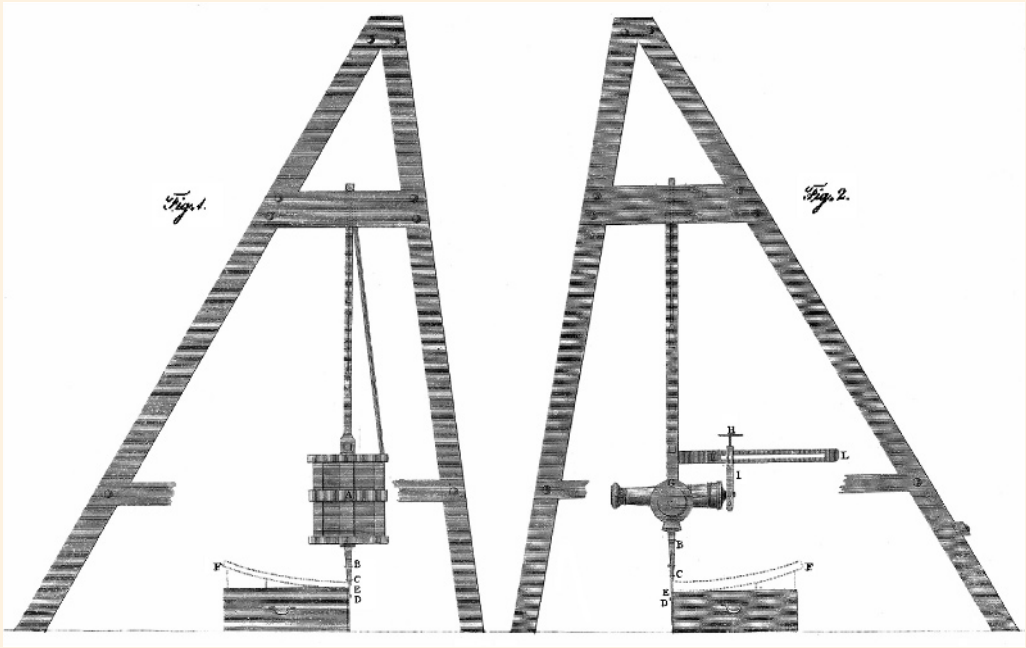

4.3 **PERCUSSION STUDIES** – 19th Century: Measurement of Shock Duration

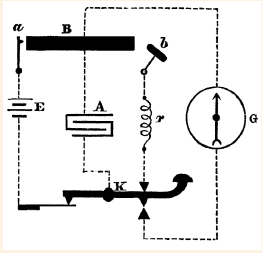

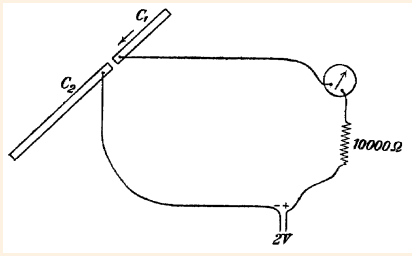

4.3–J In 1844, Claude S.M. POUILLET in France worked out an electric method for measuring the contact time of impacting bodies that was later improved by Robert SABINE in England and Carl W. RAMSAUER in Germany. ***Top, left:*** SABINE's electric apparatus, also known as the "ballistic galvanometer," was capable of measuring contact times of impacting bodies in the microsecond regime. A charged capacitor *A* was partly discharged when the impactor *b* hit an anvil *B*. The contact time was analytically determined from galvanometer readings *G* before and after impact and from the circuit parameters. [Phil. Mag. **1** (V), 337 (1876)] ***Top, right:*** RAMSAUER, improving SABINE's method, succeeded in resolving contact times as small as 1 µs. In contrast to SABINE's circuit, however, it used a battery instead of a charged capacitor. During the contact time of the two impacting rods C_1 and C_2, a certain quantity of electric charge provokes a certain deflection of a galvanometer that is proportional to the contact time and can be calibrated, for example, using the Helmholtz pendulum interrupter. [Ann. Phys. **30** (IV), 417 (1909)] ***Bottom, left:*** Peter G. TAIT, a Scottish physics professor, constructed an apparatus for measuring the duration of percussion phenomena that he humorously called "my guillotine." It used a free-falling bloc A that, sliding between vertical guide rails, collided with a test sample *B* at rest. The temporal movement and rebound of *A* was recorded on a soot-covered revolving disk *D* via a needle *E* that was connected with *A*. The contact time was evaluated by simultaneously recording the oscillations of a tuning fork *F* bearing a needle *G* writing on the soot disk *D*. ***Bottom, right:*** Percussion diagram of recorded soot traces taken with TAIT's apparatus and showing the time-resolved behavior of percussion and rebound of two elastic bodies, *A* and *B*. [Rev. Gén. Sci. Pures Appl. **3**, 777 (1892)]

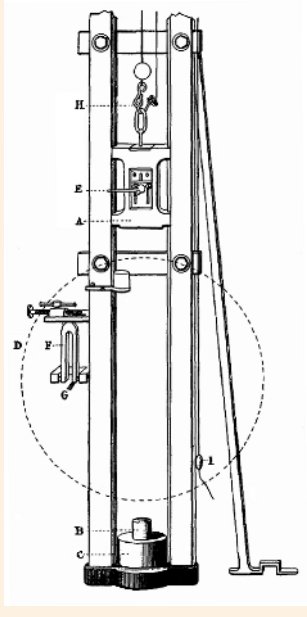

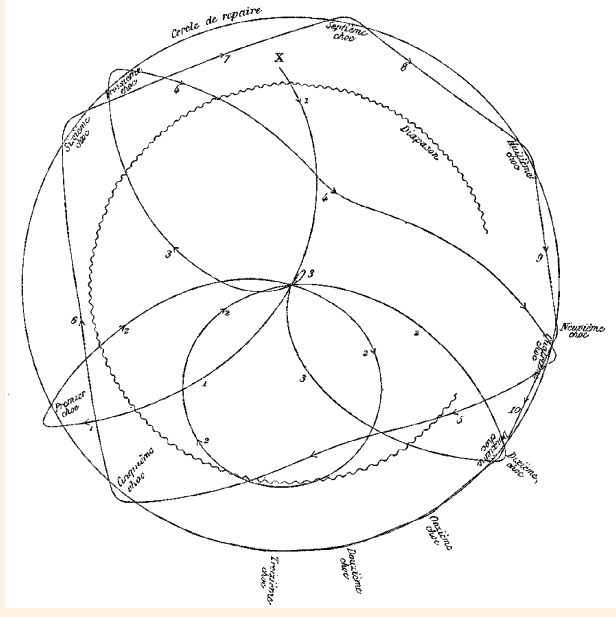

4.3 **PERCUSSION STUDIES** – 19th Century: DE CORIOLIS' Mathematical Studies on Billiards

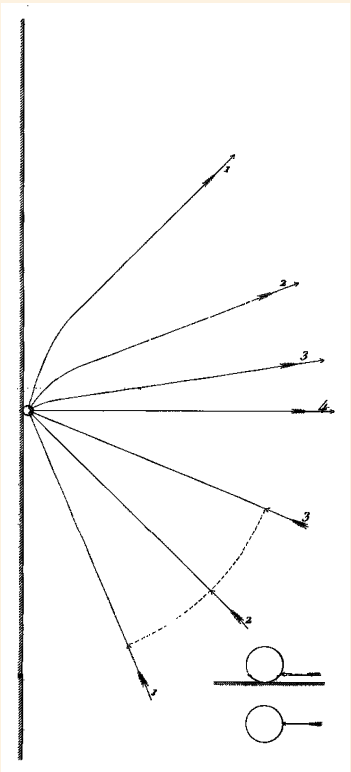

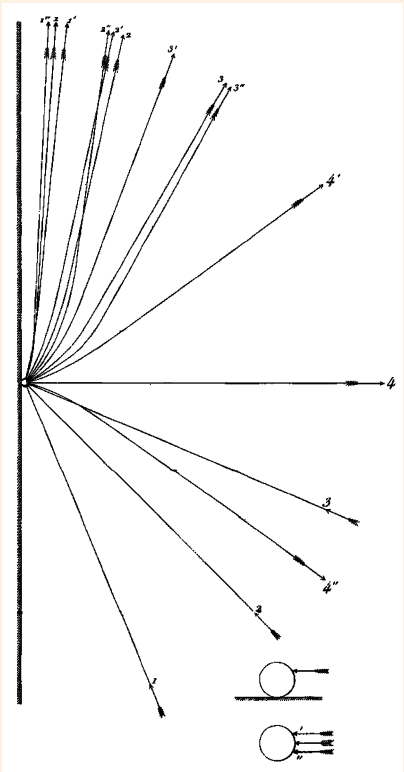

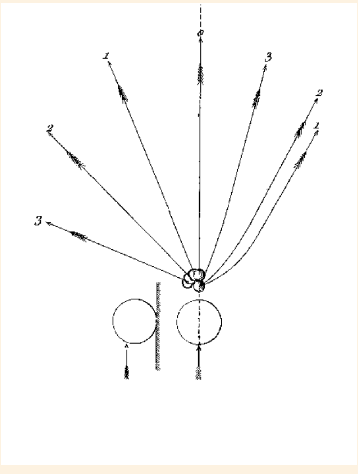

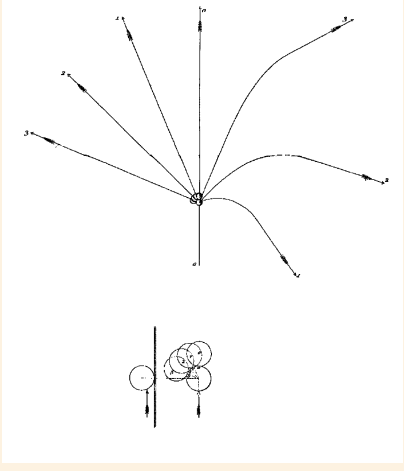

4.3–K In the early 1830s, Gaspard G. DE CORIOLIS, a French mathematics and mechanics professor at the Ecole Centrale des Arts et Manufactures in Paris, first analyzed the trajectories of billiard balls with eccentric twists considering friction between ball and cloth. ***Top:*** Deflection of cue ball at cushion. When a ball is hit below (*left*) or above (*right*) its center of gravity, the induced spin and its direction influence the ball trajectory after deflection, which results in a convex (*left*) or concave (*right*) curve, respectively. This phenomenon also depends on the angle of incidence. Obviously, the simple optical Law of Reflection that the angle of incidence equals the angle of reflection as assumed by Marcus MARCI in 1639 is no longer valid. When playing to the "side" [French *effet*] as illustrated in the right picture at bottom, which provides the ball with an additional spin around its vertical axis, the ball's trajectory after deflection can be influenced to some extent. ***Bottom:*** Collision of cue ball with an object ball. He also studied the difficult problem of when a ball, being hit above (*left*) or below (*right*) its center of gravity, strikes a second, resting ball centrally or eccentrically – a difficult task that MARCI in 1639 had tried to solve in vain. When the second ball is hit centrally (case *0–0*), it moves along a straight line in the direction of the first, striking ball. However, when the first, striking ball hits the cue ball above (*left*) or below (*right*) its center of gravity, it collides eccentrically with the second, resting ball, and the striking ball moves after collision along concave (*left*) or convex (*right*) trajectories, respectively. Note that, after collision, in both cases the trajectories of the first, striking, ball are curved (right family of curves *1*, *2*, *3*) while the trajectories of the second, struck, ball are always straight lines (left family of curves *1*, *2*, *3*), which are inclined in the direction of the striking ball. [G. CORIOLIS: *Théorie mathématique des effets du jeu de billard*. Carilian-Goeury, Paris (1835)]

4.3 **PERCUSSION STUDIES** – Oldest Known Seismoscope and 19th-Century Seismography

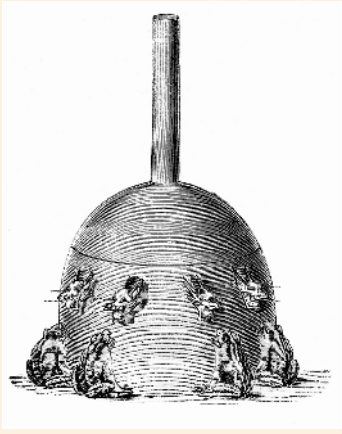

4.3–L Early seismoscopes were primitive but ingenious mechanical instruments supposed to record the direction and strength of seismic shocks. ***Top:*** The oldest known seismoscope was invented in China in A.D. 136. On the outside there are eight dragon heads, each of which contained a ball. Underneath these heads were eight frogs positioned in such a way that they were ready to receive the ball if it were shaken out of place by an earthquake, thus recording the direction of the seismic shock. [Nature **26**, 627 (1882)] ***Bottom:*** To record the strength and direction of seismic shocks, Gaetano CACCIATORE improved the mercury seismometer that Jean DE HAUTE FEUILLE had invented in 1703. CACCIATORE's mercury-horizontal seismometer consisted of a shallow, circular 10-in. (25.4-cm)-dia. bowl. In level height, its side wall was bored through eight equidistant holes. The bowl was surrounded by an annular bulge containing eight channels, corresponding to the eight holes and leading to eight small cups. The instrument had to be installed on a level pedestal in an area free of human-induced vibrations. After careful alignment of the eight holes with the four cardinal points, the bowl was filled up with mercury. Used by CACCIATORE in Palermo during the severe earthquake in 1823, he was able to prove that the seismic shocks came from the direction of the volcano Mount Etna. [Ann. Phys. Chem. **24** (II), 62 (1832)]

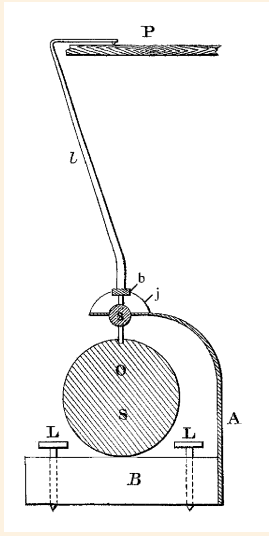

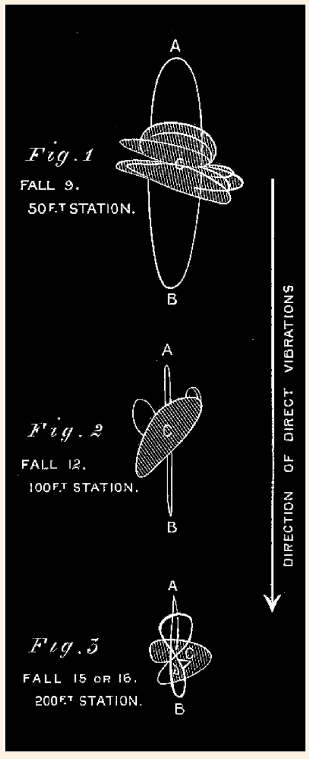

4.3–M The Englishmen John MILNE and Thomas GRAY, working as visiting professors in the 1880s at the Imperial College in Tokyo, investigated the dynamics of earthquakes. They constructed new seismographs to study the motions of the ground originating from natural and artificial earthquakes. ***Left:*** To better observe earthquakes in Japan, GRAY constructed a "rolling-sphere seismograph" that writes the Earth's vibrations directly upon a smoked glass plate by means of a pointer. Later installed at a number of different stations, it was the first seismograph to allow a clear distinction between normal and transverse vibrations, together with the maximum amplitudes of each of these two distinct movements. [Phil. Mag. **12** (V), 199 (1881)] ***Right:*** Examples of three records taken with GRAY's seismograph; each shows the motion of the ground magnified 85 times. These figures are arranged such that their greatest lengths are parallel, and the direction of greatest motion is that of a line joining the instrument and the point where the ball fell. At the commencement of a seismic shock, the needle at the pointer rested at or very near the center of curve *C*. The deflections occurred first in directions $A \rightarrow C \rightarrow B \rightarrow C$, but suddenly, when the shear waves arrived, the deflections occurred at nearly right angles to the first motion. [Phil. Trans. Roy. Soc. Lond. **173**, 863 (1883)]

4.3 **PERCUSSION STUDIES** – 19th-Century Seismography *(cont'd)*

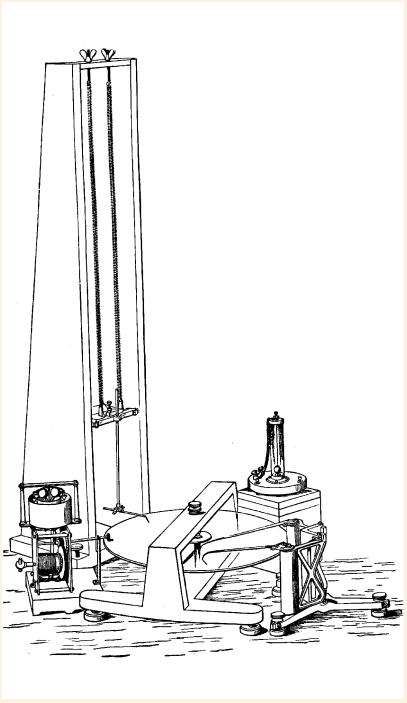

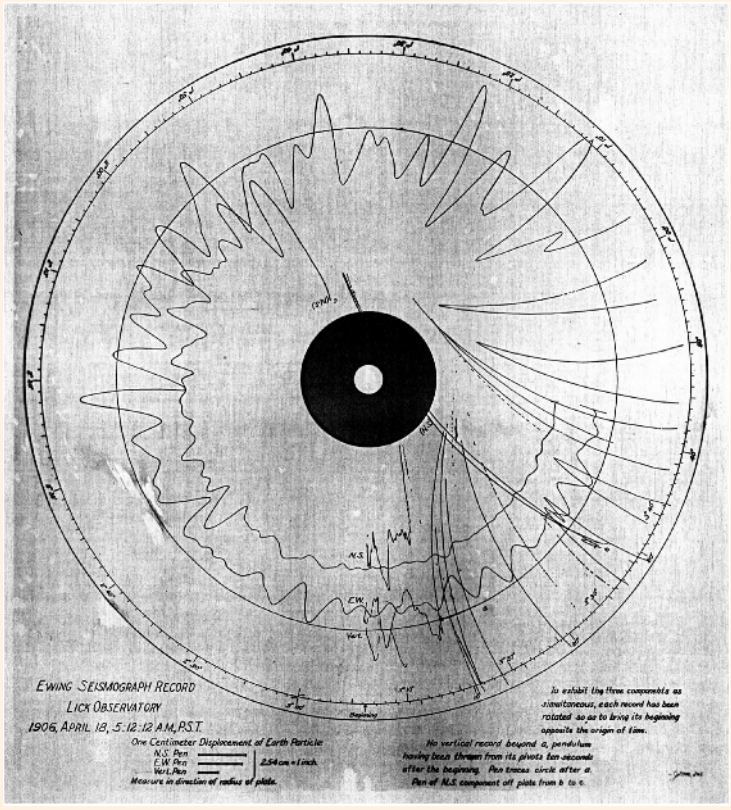

4.3–M *(cont'd)* ***Top, left:*** The first seismograph in the United States was constructed by the Scottish engineering and physics professor Sir James A. EWING and installed in 1897 at the Lick Observatory on Mount Hamilton, about 50 miles southeast of San Francisco, CA. This three-component instrument for recording motions in all directions, provided with clock and driving plate, faithfully recorded earthquake disturbances throughout the period 1887–1926. The clock was set in motion by means of a Palmieri seismograph, a small common pendulum that appears on the right in the figure behind the plate. This occurred during the preliminary tremors usually found in advance of the main movements of an earthquake. ***Top, right:*** Reproduction of the EWING seismograph record from Lick Observatory taken in the morning of April 18, 1906 at 5:12 A.M. P.S.T., when San Francisco and a wide area around the city were hit by a heavy earthquake. Ten seconds after the beginning of a series of violent shocks, the pendulum was thrown from its pivots. ***Bottom:*** Picture of Lick Observatory taken in November 1881. [Courtesy Mary Lea Shane Archives of the Lick Observatory, University of California, Santa Cruz]

4.3 **PERCUSSION STUDIES** – 19th Century: Percussion Figures

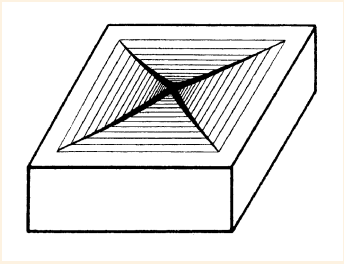

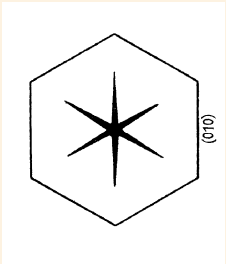

4.3–N When a crystal is hit by a pointed instrument normal to its surface, a starlike fracture pattern is produced. This so-called "percussion figure," first discovered by the German physicist Friedrich E. REUSCH (1867), is characterized by radiating lines from the point of impact that are parallel to the plane of symmetry of the crystal. For example, when a rock salt crystal is struck by a sharp blow, a four-rayed star (*left*) is formed, while a cleavage flake of mica typically shows a six-rayed star (*right*). [P. NIGGLI: *Lehrbuch der Mineralogie*. Gebr. Borntraeger, Berlin (1920), vol. I, p. 268]

4.3 **PERCUSSION STUDIES** – 20th Century: Measurement of Deformation and Force

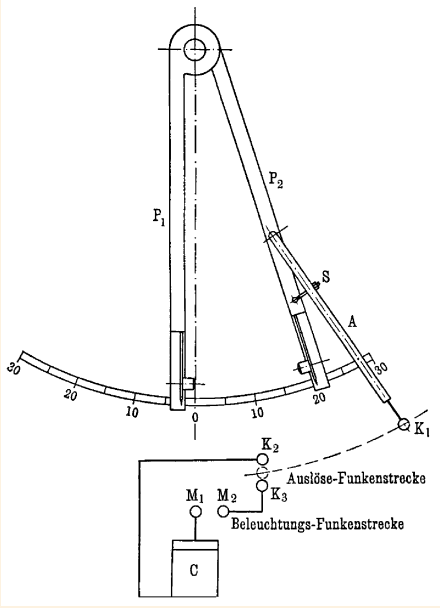

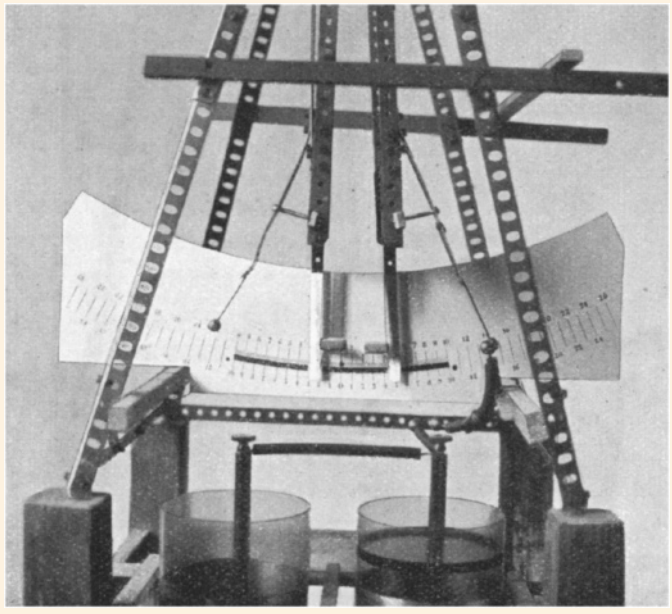

4.3–O In the early 1920s, Franz BERGER, an Austrian engineer at Vienna University, first recorded force-time profiles of colliding bodies using two different percussion apparatus: one for a stepwise recording as shown here, and a second, more advanced, one for a complete recording of the force-displacement curve. ***Left:*** Schematic of his setup. Using a twin pendulum P_1–P_2, each pendulum carries at its lower end a test cylinder, both of which collide with each other head-on. To measure the force of percussion, BERGER inserted a leaf spring between the test body and the pendulum end. The momentary displacement of the leaf spring was illuminated by a triggered spark light source M_1–M_2 and photographed using a still camera. The time delay of the flash could be adjusted at the screw S of the contact arm A that, triggering the spark gap K_2–K_3 via ball K_1, allowed one to observe different time instants within the percussion cycle. From these displacement-time data BERGER calculated the force-time profile and determined how the maximum percussion force depends on the impact velocity. ***Right:*** Photo of BERGER's percussion apparatus. [F. BERGER: *Das Gesetz des Kraftverlaufs beim Stoß*. Vieweg, Braunschweig (1924)]

4.3 **PERCUSSION STUDIES** – 20th Century: Measurement of Deformation and Force *(cont'd)*

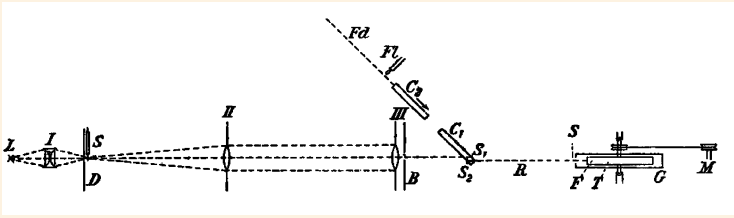

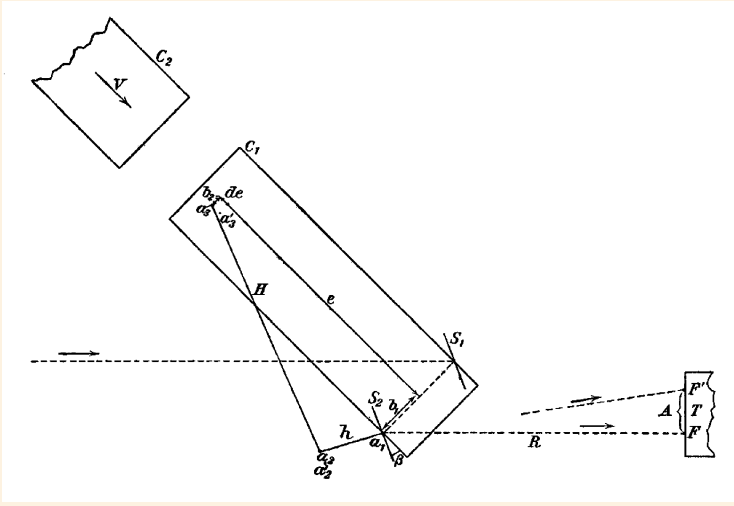

4.3–O *(cont'd)* The German physicist Carl W. RAMSAUER calculated the longitudinal elastic percussion of cylindrical bodies. He compared his results with measured data of deformation and velocities during and after percussion, and data of shock contact times. ***Top:*** He used an optical method to resolve the small deformations during and after percussion of two cylindrical test bodies C_1 and C_2, with C_1 initially being at rest and C_2 moving with velocity V. C_1 is provided with a pair of small mirrors S_1–S_2. ***Center:*** While mirror S_1 is fixed to C_2, mirror S_2 is mounted on a lever arm h and can rotate around axle a_2; S_2 is also connected with the front part of the impacted rod C_1 via a lever arm H. This provides an enlargement of the rather small deflections recorded on a film strip F mounted on a rapidly revolving drum T. His mechanical method allowed the recording of local compressions and dilatations along rod C_1. ***Bottom:*** Examples of recorded impact-induced wave profiles, shown here for five different materials, I–V, which allowed the calculation of percussion velocities after impact. In the ideal case of elastic collision that is almost realizable using helical steel springs, RAMSAUER found good agreement with Adhémar DE SAINT-VENANT's percussion theory. [Ann. Phys. **30** (IV), 417 (1909)]

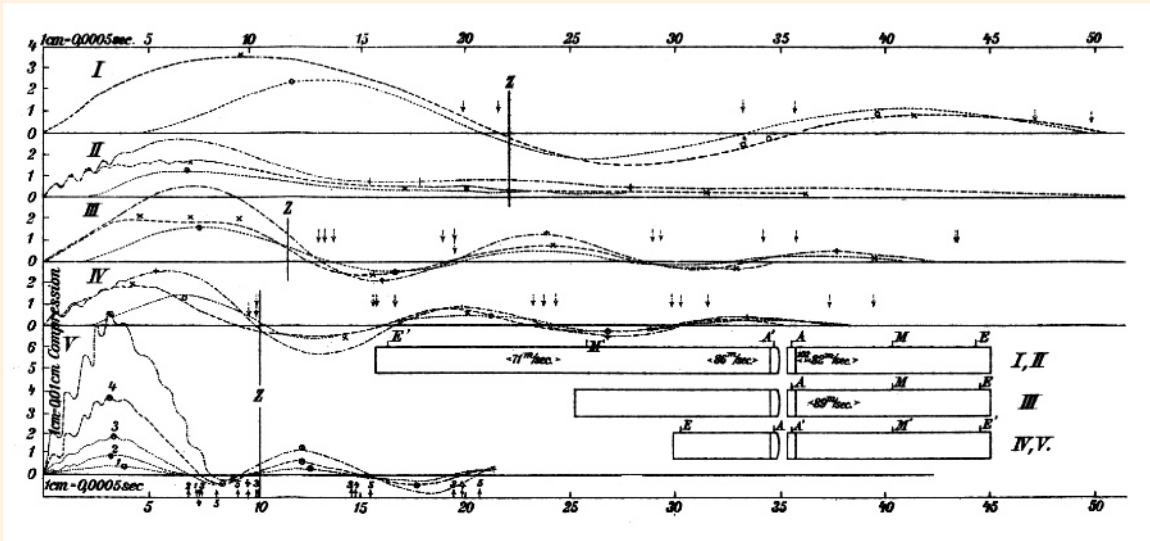

4.3 **PERCUSSION STUDIES** – 20th Century: Pressure-Bar Devices

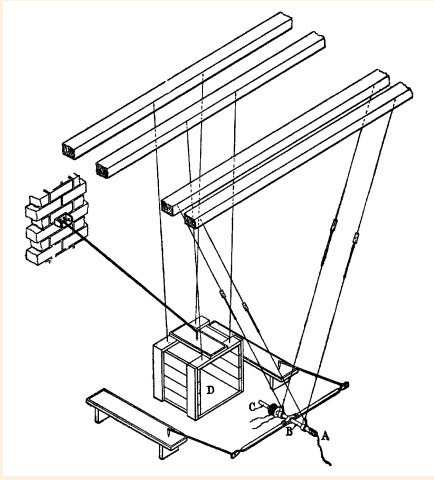

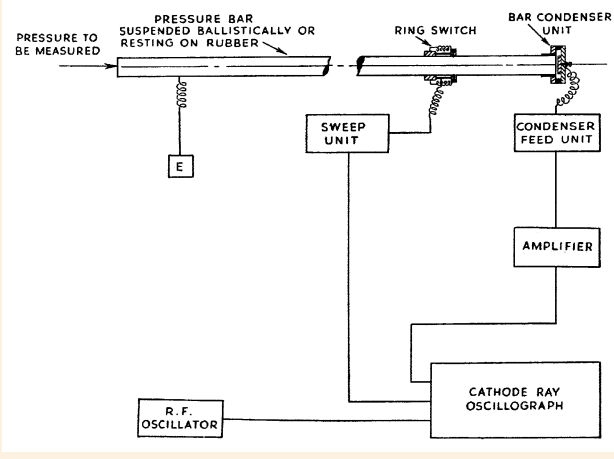

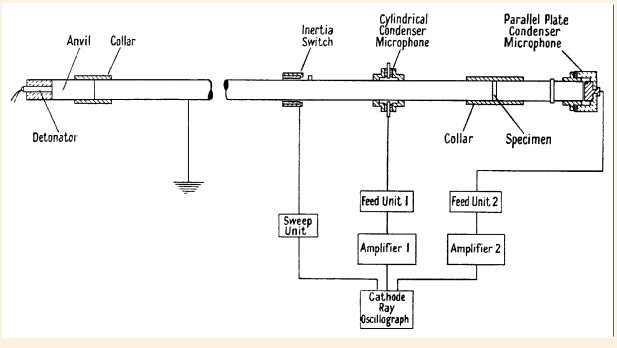

4.3–P Throughout the 20th century, various pressure-bar methods were devised for the generation of well-defined pressure pulses in order to derive dynamic stress/strain materials data. ***Top:*** Schematic of "Hopkinson pressure bar," a variant of the ballistic pendulum invented in the 1910s by the British engineer Bertram HOPKINSON. It consists of a long steel bar *B*, about 1 in. in diameter, suspended in a horizontal position by four threads so that it can swing in a vertical plane. At one end of the bar a short cylindrical pellet *C*, known as the "time piece," is wrung on. The transient pressure is applied at the other end. When a bullet impinges on the firing end of the long bar or a pressure pulse is initiated by a detonation *A*, the compression pulse is transmitted through the joint between the long and the short bar. But after reflection at the free end of the short bar this pressure pulse is converted into a pulse of tension. This causes the short rod *C* to fly off with the momentum trapped in it, which is measured with a conventional ballistic pendulum *D*. [Proc. Roy. Soc. Lond. **A89**, 411 (1914)] ***Center:*** In 1948, the British engineer Rhisiart M. DAVIES devised an electrical modification of the Hopkinson pressure bar for measuring the relation between pressure and time in experiments on high pressures of short duration. His experimental method, the so-called "Davies bar," applies a long bar to propagate the pressure pulse generated at the entrance face to the end face, which is equipped with a displacement sensor, a condenser microphone. Under the assumption that the pressure waves are elastic waves, the unknown stress-time curve can be determined by differentiating the measured displacement-time profiles. [Phil. Trans. Roy. Soc. Lond. **A240**, 375 (1948)] ***Bottom:*** In the Davies method, the pulse is propagated down the bar, only without an appreciable change in form when the pulse is long in comparison with the diameter of the bar and when there are no sudden changes in pressure. The method proposed by the British researcher Herbert KOLSKY avoids this limitation. The so-called "Kolsky pressure bar" – also known as the "split Hopkinson pressure bar" – is similar to the Davies pressure bar, except that the bar is in two parts, and a second condenser microphone and amplifier are introduced. The shock pressure pulse is produced by a detonator held against a replaceable steel anvil at the firing end of the bar. KOLSKY's method allows one to measure the stress-strain behavior of disk-shaped specimens. If a sufficiently thin specimen is inserted, the pressure pulse is effectively the same throughout the specimen during the passage of the compression pulse. This pressure is communicated along the extension bar to the condenser microphone, which delivers a displacement-time signal. The stress-time relation for the specimen is obtained by differentiation of this curve. [Proc. Phys. Soc. (Lond.) **62B**, 676 (1949)]

4.3 **PERCUSSION STUDIES** – 20th Century: Taylor Test

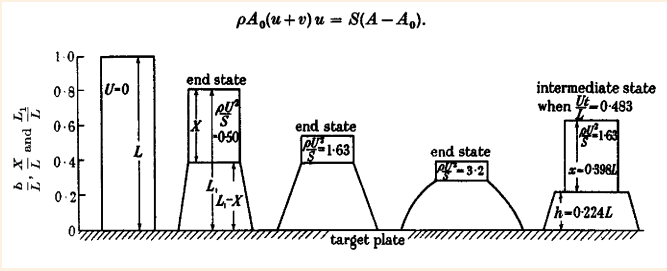

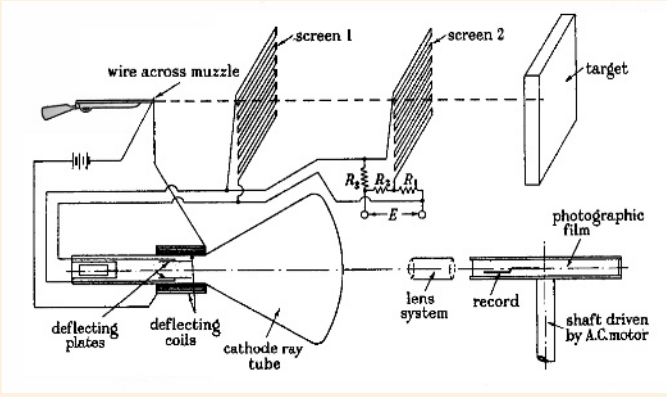

4.3–Q It has long been known that metals may be subjected momentarily to stresses far exceeding their static yield stress without suffering plastic strain. The theoretical concept for determining the dynamic yield stress is the so-called "Taylor test" devised by Geoffrey I. TAYLOR, a British applied mathematician at the Cavendish Laboratory of the University of Cambridge. It was first tested in practice by his coworker A.C. WHIFFIN, who found good agreement with theory. ***Top:*** The method allows one to determine the dynamic yield strength S of a material by using a rod made of this material and impacting it end-on at a known velocity U. TAYLOR derived a simple formula, given by

$$S = C \times U^2 (L - X)/(L - L_1),$$

with C being a constant, L the initial overall length of the test cylinder, X the unstrained length of the specimen, and L_1 the overall length of the test cylinder after impact. ***Center:*** Since the dynamic strength is proportional to the square of the striking velocity, a careful measurement of the velocity is absolutely necessary. WHIFFIN used two wire screens to subsequently deflect the bright spot of a cathode ray tube which he recorded on a film strip mounted on a rapidly revolving drum. ***Bottom:*** This picture shows examples of mushroomed steel cylinders after the test that were impacted with velocities ranging from 110 to 2,120 ft/s (33.5–646 m/s). The method of determining dynamic yield stress proved very useful for strain rates up to about 10^4 in./in./s. [Proc. Roy. Soc. Lond. **A194**, 289 (1948)]

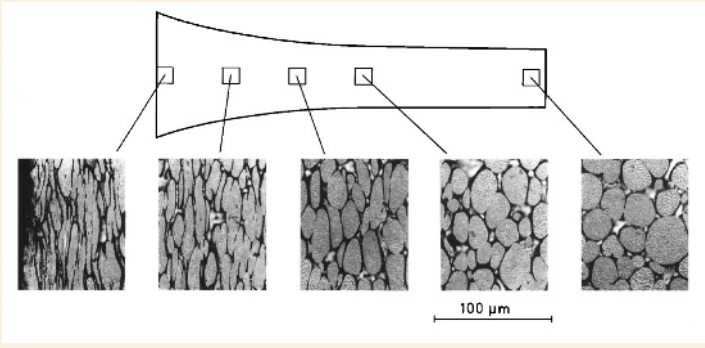

4.3–R Reinhard THAM and Alois J. STILP (EMI, Freiburg) studied the penetration depth of the plastic wave front in metal alloys by analyzing their microstructure after impact. Using 5.8-mm-dia. rods with an initial length of 58 mm made of DF-17 (a W-Ni-Fe compound made by Plansee GmbH, Germany) and impacting them on a rigid wall at 203 m/s, they measured the grain deformation and therefrom determined the dynamic compression strength. Note that deformations of the tungsten grains are particularly pronounced in the impact region on the left-hand side of the rod. [J.R. ASAY ET AL. (eds) *Shock waves in condensed matter – 1983*. North-Holland, Amsterdam (1984), p. 167]

4.3 **PERCUSSION STUDIES** – 20th Century: Examples of Ball Percussion Studies

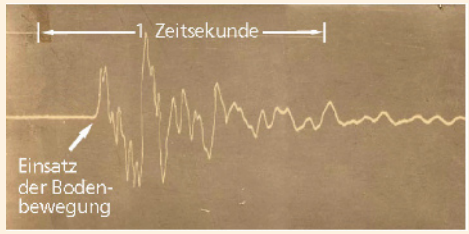

4.3–S Example of inelastic percussion at low velocity (< 17 m/s): ***Left:*** View of the "Mintrop ball," a 4,000-kg, approx. 1-m-dia. iron drop weight used in 1908 by Ludger MINTROP at Göttingen University to generate artificial earthquakes. The dropping tower, a 14-m-high steel construction, and the ball were donated by the Krupp Company. MINTROP recorded the seismic shocks at different distances from the impact site using a transportable, high-sensitivity seismograph with a magnification of 50,000. From that he derived the velocity of the earth wave. [Courtesy Institute of Geophysics, University of Göttingen] ***Right:*** Partial view of a seismogram taken in 1908 by MINTROP at a distance of 120 m from the ball impact using the Wiechert seismograph. At this close distance, the separation of ground motion into P- and S-waves is not yet fully accomplished. [From L. MINTROP's Ph.D. thesis, University of Göttingen. Girardet, Essen (1911)]

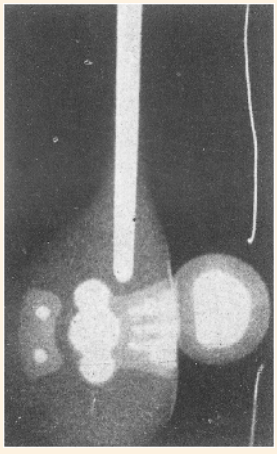

4.3–T Examples of freezing the moment of violent interaction of a golf ball with a club. ***Top:*** In 1935, Harold E. EDGERTON at MIT (Cambridge, MA), using a xenon flash lamp of short duration (< 1 µs) and a still camera, took unique reflected-light photographs of this high-speed percussion event. Note the strong elastic deformation of the ball. Because of the effect of inertia, the lower, undeformed part of the ball is still fully resting on the tee, while a tremendous percussion force is already acting on its central part. [H. EDGERTON: *Stopping time*. Stemmle, Schaffhausen (1987), p. 54] ***Bottom:*** With the advent of flash radiography in 1938 it became possible to also study the interior of shock-compressed opaque objects. The picture was taken by Charles M. SLACK at Westinghouse Electric Corporation. Note the compressed core of the golf ball. [J. Soc. Mot. Pict. Eng. **52**, No. 3, p. 63 (1949)]

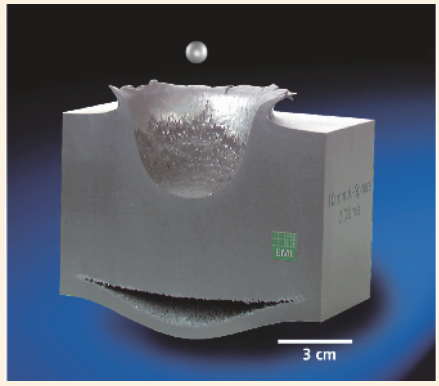

4.3–U Example of a hypervelocity impact: a 10-mm-dia. aluminum sphere impinged a plane aluminum plate at hypervelocity ($M \approx 14$). This picture well illustrates that a hypervelocity impact produces a crater that is much larger in diameter than the size of the impacting body, in this example by a factor of about 7. This is an important phenomenon for correctly interpreting meteorite impact craters. Note the well-marked spallation zone. [Dept. of Terminal Ballistics & Impact Physics, EMI, Freiburg]

4.3 **PERCUSSION STUDIES** – 20th Century: Liquids under Impact

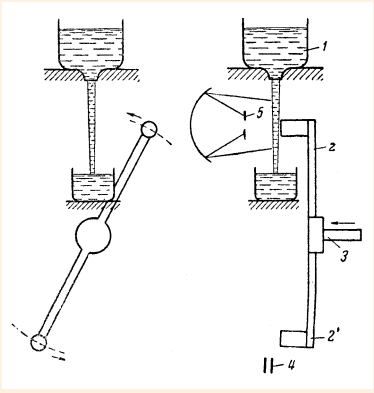

4.3–V At high impact velocities liquids can behave like solid bodies. Depending on the viscosity of the liquid and the rate of deformation, the same liquid can show plastic flow as well as brittle fracture, which was first demonstrated by Mark I. KORNFELD. ***Left:*** He generated a vertical jet of liquid by providing a hole in the bottom of a vessel *1* and used a rotating arm with two metallic segments *2* and *2'* facing each other. The first one served as an impactor and the second as a trigger of a spark light source *5*. By suddenly pushing forward the rotating arm on the axis *3*, the segment *2* strikes the liquid jet, thereby simultaneously triggering the spark light source. A still camera with open shutter was used to photograph the impact phenomenon in reflected light. He used a liquid that had a viscosity of about 50 kg s/m^2, corresponding to the consistency of honey or syrup. ***Bottom:*** "Brittle fracture" of liquid can be observed also at lower velocities when a liquid with a higher viscosity is used. [M.I. KORNFELD: *Elastizität und Festigkeit von Flüssigkeiten*. Verlag Technik, Berlin (1952), p. 74]

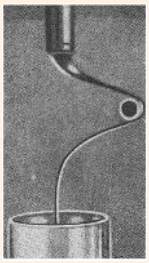

←
At a low impact velocity (< 23 m/s), the liquid jet only reveals a plastic (laminar) deformation.

→
A brittle-type destruction of the liquid jet can be observed at an impact velocity of > 23 m/s.

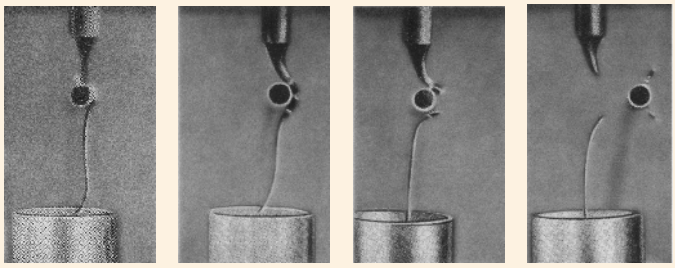

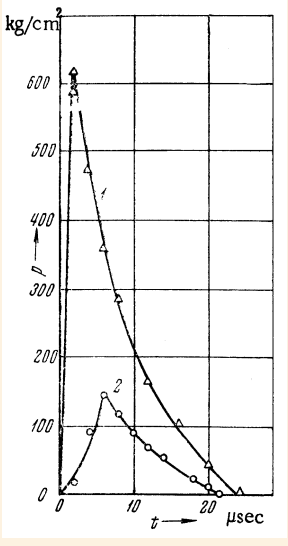

4.3–W ***Left:*** In the former Soviet Union, S.P. KOZYREV and K.K. SHAL'NEV studied the impact of liquid jets on a solid. They observed that the short duration of the initiated pressure pulse depends on the shear viscosity and impact velocity [*curve 1*, 64 m/s; *curve 2*, 32 m/s]. ***Right:*** To explain this phenomenon, they proposed a relaxation model and tested it by ballistic impact of a cylindrical projectile with a 5-bar liquid jet, a solution of rosin in mineral oil, issued from an 8-mm-dia. nozzle. Like M.I. KORNFELD {⇨Fig. 4.3–V}, they observed plastic deformation of the liquid jet at low velocity (9 m/s, *left*) and brittle fracture at a higher velocity (15 m/s, *right*). [Sov. Phys. Dokl. **15**, 513 (1970)]

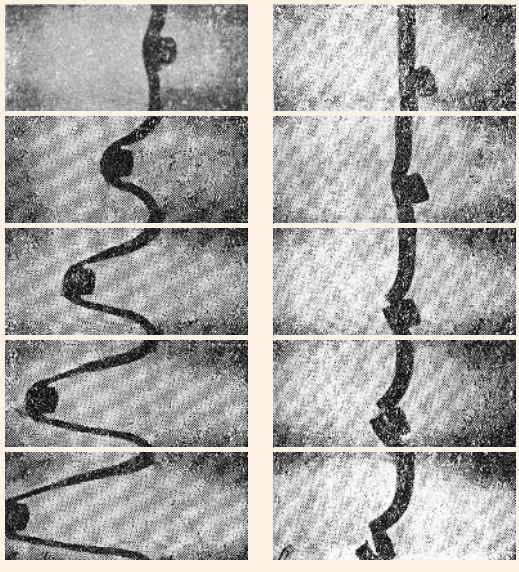

4.3 **PERCUSSION STUDIES** – 20th Century: "Sweet Spots" of Sports Equipment

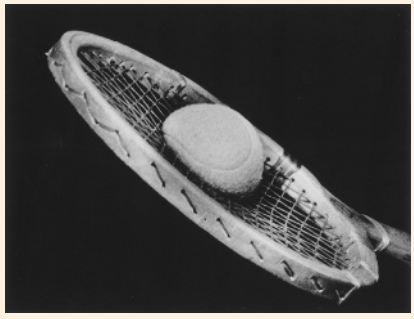

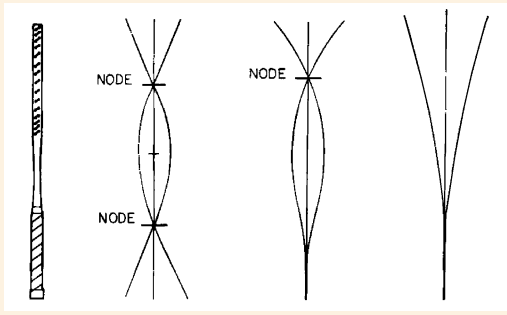

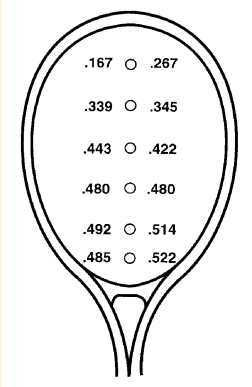

4.3–X Recent studies performed in Australia, Austria, and the United States on the impulsive force generated in handheld implements (such as tennis rackets and baseball bats) have shown that the impact point that feels best – commonly called the "sweet spot" – is usually the node of the fundamental vibration mode, not the center of percussion (COP), a well-defined spot for a rigid body rotating around a fixed axis {⇨Fig. 2.9}. The Austrian biomechanics professor Herbert HATZE {⇨1998} concluded that the concept of the COP is of limited significance when an implement is handheld because the force exerted by the hands will affect the location of the axis of rotation, which in turn affects the location of the COP. ***Top, left:*** Photo of a tennis ball in compression taken by MIT professor Harold E. EDGERTON using a xenon flash light source [Proc. 4th Int. Congress on High-Speed Photography. Helwich, Cologne (1958), p. 14] ***Top, right:*** When a ball hits a racket, it produces a transverse wave that travels along the racket and is then reflected from both the tip and the butt end. The U.S. physics professor Howard BRODY studied the vibrations of a tennis racket for the free-free (*left*) and the clamped-free (*center and right*) modes. For an impact at the vibration node, the vibrational component becomes zero. [Am. J. Phys. **49**, 816 (1981)]. ***Bottom:*** Positions of experimentally determined ball speed ratios (*left*) and calculated ball speed ratios (*right*) for a free racket according to BRODY. This ratio falls off as the impact point moves from the center of mass toward the tip. [Am. J. Phys. **65**, 981 (1997)]

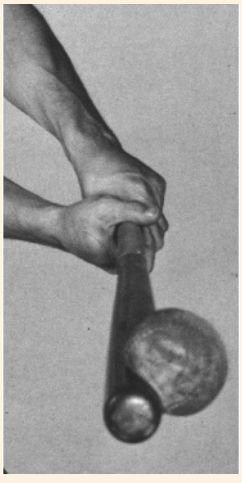

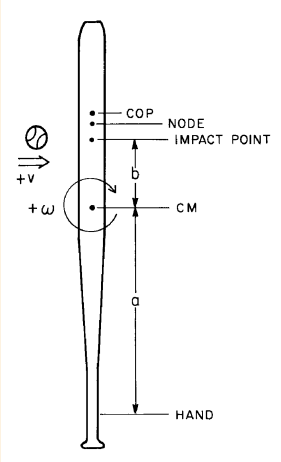

4.3–Y ***Left:*** High-speed flash photograph of a bat striking a baseball, taken by H.E. EDGERTON at MIT. The large deformation of the ball illustrates well the enormous magnitude of the impulsive force at this instant. [From his book *Stopping time.* Stemmle, Schaffhausen (1988), p. 55] ***Right:*** According to studies by Howard BRODY, there exist three "sweet spots" on a baseball bat:

(1) The center of percussion (COP), which is located ca. 17 cm from the fat or distal end of the bat. When the hands grip the bat at a distance *a* from the center of mass (CM), there is no net translational motion at that point of the bat.

(2) The node of oscillation, which is located ca. 19 cm from the end of the bat, approx. one quarter of the length of the beam. When the ball is hit at the location of the node, the hands will not "sting."

(3) The impact point, which is located at a distance *b* from the CM. When the ball is hit at an impact point that is not the COP, this leads to maximum "power," *i.e.*, to the fastest batted ball speed. The distance *b* varies between 18.2 and 8.8 cm for a bat/ball mass ratio varying between 5 and 7, respectively. [Am. J. Phys. **54**, 640 (1986)]

4.3 **PERCUSSION STUDIES** – 20th Century: Seismology of Nuclear Explosions

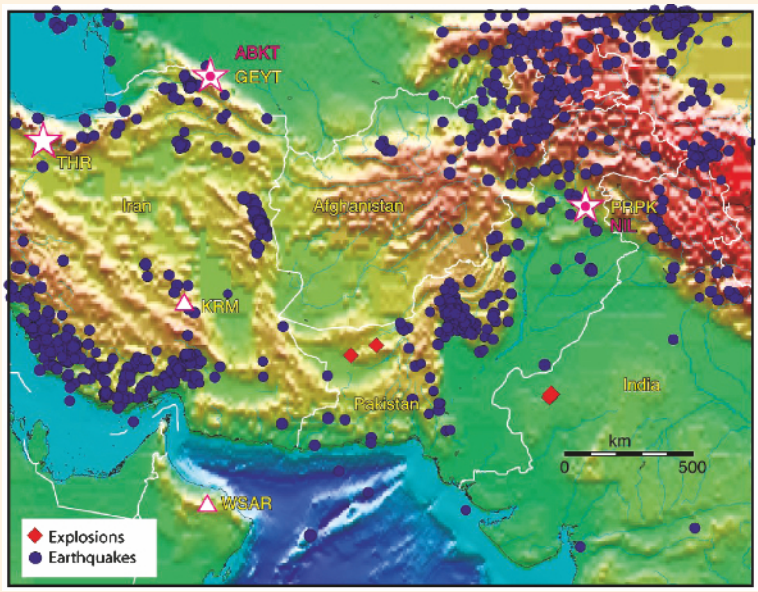

4.3–Z The Nuclear Test Ban Treaty that was signed in 1963 banned nuclear weapons tests in the atmosphere, in outer space, and under water, but permitted underground testing. The Comprehensive Test Ban Treaty (CTBT), which has hitherto been signed by 174 nations, bans *all* nuclear test explosions, including underground tests and those intended for peaceful purposes. The CTBT provides for an International Monitoring System (IMS) of automated seismic stations to record any evidence of clandestine nuclear explosions that transmit data via satellite to the International Data Center in Vienna, Austria. Teams in various countries are working to improve ways to seismically differentiate clandestine underground nuclear explosions from other sources of seismicity (*e.g.*, earthquakes and mining explosions) and to characterize them in terms of their locations, depths, and yields.

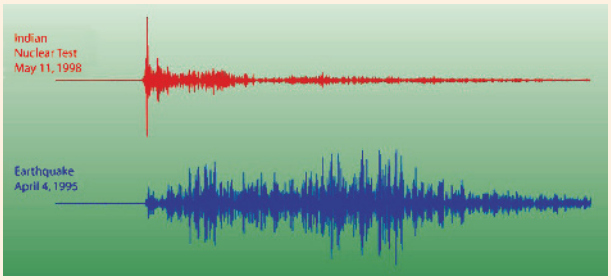

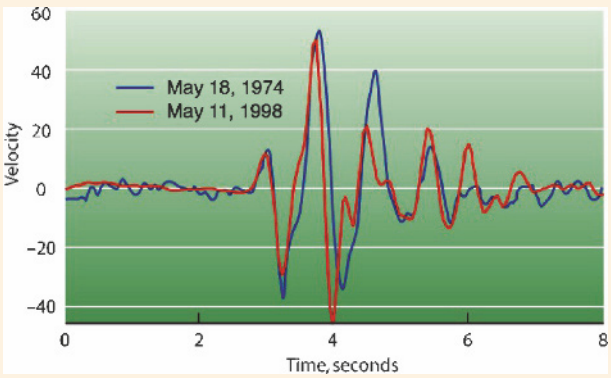

Under the auspices of the U.S. Dept. of Energy (DoE), William R. WALTER and collaborators at LLNL (Livermore, CA) worked out methods of analyzing seismograms to differentiate between nuclear explosions and other types of seismic sources. They discovered that differences in seismic P- and S-wave energy provide one method of discriminating explosions from earthquakes: seismic P-waves are compressional waves; therefore explosions should have higher P/S ratios than earthquakes. ***Top:*** This topographic map shows seismic locations both of nuclear tests (*red diamonds*) performed in India (in 1974 and on May 11 and May 13, 1998) and in Pakistan (on May 28 and 30, 1998), and earthquakes recorded in the region between 1995 and 1997 (*blue circles*), taken from the PDE (Preliminary Determination of Epicenters) catalog. Also shown are planned locations of IMS primary seismic stations (*stars*) and auxiliary seismic stations (*triangles*). ***Center:*** The seismogram of the Indian nuclear test, performed on May 11, 1998, clearly differs from that of a representative earthquake. ***Bottom:*** Seismic waveforms from different nuclear explosions show a remarkable similarity. [From LLNL's Science & Technology Review (April 1999). Courtesy University of California, LLNL; http://www.llnl.gov/str/Walter.html]

4.4 PERCUSSION AND SHOCK WAVE MODELS – Corpuscular Models and NEWTON's "Cradle"

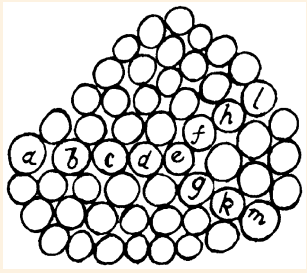

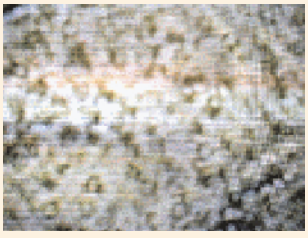

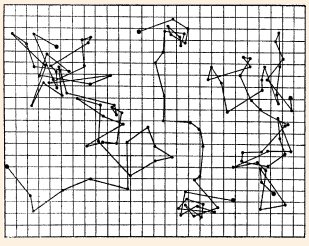

4.4–A Historic 2-D collision models. ***Top:*** Simple model of an elastic fluid used by Sir Isaac NEWTON to illustrate the transport of impulse from one individual particle to another. He writes, "If the particles *a*, *b*, *c*, *d*, *e* lie in a right line, the pressure may be indeed directly propagated from *a* to *e*, but then the particle *e* will urge the obliquely posited particles *f* and *g* obliquely … the pressure begins to deflect towards one hand and the other, and will be propagated obliquely in infinitum…" [I. NEWTON: *Principia.* S. Pepys, London (1687), Lib. II, Prop. XLI] ***Center:*** In 1992, the U.S. researcher Brian J. FORD reproduced some of Robert BROWN's famous experiments on "Brownian movement" (1827) using BROWN's own microscope. FORD's video recording on the movement of tiny particles (here fat droplets of about 1 µm in diameter in cow's milk) can be viewed on the Internet. Note that the blurring in FORD's video is caused by the primitive, single-lens construction of BROWN's microscope. [http://www.sciences.demon.co.uk/wbbrowna.htm] ***Bottom:*** The French physicist Jean-Baptiste PERRIN, studying the successive movements of small particles, quantitatively confirmed the kinetic theory of heat. Shown here are three examples of observed temporal positions of an individual grain taken through out 50 time intervals, each lasting 30 s. The particles quickly change direction, and in the microscope only a mean shift is observable. [Ann. Chim. Phys. **18** (VIII), 5 (1909)]

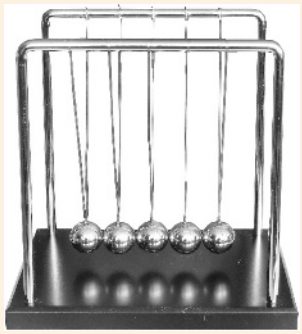

4.4–B The Newtonian demonstrator, popularly known as "NEWTON's cradle" or "balance ball," has become a widely used apparatus for demonstrating elastic percussion, the Third Law of Motion, and the Laws of Conservation of Momentum and Energy. Suspension of the balls on twin strings ensures that oscillations of all balls remain in a fixed plane, even after passing several cycles. To verify that during each collision cycle the impulse is fully propagated, the balls are suspended such that they barely touch in their positions at rest. The instrument shown here can be bought at the Deutsches Museum Shop GmbH, Munich.

4.4 PERCUSSION AND SHOCK WAVE MODELS – Shock Wave Demonstration Apparatus

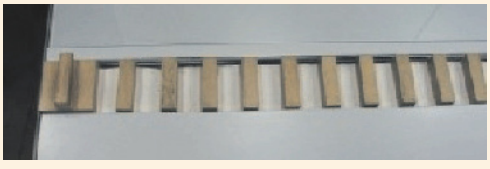

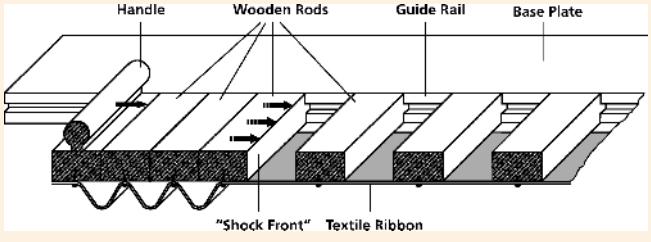

4.4–C This simple shock wave model is used to demonstrate to visitors of the Rieskrater-Museum the "shock wave" phenomenon. It consists of a couple of wooden rods mounted on a textile ribbon. Initially separated by each other, the rods, beginning from the left, are successively pushed together. In this way, the leading edge of collision proceeds successively from one rod to the other, thus illustrating the successively acceleration of particles when being hit by the shock front. [Courtesy Gisela PÖSGES, Rieskrater-Museum, Nördlingen, Bavaria]

4.4 PERCUSSION AND SHOCK WAVE MODELS – One-Dimensional Shock Wave Models

(a)

(b)

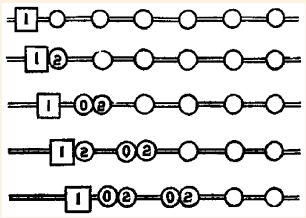

(c)

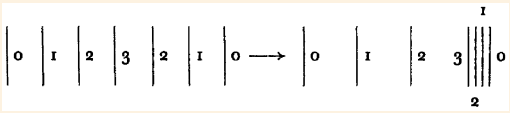

(d)

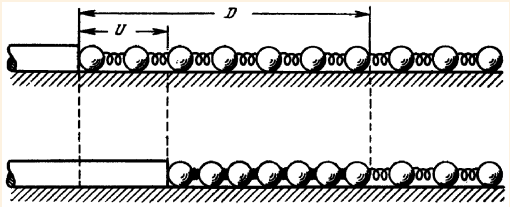

(e)

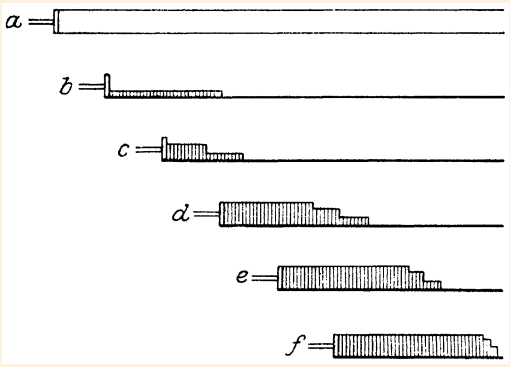

4.4–D Shock wave models arose with the discovery of the phenomenon itself, but they are also used in modern textbooks. ***(a)*** Ernst MACH's sketch of his percussion model, illustrating that a violent disturbance must propagate with a higher velocity than the sound velocity c. MACH assumed a linear row of gas molecules arranged two by two and colliding with each other (*upper row of arrows*) with velocity $u >> c$. During collision the molecules gain a velocity increase by $u + c$. After collision they rebound in the opposite direction (*lower row of arrows*). [Sitzungsber. Akad. Wiss. Wien **75** (II), 101 (1877)] ***(b)*** The British physicist Charles V. BURTON used a linear shock wave model that assumes a linear row of balls separated by an equal number of weak springs (not shown here). A piston, coming from the left side, hits the first ball and transmits its impulse to the next one. [Phil. Mag. **35** (V), 317 (1893)] ***(c)*** The shock wave model of explaining shock wave formation proposed by the British fluid dynamicist Sir M. James LIGHTHILL is very simple and plausible. LIGHTHILL says, "Note that the running of waves in the region of rising pressure, which produces a local ordering of the pressure rise into a discontinuous jump, is balanced by the gradual separation of waves from one another in any region of falling pressure, where the waves carrying the lower pressures lag behind those in front and spread the wave out as illustrated. The numbers on the waves might represent percentage excess pressure, and the right-hand figure shows the waves in the region of the rising pressure just before they have finally run together." [Mem. Manch. Lit. Phil. Soc. **101**, 1 (1959)] ***(d)*** The 1-D model of shock wave propagation of a shock wave in an elastic medium proposed by the Russian physicist Lev V. AL'TSHULER is similar to BURTON's model: The propagation of a shock wave in a substance can be modeled by a series of spheres that are elastically coupled to one another. The rate of displacement of the spheres, the "mass velocity" of substance U, is equal in this model to the velocity of a piston that causes the spheres to move. This velocity is always lower than the velocity D of the perturbation boundary separating the resting and separated spheres from those moving and gathered into a more compact mass. [Sov. Phys. Uspekhi **8**, 52 (1965)] ***(e)*** The famous "shock wave piston model," proposed by the German physicist Richard A. BECKER, explains the formation of shock waves by coalescence of discontinuous pressure pulses and by means of the formula for the sound velocity $c = (k\ \partial p/\partial \rho)^{1/2}$. The motion of the piston is thought of as being divided into a large number of small, successive motions, each separate motion producing a pressure pulse that propagates through the medium ahead at sonic velocity. Since each pressure pulse heats the gas adiabatically, which also increases the sound velocity, later pulses will tend to overtake the preceding ones. [Z. Phys. **8**, 321 (1922)]

4.4 PERCUSSION AND SHOCK WAVE MODELS – Apparatus for Demonstrating Hydraulic Jumps

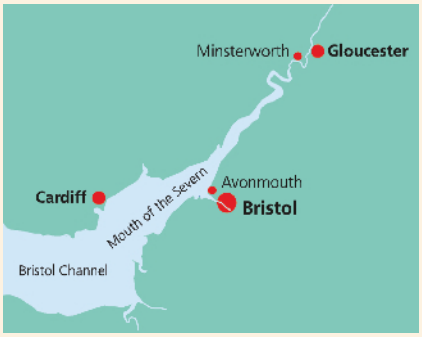

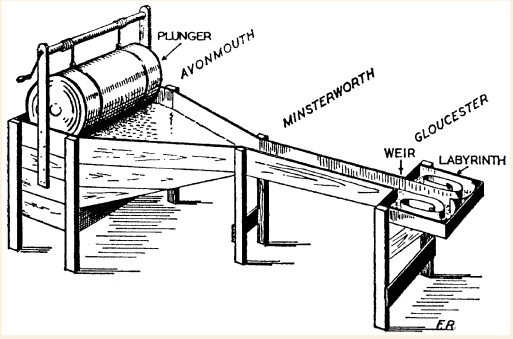

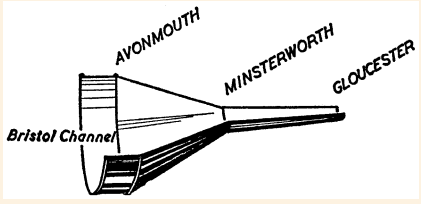

4.4–E ***Left:*** The Severn is Britain's longest river (about 290 km). The shape of its estuary is such that the water is funneled into an increasingly narrow channel as the tide rises. Between Minsterworth and Gloucester the river is less than 100 yards across, thus forming the famous "Severn Bore," one of the most studied surge waves in the world. ***Right:*** The generation of a bore can be demonstrated using this simple apparatus. It uses a funnel-shaped channel to simulate the estuary and a plunger to drive a model bore into the straight part of the funnel. At its end the wave is absorbed in a labyrinth. [F. ROWBOTHAM: *The Severn bore*. Macdonald, London (1964), p. 23]

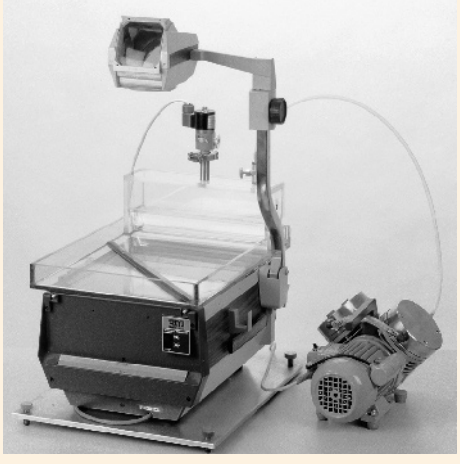

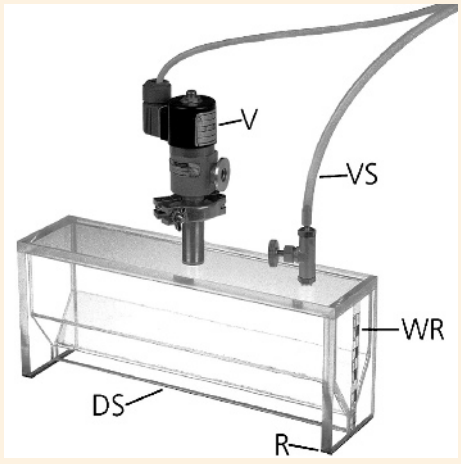

4.4–F ***Left:*** The propagation and reflection of hydraulic jumps was demonstrated by the author in an auditorium using a small water table, a wave generator, and a common viewgraph projector. A plane wave leaving the slit of a wave generator can be used to study the interaction of a hydraulic jump with a solid boundary of any desired geometry. In the example shown here, a brass bar, positioned at an oblique angle to the incident wave front, was used to illustrate regular and Mach reflection phenomena. ***Right:*** View of the used plane wave generator: *WR* – water reservoir, *DS* – discharge slot; *R* – rubber strip; *V* – air inlet valve; and *VS* – connection to vacuum pump. The strength of the hydraulic jump depends on the water level to which the water has been raised by generating a negative pressure via a vacuum pump prior to discharge. [Shock Waves **1**, 3 (1991)]

4.4 PERCUSSION AND SHOCK WAVE MODELS – Traffic Shocks

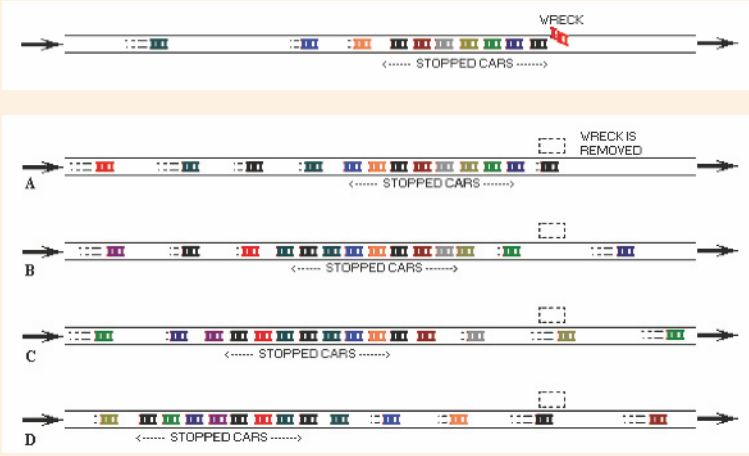

4.4–G Schematic illustrating how a "traffic shock" develops on a highway by a wrecked car. ***Top:*** A row of cars has gotten stuck behind a wreck; other cars are approaching from the left and stopping too. The traffic shock of densely concentrated cars behaves very much like the steepening process in a shock wave, leading to densely arranged air molecules at the shock front. ***Bottom:*** When the wreck (red car) has been removed, the flow is suddenly unplugged. But not all the cars can move, since most cars are stuck behind drivers who are stopped. A "jam" of cars slowly moves upstream, from left to right, while the wave of evaporation – corresponding to a rarefaction wave in shock physics – moves in the opposite direction. [Courtesy William J. BEATY. *See* his Web page *Traffic waves* (1998), http://www.amasci.com/amateur/traffic/-traffic1.html]

4.4 PERCUSSION AND SHOCK WAVE MODELS – Amusing Cartoons

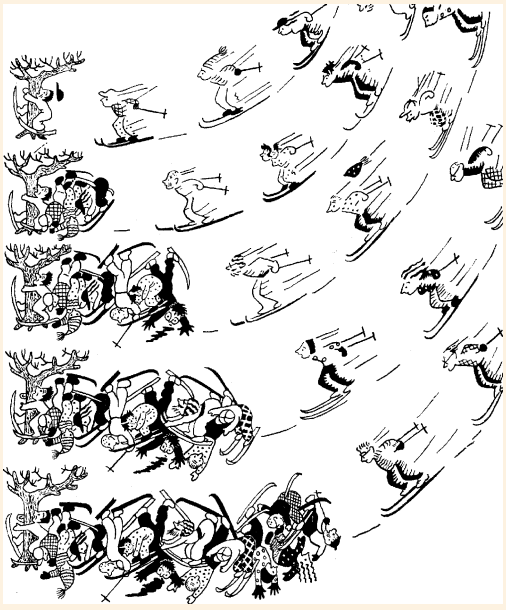

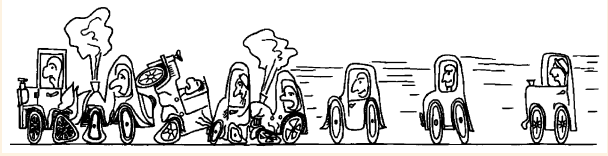

4.4–H ***Right:*** This is a picturesque example of a "traffic shock," illustrating the traffic situation when a preceding car suddenly slows down, such as by a breakdown, and drivers of subsequent cars cannot react to the new situation quickly enough. This chain-reaction-type collision, a frequently occurring phenomenon on highways, often results in dreaded mass collisions. The same mechanism that occurs in a traffic flow on long crowded roads causes the steepening of a shock wave in fluid dynamics, here each car resembling a decelerated wave. The shock front is identified with the point of collision that moves with increasing time counter to the flow of traffic. [P.A. THOMPSON: *Compressible-fluid dynamics*. McGraw-Hill, New York (1972), p. 306] ***Left:*** A similar situation might also happen to a group of skiers when a skier in front is suddenly slowed down, for example by head-on collision with an obstacle. [G.E. DUVALL and G.R. FOWLES: *Shock waves*. In: (R.S. BRADLEY, ed.) *High pressure physics and chemistry*. Academic, New York (1963), p. 213]

4.5 SHOCK WAVE VISUALIZATION – TOEPLER's Stroboscopy of Propagating Shock Waves

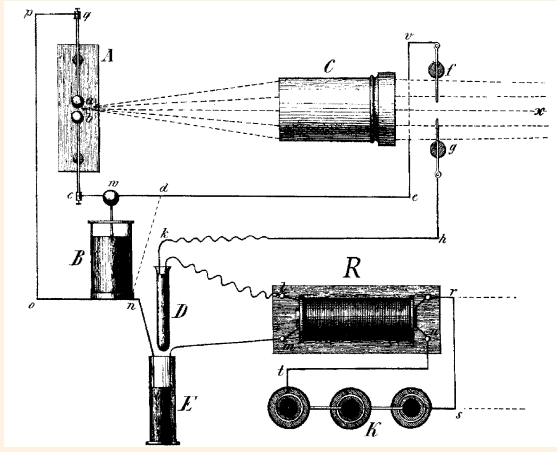

4.5–A ***Top:*** This experimental setup was used by the German physicist August TOEPLER in the mid-1860s to visualize the propagation and reflection of shock waves subjectively, using his schlieren method {⇨Fig. 4.18–A} and an electric circuit to delay the illumination spark *a–b* relative to the shock wave that he generated by the spark *f–g*. The principle involved uses two capacitor discharges that are coupled to each other via the spark gap *f–g*, the so-called "Knochenhauer circuit" {⇨Fig. 4.19–C}. The delay time between the two sparks can be varied simply by changing the immersion depth of the capacitor *D/E*. ***Bottom:*** TOEPLER's pen-and-ink drawings of what he observed as flashing pictures through his telescope. Illustrated are shock wave fronts at increasing time instants originating from a long spark *(a)*; and reflected at a solid boundary *(b)*. He also observed the spark channel and found a pinch-type plasma structure *(c)*. His drawings have often been taken erroneously as photographs, but the first photograph of a propagating shock wave was not taken until 1885 by Ernst MACH and his son Ludwig {⇨Fig. 4.5–G}. Since TOEPLER was actually the first to "see" a shock wave rather than to record it on film, his widow provided his tombstone with the following epitaph: *August Toepler – Er sah als Erster den Schall* ("August Toepler – He was the first to see the sound"). She erroneously chose the term "sound" instead of "shock wave." [A. TOEPLER: *Beobachtungen nach einer neuen optischen Methode.* Max Cohen & Sohn, Bonn (1864); plate III, figs. 1 and 10, and plate IV, figs. 5 and 11]

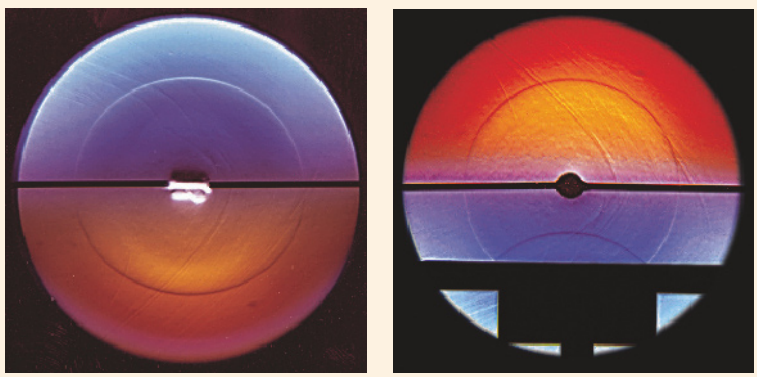

4.5–B TOEPLER's first schlieren experiments reproduced by P. KREHL (EMI, Freiburg) on the example of an air shock wave emerging from a short spark. They illustrate the propagation of the shock wave (*left*) and its reflection at a solid boundary (*right*). Since TOEPLER did not use a schlieren head corrected for chromatic aberration, he must have seen the shock wave on a colored background divided into two halves of different colors as shown here. Note the amazing relieflike structure of the shock wave front, which is typical for the schlieren method of reproducing steep density gradients. [Shock Waves **5**, 1 (1995)]

4.5 SHOCK WAVE VISUALIZATION – ANTOLIK's Soot Method

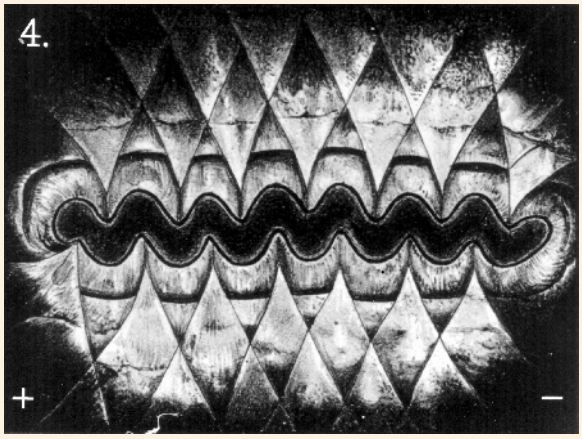

4.5–C In the mid-1870s, the Hungarian physicist and schoolmaster Károly ANTOLIK (Kaschau, Austro-Hungarian Empire) invented a curious technique of visualizing the mechanical effects originating from electric spark discharges. He generated a zigzag-shaped gliding spark between two closely spaced glass plates. When coating one plate facing the spark channel with a soot layer, he observed on this plate that conical-shaped branches were recorded in the soot layer that emerged from each concave part of the spark path. He attributed this phenomenon to electrical rather than to mechanical reasons. In reality, however, ANTOLIK recorded with his so-called "soot method" the very first irregular interaction patterns of shock waves. This was first recognized by Ernst MACH immediately after the publication of ANTOLIK's paper. [Ann. Phys. **154** (II), 14 (1875)]

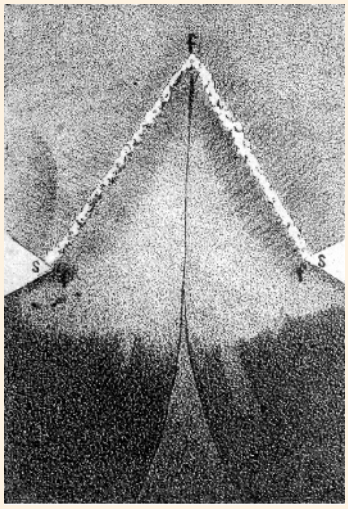

4.5–D In 1875, Ernst MACH at the German Charles University in Prague began to tackle one of the most challenging problems in shock wave physics: the oblique interaction of shock waves. ***Top:*** Ernst MACH and his student Jaromir WOSYKA, repeating ANTOLIK's experiments, reduced his complicated gliding spark geometry to a single zigzag element ("V-spark"), thus confirming that the production of conical branches is of a purely mechanical origin and that the area between them is swept clean of soot upon discharge, which they called "V-shaped propagation" [Germ. *V-förmige Ausbreitung*], later also called "soot funnel." They correctly interpreted its origin by a superposition of mechanical waves. MACH later recognized that the puzzling phenomenon was caused by aerial waves of finite amplitude – then also called "Riemann waves" [*Riemann'sche Wellen*] – the term "shock wave" [*Stoßwelle*] was not used by him until 1885. ***Bottom:*** MACH and WOSYKA, using a geometry of two opposing V-sparks (*left*), proved the existence of a straight part of the resulting interfering wave pattern, later called "Mach disk" by John VON NEUMANN. The soot transport emerging simultaneously from both sides is stopped along a straight central line where the afterflows of both shocks eliminate each other. This ingenious setup converted the transient shock wave interaction pattern *during* the discharge to an irreversible soot pattern *after* discharge. A superposition of three Mach disks (*center*), one coming from the top and two from the sides, results in an interesting Y-configuration, *cf.* enlargement (*right*). [Sitzungsber. Akad. Wiss. Wien **72** (II), 44 (1875)]

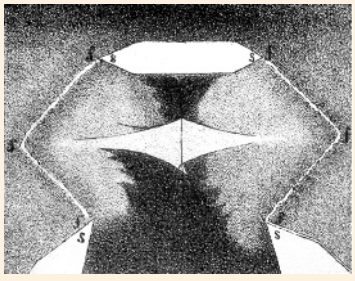

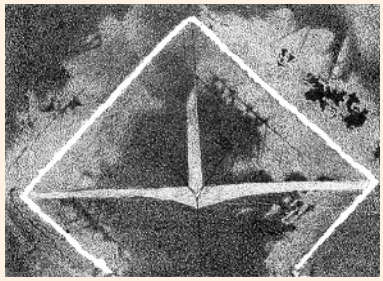

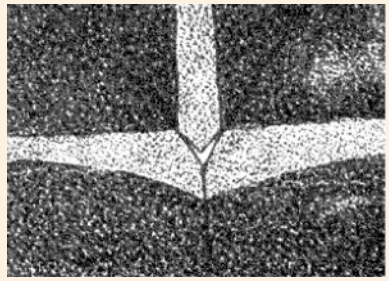

4.5 SHOCK WAVE VISUALIZATION – ANTOLIK's Soot Method *(cont'd)*

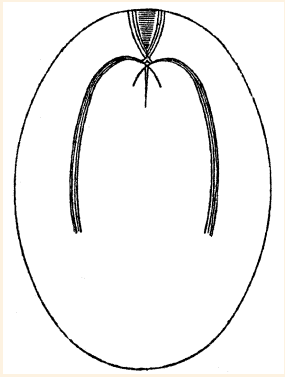

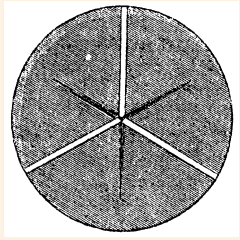

4.5–E Wenzel ROSICKÝ, one of Ernst MACH's assistants at the German Charles University in Prague, visualized focusing effects of weak shock waves in an elliptic reflector backed by a soot-coated glass plate. ***Left:*** He generated the shock wave by an electric spark discharge in one focus and observed a star-shaped interference pattern in the other focus. ***Right:*** A close-up inspection revealed that this other focus had a tri-star formation with a center completely free of soot. [Sitzungsber. Akad. Wiss. Wien **73** (II), 629 (1876)]

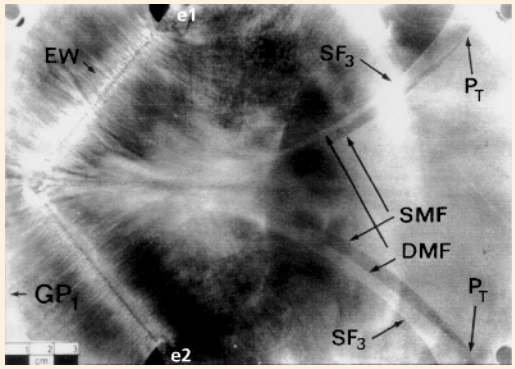

4.5–F Recording of shock interactions at higher pressure levels is possible using sand-blasted rather than plain glass plates, a discovery made by P. KREHL (EMI, Freiburg). A strong V-shaped electric gliding spark e_1–e_2 produces two concentric Mach funnels *SMF* and *DMF*, resulting from single and double Mach reflections, respectively. The third funnel SF_3 was apparently created by the interaction of primary shock waves with secondary ones from the oscillatory capacitor discharge. [*Proc. 18th Int. Symposium on Shock Waves.* Springer, Berlin (1992), p. 221]

4.5 SHOCK WAVE VISUALIZATION – Examples of Shock Wave Photography in Gases

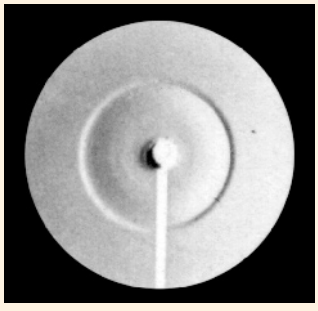

4.5–G The first schlieren photograph of a shock wave was taken in 1885 by Ernst MACH and his son Ludwig using high-sensitivity silver bromide gelantin dry plates. They generated the shock wave by discharging a Leiden jar between two closely spaced glass plates. Note the relief-type structure of the shock front, which is typical for the schlieren method of reproducing steep density gradients. [Sitzungsber. Akad. Wiss. Wien **98** (II), 1333 (1889)]

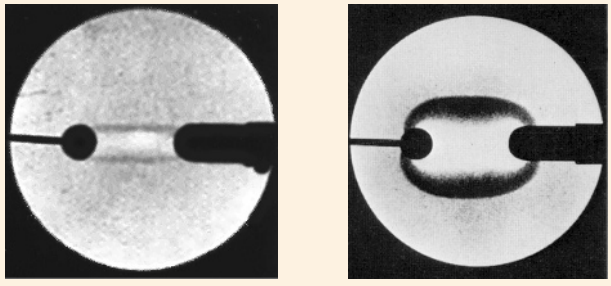

4.5–H Karl-Heinz HERRMANN at the Freie Universität Berlin took flash radiographs of shock waves emerging from a spark discharge in gases using soft Cu-K radiation ($\lambda \approx 1.5$ Å), which is essential for getting a high radiographic contrast. The two flash radiographs of the shock wave in air were taken 3 μs (*left*) and 9.5 μs (*right*) after the onset of discharge. Densitometry revealed that the density jump in the emitted wave profile is already established after the wave has traveled a few centimeters from the spark, indicating that the steepening process of the shock front is almost completed. [Z. angew. Phys. **10**, 349 (1958)]

4.5 **SHOCK WAVE VISUALIZATION** – Shock Tube Studies

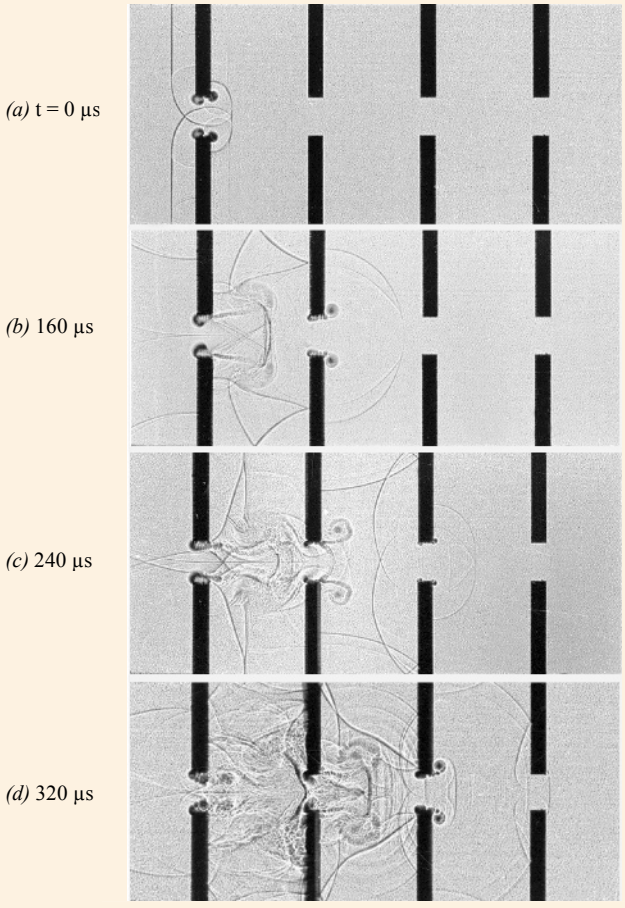

4.5–I Using the EMI Shock Tube Facility, Heinz REICHENBACH and collaborators investigated the shock attenuation in a symmetric baffle system (baffle height 110 mm). Applying the 24-spark Cranz-Schardin camera and shadowgraphy, they visualized the propagation of the shock front and the interaction with the baffle elements, *cf.* frames ***(a) – (d)***. An analysis revealed that a shock wave, here moving with $M = 1.5$ from left to right, is already absorbed by 90% after the passage of only four baffles – a surprising phenomenon due mainly to expansion. Note the vortex formation at the aperture edges that begins immediately after passage of the incident shock wave. [*Proc. 8th Int. Congr. on High-Speed Photography*, Almquist & Wiksell, Stockholm (1968), p. 362]

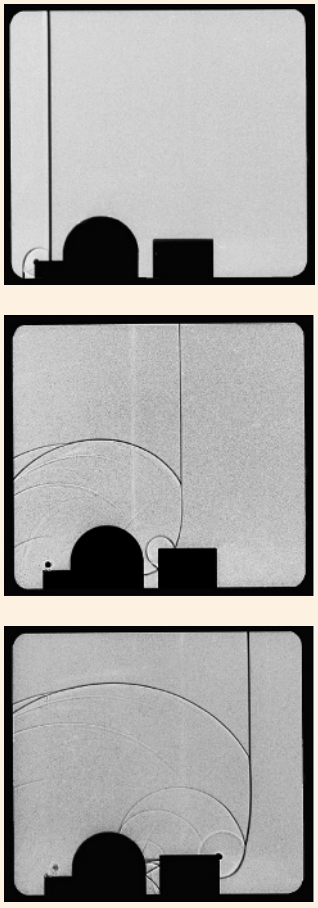

4.5–J Cinematography of a propagating plane shock wave striking a model nuclear power plant. Initially, the shock wave is reflected regularly ***(a)***, but after passing the left building block ***(b)*** it generates Mach reflection. Subsequently, the resulting Mach stem interacts with the right building model, creating for its part a second Mach reflection. Note the trapping of shock waves between the two model buildings ***(b, c)***. This series of shadowgraphs was also recorded with the Cranz-Schardin multiple-spark camera. [Photos by W. SCHÄTZLE and W. GEHRI; EMI-Archives, Freiburg]

4.5 **SHOCK WAVE VISUALIZATION** – Whip Cracking

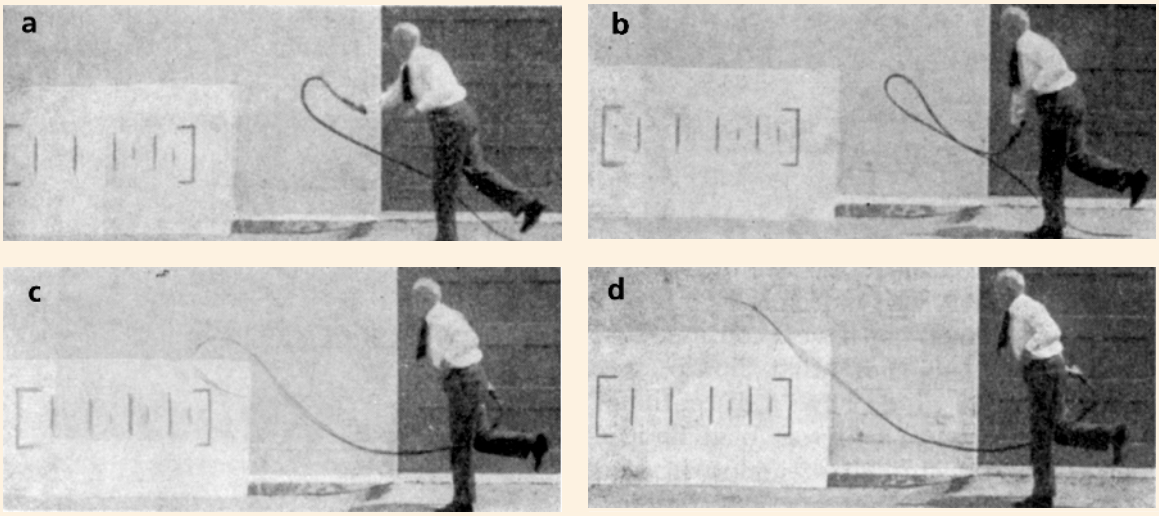

4.5–K ***Top:*** Barry BERNSTEIN and collaborators at the U.S. Naval Research Laboratory (Washington, DC) visualized the motion of the whip lash before, during, and after whip cracking. Frames *a–d* were taken with a movie camera at 4,000 frames/s, the heavy vertical lines are one foot apart. Frames *c* and *d* were taken before and shortly after the whip cracked. Note that the loop starts near the handle and propagates down until it reaches the whip tip where it generates the sharp cracking sound. [JASA **30**, 1112 (1958] ***Bottom, left:*** In 1927, Zéphirin CARRIÈRE, a French physicist and clergyman at the Institut Catholique (Toulouse, France), was the first to succeed in visualizing the shock wave emerging from the whip tip of a simulated *laboratory whip*. He performed this difficult task by using schlieren photography and a spark point light source. Almost 30 years later, he resumed his studies and was able to improve the contrast of his photos. [Cahier de Physique No. 63, p. 5 (1955)] ***Bottom, center:*** BERNSTEIN ET AL. (*see above*) were the first to successfully photograph the shock wave emerging from the tip of a *real whip*, in their studies a 12-ft (3.66-m)-long bull whip. Using a still camera and flash shadowgraphy, they recorded snapshots of the propagating shock wave at different time instants. [JASA **30**, 1112 (1958)] ***Bottom, right:*** More recent experiments on whip cracking, carried out at EMI, Freiburg by Peter KREHL and collaborators in March 1995 using high-speed videography and laser stroboscopy, revealed that the supersonic motion of the tuft is only a *conditio sine qua non*, but that the essential mechanism of shock generation occurs in the final stage of acceleration and is due to the abrupt flapping of the tuft at the turning point – *i.e.*, when, as illustrated in the schematic, the tuft flaps from position "8" into position "9". [Shock Waves **8**, 1 (1998)]

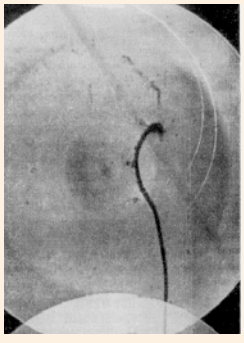

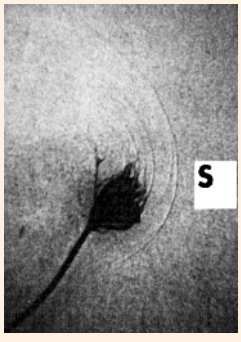

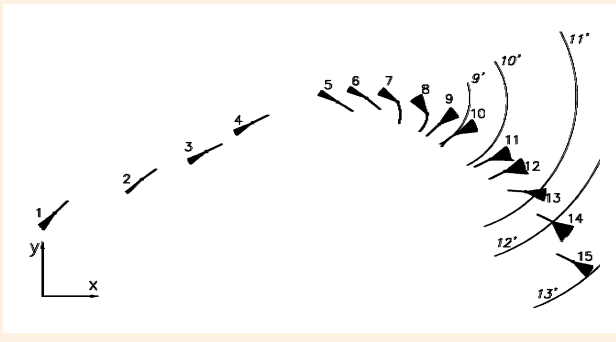

4.5 SHOCK WAVE VISUALIZATION – Muzzle Blast and Head Wave

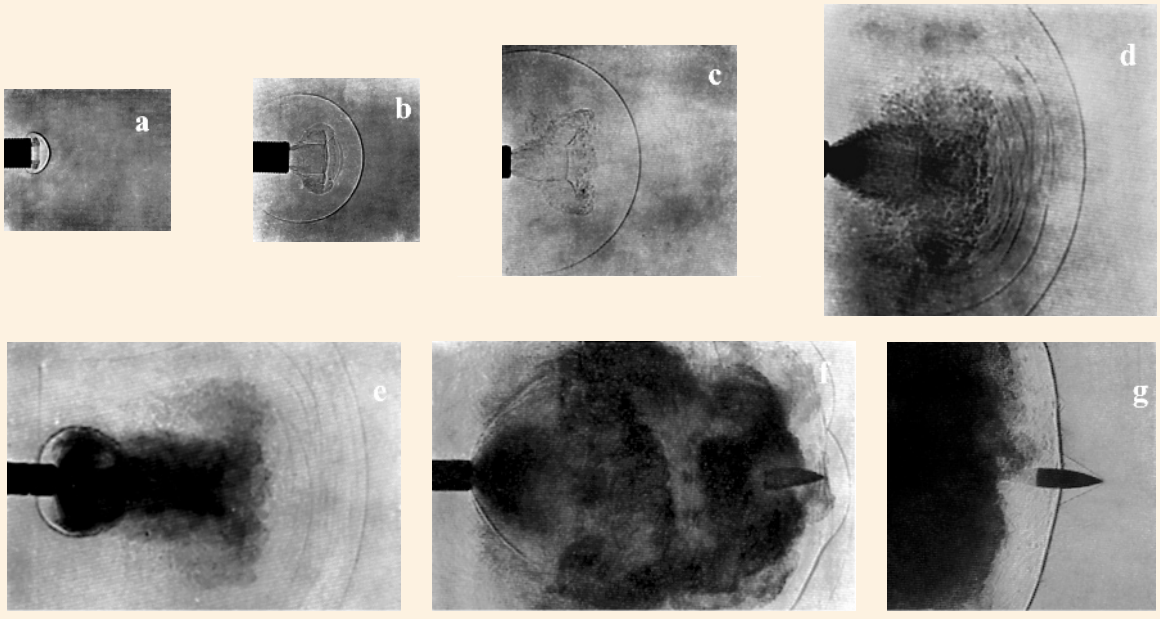

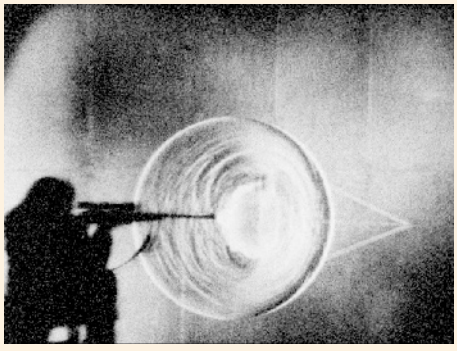

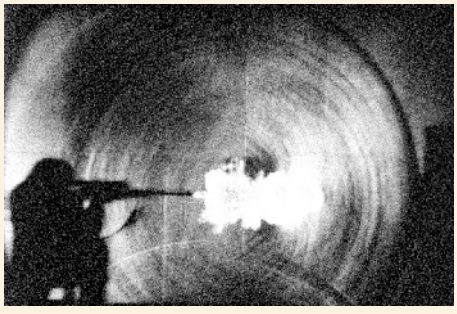

4.5–L High-speed cinematography revealed hitherto unknown flow phenomena in the environment of the muzzle and established *Intermediate Ballistics*, a new branch of ballistics. ***Top:*** Muzzle phenomena observed at the German rifle Mauser M98 while firing an S-bullet (v_0 = 880 m/s): *(a)* the air, compressed in the barrel in front of the accelerating projectile, creates a weak shock wave that has already partly left the muzzle; *(b), (c)* the shock wave expands spherically, and an air cushion has piled up between muzzle and shock front; *(d)* some powder smoke, leaking between barrel and projectile, already begins to leave the muzzle; *(e)* in this moment, the projectile base has just passed the muzzle, and the main part of the powder smoke can leave the barrel, which, impinging on the surrounding air, produces a second, stronger shock wave – the so-called muzzle blast; *(f)* the powder smoke, initially emerging from the muzzle with velocity v_0, decreases in velocity because of aerodynamic drag effects; and *(g)* after a certain distance from the muzzle, the head wave overtakes the muzzle blast, which quickly loses in strength because of its 3-D expansion. Note that the head wave, sitting rooflike above the muzzle blast, does not extend beyond the front of the muzzle blast. [C. CRANZ: *Lehrbuch der Ballistik*. Springer, Berlin; vol. II (1926): *Innere Ballistik*, pp. 443-449] ***Bottom:*** These schlieren pictures show the formation of the muzzle blast and the head wave upon firing a Remington 0.30-06 high-powered rifle. Taken on a scale an order of magnitude larger than previously done by others with the Full-Scale Schlieren System at Penn Sate University {⇨Fig. 4.5–N}, they allow one to observe and study the entire process, including shock wave reflections, bullet impact upon a target, and hearing protection for the shooter. Note that near the muzzle the head wave propagates almost twice as fast as the muzzle blast. The images appear somewhat grainy and indistinct because they are individual frames from a high-speed movie shot at 30,000 frames/s by way of a drum camera. [Courtesy Prof. Gary S. SETTLES, Gas Dynamics Laboratory, Penn State University, PA]

4.5 SHOCK WAVE VISUALIZATION – Color Schlieren Photography

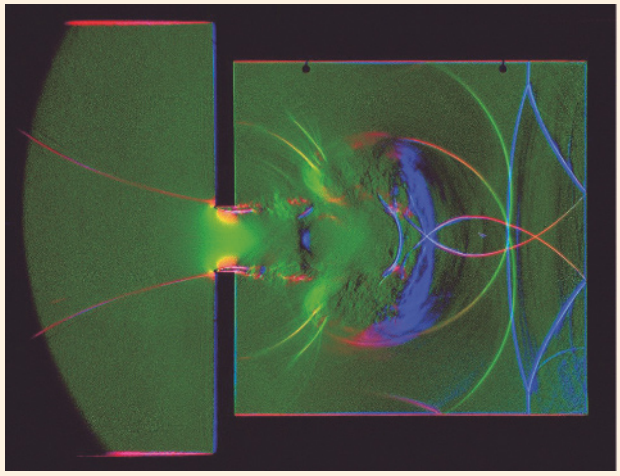

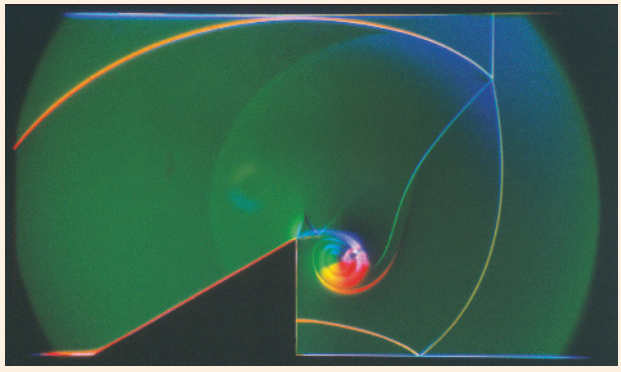

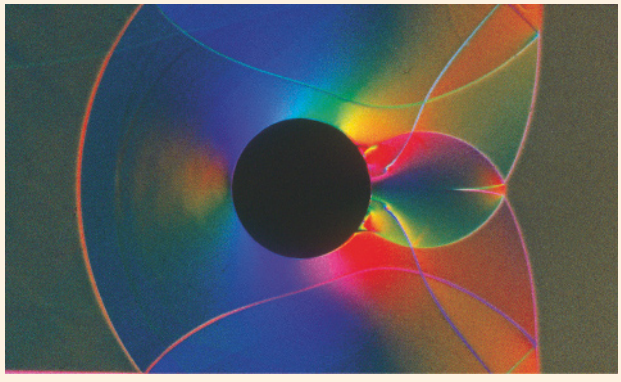

4.5–M Color schlieren photography is an extension of the original black-and-white schlieren photography and has the advantage that a specific hue can be better distinguished by the eye than a corresponding luminance within a gray-scale on a black-and-white schlieren photograph. The shock-tube pictures presented here were made with a multi-color filter in place of the knife edge. In all three cases shown here the incident shock wave propagates from left to right. ***Top:*** Schlieren photo of an aerial shock wave of strength $p_1/p_0 = 2.15$, propagating in air with a Mach number of $M = 1.41$ and penetrating through an aperture into a dead-end chamber. The picture was taken at a time instant shortly after reflection of the incident shock wave at the end of the chamber. Note that a complex reflection pattern is created, including both regular reflection and irregular (or Mach) reflection. A symmetric four-sector bicolor (blue/green) filter was used that reproduced the pressure gradients in different colors. The reflected shock wave, propagating from right to left, is reproduced in a bluish color, while several subsequent weaker shocks, still propagating from left to right, are reproduced in a greenish color. The following two pictures were taken with a three-sector tricolor (blue/green/red) filter. ***Center:*** Interaction of an aerial shock wave ($p_1/p_0 = 2.27$; $M = 1.45$) with a 30° wedge that generates Mach reflection. The picture was taken at a moment after the Mach stem had already passed the wedge top. The flow behind the Mach stem, after having entered the undisturbed corner below the edge, has created a counter-clockwise rotating vortex near the edge of the wedge. This motion has also been communicated to the slip line. Shock wave diffraction over a knife edge was first studied in 1958 by Hubert SCHARDIN at ISL (Saint-Louis, France) using black-and-white schlieren photography. [Courtesy Dr. P. NEUWALD, EMI, Freiburg] ***Bottom:*** This picture shows a complex wave interaction pattern generated by a plane shock wave ($p_1/p_0 = 2.39$; $M = 1.48$), propagating into nitrogen at atmospheric pressure and being diffracted at a circular cylinder. The single wave front on the left-hand side is the reflected wave. The two diffracted waves, propagating from left to right, have interacted and created a Mach disk that propagates along the axis of symmetry and varies in width. The diffracted waves, after being reflected at the tube walls, have created two Mach stems. [Courtesy Dr. Harald KLEINE, Stoßwellenlabor of RWTH, Aachen]

4.5 SHOCK WAVE VISUALIZATION – Color Schlieren Photography *(cont'd)*

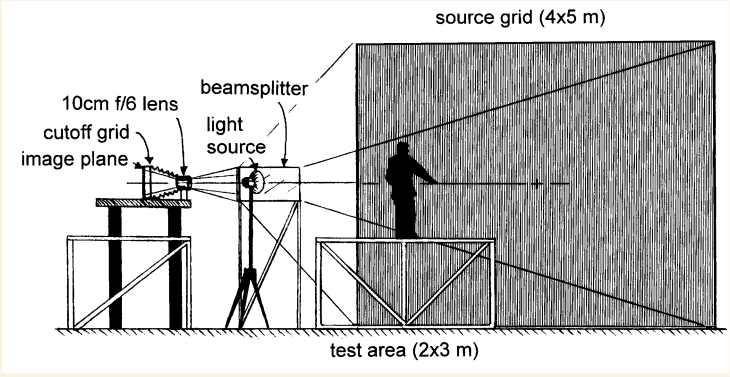

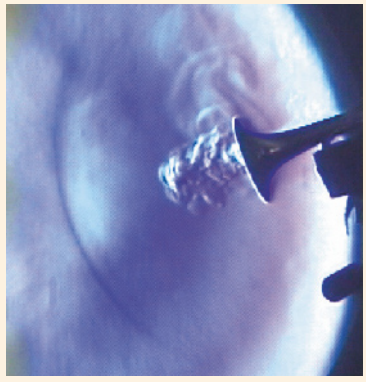

4.5–N Gary S. SETTLES, a professor at the Gas Dynamics Laboratory of Penn State University (University Park, PA), developed a sensitive large-aperture schlieren optical instrument that proved very useful in studying at full scale both heat- and shock-wave-generated schlieren flows. ***Left, top:*** Schematic of his Full-Scale Schlieren System, the largest indoor schlieren system in the world; the field-of-view is 2.9×2.3 m^2. Based on the lens-and-grid principle first developed in Germany by Hubert SCHARDIN in the late 1930s, it essentially consists of (1) a high-intensity light source of small dimension, (2) a large front-lit retroreflective source grid that covers one wall of the laboratory, (3) a cutoff grid that is a precise negative image of the source grid, and (4) for recording purposes either a high-speed movie camera system or a still camera for operation in single-frame mode. Contrary to classic schlieren methods using transparent light, the lens-and-grid method views the object in reflected light, which is more informative and realistic than imaging of contours only. ***Left, center & bottom:*** To study onboard explosions in an aircraft, full-scale schlieren flow visualizations of an explosion in a mockup aircraft cabin were performed. The blast waves, with Mach numbers ranging between 1.0 and 1.2 at a distance of about 1 m from the blast center, were generated by the detonation of an oxygen-acetylene gas mixture in a small toy balloon which, depending on its size, were equivalent to the yield of about 1 to 10 grams of TNT. The schlieren images show the blast propagation beneath full-size aircraft seats occupied by mannequins, both in side view (*center*) and front view (*bottom*). [Shock Waves **12**, 267 (2003)] ***Right:*** B.H. PANDYA, G.S. SETTLES, and J.D. MILLER at Penn State University visualized gasdynamic phenomena at the exit of a trumpet. Especially for loud, high-pitched trumpet notes they observed the emission of weak shock waves, which are the result of cumulative nonlinear acoustic propagation inside the trumpet bore. Though of weak intensity, ranging from 118 to 124 peak dB (A) and thus only marginally propagating above the sound speed, they can clearly be visualized with SETTLES' Full-Scale Schlieren System. The schlieren pictures shown here were made in single-frame mode using a xenon flash tube and 120-size ISO 800 color negative film. [JASA **114**, 3363 (2003)]

4.6 **HEAD WAVE STUDIES** – HUYGENS' Principle of Wave-Front Construction

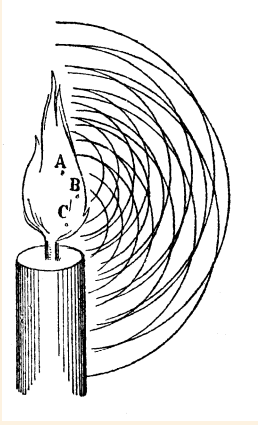

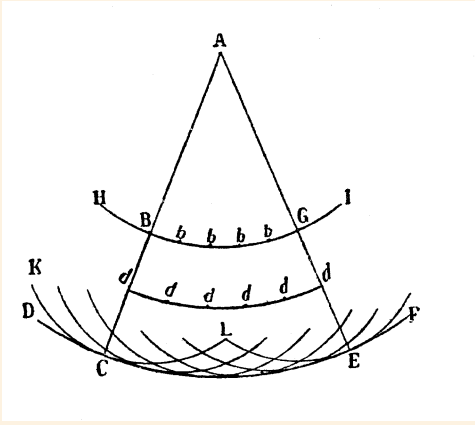

4.6–A The Dutch natural philosopher Christiaan HUYGENS suggested (i) that each point on the surface of a wave front acts as a point source for outgoing spherical waves ("wavelets") which advance with a speed and frequency equal to that of the primary wave at each point in space, and (ii) that the sum of the wavelets produces a new wavefront – so-called "Huygens principle." To some extent the method is also useful for constructing the front of a shock wave. HUYGENS, not yet knowing the features of a shock wave, assumed that the wavelets had very small amplitude and that the wavefronts were a linear superposition of wavelets. [C. HUYGENS: *Traité de la lumière*. Vander Aa, Leiden (1690)]

4.6 **HEAD WAVE STUDIES** – DOPPLER, Father of the Head Wave Phenomenon

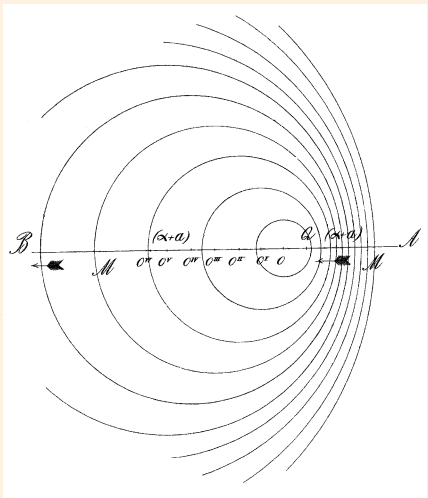

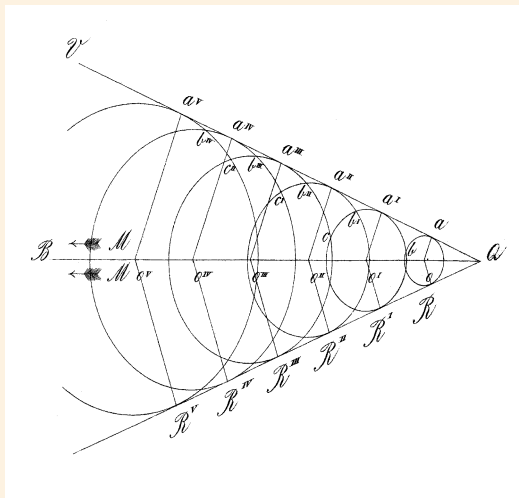

4.6–B Christian DOPPLER's schematics of a wave phenomenon arising from a disturbance moving along a straight line with a constant velocity u with respect to the sound velocity a of the surrounding medium. ***Left:*** Formation of waves in front of an object moving with subsonic velocity. ***Right:*** For supersonic motion the disturbances emitted from the moving object form the typical "Mach cone." If the body's speed is not constant along a straight course, the region of disturbance would be bounded by curved lines and its shape would also change with time. DOPPLER also derived the famous formula for the half-cone angle, given by $\sin\alpha = a/u$. In the period 1886–1887, Ernst MACH and Peter SALCHER first proved his theoretical model by visualizing the "head wave" in their supersonic ballistic experiments. [Abhandl. Böhm. Gesell. Wiss. Prag **5** (V), 293 (1848)]

4.6 **HEAD WAVE STUDIES** – DOPPLER, Father of the Head Wave Phenomenon *(cont'd)*

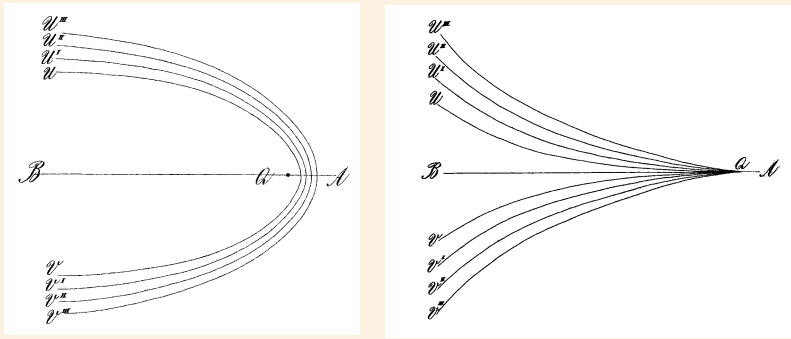

4.6–C DOPPLER, then a professor at the Technical State Academy (Prague, Austro-Hungarian Empire), also constructed head wave geometries at four successive time instants for an object moving along a straight trajectory with a supersonic velocity decreasing with time (*left*) and increasing with time (*right*); *i.e.*, for a decelerating and an accelerating object, respectively. [Abhandl. Böhm. Gesell. Wiss. Prag **5** (V), 293 (1848)]

4.6 **HEAD WAVE STUDIES** – Surface Wave Pattern Produced by a Moving Body in Water

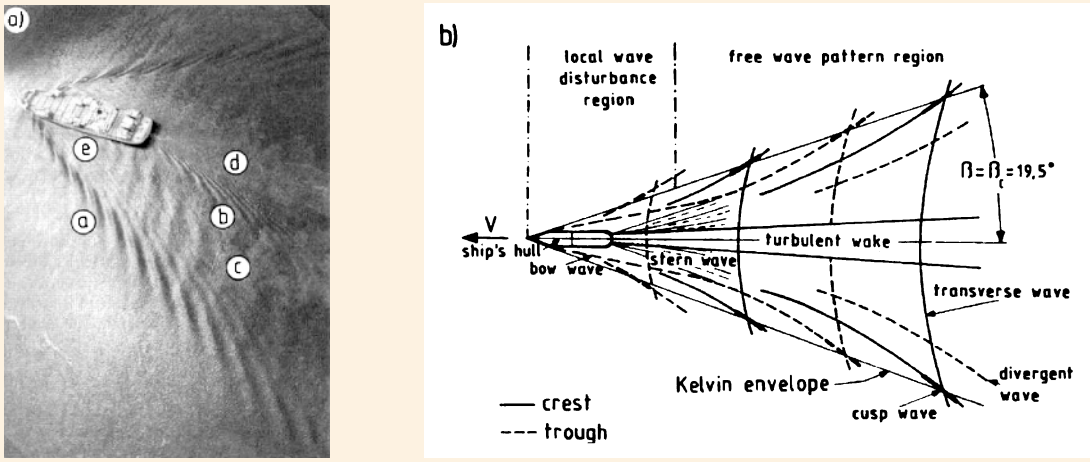

4.6–D ***Left:*** Aerial photograph showing the components of a ship wake pattern: *a* – bow wave, *b* – stern wave, *c* – transverse wave, *d* – turbulent wake, and *e* – turbulent region, adjacent to ship's hull. ***Right:*** When a ship travels through water, it generates a conical wave pattern. A closer inspection of the wave drawn in water, the so-called "bow wave," was carried out in 1871 by William THOMSON, the later Lord KELVIN [Phil. Mag. **42** (IV), 368 (1871)]. His study revealed that the wave front is not made up of only a single wave front, as in the case of the Mach head wave generated by a supersonic projectile, but is rather composed of a number of short waves (or cusp waves). They typically have wavelengths between 10 and 40 m and amplitudes between 0.2 and 1 m. They are not arranged parallel to the two lines emanating from the bows but are inclined at a certain angle to them. These component waves travel forward through the lines from the bows, at the same time as they travel outward with them, as the lines get gradually farther and farther apart. The envelope of these short waves is called the "Kelvin envelope" or "Kelvin wake." The angle between the waves in the "Kelvin arms" of a wake is independent of the ship's velocity and, contrary to a head wave generated by a supersonically moving object, is always 39°, *i.e.*, the Mach number for motion on water is $1/\sin 19.5° = 3$. [*Ship wakes.* ESA, Earth Observation Applications, Earthnet Online; http://earth.esa.int/applications/ERS-SARtropical/oceanic/shipwakes/intro/index.html. Courtesy R. DOERFFER, GKSS, Geesthacht, Germany]

4.6 **HEAD WAVE STUDIES** – MACH and SALCHER: Prelude to a Pioneering Ballistic Experiment

Dear Professor [Salcher],

I am very grateful to you for your kind intention to do the experiment, and if you don't mind I communicate right away some experiences and remarks.

I believe that an infantry rifle will be sufficient to do the experiment. Most important is that the projectile velocity surmounts the sound velocity. It will be sufficient at first to observe the phenomenon optically and later to photograph it. For its representation an additional illumination is certainly not required. This setup should work with this type of experiment as well as when photographing the bullet. The closing spark of a battery of jars, corresponding to a capacity of a free 12-m-diameter ball and in my case charged up to a voltage of about1-cm gap length, has two gaps, I and II. Passing in front of the lens O, the bullet passes II, which triggers the illumination spark I.

The rifle will be positioned several meters away from II in order to prevent smoke from entering the field of view.

As electrodes in II I have applied end-melted glass tubules into which very thin wires were inserted. The straight parts stand vertically with respect to the trajectory of the bullet, and their distance is slightly smaller than the diameter of the projectile. Annoying are the small glass fragments that could easily scratch the lens. Besides, using another method I could not provoke precise triggering and have preferred to position II farther away from the lens.

The setup would differ from that for photographing the bullet only by insertion of the aperture B, which at its border retains the picture imaged by the lens O from the telescope focused on II. For this experiment Toepler's time delay method would be too unreliable. If necessary I could supply you with a better triggering that is easy to produce.

I expect that the projectile will carry an envelope of compressed air of an approximate geometry as shown opposite. The apex of the truncated cone will doubtless depend on the ratio of the sound velocity to the projectile velocity.

I would be very happy if you succeeded with the experiment. I am entirely satisfied with having stimulated it.

Very sincerely, yours E. MACH

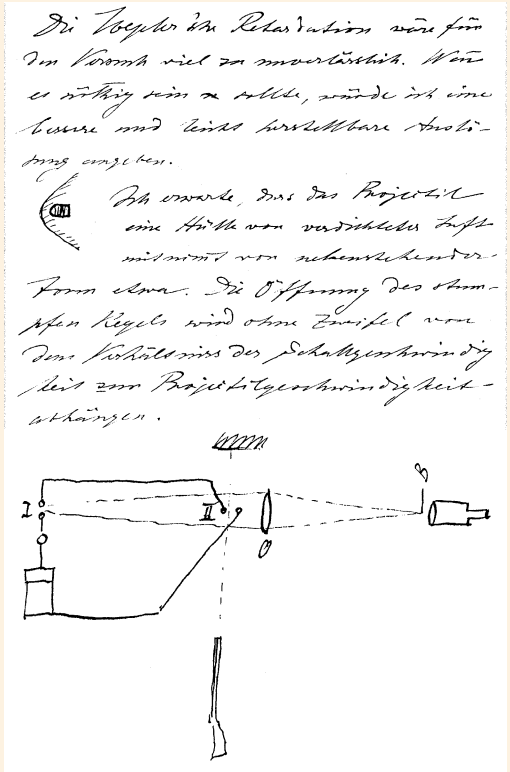

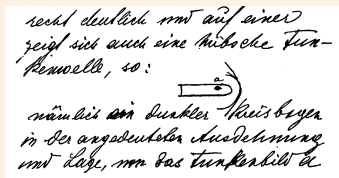

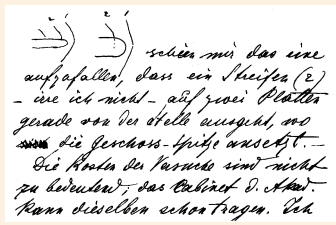

4.6–E ***Top, left & right:*** Ernst MACH assumed that a head wave should surround a projectile flying at supersonic speed. In his letter to Peter SALCHER dated February 16, 1886, he specified his idea for an appropriate setup to visualize the head wave. This historically important letter, until 1990 assumed lost, was rediscovered by the author in private archives of the Salcher family. [Courtesy Dr. Günther SALCHER, Hermagor, Austria] ***Bottom:*** In a letter (*left*) to MACH dated May 21, 1886, SALCHER fully confirmed MACH's speculation by including a sketch of the head wave. It also shows a circular wave emitted from a spark gap that, triggered by the projectile, activated the spark light source. In a further letter (*right*) to MACH dated May 23, 1886, SALCHER also visualized so-called "Mach lines" that arise from the rough surface of a supersonic projectile. He wrote, "A stripe (*2*) – if I'm not mistaken – goes out exactly from the place where the nose of the bullet begins." Both of SALCHER's letters mentioned above belong to a collection of 140 letters that he had sent to MACH at a time when they were both involved in the visualization of head waves and free-air jet phenomena (1886–1889). They are now kept at the Archives of the Deutsches Museum, Munich. MACH's letters to SALCHER are kept at Dr. Günther SALCHER's private archive at Hermagor.

4.6 **HEAD WAVE STUDIES** – First Experimental Evidence

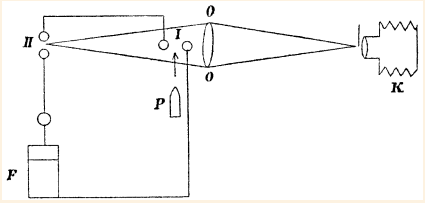

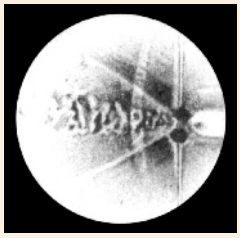

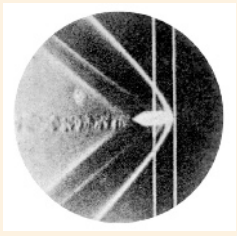

4.6–F In May 1886, E. MACH and P. SALCHER first reported in a short note on their observed head wave phenomenon. More detailed data were published by them in 1887. ***Left, top:*** Schematic of their experimental setup to capture a supersonic projectile *P* in flight using TOEPLER's schlieren method. Note the great similarity with MACH's previous sketch {⇨Fig. 4.6–E}. They took the picture in a darkened room about 2 to 4 m away from the muzzle. After opening the camera shutter and firing the rifle, the light source was triggered when the projectile *P* entered the electrode spacing of the spark gap *I*, which, causing a breakdown, triggered the illumination spark gap *II*. [Sitzungsber. Akad. Wiss. Wien **95** (IIa), 764 (1887)] ***Left, bottom:*** Since the intensity of their spark point light source, as well as the sensitivity of the first commercially available silver bromide gelantin dry plates, was limited, they reduced the schlieren picture to a small size of only some millimeters in diameter, thus obtaining sufficient exposure density on film. ***Center & right:*** These two schlieren pictures of the head wave, generated by a supersonic projectile flying from left to right, are among the very first ones they took. The vertical line (*left*) is a wire with a spark gap inserted for triggering the spark light source. They observed that triggering is more reliable when using two parallel lines acting as a spark gap (*right*). SALCHER used a Guedes infantry rifle (v_0 = 530 m/s), which resulted in a Mach cone angle of $2\alpha \approx 80°$. [EMI-Archives, Freiburg]

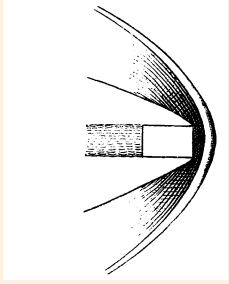

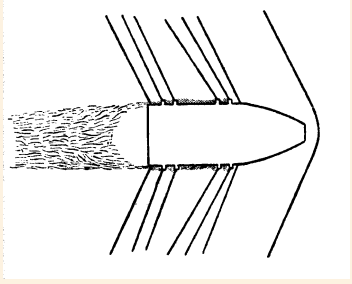

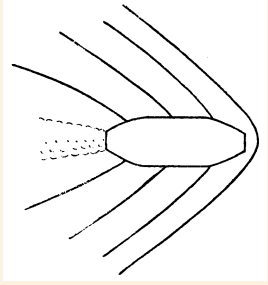

4.6–G MACH and SALCHER visualized head wave phenomena not only of small shots, but also of 9-cm-caliber projectiles – a difficult experimental task that had to be done in the harsh environment of a shooting range. Observing similar head wave phenomena as in the case of small shots, they correctly concluded that large shots could be simulated also in small-scale model experiments. ***Left:*** Blunt-headed projectiles typically reveal a double-layer structure of the head wave. ***Center and right:*** In the case of a projectile with guiding rings, vortices are already created at the first ring. Note the series of secondary head waves emerging from the periphery of the projectile, so-called "Mach lines." For projectiles provided with guiding rings they emerge under different Mach angles. In all cases, a train of vortices is followed behind the projectile stern. These vortices produce additional aerodynamic drag. [Sitzungsber. Akad. Wiss. Wien **98** (IIa), 41 (1889)]

4.6 **HEAD WAVE STUDIES** – Other Optical Methods

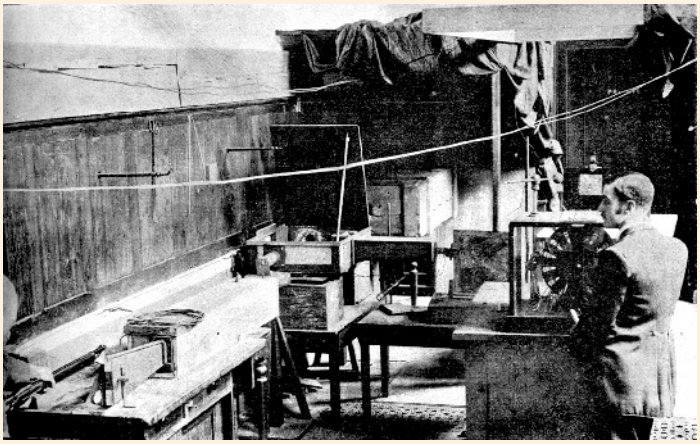

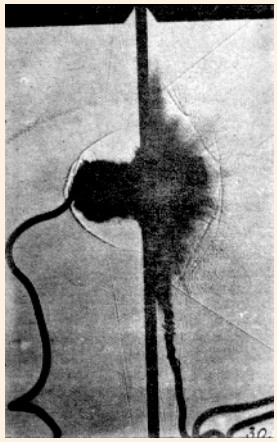

4.6–H In the early 1890s, Charles V. BOYS in England repeated MACH and SALCHER's ballistic photography of supersonic projectiles in free flight, but he used the silhouette rather than the schlieren method. ***Left:*** This photo shows BOYS' laboratory at the Royal College of Science in London. The rifle, operated by an assistant at the very left, was fired into a "recording box" that, shown here in the center with its open cover, contained the film plate and the spark light source. Its pulse capacitor was charged up via a Whimphurst influence machine. After leaving the recording box, the bullet was caught behind in a second box. ***Right:*** BOYS also studied the penetration and perforation phenomena of a glass plate struck by a projectile flying here from right to left. The expansion of the cloud of debris is clearly resolved. The two wires were used for triggering purposes of the spark light source. [Rev. Gén. Sci. Pures Appl. **3**, 661 (1892)]

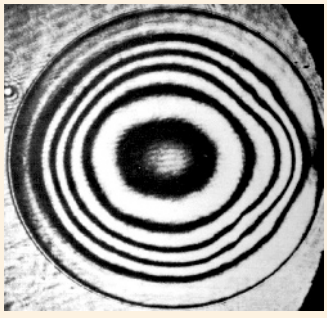

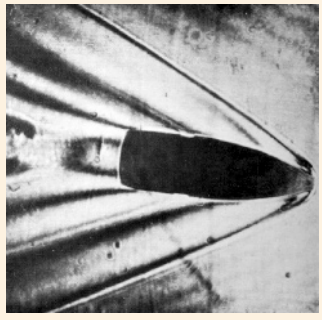

4.6–I ***Left:*** This is Hubert SCHARDIN's famous color schlieren photo of a supersonic projectile penetrating the flame of a candle. Outside of the Mach cone, in the so-called "zone of silence," the candle schlieren are not yet disturbed by the head wave. Note the train of vortices behind the projectile tail. (EMI-Archives, Freiburg) ***Right:*** Flash holography allows one to record a shock wave in three dimensions and to subsequently analyze details according to the required sensitivity such as corresponding to the schlieren method, shadowgraphy, or differential interferometry. Example of a flash hologram (*left*) of a supersonic projectile using a Q-switch ruby laser and applying holographic interferometry, and a reconstruction of the hologram (*right*). [Courtesy Drs. A. HIRTH and P. SMIGIELSKI, Rept. T16/69, ISL, Saint-Louis, France (1969)]

4.6 **HEAD WAVE STUDIES** – Other Optical Methods *(cont'd)*

↑ Although Andy GREEN, an RAF fighter pilot in his real job, still drove the 10-ton jet-mobile at subsonic speed (M = 0.95), close to the ground it produced a bow shock that extended out about 150 ft on either side of the vehicle.

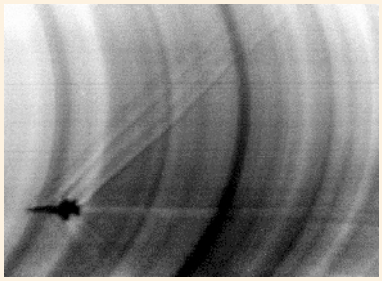

4.6–J The visualization of head waves produced by a full-sized supersonic vehicle is a particular challenge for high-speed photographers because it requires monitoring of a large field of view that is not directly accessible using conventional optical laboratory methods. ***Top, left:*** Aerial photo of shock bow wave generated by British supersonic jet car "ThrustSSC" {⇨Fig. 4.20–N} in the Black Rock Desert of Nevada. The photo was taken on October 8, 1997 from a microlight spotter aircraft, shortly before reaching Mach 1. Only 3 days later, GREEN broke the sound barrier. [Courtesy British Microlight pilot Richard MEREDITH-HARDY] ***Top, right:*** An array of head waves, emerging from different parts along the supersonic jet car, is visible against the background. [Courtesy U.S. photographer Chris ROSSI; http://ourworld.compuserve.com/homepages/Andy_Graves/SSC_pics.html] ***Bottom:*** The largest field-of-view schlieren photo (96×71 m^2) ever captured on film, taken of a full-sized aircraft Northrup T-38 at supersonic flight against the Sun. The plane (total length 14.12 m) was at 11.6 km altitude and at a slant distance of 19.5 km. [Courtesy Dr. Leonard M. WEINSTEIN, NASA Langley Research Center, Hampton, VA]

4.6 **HEAD WAVE STUDIES** – Model Sonic Boom Studies

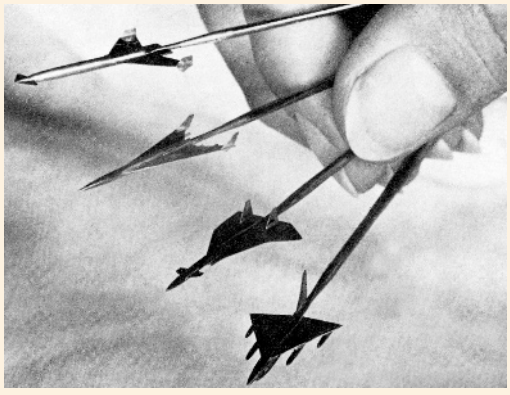

4.6–K To study sonic boom effects in the Langley 4×4-ft^2 (1.22×1.22-m^2) supersonic wind tunnel, Harry W. CARLSON and Odell A. MORRIS at NASA's Langley Research Center (Hampton, VA) used precision miniature models of supersonic transport and bomber configurations, only about 1 in. in overall length. They visualized the resulting head wave and flow field up to M = 2 using a schlieren technique and measured the model-induced pressure-time profile, the so-called "N-wave," using a differential pressure gauge. Model vibration as well as nonuniform and nonsteady tunnel flow were the prime difficulties encountered in this method of sonic boom testing. [J. Aircraft **4**, 245 (1967)]

4.6 **HEAD WAVE STUDIES** – Pressure Measurements Around a Flying Projectile

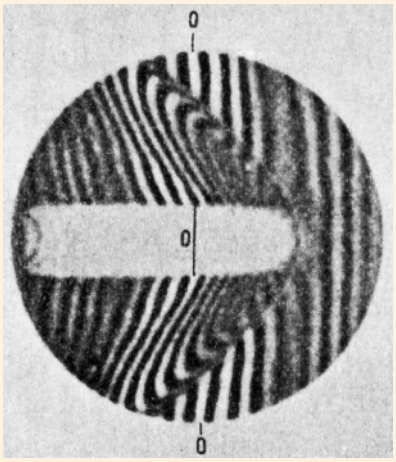

4.6–L Flash interferogram of a head wave generated by a supersonic steel projectile (v_0 = 620 m/s) taken by Ludwig MACH on August 15, 1893 with the Mach-Zehnder interferometer. To provide sufficient light intensity – the crucial condition particularly for this optical method – MACH used the continuous spectrum of an electric point spark and positioned a concave mirror at the back of the spark. He used high-sensitivity dry plates of the Schleussner Co., which had to be developed for a period of 1.5 h. Note that his original photo had a diameter of only 4 mm. From the shift of the system of interference lines he also tried to estimate the density and pressure behind the projectile head, a delicate problem. Using the Fresnel principle and converting densities into pressures, he estimated for a distance of 19 mm behind the projectile tip a maximum compression of 0.2 bar and at the tail a rarefaction of 0.07 bar. He correctly concluded that the projectile, pushing the air to the sides, had only slightly compressed the surrounding air. His studies provided the first quantitative evidence that Louis H.F. MELSENS' hypothesis (1872), that a supersonic projectile carries with it large masses of compressed air, was not correct. [Sitzungsber. Akad. Wiss. Wien **105** (IIa), 605 (1896)]

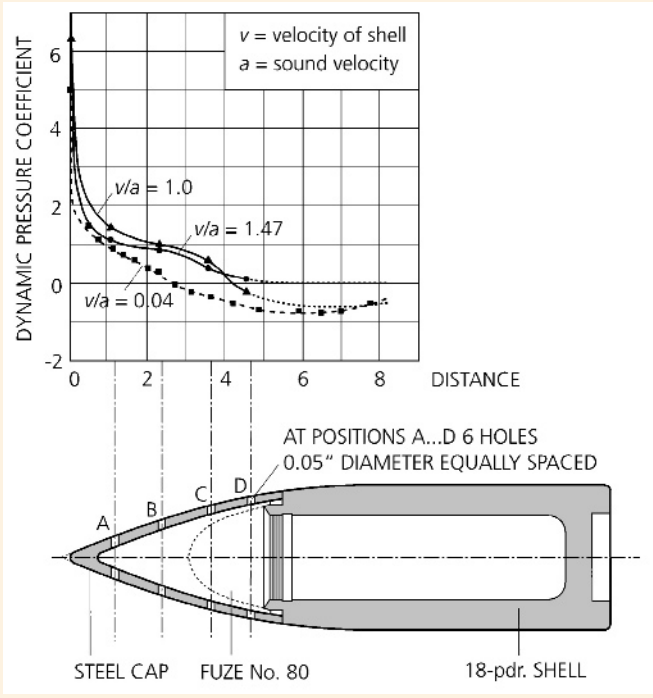

4.6–M In England, Leonard BAIRSTOW, Ralph H. FOWLER, and Douglas R. HARTREE used an ingenious method of measuring the pressure at different locations along the head of an 18-pdr. shell moving at high velocity. Each location of measurement was connected with a time fuse being affected by the actual pressure during flight. It is well known that the rate of burning of a time fuse depends on pressure. The measurements were carried out in two steps: (i) At first this dependency between the external pressure and the time was determined by laboratory experiments. If the circumstances of the shell's motion are known, this leads at once to a relation between the dynamic pressure, the velocity of the shell, and the prevailing atmospheric conditions. Depending on the projectile velocity, the time fuse burns slower or faster, eventually igniting the charge. (ii) Then the observers measured the time and location of the explosion. The results obtained for the derived dynamic pressure coefficient, $p/\rho v^2$, are shown here schematically for different velocity ratios v/a, with v as the projectile velocity, a as the sound velocity, ρ as the density, and p as the overpressure (or underpressure) with regard to the quiescent air. The curve for $v/a = 0.04$ (*broken line*) was obtained in wind-tunnel experiments. Note that in 1920 the term *Mach number*, here the ratio v/a, had not yet been coined. [Drawings by EMI, Freiburg; after Proc. Roy. Soc. Lond. **A97**, 202 (1920), Figs. 1 and 3]

4.6 **HEAD WAVE STUDIES** – Blunt Body Concept

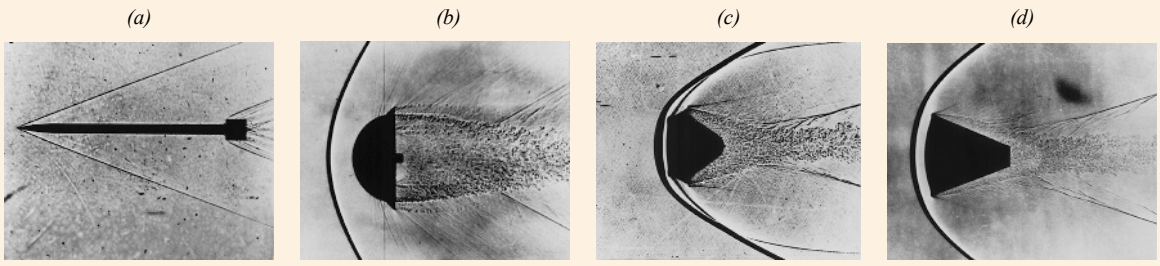

4.6–N Example of aerodynamic research contributing to the U.S. Project Mercury, the first series of manned space flights conducted in the period 1961–1963. In 1952, H. Julian ALLEN at NACA's Ames Aeronautical Laboratory pioneered the Blunt Body Theory, which made possible the heat shield designs embodied in the Mercury, Gemini, and Apollo space capsules, enabling astronauts to survive the fiery reentry into the Earth's atmosphere. A blunt body produces a shock wave in front of the vehicle that actually shields the vehicle from excessive heating. As a result, blunt body vehicles can stay cooler than pointy, low-drag vehicles. ***(a)*** Initial concept. ***(b)*** Blunt body concept 1953. ***(c)*** Missile nose cones 1953–1957. ***(d)*** Manned capsule concept 1957. Later versions of spacecraft used the blunt body design and an ablative surface [Courtesy NASA; http://www.centennialofflight.gov/essay/Evolution_of_Technology/reentry/Tech19G3.htm]

4.6 **HEAD WAVE STUDIES** – Phenomena at Hypersonic Velocities

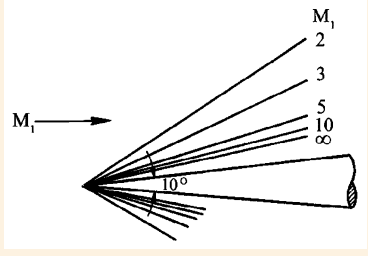

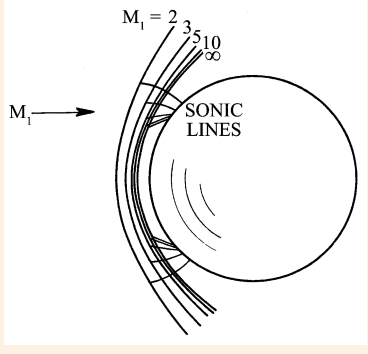

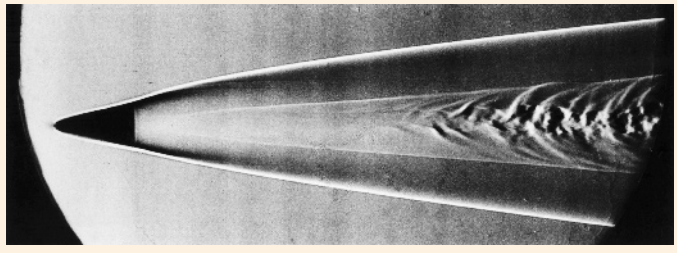

4.6–O ***Left:*** Illustration of the effect of high Mach numbers at hypersonic flight. For a slender pointed body or a wing with a sharp leading edge (*top*) the shock may be attached, or detached, *i.e.*, standing off from the surface, if the nose of the body or the wing leading edge is blunt (*bottom*). For a perfect gas with $\gamma = 1.4$, the angle between the shock and the body decreases with increasing Mach number M_1, until slightly above $M_1 = 10$ a limiting shock position is reached. This typical feature of hypersonic flight holds both for a slender cone (*top*) and a blunt body such as a ball (*bottom*). In the latter case, the shock stands off from the body by an amount that decreases as M_1 increases. Just behind the front part of the shock the flow passes through the local velocity of sound at the sonic line and then becomes supersonic. [R.N. COX and L.F. CRABTREE: *Elements of hypersonic aerodynamics*. The English Universities Press, London (1965), pp. 8-9] ***Right:*** Photo of a wake behind a conical projectile flying at 4,113 m/s through the air at 0.13 bar. Interest in wakes very far downstream has been stimulated by observations of entry vehicles entering the atmosphere, which may leave ionized trails thousands of feet long. In the 1950s, various criteria were worked out to calculate the transition point from laminar to turbulent flow. [B.C. JAEGGY: Rept. CO 229/85, ISL, Saint-Louis, France (1985)]

4.7 NOZZLE STUDIES AND APPLICATIONS – Early Safety Valve Constructions

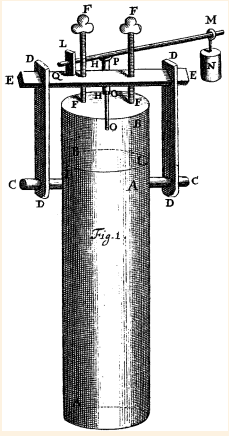

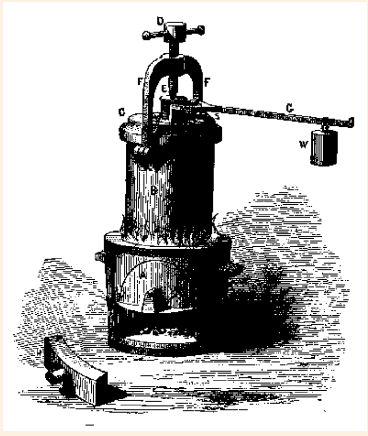

4.7–A ***Left:*** In 1679, the French-born British physicist Denis PAPIN designed the first safety valve to prevent an explosion of his "steam digester," the first pressure cooker. It consisted of a small plate *P* covering the exit hole of a pipe *H-H* in the cooker lid and loaded by a weight *N*. When the pressure exceeded a certain value, *P* was lifted so that the steam could escape. [D. PAPIN: *A new digester or engine for softening bones*. Bonwicke, London (1681)] ***Right:*** View of PAPIN's digester. [http://www.ledenispapin.com/digesteur.htm]

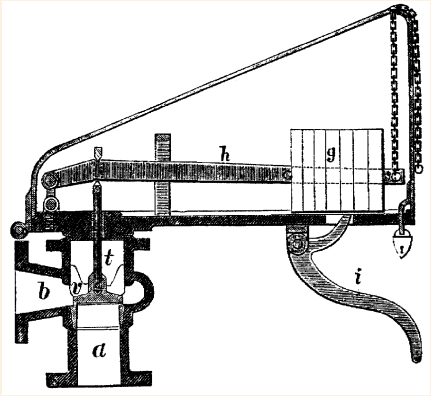

4.7–B PAPIN's valve was also used in steam boilers and modified in many ways. To avoid unauthorized manipulations of the valve – one of the numerous reasons for disastrous steam boiler explosions – it was enclosed by a case and secured by a locker. The so-called "safety valve" became one of the most delicate elements of steam engines and stimulated nozzle outflow research. [*Brockhaus Enzyklopädie*. Brockhaus, Leipzig (1898), vol. IV, p. 728]

4.7 NOZZLE STUDIES AND APPLICATIONS – Predecessors of Steam Turbines

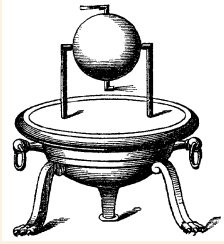

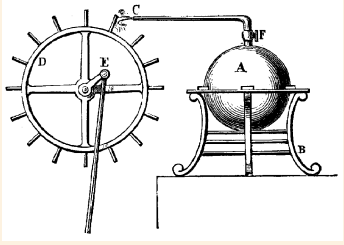

4.7–C Early steam engines were used for demonstration purposes or as children's toys, but never gained any technical importance. ***Top:*** The "steam ball" [*aeolipile*], the first steam turbine, was described by HERON of Alexandria in his *Pneumatica* (A.D. 100). Based on Sir Isaac NEWTON's Third Law of Motion, his mechanical principle of reaction, it consists of a ball filled with steam and is provided with a number of fine nozzles arranged in a tangential direction around the ball. Steam emerging from these nozzles sets the steam ball in rotation. [*Meyers Konversations-Lexikon*. Bibliogr. Inst., Leipzig (1894), vol. 4, p. 525] In earlier centuries, HERON's small steam turbine was often demonstrated in physical cabinets. The reaction principle was later resumed and successfully applied on an industrial scale in Andreas SEGNER's water reaction turbine (1750) and in Charles PARSON's steam reaction turbine (1884). ***Bottom:*** Schematic of Giovanni BRANCA's "steam wheel" (1629), which is based on the impulse (or action) principle. The steam emerging from a narrow nozzle is directed toward the blades of a small paddle wheel. The principle of action was later resumed in DE LAVAL's impulse turbine, which used a special nozzle of convergent-divergent geometry, the so-called "Laval nozzle." The very high steam speed at the exits of Laval nozzles, impinging on blades projecting from a wheel, resulted in a high turbine efficiency (1888). [*Meyers Konversations-Lexikon*. Bibliogr. Inst., Leipzig (1875), vol. 4, plate *Dampfmaschine I*]

4.7 NOZZLE STUDIES AND APPLICATIONS – Forerunners of the Laval Nozzle

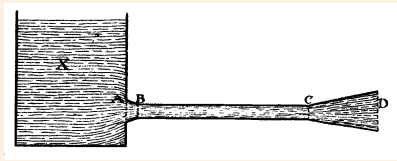

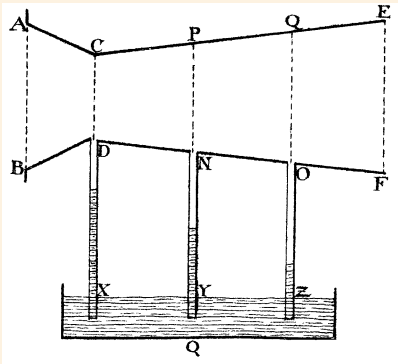

4.7–D ***Left, top:*** In the 1790s, the Italian physicist Giovanni B. VENTURI, experimenting with the outflow of water from vessels, observed that the rate of outflow could be increased by attaching to the end of a drain pipe a conical diverging tube, thus inventing the diffuser principle. ***Left, bottom:*** While studying the flow in a convergent-divergent tube, VENTURI noticed that in the constriction the flow speed increased and the pressure decreased, an important phenomenon used in the so-called "Venturi tube" to measure fluid flows, and as a pump. [Ann. Phys. **2**, 418 (1799)] ***Right:*** In the mid-1870s, the German KÖRTING Brothers at Hannover used a divergent nozzle in their steam injection pump, even before Gustaf DE LAVAL. However, their patent application was rejected. This is a more recent schematic of a steam jet vacuum pump. A supersonic jet velocity improves the pump efficiency. [After R. VON MILLER (ed.) *Lexikon der Energietechnik und Kraftmaschinen*. Deutsche Verlagsanstalt, Stuttgart (1965), vol. 6, p. 188]

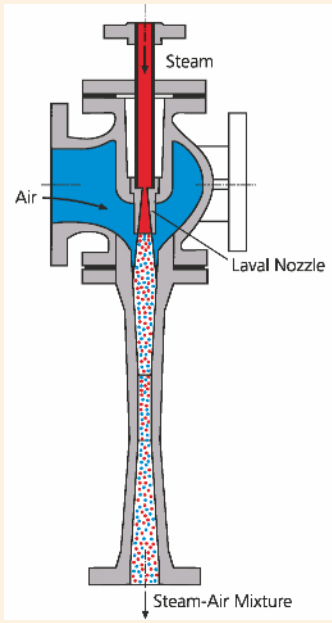

4.7 NOZZLE STUDIES AND APPLICATIONS – Use of the Venturi Nozzle in the First Wind Tunnel

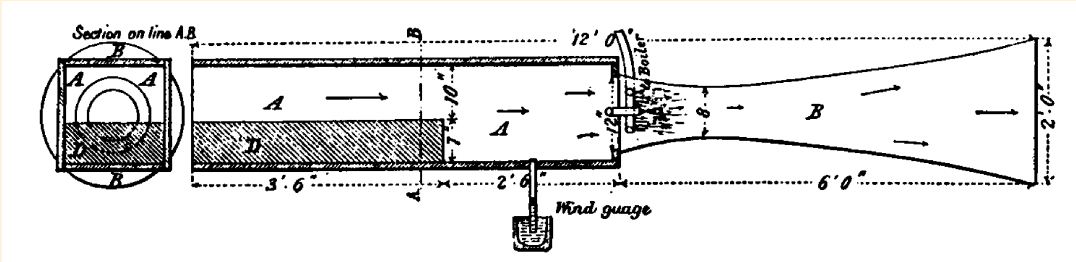

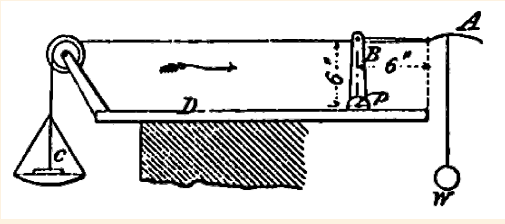

4.7–E ***Top:*** The very first wind tunnel constructed in 1884 by the Englishman Horatio F. PHILLIPS used a diffusor throat at its exit – in a sense a Venturi tube, the forerunner of the Laval nozzle. The device had a rectangular cross section and applied a system of steam nozzles that accelerated the air in the nozzle, thus creating an almost steady flow over the test object up to a maximum flow velocity of 18 m/s. ***Left:*** PHILLIPS positioned an airfoil *A* about 1 m in front of the steam nozzle and measured the lift with a balance, a method that quickly became a standard technique in continuous-flow wind tunnels. [Engineering (London) **40**, 160 (1885)]

4.7 NOZZLE STUDIES AND APPLICATIONS – First Use of Laval Nozzle in a Steam Turbine

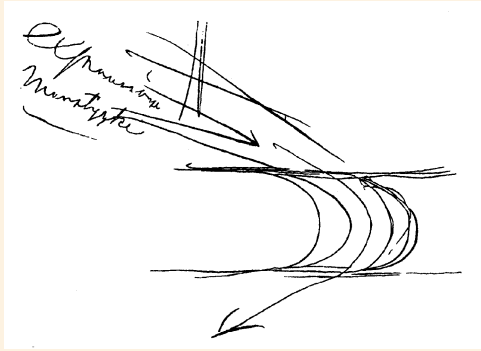

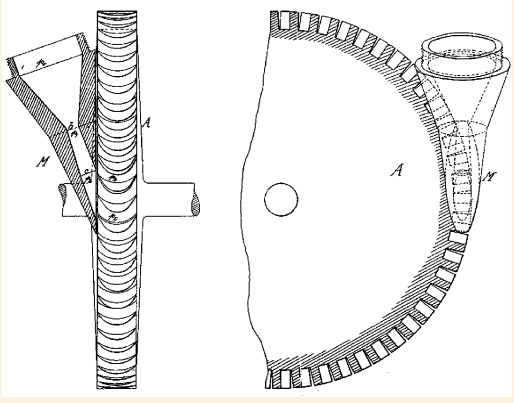

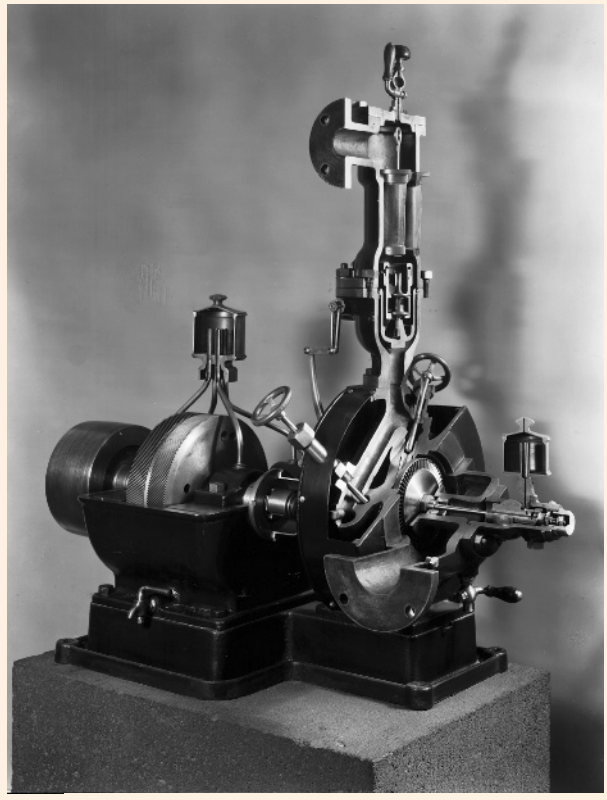

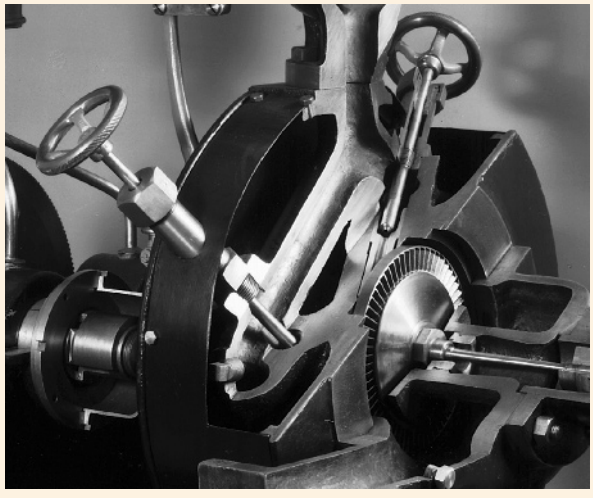

4.7–F Gustaf DE LAVAL, a Swedish mechanical engineer, dedicated much time to optimizing the geometry of steam nozzles for use in steam turbines. He correctly recognized by experimentation that a divergent geometry significantly increased the velocity of the steam jet, thus improving the efficiency of steam turbines. ***Left, top:*** His sketch of the first axial impulse blade with a rather modern aerodynamic blade form and a supercritical nozzle, dated 1888. His Swedish handwriting reads *expansion munstycke*, meaning "expansion nozzle." [I. JUNG: *De Laval Memorial Lecture 1973*, Roy. Swed. Acad. Eng. Sci. (1973)] ***Left, center:*** Schematic of the Laval nozzle as used in his steam turbine. Note the divergent nozzle exit geometry [C.G.P. DE LAVAL: *Steam inlet channel for rotating engines*. Swed. Patent No. 1,902 (1888)] ***Right:*** Photograph of Laval's steam turbine from 1888, the first to employ Laval nozzles. ***Left, bottom:*** Enlargement of a cut through the injection system, showing the turbine wheel and two Laval steam nozzles in more detail. [Courtesy Deutsches Museum, Munich]

4.7 **NOZZLE STUDIES AND APPLICATIONS** – Steam Flow in a Divergent Nozzle

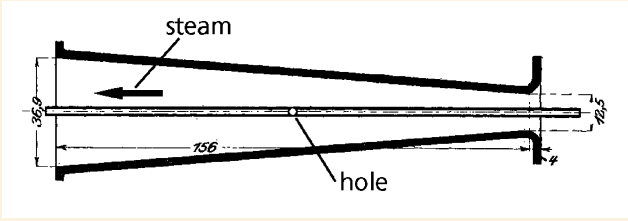

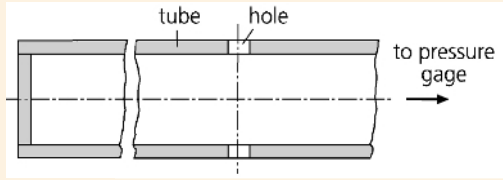

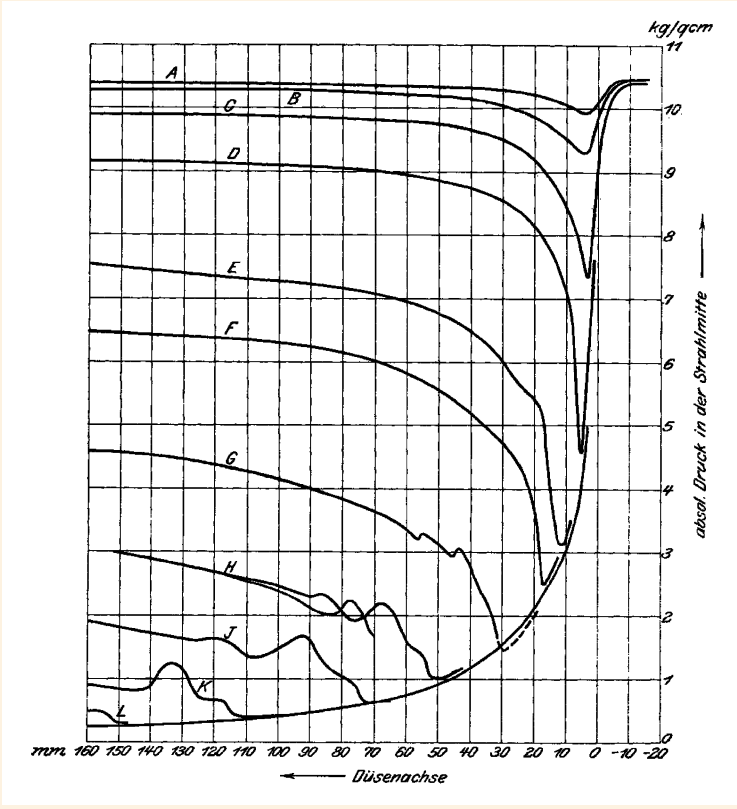

← The parameter of the family of curves (*A*, *B*,…*L*) is the backpressure that is adjustable over any desired range by closing a valve downstream of the nozzle exit. Note that the pressure drop initially follows the line of free expansion but, depending on the chosen backpressure, rapidly increases. Nozzle characteristics range from subsonic flow at high backpressure (*A*…*C*) to supersonic flow at low backpressure (*D*…*L*).

4.7–G Aurel B. STODOLA, a Hungarian-Swiss mechanical engineer at ETHZ, made the first axial pressure measurements of supersonic flow inside a Laval nozzle. ***Left, top:*** Using a 156-mm-long divergent nozzle with a steam entrance diameter of 12.5 mm and an exit diameter of 36.9 mm, STODOLA measured the axial pressure by moving a tubular gauge in the axial direction. The thin tube, closed at the left end and connected to a mechanical pressure gauge at its right end, allowed one to measure the pressure variation along the nozzle axis. ***Right:*** The tube was provided with a small hole drilled perpendicular to the tube axis and connected with a manometer. [By the author] ***Left, bottom:*** Diagram showing curves of measured absolute steam pressures along nozzle axis. STODOLA correctly interpreted the strong increases in pressure as a "condensation shock" [Germ. *Verdichtungsstoß*], such as was derived theoretically in 1859 by the German mathematician G.F. Bernhard RIEMANN. At low backpressures (curves *H* to *L*), the local pressure shows small oscillations that, however, are quickly used up by friction when approaching the nozzle exit. [A.B. STODOLA: *Die Dampfturbinen*. Springer, Berlin (1903), p. 19]

4.7 NOZZLE STUDIES AND APPLICATIONS – Laval Nozzles as Power Generators in Aeronautics

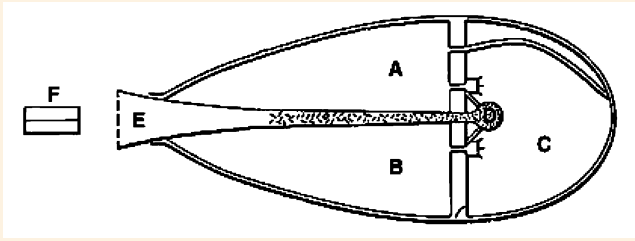

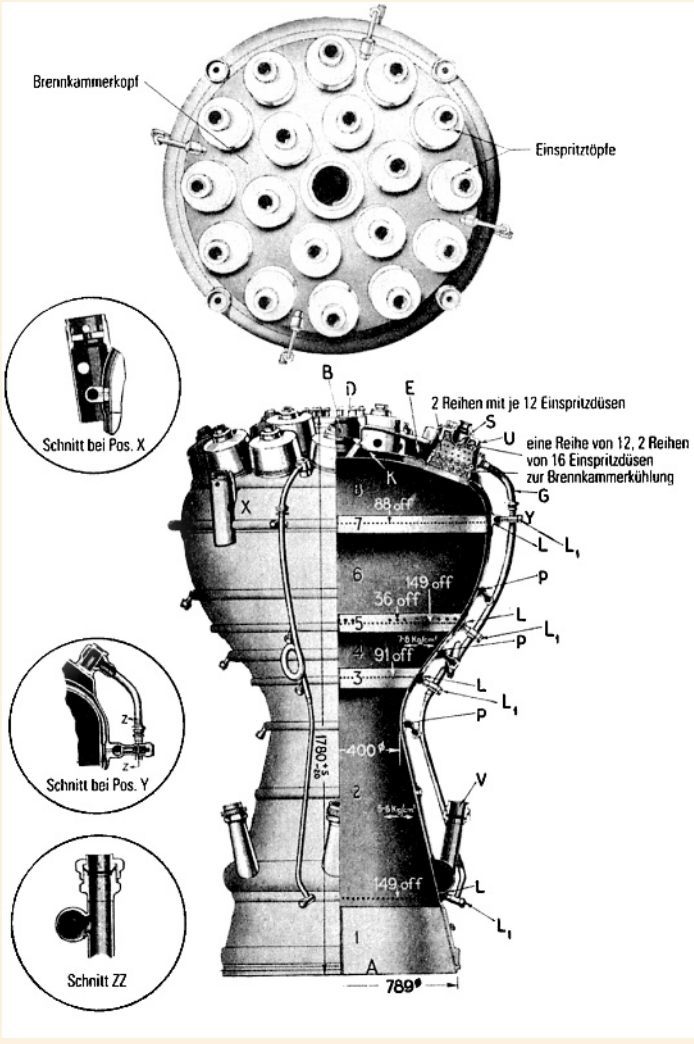

4.7–H The concept of a convergent-divergent nozzle geometry, the so-called "Laval nozzle," had also been proposed for propulsion purposes, particularly to realize in this way a high exit velocity of the hot exhaust gases. ***Top:*** The Russian rocket pioneer Konstantin E. TSIOLKOVSKY proposed manned rocketry in the 1890s. This is a conceptual sketch of a liquid fuel rocket from his 1903 milestone paper entitled *Exploration of Cosmic Space by Means of Reaction Devices* (Nauchnoe Obozrenie). The letters, here added later, designate: *A* – tank with freely evaporating liquid oxygen kept at very low temperature; *B* – tank with liquid hydrogen (or hydrocarbon); *C* – crew and breathing equipment; *D* – burning chamber; *E* – exhaust nozzle; *F* – rudders, positioned in the stream of the exhaust gases, serving for flight control (a method which was later used in the German V2). The rocket thrust chamber and a partition wall separate the fuel and oxidizer. [Uranos Group, *see* http://www.uranos.eu.org/biogr/ciolke.html] ***Bottom:*** View of the 1.83-m-long engine of the German WWII rocket A-4, in 1943 renamed V2 (meaning "Vengeance Weapon 2"). The rocket engine consisted mainly of an 18-nozzle injection system, a spherical combustion chamber, and a common exhaust nozzle, a large 25° conical Laval nozzle. A small, only 30-cm-diameter two-stage 500-hp turbo-centrifugal pump (not shown here) – in WW II a riddle to allied secret services – injected the propellant (liquid oxygen and a fuel mixture consisting of 75% ethyl alcohol and 25% water) into the combustion chamber. The hot combustion gases, leaving the combustion chamber at a temperature of about 2,400 °C and expanding to ambient pressure, were accelerated up to 2,000 m/s, thus producing by the exhaust blast a thrust of 55,000 pounds for about 1 min. The A-4, weighing about 13.5 tons at takeoff, reached a maximum speed of over $M = 4$ {⇨Fig. 4.20–C}. Its maximum range was about 320 km. [M.J. NEUFELD: *The rocket and the Reich*. Free Press, New York (1995), p. 98]

4.8 SUPERSONIC JET PHENOMENA – SALCHER's and MACH's First Free Air Jet Studies

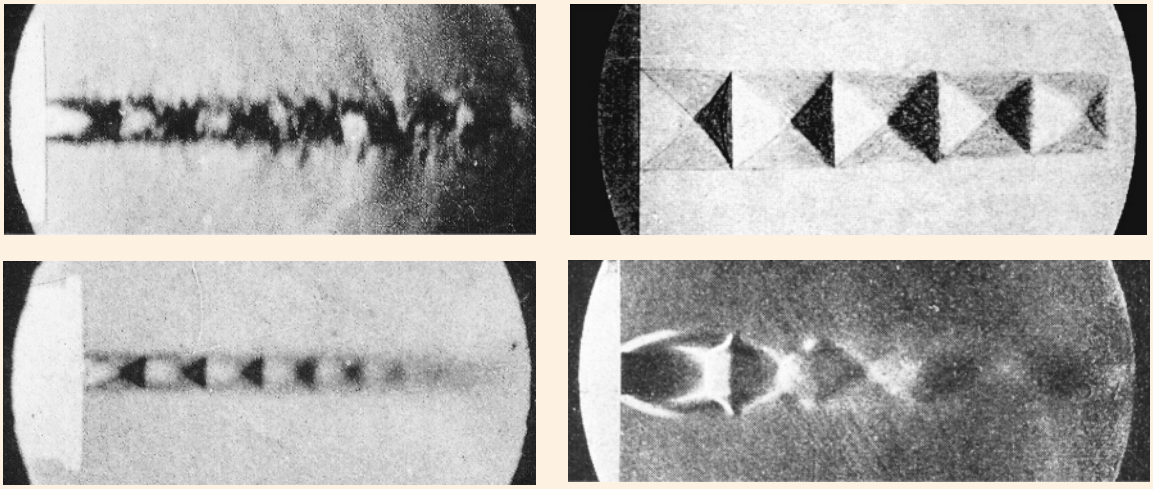

4.8–A Ernst MACH at the Charles University in Prague inspired a number of studies on the rapid outflow of gases from small orifices that brought to light many new supersonic flow phenomena. ***Left:*** Together with Peter SALCHER, an Austrian physics professor at the Royal Naval Academy in Fiume, he made the first schlieren photos of a supersonic air jet emerging from a 4.5-mm-dia. nozzle operated at a pressure of 37 bar. They used two different methods of illumination: flash illumination (*top*) provided by an electric spark is useful to visualize momentary nonstationary phenomena, such as vortices. On the other hand, they are suppressed when a long-duration illumination is used, such as a Geissler-discharge tube (*bottom*), which shows more clearly the stationary wave pattern. [Sitzungsber. Akad. Wiss. Wien **98** (IIa), 1303 (1889)] ***Right:*** Ludwig MACH, resuming these experiments in the mid-1890s, studied more closely the wave pattern inside supersonic free air jets resulting from different reservoir pressures and nozzle shapes. At low pressure he observed a crossed wave pattern in the case of regular shock reflection (*top*). At higher pressures, the crossed wave pattern transformed into a new wave front at the point of intersection (*bottom*) – the so-called "Mach disk," a result of a symmetric irregular shock interaction. [Sitzungsber. Akad. Wiss. Wien **106** (IIa), 1025 (1897)]

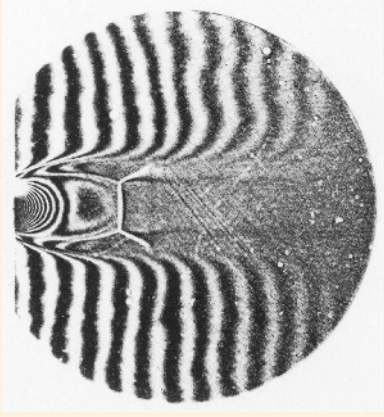

4.8–B Flash interferogram of an air jet, emerging under 20 bar from a cylindrical nozzle with a 7.5-mm dia. and propagating from left to right. The mouth of the nozzle is on the far left side and not visible in the picture. This interferogram was taken in July 1893 by Ludwig MACH using the famous "Mach-Zehnder interferometer," a construction invented in 1891 by him and, independently, by Ludwig ZEHNDER at the University of Würzburg, a Ph.D. student of Prof. Wilhelm Conrad RÖNTGEN. The picture clearly shows the formation of a steady "Mach disk" in front of the nozzle exit. [Sitzungsber. Akad. Wiss. Wien **106** (IIa), 1025 (1897)]

4.8 SUPERSONIC JET PHENOMENA – EMDEN's First Steam Jet Studies

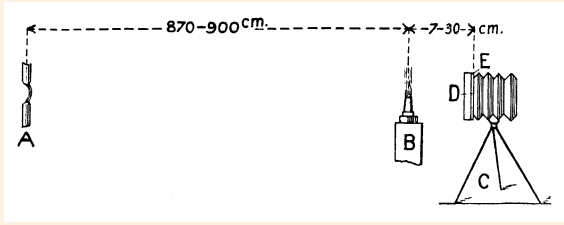

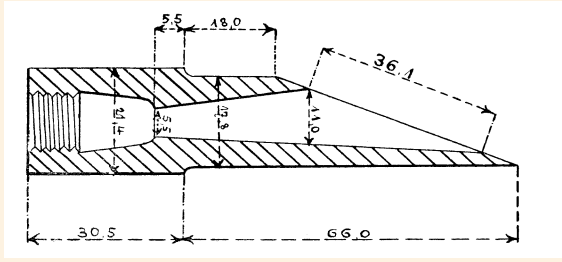

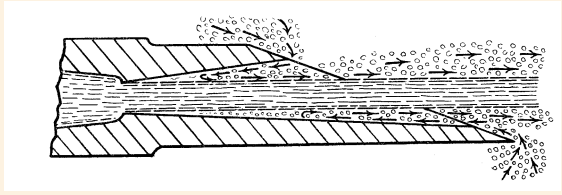

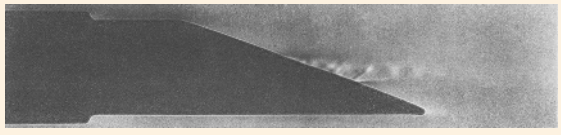

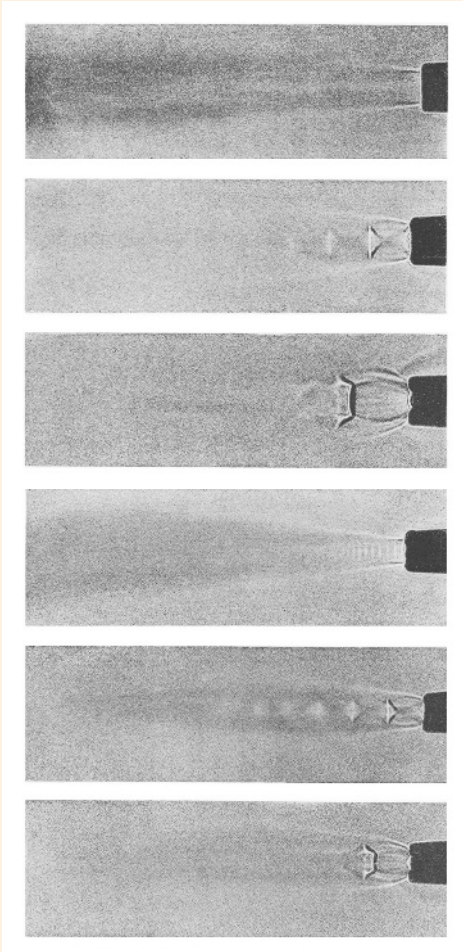

4.8–C Paul EMDEN, a Swiss physicist at the University of Basel, first demonstrated in the early 1900s that the stationary jet structures of divergent nozzles operated with steam are very similar to those operated with air, thereby referring to studies of his brother Robert EMDEN who in 1898 carried out nozzle outflow experiments at the TH Munich using pressurized air. ***Left, top:*** P. EMDEN, using a carbon arc lamp as an intense point light source and a standard camera with a shutter, photographed the jet structure in transmitted light. ***Left, bottom:*** For cylindrical, slightly divergent nozzles 3.63 mm *(a–c)* and 2.65 mm *(d–f)* in diameter he obtained a pattern of standing waves. Note the Mach reflection in *(c)* and *(f)*. ***Right, top:*** Dimensioned sketch of an original Laval nozzle made in Germany by the Maschinenbauanstalt Humboldt AG in Köln-Kalk, which produced Laval turbines under license. ***Right, center:*** Schematic showing the steam flow. The low pressure at the edge of the orifice sucks in air; thus the steam jet produces a pumping action – a detrimental effect that reduces the outflow velocity. ***Right, bottom:*** This picture of a narrow stationary air jet emerging from a Laval nozzle at a pressure of 1.8 atmospheres reveals a similar wave pattern as obtained with cylindrical divergent nozzles. Assuming that the standing-wave patterns are produced by normal sound waves – rather than by shock waves – P. EMDEN erroneously concluded that the jet velocity could not exceed the velocity of sound. [P. EMDEN: Ph.D. thesis, University of Basel (1903), publ. by R. Oldenbourg, Munich (1903)]

4.8 SUPERSONIC JET PHENOMENA – PRANDTL's and MEYER's Nozzle and Jet Studies

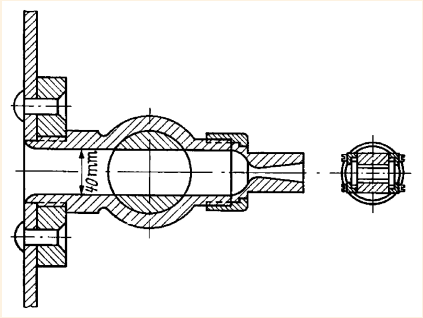

↑ The test nozzle was attached to a 40-mm-dia. ball valve.

4.8–D In the early 1900s, Ludwig PRANDTL and Theodor MAYER at Göttingen University studied steady air flow fields inside and outside of plane nozzles enclosed between two parallel glass plates using the schlieren method which reproduces regions of compression and expansion as dark and bright areas, respectively. ***Left, top:*** Experimental setup. ***Left, bottom:*** Schematics of three main jet types: jet emerging *(a)* from a parallel nozzle with supersonic velocity; *(b)* from a convergent nozzle with sound velocity; and *(c)* from a divergent nozzle showing a more simplified jet structure. *Arrows* in the schematics indicate the direction of density gradients. ***Right:*** Schlieren pictures of jet structures: *(a)* jet emerging supersonically from a divergent nozzle, exhibiting in the case of overpressure ($P_{JET} > P_0$) a series of crossing fans of expansion and compression waves; *(b)* supersonic jet in the case of equal pressure ($P_{JET} = P_0$), revealing a more uniform structure; and *(c)* jet emerging with sound velocity from a parallel nozzle, showing disturbances. In all cases the flow propagates from left to right. [Physik. Z. **8**, 23 (1907)]

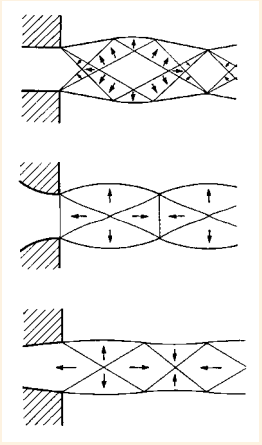

(a)

(b)

(c)

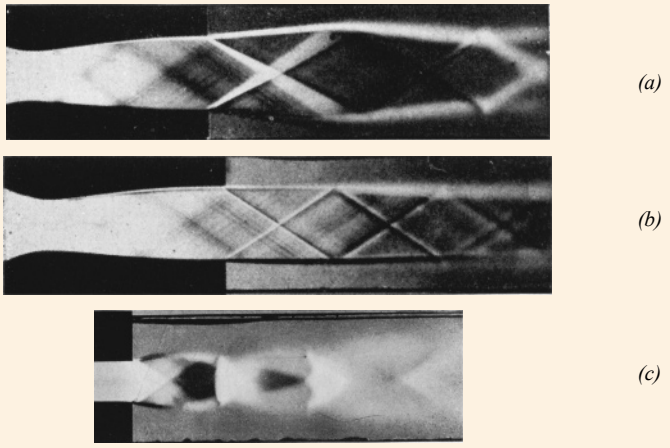

(a)

(b)

(c)

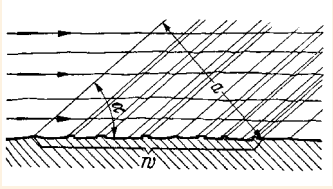

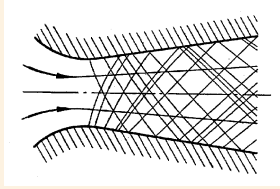

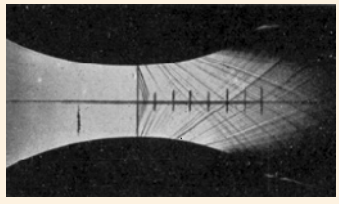

4.8–E Schematics of the interaction of a supersonic flow with wall discontinuities in a parallel flow *(left)* and a divergent flow (*center)*, which creates an oblique pattern of lines, so-called "Mach lines," similar to lines generated at the rough periphery of a supersonic projectile. [Phys. Z. **8**, 23 (1907)] The flow through a Laval nozzle (*right*) was chosen such that sound velocity was reached at the passage of the narrowest part of the nozzle, which generates a supersonic flow in the expanding section. To improve optical visualization, the roughness of the nozzle wall was artificially increased using sandpaper. [Th. MEYER; Ph.D. thesis, University of Göttingen (1908)]

4.8 SUPERSONIC JET PHENOMENA – THOMER's First Radiographs of Detonating Shaped Charges

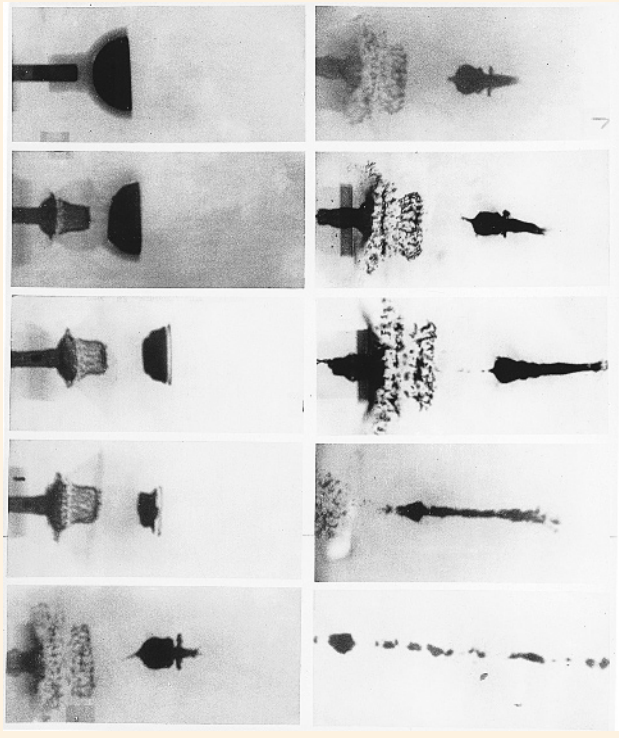

4.8–F This series of historic flash radiographs of hemispherical shaped charges was made in 1941 by Gustav THOMER at Prof. Hubert SCHARDIN's Ballistic Research Laboratory of the Technische Akademie der Luftwaffe (Air Force Technical Academy) in Berlin-Gatow and published in November 1941 in a secret institute report. In order to illustrate the evolution of the jet phenomenon, the pictures were taken from different charges at different time instants and assembled to a chronology of a detonating hollow charge, a technique called "pseudocine radiography." The time proceeds from *top* to *bottom*, and from *left* to *right*. The jet formation and propagation as well as its subsequent rupture into a number of droplets is clearly resolved. [Courtesy Dr. Pascale LEHMANN, ISL, France; Proc. Flash Radiography Symp.. 36th Natl. Fall Conf. of American Society for Nondestructive Testing (ASNT), Houston, TX (1976), pp. 1-14]

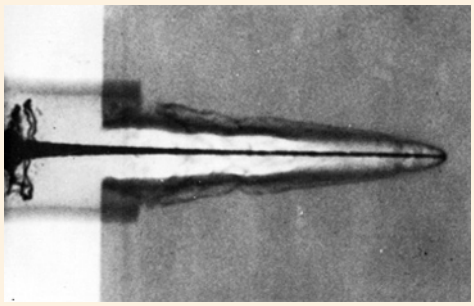

4.8–G ***Left:*** Flash radiograph of a supersonic jet resulting from a shaped charge and penetrating a duralumin target. Note that the shock wave initiated in the target is not visible. In detonating shaped charges, most of the jet formed moves at hypersonic speed, the tip traveling in the 10–14 km/s region and the jet tail at a lower velocity. [F. JAMET and G. THOMER: *Flash radiography*. Elsevier, Amsterdam (1976), p. 137] ***Right:*** View of a "slug," the back part of the collapsing liner that travels along the same direction as the jet but at much lower velocity than the jet tail. In this well-preserved form, it is only occasionally found after detonation of shaped charges [Courtesy Dr. Norbert HEIDER, EMI, Freiburg]

4.8 SUPERSONIC JET PHENOMENA – Formation and Structure of Liquid Jets

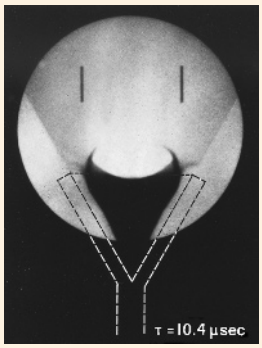

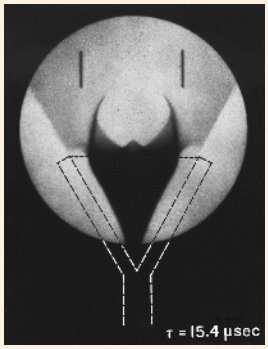

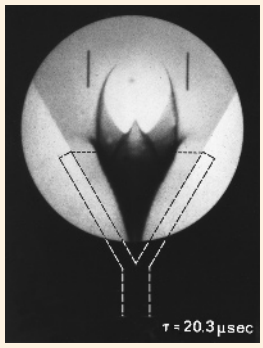

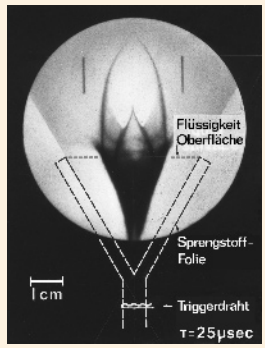

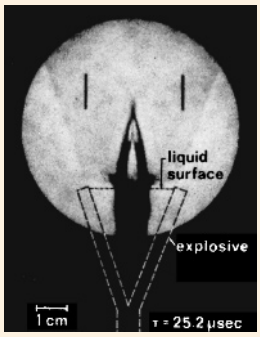

4.8–H Peter KREHL, Werner HEILIG, and Ulrich HORNEMANN at EMI, Freiburg, studied unsteady Mach reflection in organic liquids. ***Top:*** This series of flash radiographs from the formation of supersonic liquid jets was obtained when a plane hollow 60° cone of a solid explosive (nitropenta), filled with a liquid (carbon tetrachloride, CCl_4), was ignited at its cone tip. The region of interaction of the two head waves, indicated by the two detonation waves in the liquid, results in "inverse Mach reflection," a regressive type of irregular reflection. The liquid, squeezed and accelerated along the cone axis, is thrown out as a two-jet phenomenon. The two outer jets are formed first, followed by the generation of the two inner jets. Both branches of outer and inner jets move at a velocity of about 1,000 m/s. ***Bottom:*** At decreasing cone angle, here shown for a 40° cone geometry, the intersection of the two colliding head waves just before reaching the surface is regular, but the typical ejection phenomenon is again obvious. However, the jet formation becomes now increasingly focused in the axial direction, and the jet velocity increases. [Proc. 11th Int. Symp. on Shock Tubes and Waves, Seattle (July 1977), p. 303]

↑ Optical shadowgraph of a petroleum jet (*top*) and X-ray shadowgraph of a nitromethane-methanol jet (*bottom*), emerging from a 2-mm- and a 4-mm-dia. cylindrical nozzle, respectively, at a velocity of about 410 m/s into the atmosphere.

4.8–I The dynamics of pulsed supersonic jets emerging from nozzles and injected into a gas at atmospheric or high static pressures can be studied using optical photography, flash X-rays, and bursts of electrons. In most combustion applications, the jet should break up into a spray of droplets as fine as possible. ***Left:*** Liquid jets – particularly with diameters exceeding several millimeters – often show in optical shadowgraphy a plumelike disintegration (*top*). However, flash soft radiography reveals that the liquid jet core still exists for a distance of many nozzle diameters (*bottom*). [Courtesy Dieter WARKEN, EMI Archives, Freiburg] ***Right:*** Flash soft radiography can also resolve density discontinuities in the jet core such as caused by shock waves that propagate in the core as in a wave guide. [Picture by Peter KREHL (EMI Archives, Freiburg). Proc. 12th Int. Symp. on Ballistics, San Antonio, TX (1990); Proc. 19th Int. Congr. on High-Speed Photography and Photonics, Cambridge, U.K. (1990)]

4.8 SUPERSONIC JET PHENOMENA – Generation of Microjets

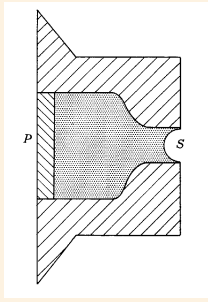

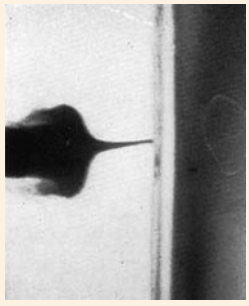

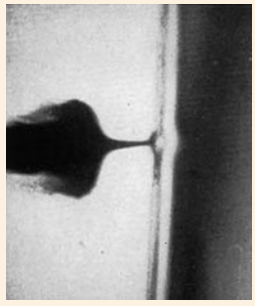

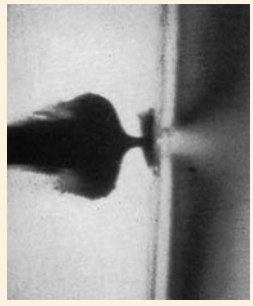

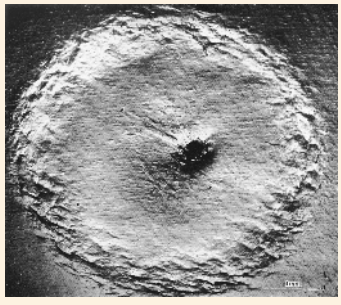

4.8–J In the 1960s, Frank P. BOWDEN and John H. BRUNTON at Cavendish Laboratory (Cambridge, U.K.) studied the formation of microjets in liquids under the influence of impact or shock. ***Top, left:*** Schematic of generating small high-velocity liquid jets. A small amount of water is held in a strong steel container with a small hole in it. A sudden pressure pulse is generated, *e.g.*, by firing a bullet on the rubber plug *P*. When the shock wave reaches the curved free surface *S*, the water emerges as a tiny Munroe jet at much higher velocity. ***Top, right:*** A three-frame series showing the microjet formation process and its interaction with a steel surface; interframe time is 0.8 µs. This technique of liquid jet generation was later refined and used in rain erosion studies. ***Bottom:*** Example of a 4-mm-dia. crater formed by liquid impact on stainless steel. Near its center a second small but deep crater has been formed by a microjet. [Phil. Trans. Roy. Soc. Lond. **A260** (1966), plates 10 and 11]

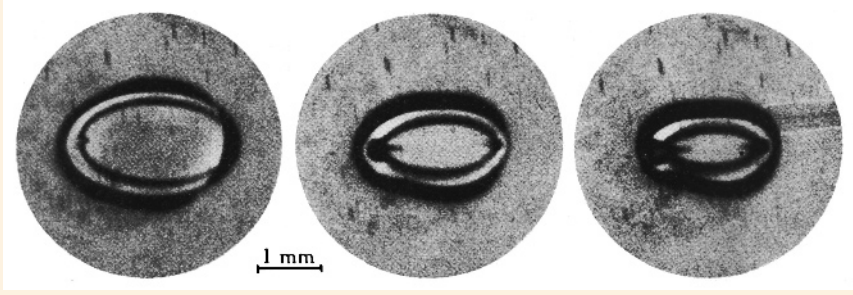

4.8–K There is strong evidence that microjets play a significant role in the initiation process of liquid high explosives. The initiation by impact or shock is essentially a thermal process in which a small region of the explosive is heated to a temperature at which reaction can occur. Shock heating requires very high pressures (ca. 60 to 100 kbar). However, if a discontinuity – such as a bubble or cavity – is present in the liquid explosive, the energy of the shock can be concentrated in a small region, and a localized "hot spot" can be formed that initiates detonation. Frank P. BOWDEN and M.P. MCONIE at Cavendish Laboratory demonstrated that an annulus of nitroglycerin, which had trapped a single cavity containing air and was struck by a falling hammer, generated tiny jets in the regions of maximum curvature. These so-called "microjets" project at about 30 to 50 m/s into the central cavity as the cavity is compressed. ***Left:*** Beginning of jet formation, here starting at the left inner wall of the bubble. ***Center:*** 10 µs later, a second jet is formed at the opposite end of the cavity. ***Right:*** After another 5 µs, two jets have formed that later collide head on. The initiation of microjets will aid adiabatic heating of the entrapped gas and initiation of detonation. [Nature **206**, 380 (1965); Phil. Trans. Roy. Soc. Lond. **A260**, 94 (1966)]

4.8 SUPERSONIC JET PHENOMENA – Astrophysical Jets

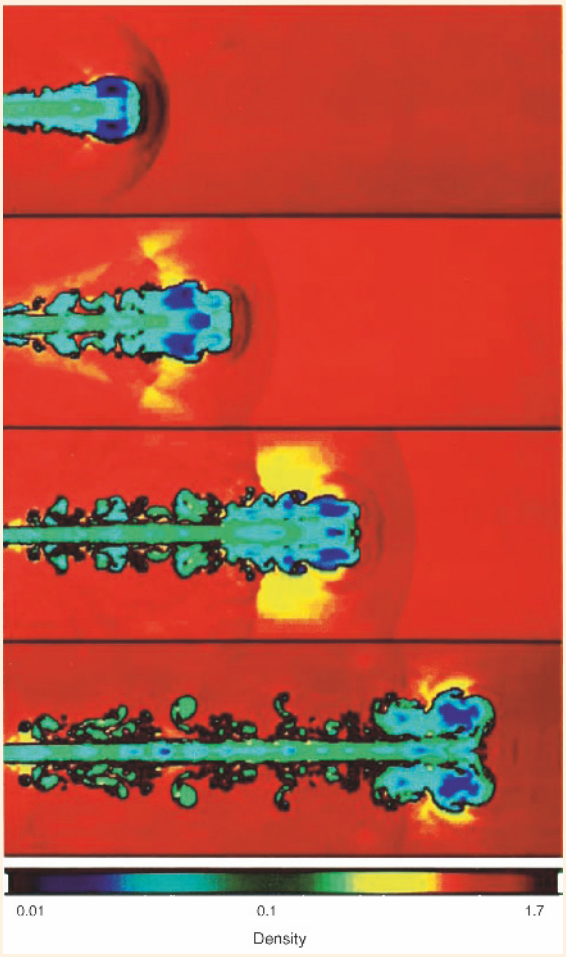

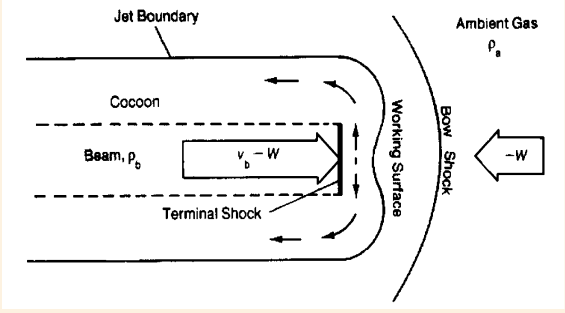

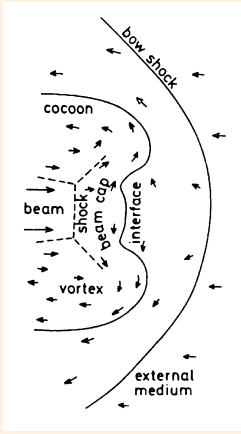

← Detail of an astrophysical *terminal jet shock* structure originating from a powerful radio source. The beam gas does not collect at the region of impact, the so-called "beam cap," but is shock-decelerated and deflected sideways to form a low-density backward-flowing cocoon around the forward-moving beam. At the terminal shock the jet gas is heated and flows into the cocoon. The interface is the contact discontinuity between the shocked jet material and the shocked intracluster material.

4.8–L Astrophysical jets are mysterious phenomena that can extend in a remarkably collimated manner from the center of a radio galaxy to distances of thousands or millions of light-years. In order to study nonlinear features of supersonic jet flow that may explain the unusual stability of extragalactic jets, astrophysicists at the MPI für Physik und Astrophysik (Garching, Germany) performed numerical studies using a high-resolution gasdynamic code. ***Left, top:*** Numerical simulation of the evolution of a supersonic jet (M = 3) expanding from a narrow orifice into a quiescent gas; the calculated gas density varies according to the color code *(e)*. Stages of jet formation: *(a) & (b):* Establishment and turnover of jet cocoon, which is composed of gas that has passed through the terminus of the jet. *(c) & (d):* Subsequent mixing of cocoon and ambient gas, which leaves intact only a lobe of cocoon gas at the jet head. The bow shock, driven by the supersonically advancing jet head, is revealed by the jump in density it produces. [M.D. SMITH, M.L. NORMAN, K.H.A. WINKLER, L. SMARR, MNRAS **214**, 67 (1985); Los Alamos Sci. Mag. **12**, 38 (Spring/Summer 1985)] ***Left, bottom:*** Flow schematic of the jet head. The working surface or "beam cap" maintains a high pressure of order M^2 higher than the static pressure of the external medium. ***Right:*** The above jet morphology was used to explain the possible physical conditions in extragalactic radio sources. This schematic shows a detail of the expected double-shock structure at the jet terminus as the result of an expanding radio source on the external medium. The Mach disk or "jet shock" effectively stops the incoming jet, and the bow shock accelerates and heats the ambient medium The beam shock and cap correspond to observed radio hotspots, and the cocoon corresponds to the radiolobe of a radio galaxy.

4.9 **WIND TUNNELS** – Pioneering Supersonic Devices in France and England

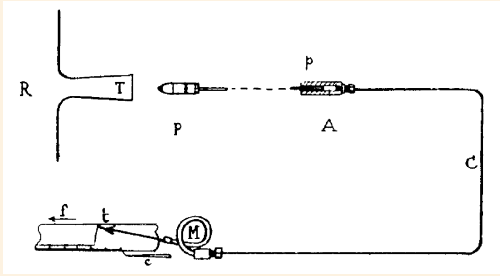

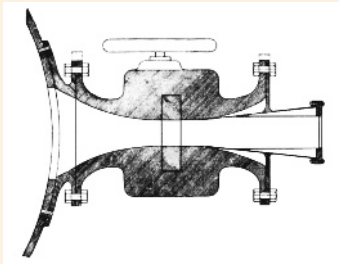

4.9–A ***Left:*** Eugène HUGUENARD and Jean André SAINTE-LAGUË, two French researchers at Paris, apparently built the first supersonic test facility for aeroballistic studies. They generated a supersonic flow emerging from a Laval nozzle *T* that was operated by discharging a high-pressure air reservoir *R* via *T* and reached flow velocities up to 450 m/s. To record the drag force of a projectile *P* they used a piston gauge *A* coupled to an oil-pressurized manometer *M*. Note that the projectile was positioned in front of the Laval nozzle and not within it. ***Right:*** This is a close-up view of their Laval nozzle illustrating its geometry. [La Technique Aéronautique **15**, 346 (1924)]

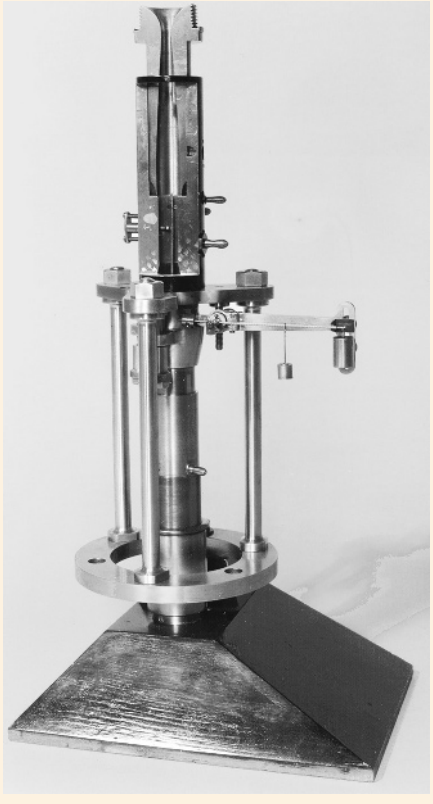

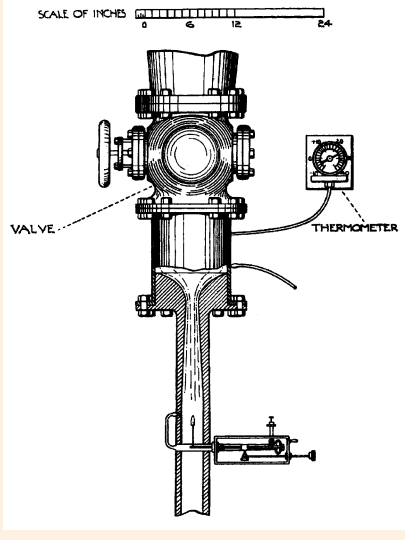

← The NPL supersonic wind tunnel employed a converging/diverging nozzle ranging from 0.515 to 0.8 in. (13 to 20.6 mm) in diameter; the test body was fully emerged in the Laval nozzle. To minimize any wall effects on the air flow around the model, only tiny model projectiles with a diameter not exceeding 0.09 in. (2.3 mm) could be used. The drag force was measured with a small balance. To provide a uniform flow, a honeycomb and guide-blade system were later inserted between stop valve and nozzle. [Proc. R. Soc. Lond. **A131**, 122 (1931)]

4.9–B ***Left:*** View of world's first supersonic wind tunnel ($M = 2$), a continuously working miniature facility devised by the British engineer Thomas E. STANTON and collaborators at NPL (Teddington, U.K.). The apparatus, first operational in 1921, was applied on ballistic drag studies. [Crown Copyright 1980. Reproduced by permission of controller of H.M.S.O. Courtesy National Physical Laboratory (NPL), Teddington, U.K.] ***Right:*** Schematic of STANTON's improved wind tunnel. A considerable increase in the scale of experiments became possible by equipping the laboratory with a large air-compressing plant (2,000 m^3/min) that allowed one to increase the speed up to $M = 3.25$ at a 3.07-in. (79.5-mm)-dia. test section.

4.9 **WIND TUNNELS** – Prewar Supersonic Facility at TH Aachen

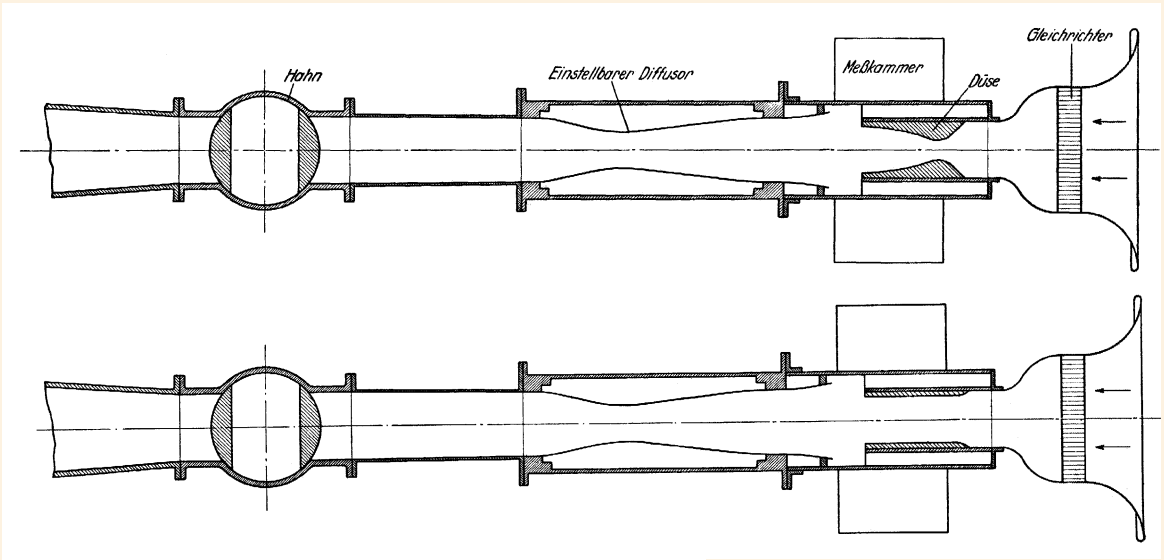

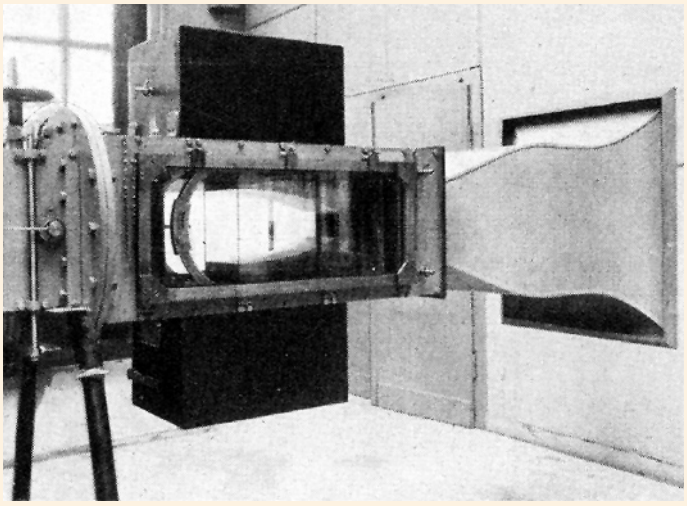

4.9–C ***Top:*** Schematic of supersonic wind tunnel (M = 3.3) at Prof. Carl WIESELSBERGER's Aerodynamic Institute of TH Aachen. The so-called "blow-down-type facility," designed and operated by his assistant Rudolph HERMANN, used a vacuum tank of 90 m^3 that alternatively allowed the operation of two test sections: either of 10×10 cm^2 (running time 25 s) or of 20×20 cm^2 (5 s). The device was provided with a three-component inductive balance for drag measurements and an optical schlieren system. ***Bottom:*** The curved walls of the Laval nozzle, constructed graphically by the method of characteristics, were carefully fabricated and covered with a layer of plaster of Paris that furnished the necessary surface smoothness. The nozzle was enclosed on both sides by heavy glass plates for schlieren or interferometric visualization. The large Peenemünde facility {⇨Fig. 4.9–E} was designed on the model of the Aachen supersonic wind tunnel. [Luftwissen **4**, 301 (1937)]

4.9 **WIND TUNNELS** – Continuous-Flow Closed-Circuit Supersonic Facility at ETH Zurich

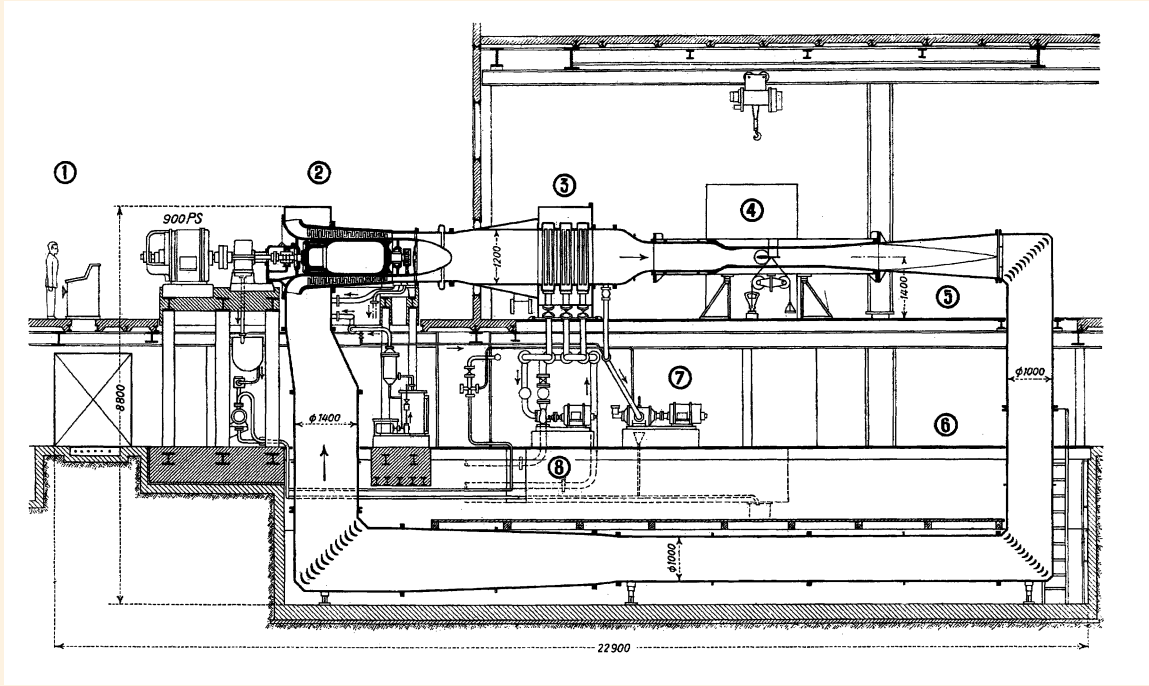

← View of open test section showing Laval nozzle geometry. Note that the flow direction is from left to right. The upper porthole is the field of view for schlieren, shadow, or interferometer visualization; the lower porthole is used to accept the reference beam of a Mach-Zehnder interferometer. [Courtesy Prof. Leonhard KLEISER, Institut für Fluiddynamik, ETH Zürich]

4.9–D ***Top:*** Schematic of Prof. Jakob ACKERET's famous continuously operated closed-circuit supersonic wind tunnel (1933), the first of its kind in the world, which allowed Mach numbers up to two and stationary flow visualization. The device allowed one to vary the Mach number and, independently, the Reynolds number. *1* – power house; *2* – axial fan with 13 steps ranging from 0 to 3,900 rpm; *3* – air cooler with 750,000 kcal/h; *4* – test section 40×40 cm^2; *5* – ground floor; *6* – basement; *7* – vacuum pump; and *8* – cooling water pump. [Interavia **1**, 1 (1946)] The facility, further developed, is still in operation at ETH Zurich. ***Bottom:*** View of Laval nozzle.

4.9 **WIND TUNNELS** – Supersonic Intermittent Indraft Facility at Heeresversuchsanstalt Peenemünde

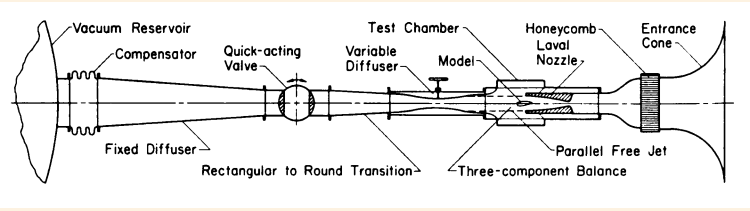

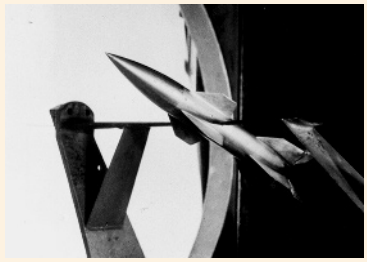

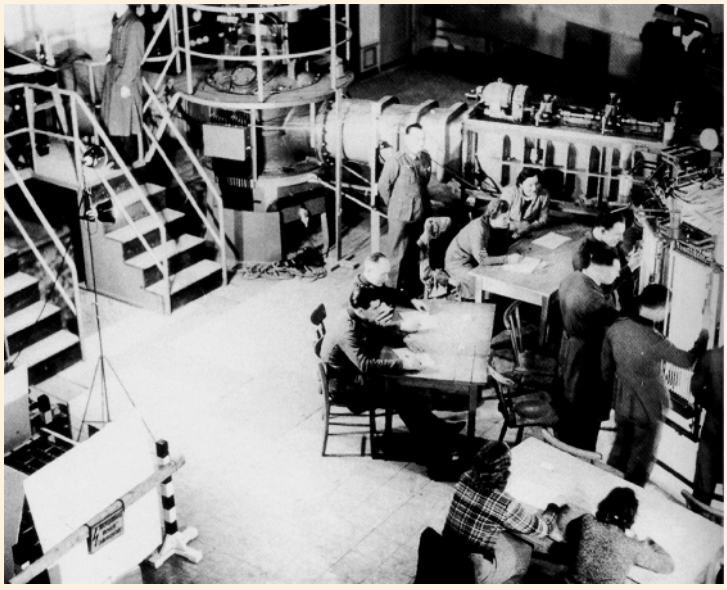

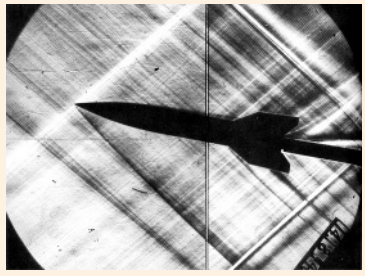

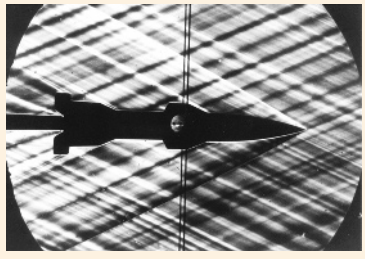

4.9–E ***Left, top:*** Schematic of supersonic intermittent indraft wind tunnel at the Heeresversuchsanstalt (HVA) Peenemünde, designed in 1937 by Dr. Rudolph HERMANN for model testing of rockets, gun-fired projectiles, and missiles up to velocities of Mach 5. It had a 40×40-cm^2 test section. A system of large rotary vacuum pumps was provided to evacuate a huge steel sphere with a diameter of more than 12 m. The blow-down operation was initiated by opening a special valve leading to the wind tunnel, which caused air to rush through the test section into the vacuum sphere throughout a running time of 20 to 25 s, depending on the chosen Mach number. A set of differently shaped Laval nozzles was used to obtain a supersonic flow, free of shocks, ranging from $M = 1.22$ to 5.18. Since Peenemünde is located on the Baltic Sea and has a humid climate, the air entering the wind tunnel from outside had to pass an extensive drying system at low speed (installed in 1940). This provided a shock-free flow up to $M = 5.2$. [Proc. 32nd Int. Astronautical Congr., Rome (1981). Pergamon, Oxford (1982), p. 436] ***Left, bottom:*** View of the test section of one of Peenemünde's wind tunnel testing facilities – then the most advanced in the world. Aerodynamic pressure loading at many locations along the surface of rocket models was measured with the help of mercury manometers attached to tiny tubes leading to small holes in the surface of the test model. To observe and record the gauge data during the short operation time of the wind tunnel, each gauge was assigned to a technician. The schlieren-optical system had two nearly parabolic mirrors, 50 cm in diameter each, with a focal length of 10 m. Schlieren pictures were taken with various types of high-speed cameras and light sources. Aerodynamic forces like drag, lift, and pitching were measured by a three-component balance. [P.P. WEGENER: *The Peenemünde wind tunnels*. Yale University Press, New Haven *etc.* (1996)] ***Right:*** One of the main tasks of HERMANN's group was the model study of the aerodynamic behavior of the supersonic rocket A-4 or "V2" (*center*), the first ballistic missile ($M_{max} > 4$), and the supersonic winged "Wasserfall" (*top & bottom*), an anti-aircraft missile ($M_{max} \approx 2$). The models were mounted on a rod and could be exposed under different yaw angles to the supersonic flow. [Courtesy Historisch-Technisches Informationszentrum Peenemünde]

4.9 **WIND TUNNELS** – Slotted Throat of Supersonic Facility at NACA, Hampton, VA

4.9–F To eliminate any net effects of the walls on wind tunnel test results, a research program was devised at NACA in the mid-1940s with the idea of absorbing shock waves by means of longitudinal openings, or slots, in the test section – a combination of opposite effects of open and closed walls. This, however, required an increasing power of the air compression plant. The slotted throat avoided the so-called "choking effect" on the achievable speed due to the presence of a test model and permitted a full spectrum of transonic flow studies, thus becoming a milestone in the evolution of high-speed wind tunnels. The first successful slotted tunnel was a 12-in. (30.48-cm) model tunnel with a maximum useful Mach number of 1.26, which was applied only for tunnel development (1947). The view of the NACA 8-ft (2.44-m) slotted throat shows the diffuser-entrance flaps. [NASA Rep. SP-445 (1980)]

4.9 **WIND TUNNELS** – Ludwieg Tube Facility at AVA, Göttingen

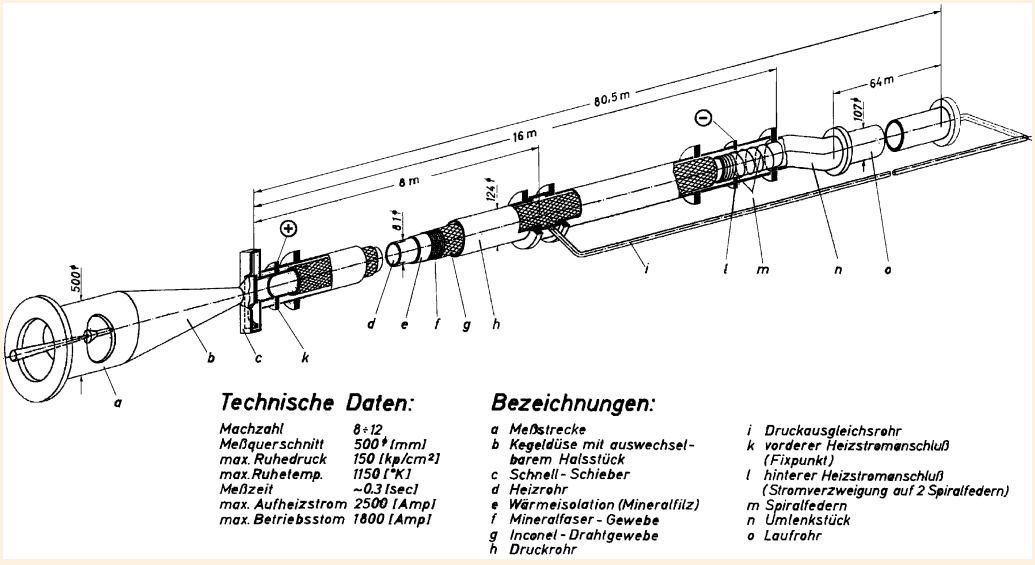

4.9–G Schematic of a particular type of hypersonic wind tunnel – the so-called "Ludwieg tube" – at the Aerodynamische Versuchsanstalt (AVA) in Göttingen. The principle, invented in 1955 at AVA by the German fluid dynamicist Hubert LUDWIEG, allows a wide range of operation, ranging from Mach 3 to 12. The facility, which had a test cross section *a* of 50×50 cm^2, had a pressure storage, designed as a pressure tube *h*, which was connected to test chamber *a* via a fast-closing valve *c*. The inserted conical nozzle *b* provided a parallel flow in *a*. [AVA Rep. 68A77, Göttingen (1968)]

4.9 **WIND TUNNELS** – First Hypervelocity Facilities

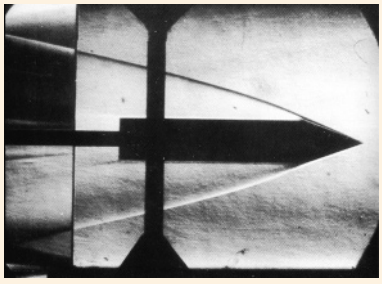

↑ ERDMANN used a plane nozzle with an extremely narrow slit at the throat, followed by two symmetrical, sharply opening nozzle walls enclosed in parallel plate-glass sidewalls.

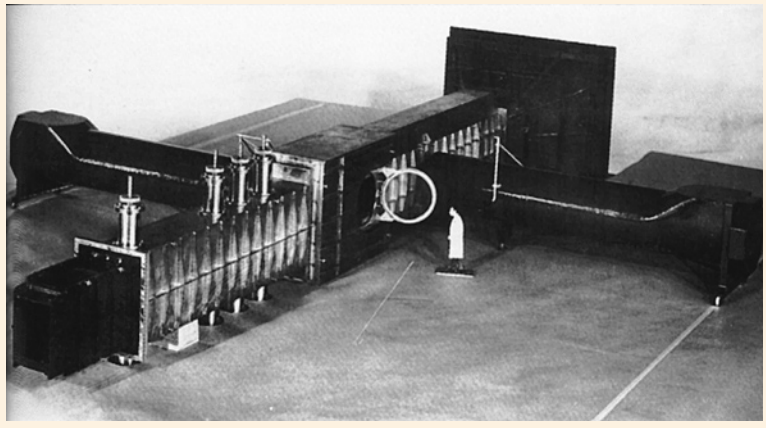

4.9–H ***Left:*** First schlieren photo of a hypersonic flow close to $M = 9$, taken in 1943/1944 by Siegfried F. ERDMANN at Heeresversuchsanstalt (HVA) Peenemünde shortly before evacuation of the facility to Kochel in the Bavarian Alps. ***Right:*** Model of the hypersonic wind tunnel ($M = 10$) as planned in 1944 at the German Rocket Center. It was considered to operate this huge wind tunnel facility by the nearby 120-MW Walchensee Hydroelectric Power Plant. [P.P. WEGENER: *The Peenemünde wind tunnels. A memoir.* Yale University Press, New Haven, CT (1996)]

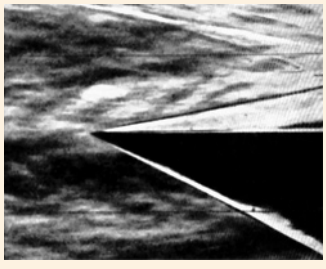

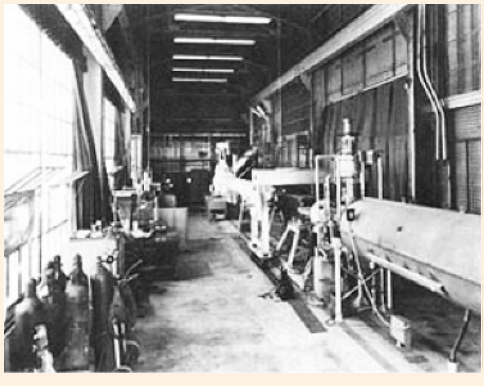

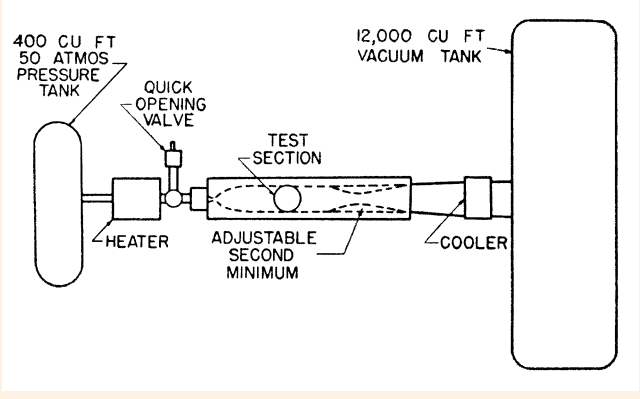

4.9–I After World War II, hypersonic wind tunnel studies were resumed first in the United States. Dr. John V. BECKER at Langley Aeronautical Laboratory built an 11-in. (279-mm) dia. hypersonic tunnel that first became operational in November 1947 – the first operation of a hypersonic tunnel in the United States. ***Left, top:*** Schlieren photograph of the boundary layer and shock on a flat surface aligned with the flow at $M = 6.9$. ***Right:*** Schematic, shown here with a conventional single-step nozzle that produced uniform flow up to $M = 6.9$. [J. Appl. Phys. **21**, 619 (1950)] ***Left, bottom:*** View of NACA's 11-in. dia. hypersonic wind tunnel. An electric heater was incorporated in front of the test section to prevent liquefaction. [NASA SP-4305 (1987)]

4.10 **SHOCK TUBES** – VIEILLE's Pioneering Setup

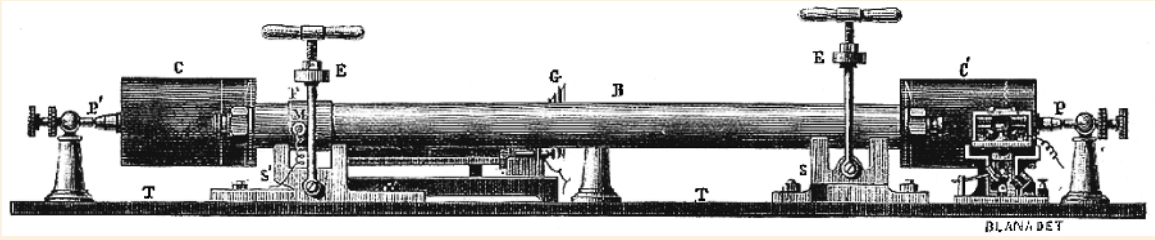

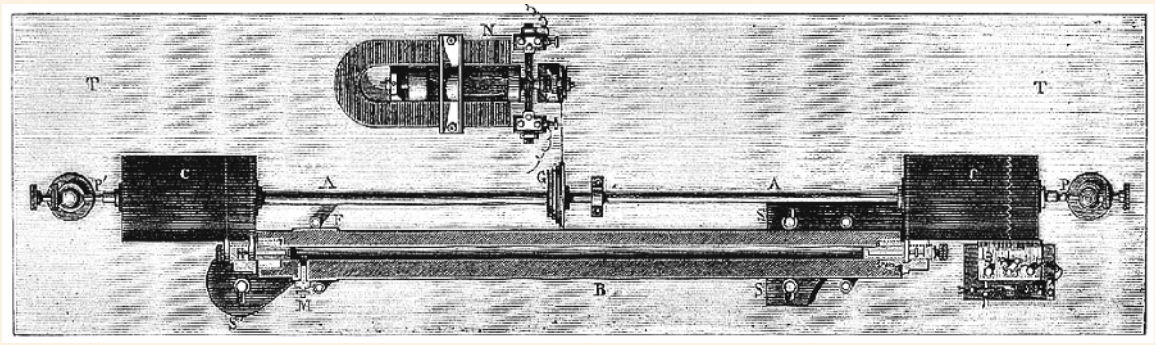

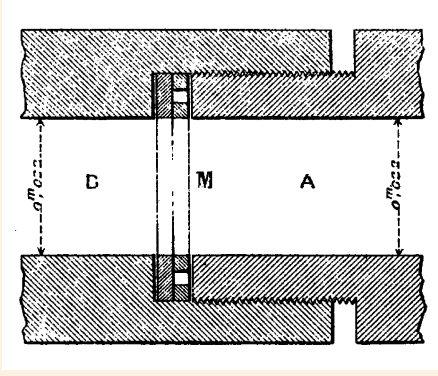

4.10–A ***Top & center:*** Side view and top plan view of the first "shock tube" invented in the late 1890s by the French physicist Paul VIEILLE at the Laboratoire Central of the Service des Poudes et Salpêtres in Paris. It allowed gas dynamicists to study in detail the propagation and reflection of shock waves. Its length ranged from 1 to 32 m. To measure pressure-time profiles at two different locations, two small pressure pistons, spring-loaded and positioned perpendicular along the tube axis, were applied. Their temporal displacements were recorded on two synchronously rotating, smoke-covered drums [Mém. Poudres Salpêtres **3**, 177 (1890)]. ***Bottom:*** Drawing of his membrane holder. The 22-mm-diameter membrane *M* ruptured after reaching a critical burst pressure, which generated the shock wave. VIEILLE tested various membrane materials and measured corresponding burst pressures p_R, *e.g.*, for a 0.6- to 1.5-mm-thick glass plate: $p_R = 5–35$ bar; for a 0.27-mm-thick collodion foil: $p_R = 25–30$ bar; and for a sheet of paper: $p_R = 0.95–1$ bar [C. R. Acad. Sci. Paris **129**, 1228 (1899); Mém. Poudres Salpêtres **10**, 177 (1900)].

4.10 **SHOCK TUBES** – BLEAKNEY's Triggerable Shock Tube

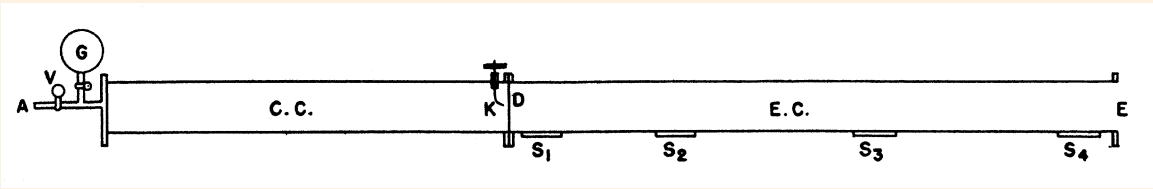

4.10–B During World War II, Walker BLEAKNEY, a U.S. professor of applied physics, and his team at the Shock Wave Laboratory of Princeton University (Princeton, NJ) took up and refined VIEILLE's shock tube technique – thereby also coining the term "shock tube." They introduced a sliding pin *K* for rupturing the diaphragm *D*, which allowed for an easier triggering of attached diagnostic instrumentation. Their pioneering setup basically consisted of a compression chamber *CC* and an expansion chamber *EC*. Air was pumped into *CC* through the inlet *A*, pressure read by gauge *G*, valve *V* closed, and then knife *K* pushed into diaphragm *D*. The shock wave, propagating down the tube *EC*, was monitored by pressure gauges $S_1 ... S_4$ positioned sideways along the tube wall before escaping through the open end *E* of the shock tube. [Rept. OSRD No. 1519 (1943), Princeton University Station]

4.10 **SHOCK TUBES** – Special Types

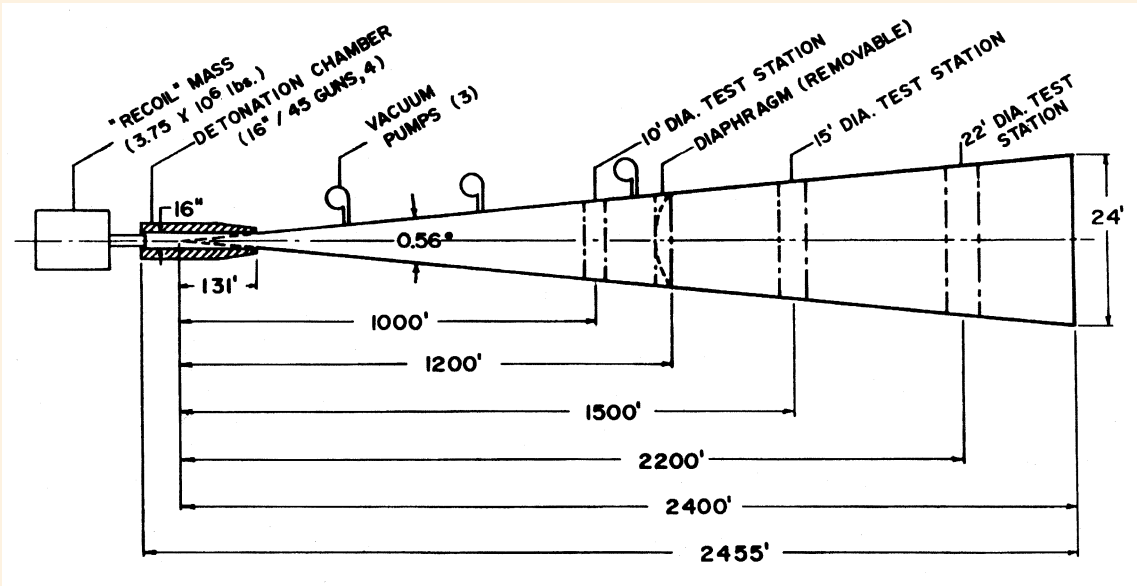

4.10–C Based upon the "Filler tube" (1960), a divergent conical blast simulator driven by a high explosive charge at the apex, the U.S. engineer D.W. CULBERTSON and collaborators at the Naval Weapons Laboratory (Dahlgreen, VA) constructed a large-scale, explosive-driven, conical shock tube to simulate free-air blast waves from a nuclear explosion in the kiloton-yield range. Their simulator applying TNT in a detonation chamber was set up at Dahlgreen. [Proc. 7th Int. Shock Tube Symp., University of Toronto Press, Toronto (1970), p. 396]

4.10 **SHOCK TUBES** – Special Types *(cont'd)*

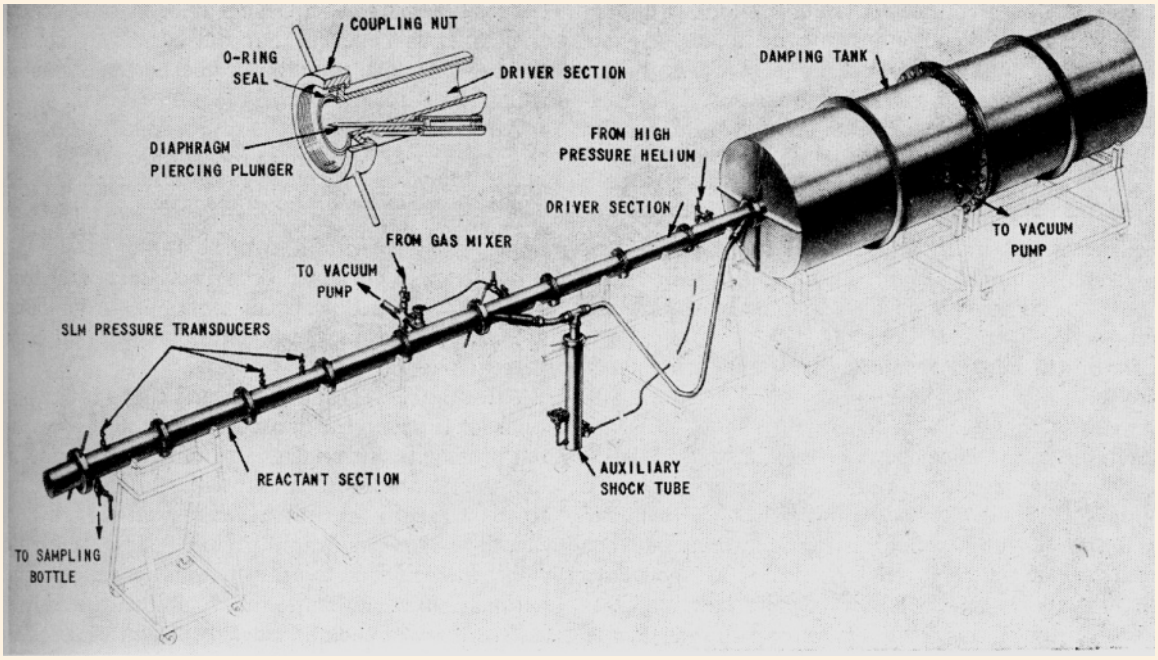

4.10–D Herbert S. GLICK and collaborators at the Aeronautical Laboratory of Cornell University (Ithaca, NY) designed the first single-pulse chemical shock tube. The reactant gas was first compressed by the incident shock. After being reflected at the closed end of the tube, the test gas was further compressed and heated, thus allowing gas dynamicists to process a reactant gas sample with a single closely controlled, high temperature pulse in the order of several milliseconds. [J. Chem. Phys. **27**, 850 (1957)]

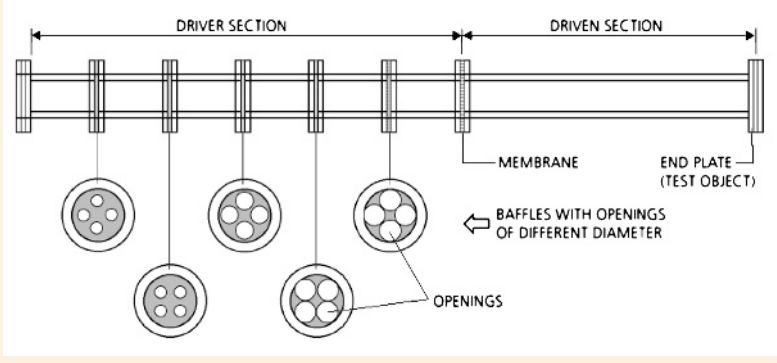

4.10–E In the 1960s, Hubert SCHARDIN and Heinz REICHENBACH at EMI, Freiburg designed an "equal-pressure shock tube" for testing objects subjected to a pressure jump of a long, even infinitely long, duration [Germ. Patent No. 1,273,850 (1968)]. It differed from a common shock tube in that the driver section contained a series of baffles for attenuation of transient shock and rarefaction waves. The test object was placed in front of the end plate, or served to hermetically terminate the end of the shock tube. [EMI-Archives, Freiburg]

4.10 **SHOCK TUBES** – Special Types *(cont'd)*

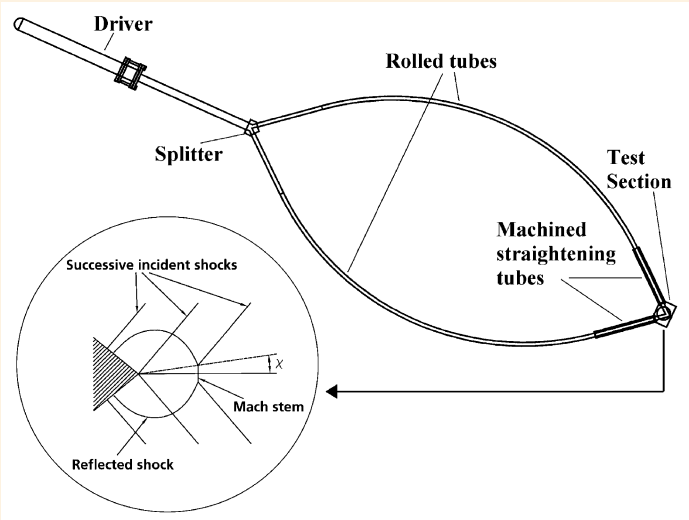

4.10–F Beric W. SKEWS, a gas dynamics professor at the University of Witwatersrand (Johannesburg, South Africa) and collaborators constructed a unique bifurcated shock tube to study the interaction of two-plane shock waves. An initially plane shock wave is split symmetrically into two equal shock waves and then recombined at the trailing edge of a wedge. The plane of symmetry acts as an ideal rigid wall, thus eliminating any thermal and viscous boundary layer effects. [Courtesy Prof. B.W. SKEWS; Proc. 22nd Int. Congr. on High-Speed Photography and Photonics, Santa Fe, NM (1996). SPIE vol. 2869, SPIE, Bellingham, WA (1997), p. 623]

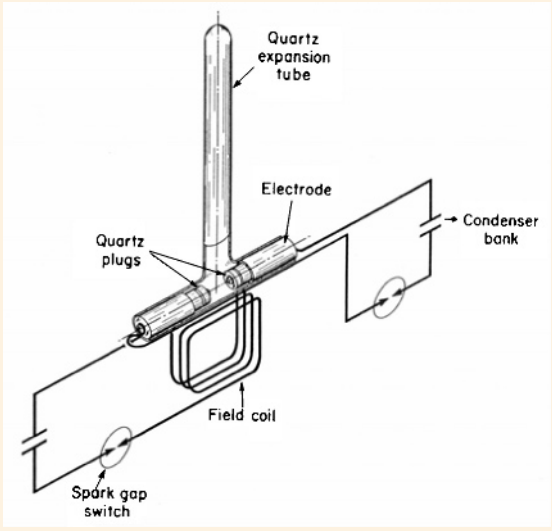

4.10–G A.C. KOLB at the U.S. Naval Research Laboratory (Washington, DC) built a T-tube arrangement for electromagnetic generation of very strong shock waves up to Mach numbers > 100 and temperatures on the order of 100,000 K. [3rd Lockheed Symp. on Magnetohydrodynamics, Palo Alto, CA (1956). Stanford University Press (1958), p. 76]

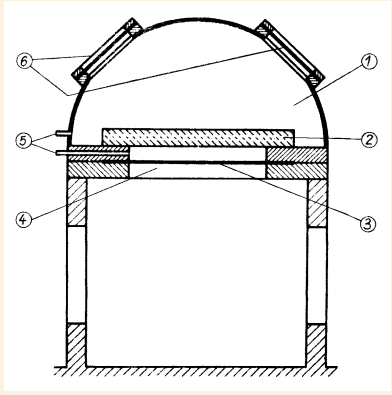

4.10–H In 1960, Hubert SCHARDIN and Manfred FRÖBÖSE at ISL (Saint-Louis, France) designed a blast simulator for full-scale testing of structural elements (*e.g.*, doors, windows, wall panels), consisting of a hemispherical pressure vessel *1* that contained the test structure *2* at its bottom and a lower chamber *4*, both being separated by a membrane *3*. The test structure was shock-loaded by suddenly destroying the membrane *3*. The shape of the pressure-time profile could be additionally controlled by destroying sequentially further membranes *6*. [ISL-Bericht 6/62 (1962)]

4.10 **SHOCK TUBES** – Special Types *(cont'd)*

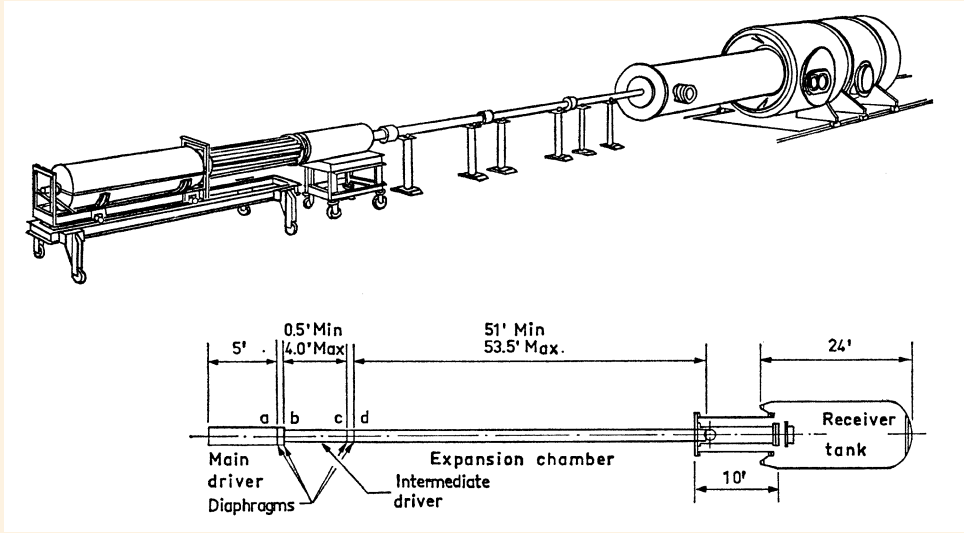

4.10–I Bo LEMBCKE, a Swiss mechanical engineer at MIT (Cambridge, MA) observed that when a shock tube configuration with a large area driver, separated from the shock tube by a diaphragm downstream of the area change, is used, two shock waves appear at the end of the shock tube. The double-driver self-timing shock tube at Cornell Aeronautical Laboratory, closely following this principle, applied a 5-in. (12.7-cm)-diameter main driver that could heat the driver gas (*e.g.*, helium or hydrogen at 2 kbar) up to a temperature of 700 K. The two shock waves reach the test section one after the other before entering the receiver tank. So-called "double-shock shock tubes" are useful for simulating blast loading effects on supersonically moving bodies. [AIAA J. **1**, 1417 (1963); FFA-Rept. 109, Aeronautical Research Institute of Sweden, Stockholm (1967)]

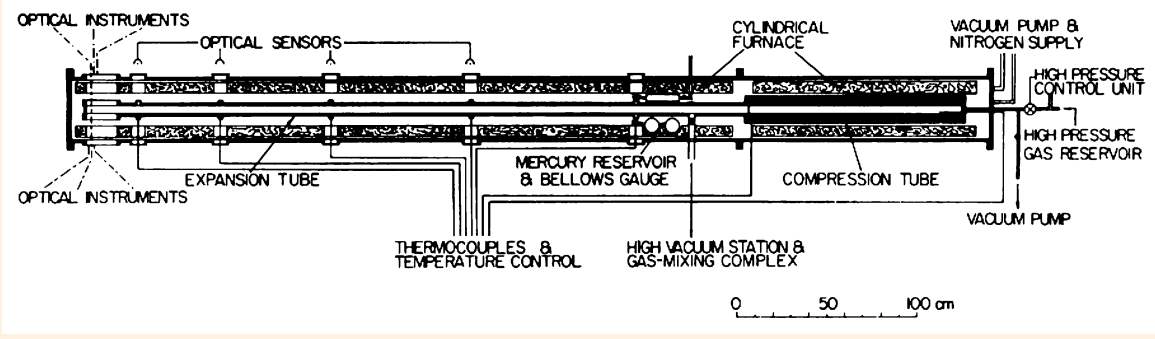

4.10–J In the 1960s, Yong W. KIM and Otto LAPORTE, two shock physicists at the University of Michigan (Ann Arbor, MI), constructed a heated shock tube as a spectroscopic source for studying metallic vapors at high temperatures. Their "mercury shock tube" consisted of three major parts: the main shock tube, a cylindrical furnace surrounding it, and a large outer tube within which both were contained. It provided a thermodynamically well-defined discontinuity followed by a uniform flow at high temperature. The shock-tube temperature could be raised up to 400 °C. [Phys. Fluids **12**, I:61 (1969)]

4.10 **SHOCK TUBES** – Special Types *(cont'd)*

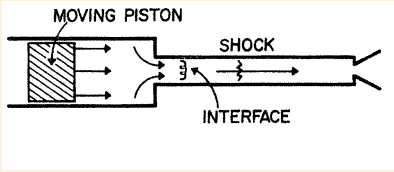

4.10–K Ray J. STALKER, an aeronautical engineering professor at the Australian National University (Canberra) proposed his "free-piston shock tunnel" – later known as the "Stalker tube." It uses a heavy piston to achieve isentropic compression of a helium driver gas. The shock-tube diaphragm ruptures before the piston compression stroke is complete. The resulting very high shock speeds allow model testing at hypersonic speeds. With his prototype gun STALKER achieved a shock wave velocity of 5,334 m/s. [AIAA J. **3**, 1170 (1965)]

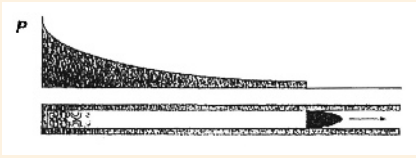

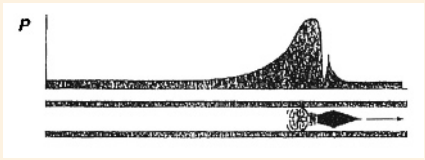

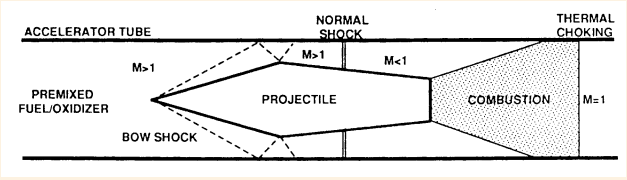

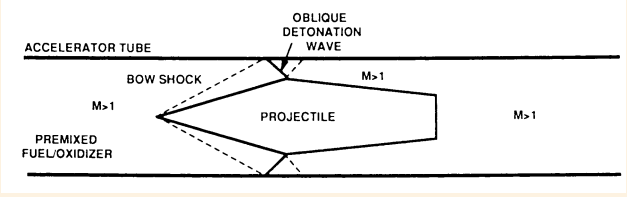

4.10–L ***Top:*** Principle of the ram accelerator (*right*) when compared to classical interior ballistics (*left*). In a ram accelerator the projectile, behaving like a surfboard riding on a wave propagating in a tube, is continuously accelerated by the combustion generated overpressure at its rear end. [G. SMEETS: IUTAM Symp. on Combustion in Supersonic Flows. Kluwer, Dordrecht (1997), p. 228] ***Center & bottom:*** The first ram accelerator, devised and built by Abraham HERTZBERG and collaborators at the University of Washington (Seattle, WA) used the chemical energy of a driving gas for accelerating projectiles to hypersonic velocities (up to 12 km/s). It consisted of a steel tube filled with a gaseous mixture of fuel, oxidizer, and diluent. The most popular gases were methane, oxygen, and nitrogen. To reduce the length of the tube, the mixture was pressurized. A projectile resting on a sabot was fired from a conventional powder gun into the ram accelerator. The projectile compressed the mixture to the point of ignition. Thrust was generated by the mixture expanding behind the projectile. The two schematics illustrate two different drive modes: subsonic combustion wave (*top*) and overdriven detonation wave (*bottom*), which enabled efficient acceleration to higher velocities. [Proc. 37th Meeting of Aeroballistic Range Association (ARA), Québec (1986). Defense Research Establishment Valcatier, Québec (1986)]

4.11 SHOCK WAVE GENERATION – Snapping Belts and Whip Cracking

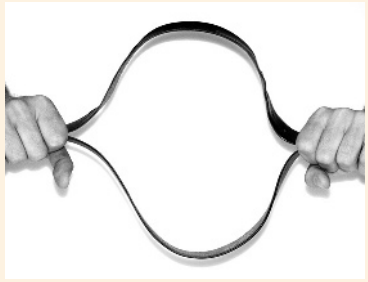

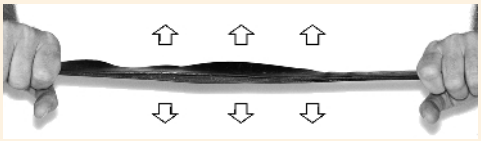

4.11–A ***Left:*** The "snapping belts" are a very primitive way of generating aerial waves of final amplitude: two belts' ends are firmly held together at both sides at the starting position (*top*) and then rapidly moved apart (*bottom*). This results in a peak pressure of about 130 dB ref. 2×10^{-4} μbar. However, although the ear has the impression of a sharp report, it is in the strict sense not a shock wave because the pressure front does not have the typical steplike rise. [EMI-Archives, Freiburg] ***Right:*** View of a Black Forest whip cracker in his traditional costume at Shrovetide. The cracking sound of a whip is indeed a shock wave, albeit a weak one. [Shock Waves **8**, 1 (1998)]

4.11 SHOCK WAVE GENERATION – Plane-Wave Generators

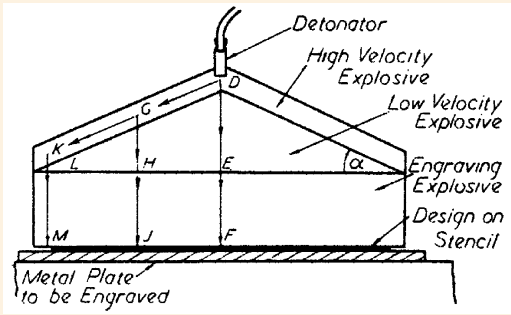

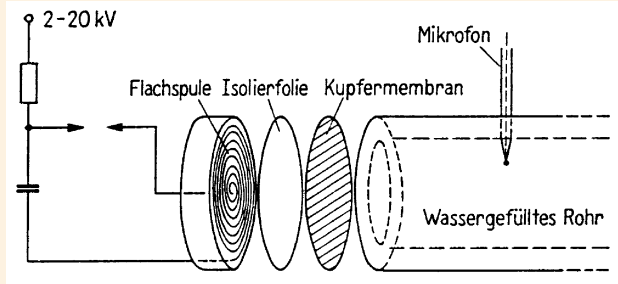

4.11–B Examples of plane-wave generators: ***Left:*** J.H. COOK at Imperial Chemical Industries (Stevenston, U.K.) used a novel explosive arrangement for engraving purposes. It applied a conical geometry assembled from explosives of different detonation velocities to tailor a plane detonation wave. His method of generating plane shock fronts was widely adopted in shock wave research. [Research **1**, 476 (1948)] ***Right:*** Wolfgang EISENMENGER, a German physics professor at Göttingen University, used an electromagnetic shock wave generator that could produce plane shock fronts in liquids with a diameter of 5 cm and shock pressures up to 700 bar. Today this principle is used in shock lithotripters. [Acustica **12**, 185 (1962)]

4.11 SHOCK WAVE GENERATION – Plane-Wave Generators *(cont'd)*

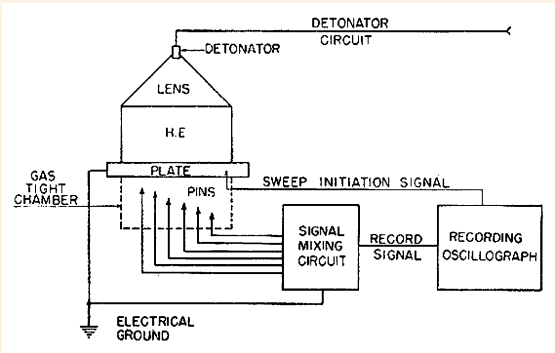

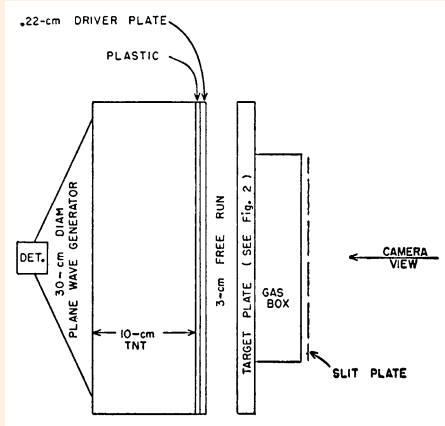

4.11–C ***Left:*** Roy W. GORANSON and collaborators at LASL (Los Alamos, NM) introduced the "electrical pin method" to measure free-surface velocities of shocked solid samples. Together with measured shock front velocities, it allowed for the determination of Hugoniot data. [J. Appl. Phys. **26**, 1475 (1955)] ***Right:*** Schematic of the "flyer plate method" as used by Robert G. MCQUEEN and Stanley P. MARSH at LASL to determine Hugoniot curves of solids. The method applied an explosive plane-wave generator {⇨Fig. 4.11–B} to accelerate a thin plate that, upon impact, generated an intense plane shock wave in the test specimen. [J. Appl. Phys. **31**, 1253 (1960)]

4.11 SHOCK WAVE GENERATION – Gun-Type High-Velocity Accelerators

Behind piston *P* traveling in a bore *H* of a cylinder *D* is a conventional powder chamber *C*, loaded with nitrocellulose propellant. →

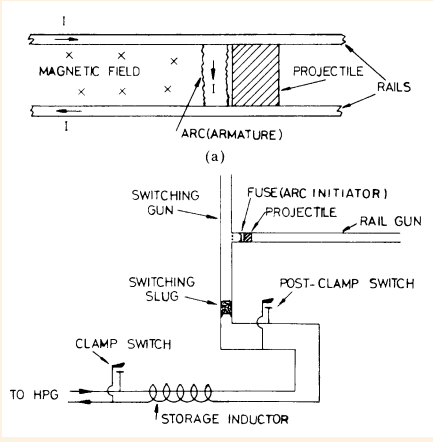

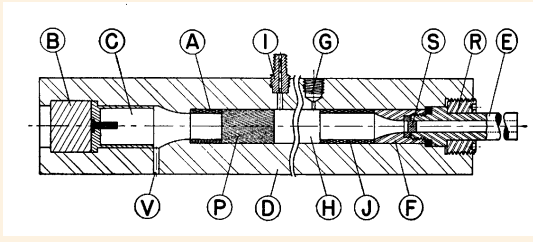

4.11–D Schematics of high-velocity guns. ***Left:*** The "rail gun" was invented in France by André FAUCHON-VILLÉPLÉE (1916). In Germany, Joachim HÄNSLER (1944) built the first practical device, his objective was to use rail guns in the battlefield. The method was later taken up by Scott C. RASHLEIGH and Richard A. MARSHALL. Their setup shown here could accelerate 2.5 g up to 5,900 m/s. ***Right:*** William D. CROZIER and William HUME (Socorro, NM) first proposed a "light gas gun," using a column of hydrogen or helium instead of conventional powder gas. [J. Appl. Phys. **28**, 892 (1957), Ibid. **49**, 2540 (1978)]

4.11 SHOCK WAVE GENERATION – Other Methods

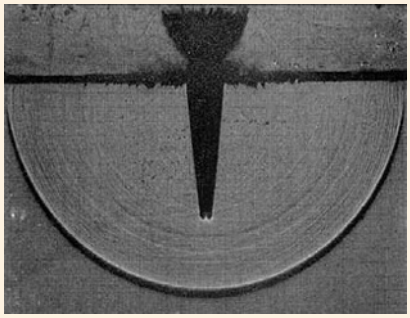

4.11–E J. Howard MCMILLEN and E. Newton HARVEY at Princeton University (Princeton, NJ) studied "water impact waves" generated by fast moving objects striking a water surface. Using flash shadowgraphy they visualized the shock wave produced by a vertical shot of a $^{4}/_{32}$-in. (3.2-mm)-dia. steel sphere and noticed that the wave front geometry was not hemispherical but rather ellipsoidal: since the water pressure was higher in shot direction, the wave propagated there supersonically but in perpendicular direction only sonically. [J. Appl. Phys. **17**, 541(1946)]

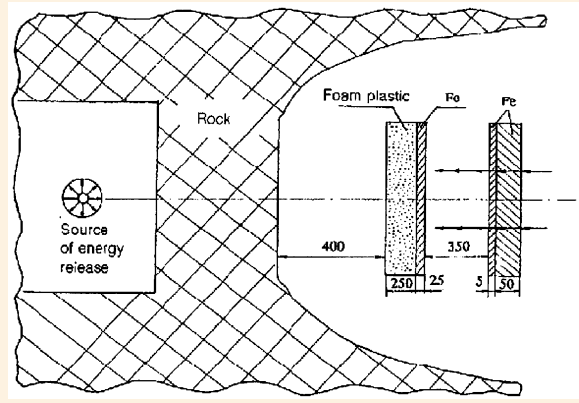

4.11–F Ryurik F. TRUNIN and collaborators at VNIIEF (Sarov, Russia) determined the shock compressibility of iron up to 100 Mbar using the speed of flight of an iron striker that was set off with the help of the energy of an underground nuclear explosion. The mean velocity of the shock wave in the target was measured using a system of electric-contact sensors. The mass velocity was close to half the velocity of the striker iron plate, which was provided at its front side with a foam to absorb the neutron flux of the explosion and to drive the iron striker by its explosion products. [Sov. Phys. JETP **76**, 1095 (1993)]

4.11 SHOCK WAVE GENERATION – Laser-Induced Spark

Incident
laser beam ⇨

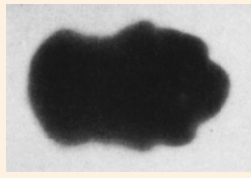

4.11–G Russell G. MEYERAND JR. and collaborators at United Aircraft Research Laboratories (East Hartford, CT) studied the interaction of extremely high-intensity laser radiation with air. ***Left:*** A laser pulse from a Q-switched ruby laser, focused by a simple lens in air at atmospheric pressure – a so-called "laser spark" – produced a bright flash, resulting in the emission of a blast wave, causing a sharp report. ***Right:*** The breakdown that developed in an elongated, egg-shaped plasma region showed a curious structure: it was rounded on the left side, the direction from which the laser beam was incident, and lobed on the right or downstream side. [Proc. 6th Int. Conf. on Ionization Phenomena in Gases. S.E.R.M., Paris (1963), vol. II, p. 479]

4.11 SHOCK WAVE GENERATION – Laser-Supported Detonation (LSD)

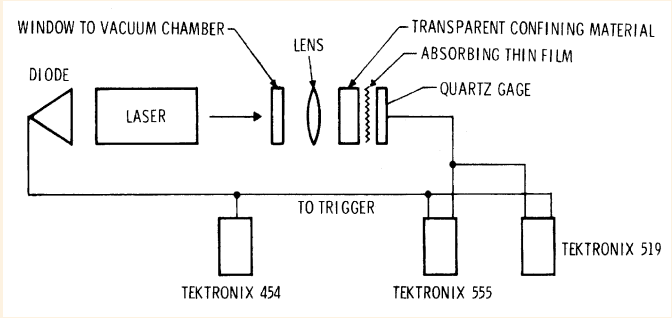

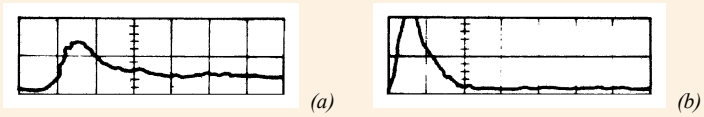

4.11–H N.C. ANDERHOLM at Sandia Laboratories (Albuquerque, NM) reported on a method of generating ultrashort stress pulses of 34 kbar using a pulsed ruby laser (7 J in 12 ns). ***Top:*** Schematic of experimental setup. The laser beam is focused into a 6-mm-dia. region. A transparent material is used to impede the expansion of the vaporized absorber. ***Bottom:*** The high-resolution stress pulse *(a)* was recorded with a Sandia-type quartz gauge (horiz. scale 20 ns/div); its rise time was nominally the laser pulse width *(b)*. [Appl. Phys. Lett. **16**, 113 (1970)]

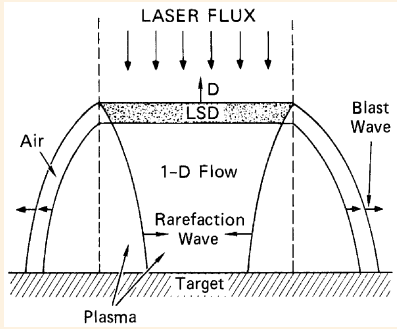

4.11–I When matter is irradiated by an ultrashort high-intensity laser pulse, it provokes a "laser-supported detonation" (LSD) wave. Samuel HOLMES at SRI International (Menlo Park, CA) proposed a detonation model for the plasma zone. Using ytterbium pressure gauges, he measured the surface pressures produced by a pulsed 200-J CO_2-laser beam on an Al target to be around 140 bar. [*Shock waves in condensed matter – 1983*. North-Holland, Amsterdam (1984), p. 339]

4.11 SHOCK WAVE GENERATION – Laser-Propelled "Lightcraft"

4.11–J In 1987, Leik MYRABO, a U.S. professor of engineering at Rensselaer Polytechnic Institute (Troy, NY) had the idea of a "lightcraft" – a vehicle driven by a train of high-power laser pulses. Experiments using a 10-kW CO_2 laser were carried out at the USAF Research Laboratory (Edwards AFB, CA). ***Left:*** The optical surface of the lightcraft was used to focus a horizontal laser beam into the rear of the vehicle, where it was absorbed by the air inside the engine, thus creating a laser-supported detonation. This picture shows the plasma induced in the 14-cm-dia., 50-g Al lightcraft model from a single laser pulse. ***Right:*** Superposition of four pictures illustrating the starting phase. A high-pressure, high-temperature plasma is used to create the thrust that propels the lightcraft into the sky. In October 2000, a spin-stabilized lightcraft reached a record height of 71 m. [AIAA 98-1001 (1998)]

4.12 SHOCK FRONT ANALYSIS – In Gaseous Matter

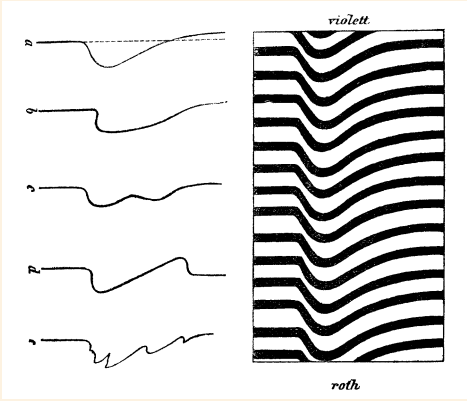

4.12–A Ernst MACH and J. VON WELTRUBSKY (Charles University, Prague), using a Jamin interferometer and a spark light source, observed the shifting of diffraction lines behind a blast wave that they generated by repeatedly operating an electric spark discharge. They visualized interferograms of the blast wave at different time instants (*right*) and then determined the corresponding density profiles (*left*). Note that the interferograms are drawings of what they observed and not photographic records. High-sensitive film was not yet available. [Sitzungsber. Akad. Wiss. Wien **78** (II), 551 (1878)]

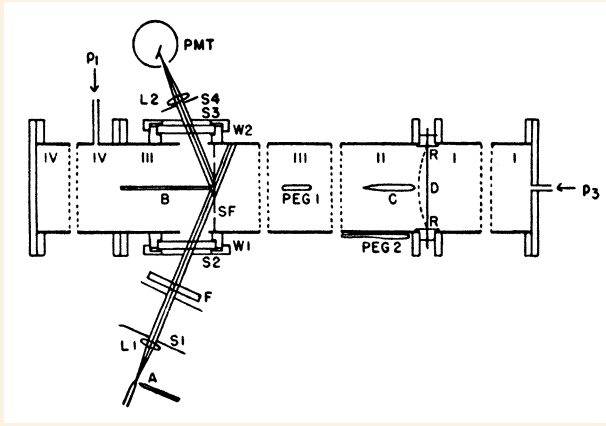

4.12–B George R. COWAN and Donald F. HORNIG at Brown University (Providence, RI) tackled the difficult task of measuring the shock front thickness in gases. Using an optical reflection method, they obliquely directed an intense collimated beam of nearly monochromatic light onto the shock front *SF* and recorded the weakly reflected light (reflectivity 4×10^{-6} in N_2 at $M = 1.3$) by a photomultiplier tube *PMT*. The main problem was the detection of the weakly reflected light against a background of scattered light. They found the shock front thickness to be significantly greater than hitherto predicted theoretically based on the Navier-Stokes equations. [J. Chem. Phys. **18**, 1008 (1950)]

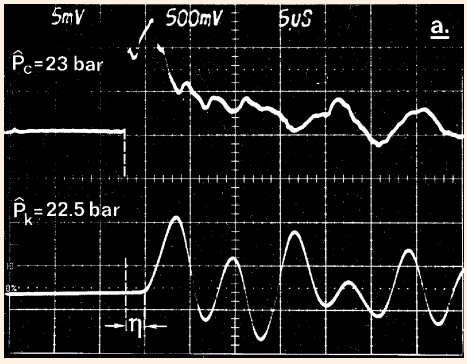

4.12–C In gas dynamics, piezoelectric gauges are widely used to record shock-pressure profiles. However, their rise time is not short enough to truly record the steep rise at the shock front. On the contrary, piezoresistive gauges have rise times of < 100 ns and since the early 1960s have been advantageously applied to high pressures in solid-state shock wave physics. To extend the use of piezoelectric gauges to very low pressure levels, P. KREHL (EMI, Freiburg) used a pulsed, double-compensated Wheatstone bridge in order to compensate for the enormous offset originated from the slightest changes in temperature. To demonstrate the feasibility of piezoresistive carbon gauges for laboratory studies, head-on and side-on shock-wave-collision experiments were carried out in a shock tube. ***Top:*** This picture compares head-on pressure-time profiles recorded with a carbon gauge (*upper trace*) and a piezoelectric gauge (Kistler model 603 E, *lower trace*). Obviously, a piezoelectric gauge has a much larger rise time and requires more time to reach stress equilibrium. ***Bottom:*** View of a thin 50-Ohm piezoresistive carbon shock pressure gauge, Dynasen model 15-300-E. The sensitive element, a 1.5×1.5-mm^2-sized carbon film *CF* manufactured by Dynasen Inc. (Goleta, CA) is connected to two electrical leads *L* that are encapsulated between two layers of thin Kapton foils. [Rev. Sci. Instrum. **49**, 1477 (1978)]

4.12 SHOCK FRONT ANALYSIS – In Space

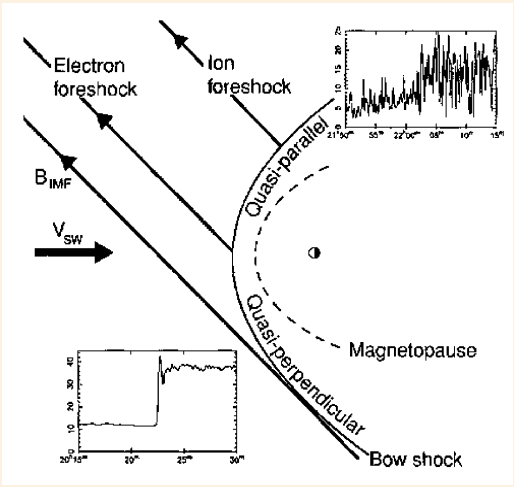

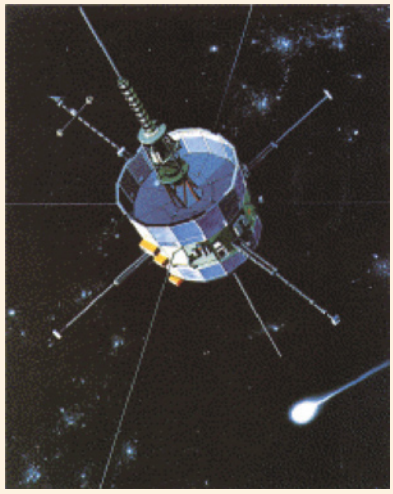

← An artist rendering showing the 469-kg ISEE space probe in orbit. This Explorer-class heliocentric satellite was used in the ISEE program to investigate the structure of the solar wind near the Earth and the shock wave that forms the interface between the solar wind and the Earth's magnetosphere. [Courtesy NSSDC and NASA]

4.12–D ***Left:*** Schematic of Earth's bow shock in equatorial plane as given by David BURGESS. Since in space plasmas the mean free path between collisions is very large, plasma processes, related to the changes in electric and magnetic fields, govern the width and internal structure of the shock layer. The Earth's bow shock has a width of between roughly 100 km and 1,000 km, depending on the shock and plasma parameters. The direction of the upstream solar wind flow is indicated schematically by V_{SW}. Examples of different types of shock crossing – *e.g.*, the "quasi-perpendicular bow shock" and the "quasi-parallel bow shock" – are shown as time series of the magnetic field magnitude in nanoTesla (nT). [*Encyclopedia of astronomy and astrophysics.* Institute of Physics, Bristol (2001), vol. 2, p. 1565] ***Right:*** View of ISEE spacecraft that took the magnetic profiles of the shock. [http://www.friends-partners.org/mwade/craft/isee.htm]

4.12 SHOCK FRONT ANALYSIS – In Solid Matter

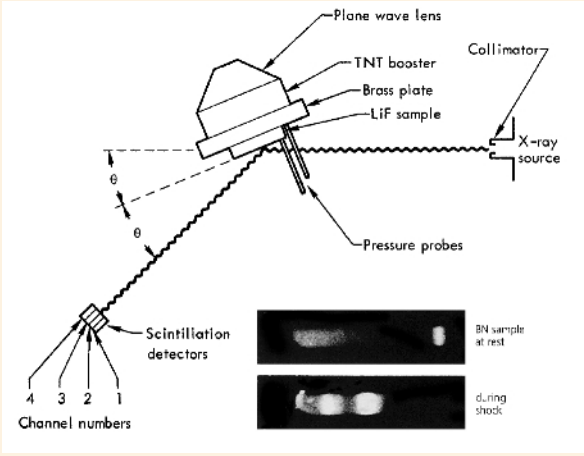

4.12–E To study the microcrystalline state of shock-compressed lithium fluoride (LiF) behind the shock front, Quintin JOHNSON and collaborators at LLNL (Livermore, CA) applied the flash X-ray diffraction technique. Their experimental setup is shown here schematically. The test sample was compressed using a COOK-type, planar shock wave generator {⇨Fig. 4.11–B}. Either film or a detector array was applied to record the shock-induced shift of diffraction lines, which allowed for the estimation of the compression of the unit cell. [Phys. Rev. Lett. **25**, 1099 (1970)] In another study, using shock waves to compress boron nitride (BN) up to 245 kbar, they obtained the first evidence of a shock-induced phase transition that showed up in the origin of new lines in the flash X-ray diffraction pattern. [Phys. Rev. Lett. **29**, 1369 (1972)]

4.12 SHOCK FRONT ANALYSIS – In Solid Matter *(cont'd)*

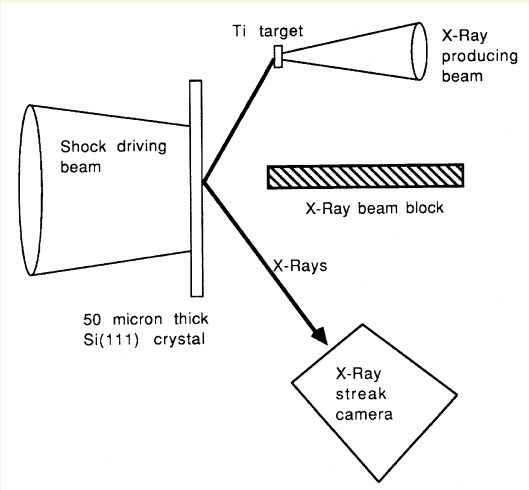

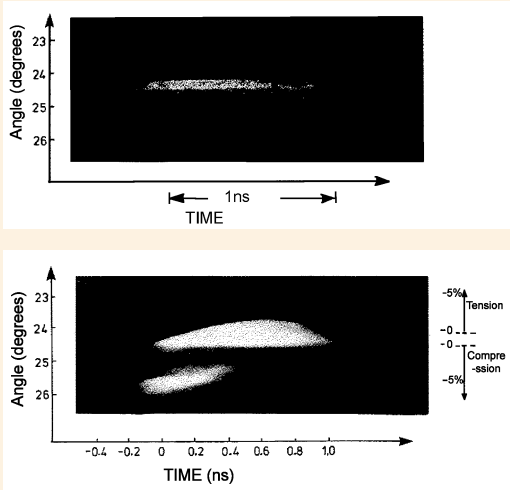

4.12–F Justin S. WARK at Oxford University, together with researchers at Imperial College (London, U.K.) and the Naval Research Laboratory (Washington, DC) measured the compressive and tensile strain during breakout of a 100-kbar shock wave which was launched into a 50-μm-thick single crystal of silicon <111>. ***Left:*** As shown in the schematic of their experimental setup, they used a 100-J 1.05-μm laser pulse which they split into two arms. One arm was focused to a small focal spot generating the shock wave; the second laser beam, synchronous but delayed with respect to the shock driving beam, was focused to a tight spot on a separate target, thus acting as an intense line X-ray source emitting at 23.6 Å. ***Right:*** Changes in interatomic spaces were deduced from a resultant shift in Bragg angle. The upper trace is the diffraction from the crystal at rest, the lower trace from the shocked crystal. [J. Appl. Phys. **68**, 4531 (1990); Proc. 18th Int. Symposium on Shock Waves, Springer, Berlin (1992), p. 393]

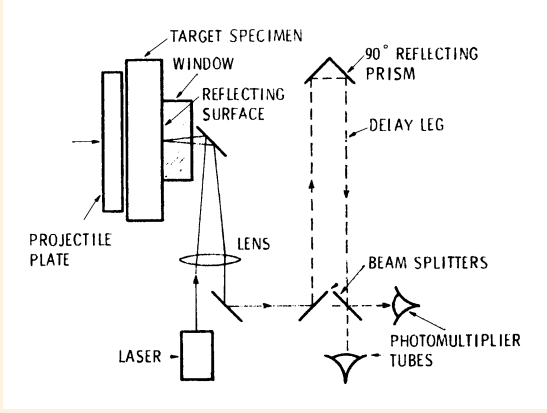

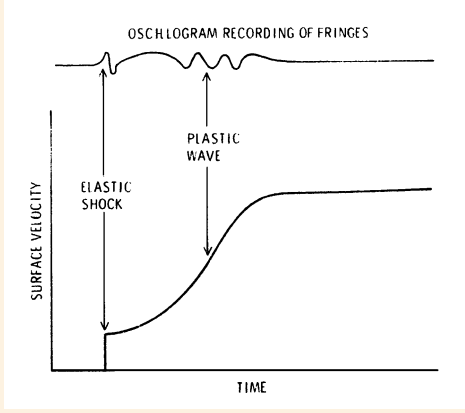

4.12–G James N. JOHNSON and Lynn M. BARKER at Sandia Laboratories (Albuquerque, NM) first used laser interferometry to measure the free rear surface velocity *vs.* time of an impact-loaded metal plate. ***Left:*** Schematic of measurement system. ***Right:*** The evaluated velocity-time profile, here shown in aluminum, allows one to determine the thickness of the plastic wave and to compare it with the dislocation model of plastic flow. [J. Appl. Phys. **40**, 4321 (1969)]

4.12 SHOCK FRONT ANALYSIS – Hydraulic Jumps in Water

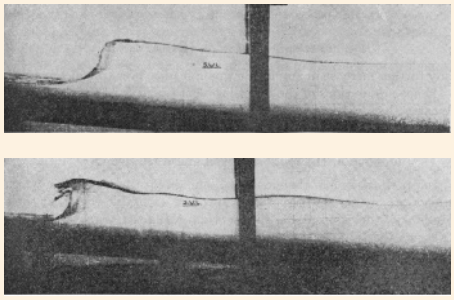

↑ Photographs of the breaking and formation of what looks like a jet (*bottom*) at the summit of the wave.

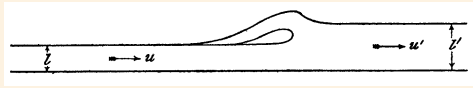

4.12–H Since the propagation velocity v of a hydraulic jump in shallow water of depth h is approximately given by $v = (gh)^{1/2}$ with g as the gravitational acceleration, the wave crest in shallow water travels faster than the wave trough, and the front, leaning forward, generates a "breaker" or "roller". Obviously, the front of a water wave can never be as steep as in the case of a shock wave. ***Left, top & center:*** Propagation of a long wave in shallow water. [J.J. STOKER: *Water waves*. Interscience Publ., New York (1957), p. 373] ***Left, bottom:*** Sketch of the wave front of a tidal wave made by Lord RAYLEIGH. [Reprinted with permission from Proc. Roy. Soc. Lond. **A81**, 448 (1908). © 2007, The Royal Society] ***Right:*** Two tsunami logos (*left* and *center*) adopted by the 19th Session of ITSU (2003); and international tsunami hazard sign (*right*).

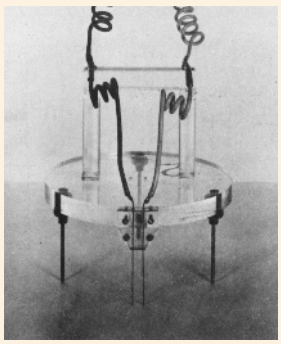

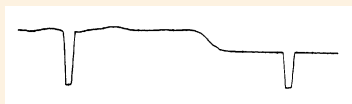

Distilled water

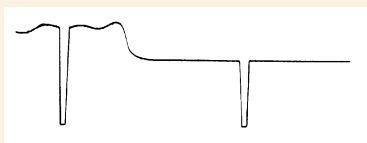

Isoquinolium bromide solution

4.12–I In the 1940s, Harry E. CROSSLEY JR. at CalTech (Pasadena, CA) performed so-called "water table" studies of hydraulic jumps. ***Left:*** He used an electrolytic gauge for measuring the height of a propagating hydraulic jump. The change in the electrical resistance between two metal wires immersed in the working fluid served as a measure for the instantaneous water height. The short interruptions in the recorded wave profiles were due to an automatic current interrupter that broke the gauge circuit at intervals of approx. 0.6 s. ***Center:*** The wave profile of a hydraulic jump propagating in pure water was not as discontinuous as desired. CROSSLEY observed that by adding a detergent (such as isoquinolium bromide) to the distilled water the slope of the wave front substantially increased. [Hydrodynamics Laboraory Rept. N-54.1, CalTech (1949)] ***Right:*** Immersion gauges suffer from difficulties attributable to the erratic dynamic behavior of the meniscus and large disturbances around the gauge when fluid velocities become large. Bradford STURTEVANT at Harvard University (Cambridge, MA) developed an optical depth gauge with fast response time for laboratory studies of water waves using the absorption of infrared light by water. [Rev. Sci. Instrum. **37**, 1460 (1966)]

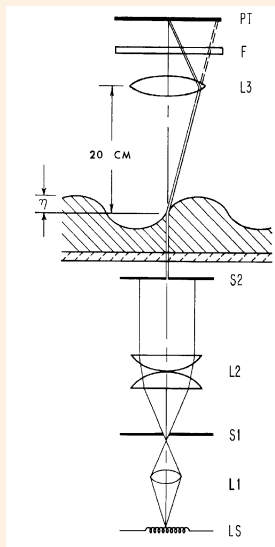

↑ Schematic of STURTEVANT's optical-depth gauge: A beam of light from a light source *LS*, collimated by slits *S1* and *S2*, is projected from below through the glass bottom of a water table. After passing through the water, the attenuated beam is focused by a lens *L3* through an infrared filter *F* onto an infrared-sensitive phototube *PT*.

4.13 **MACH EFFECT** – Interactions of Hydrodynamic Jumps

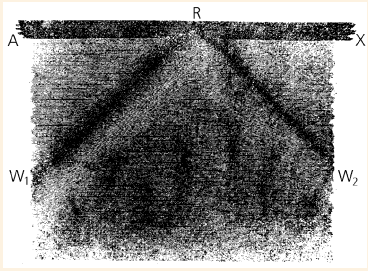

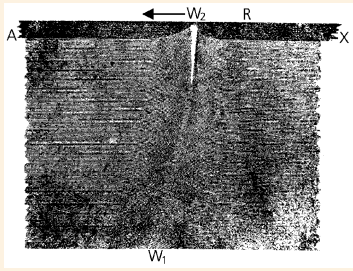

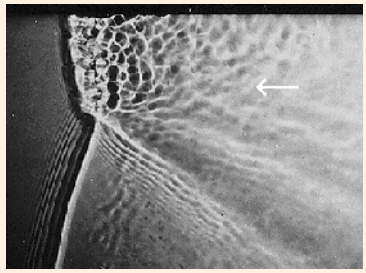

4.13–A Early studies of hydraulic jumps in shallow water. ***Left:*** In the period 1833–1840, the English engineer John Scotch RUSSELL studied the oblique reflection of solitary waves on a vertical plane surface immovable at *R*. For an incident water wave (W_1–R) with an angle less than 30° he observed regular reflection, the reflected wave (W_2–R) being equal in angle and quantity. Note that his pictures are copper-plate impressions and not photographic snapshots. They were prepared after drawings that he made immediately after observation. ***Center:*** The magnitude of the reflected wave diminishes as the angle of incidence increases. Then the velocity of the incident wave (W_1–R) increases near the wall and moves forward rapidly, thus forming a wave front with a high crest (W_1–W_2) at right angle to the resisting surface, also accompanied by the disappearance of the reflected wave. His observation of irregular reflection which he called a "lateral accumulation" is actually the "Mach effect," which Ernst MACH and Jaromir WOSYKA recovered in 1875 by studying the interaction of aerial weak shock waves originating from an electric gliding spark. [J.S. RUSSELL: *Report on waves (1833–1840).* Rep. Meet. Brit. Assoc. **14**, 311 (1844)] ***Right:*** Reflection of a hydraulic jump at a solid boundary under an angle of about 75°. Very similar to RUSSELL's result (*center*), the Mach stem emanating almost perpendicularly from the wall is well pronounced, but the reflected wave diminishes in amplitude and at a large angle of incidence becomes barely visible. [Photo taken in 1990 by the author]

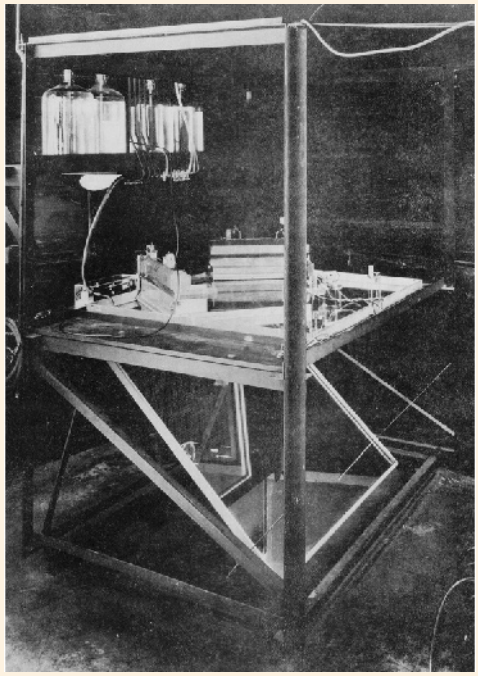

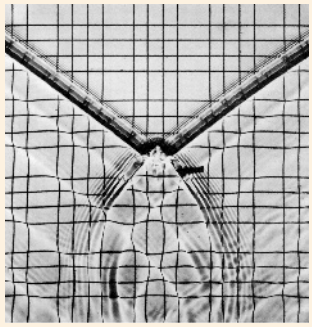

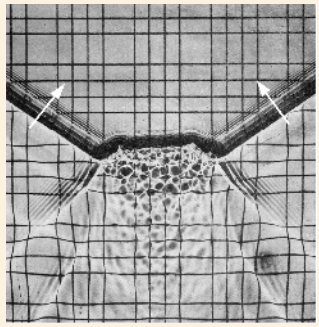

4.13–B ***Left:*** View of CalTech's ripple tank as used in the 1940s to model the interaction of hydraulic jumps. It consisted of a shallow glass-bottom tank; the hydraulic jumps or "surface shock waves" were produced by two 24-in. (61-cm)-long slit generators. Snapshot silhouette photography was used to visualize the wave interference phenomena. ***Center & right:*** Two shadowgraphs showing the interaction of two upward moving hydraulic jumps in shallow water under an angle of 56°, taken at two time instants τ after beginning of interaction. The strength of a hydraulic jump, defined as $\xi = (h_1/h_2)^2$, is analogous to the pressure ratio across a compression shock in a perfect gas with $\gamma = 2$. At $\tau = 0.45$ s (*center*), the region of interaction shows the beginning of Mach reflection, while at $\tau = 1.25$ s (*right)* the Mach disk has been clearly established. [H.E. CROSSLEY JR.: *Analogy between surface shock waves in a liquid and shocks in compressible gases*. CalTech Rept. N-54.1 (1949)].

4.13 **MACH EFFECT** – Shock Interactions in Gases

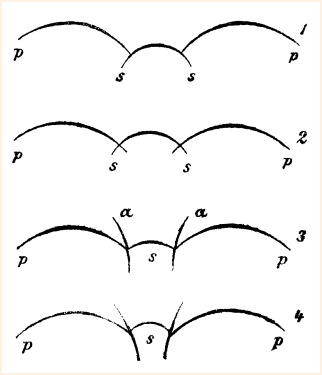

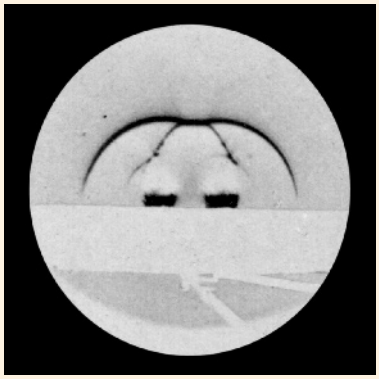

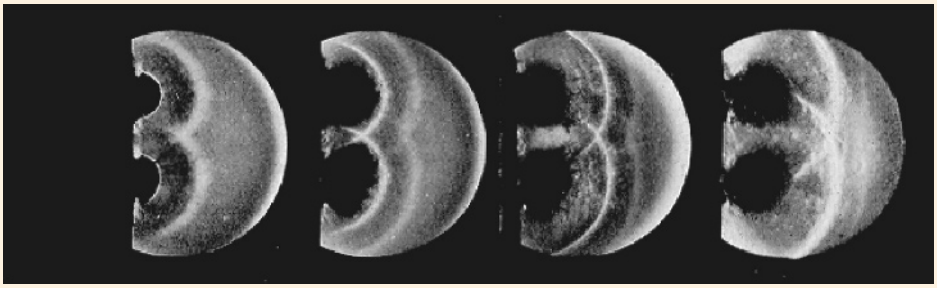

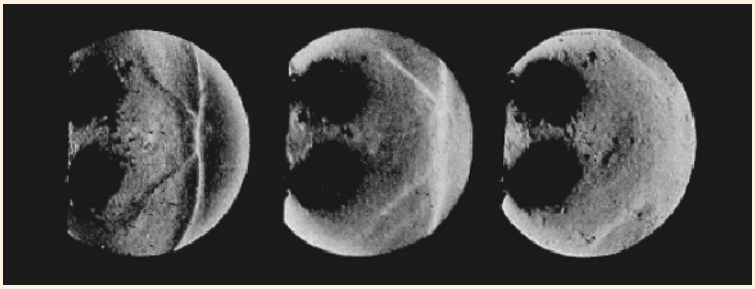

4.13–C Steps of disclosing the riddle of "Mach reflection." ***Top, left:*** Ernst MACH (German Charles University, Prague) studied the intersection of two spherical spark (weak shock) waves *p* in air. Since high-sensitivity photo plates were not yet available to him, he visualized the schlieren pictures subjectively. His schematic clearly shows that he correctly interpreted the newly formed secondary wave front *s*–*s* as the result of increased density at the point of interaction of the two primary waves *p p*. Note that the distance *s*–*s* increases in size with increasing time ($t_1 > t_2 > t_3 > t_4$). [Sitzungsber. Akad. Wiss. Wien **78** (II), 467 (1878)] ***Top, right:*** First published photo of "Mach reflection," taken by Ernst and Ludwig MACH. The two closely spaced point sparks emit shock waves that, obliquely interacting under a sufficiently large angle of incidence, create the so-called "Mach bridge" or "Mach disk." They also obtained quite similar results by simultaneously igniting two small quantities of a high explosive, thus proving that the effect is indeed of mechanical rather than of electric nature. [Sitzungsber. Akad. Wiss. Wien **98** (IIa), 1333 (1889)] ***Center & bottom:*** Shortly after their invention of the "multiple-spark camera," Carl CRANZ and Hubert SCHARDIN (Institut für Technische Physik, Berlin) made the first series of oblique shock interactions. This series of shadowgraphs showing the evolution of the Mach disk fully confirmed MACH's interpretation of the origin of this nonlinear superposition phenomenon. The aerial shock waves were generated by two small piles of detonating silver fulminate. The spherical waves, interacting with each other, formed the typical "Mach disk," here beginning in the fourth frame (*left* to *right*). [Z. Phys. **56**, 147 (1929)]

4.13 **MACH EFFECT** – Shock Interactions in Gases *(cont'd)*

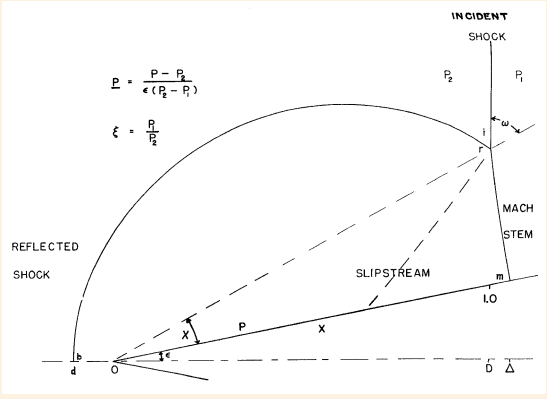

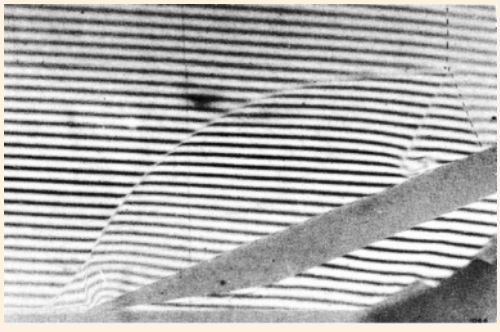

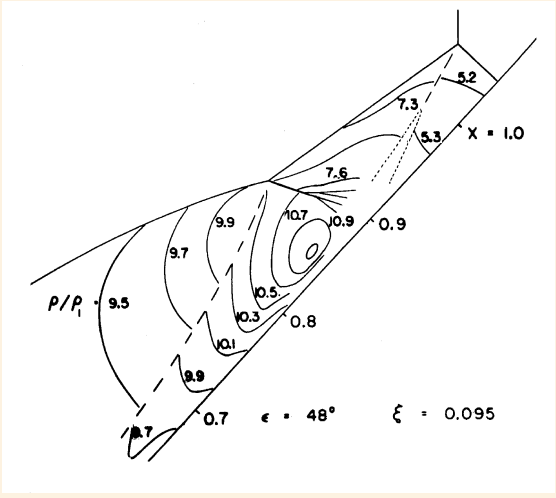

4.13–D ***Left:*** Schematic (*top*) and corresponding photograph (*bottom*) of "single Mach reflection," taken by Donald R. WHITE at Palmer Physical Laboratory of Princeton University (Princeton, NJ) using a shock tube and Mach-Zehnder interferometry. ***Right:*** WHITE's schematic of a strong shock wave interaction at a wedge, giving rise to a second slipstream and a second triple point. This unique shock interaction phenomenon was later called the "double Mach reflection." [D.R. WHITE: *An experimental survey of the Mach reflection of shock waves*. Tech. Rep. II-10, Dept. of Physics, Princeton Univ. (1951)]

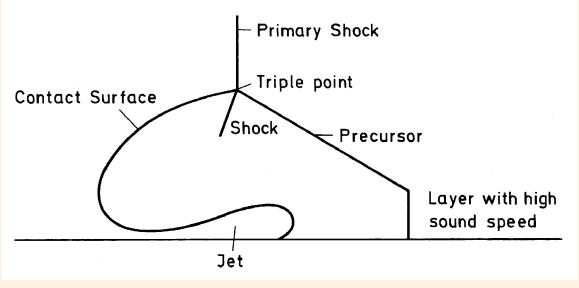

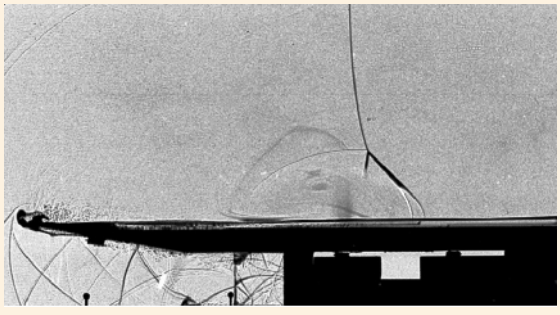

4.13–E Heinz REICHENBACH and collaborators (EMI, Freiburg) performed laboratory-scale air-blast precursor experiments in a shock tube. ***Left:*** The primary shock ($M = 1.66$), here moving from left to right over an electrically heated surface, propagates faster in the hot gas layer than in the rest of the atmosphere, thus creating a "precursor" wave that encounters the primary shock in the cool gas at an angle different from 180°. ***Right:*** At the same time, a complex three-shock configuration is created, similar to that created by classical Mach reflection. The contact surface is marked by a shear flow, which causes the cool gas to move towards the ground in a forward direction. [Rept. E22, EMI, Freiburg (1985)]

4.13 **MACH EFFECT** – Shock Interactions in Gases *(cont'd)*

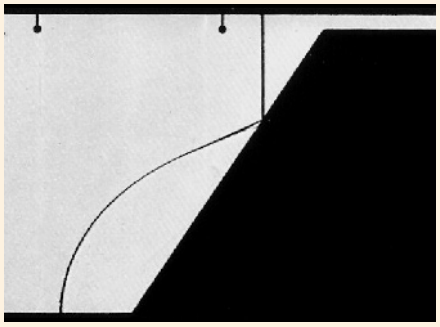

(a)

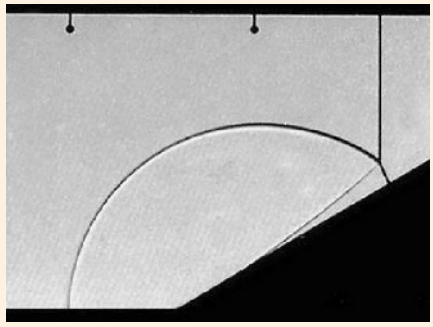

(b)

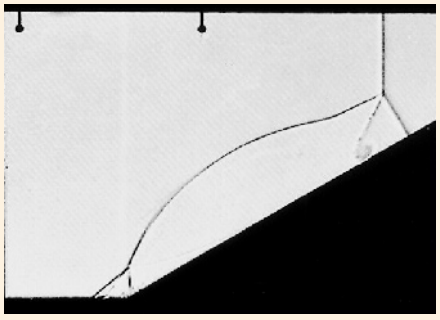

(c)

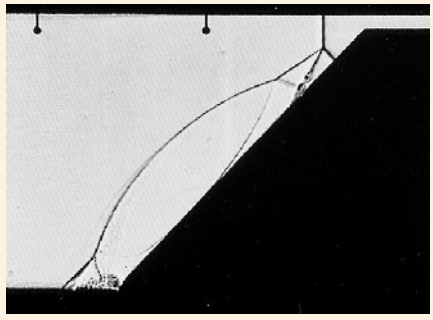

(d)

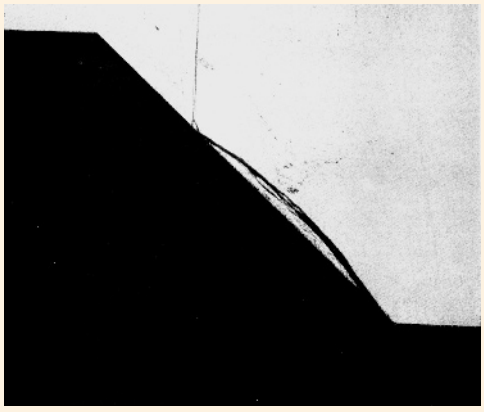

(e)

(f)

4.13–F Types of oblique shock wave reflections in a pseudo-stationary gasdynamic flow {⇨Fig. 2.14}, generated in a shock-tube arrangement and visualized using the shadowgraph method. ***(a)*** Regular reflection. ***(b)*** Single Mach reflection. ***(c)*** Complex Mach reflection. ***(d)*** Double Mach reflection. [Courtesy Dr. Werner HEILIG, EMI, Freiburg] ***(e)*** Terminal double-Mach reflection. ***(f)*** Enlargement of ***(e)*** showing the region of the two triple points in more detail. This unusual shock wave reflection configuration as shown here is only possible in low-gamma gases, *e.g.*, in isobutane and sulfur hexafluoride ($\gamma \approx 1.094$ at room temperature). [J.T. URBANOWICZ, UTIAS Tech. Note No. 267, University of Toronto (1985)] Note that in *(a)–(d)* the incident shock wave propagates from left to right; in *(e)* and *(f)*, however, from right to left.

4.13 **MACH EFFECT** – Shock Interactions in Liquids

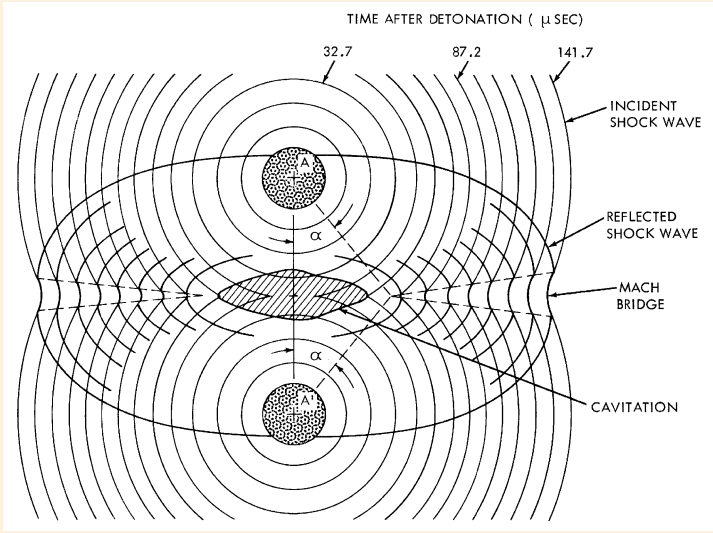

4.13–G ***Left:*** In 1943, Ralph W. SPITZER and Robert S. PRICE at the Underwater Explosives Research Laboratory (Woods Hole, MA) first confirmed John VON NEUMANN's assumption that the Mach reflection also exists in water. Using two spherical 50-g tetryl charges, 8.4 in. (21.3 cm) apart and fired simultaneously under water, they photographed the Mach intersection at a distance of 12 in. (30.5 cm) from the charges, where the fronts of the interacting shock waves formed an angle of 142°. However, at the low pressure levels they did not observe any slipstreams. [R.H. COLE: *Underwater explosions*. Dover, New York (1948), plate III] ***Right:*** Time profiles of collision of two equal spherically expanding underwater shock waves emerging from two equal charges *A* and *A'*, and the formation of the so-called "Mach disk" (or "Mach bridge"). Note that a lens-shaped cavitation zone is created between both detonating charges. [N.L. COLEBURN and L.A. ROSLUND: *Collision of spherical shock waves in water*. Rept. NOLTR 68-110, U.S. Naval Ordnance Laboratory, White Oak, MD (1968)]

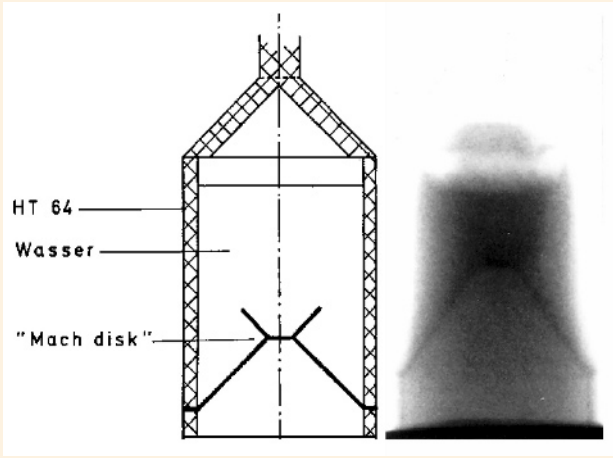

4.13–H Flash radiograph of Mach reflection in water taken by Klaus HOLLENBERG and Ferdinand MÜLLER (Physics Dept., University of Düsseldorf). The 40-mm-dia. water column is surrounded by a hollow cylinder of the high explosive HT64 (a mixture of hexogen and TNT), which has an outer diameter of 50 mm. After ignition at the top, the coaxial detonation wave generates a "Mach disk," which steadily moves in axial direction downwards with constant width. This simple configuration allows the generation of axial pressures in water up to 2 Mbar. Since the X-ray absorption of water is rather low, it is very difficult to obtain high-contrast flash radiographs, and a special "flash soft X-ray tube," operated at high current but low voltage (< 30 kV), is required to resolve the density jump at the shock front. [Bericht 1/7, Arbeitsgruppe für Physik der Hochdruckplasmen und Impulsentladungen (AGD), Fraunhofer-Gesellschaft e.V. Physikalisches Institut I, Universität Düsseldorf (1971)]

4.13 MACH EFFECT – Shock Interactions in Liquids *(cont'd)*

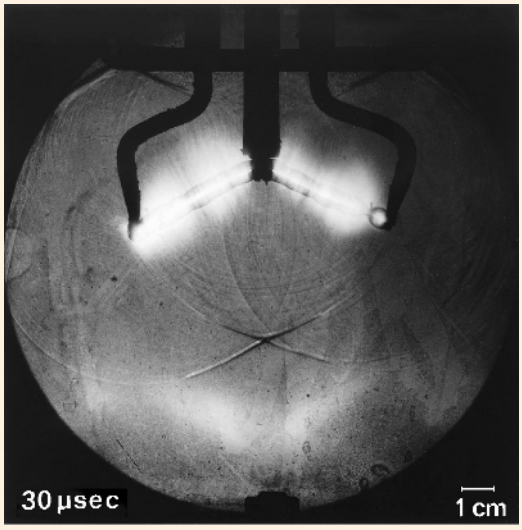

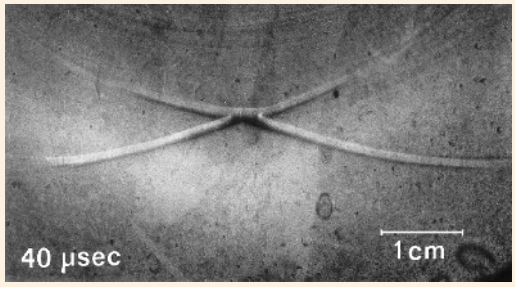

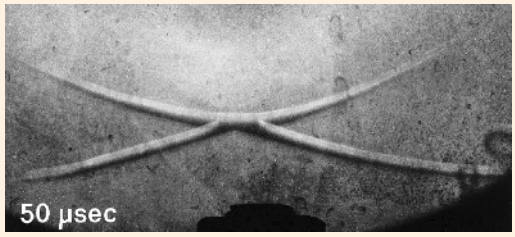

4.13–I ***Left:*** Optical snapshot shadowgraphy of two interacting cylindrical shock waves in water, generated by two 4-cm-long exploding Cu wires arranged in a "V-geometry" at an angle of 130°. At a distance of about 4 cm from the wire, the geometry of the shock waves begins to transform into a spherical one. This increases the angle of incidence – thus favoring Mach reflection, which in this example begins at about 30 µs. ***Right:*** At 40 µs (*top*) and 50 µs (*bottom*), the Mach disk has more grown in width. [Photos by the author]

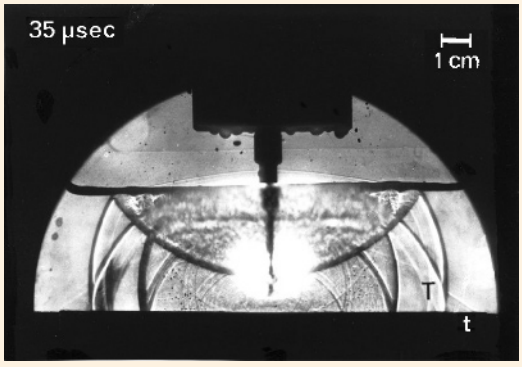

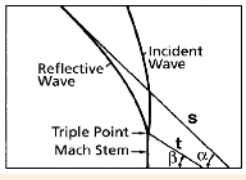

4.13–J ***Top:*** In the 1930s, the German physicist Oswald VON SCHMIDT at Humboldt University in Berlin demonstrated that head waves arise when a disturbance is generated at or near the interface of two media with different sound (or shock) wave propagation velocities {⇨Fig. 4.14–O}. This so-called "Schmidt head wave" (SHW) commonly encompasses a family of such head waves that emerge under different angles, α_L, α_T, and α_S, according to the relation $\alpha_{L,T,S}$ = arc sin $u_1/(u_2)_{L,\,T,\,S}$. Here u_1 denotes the sound velocity in the upper (here liquid) half space; the velocities $(u_2)_{L,\,T,\,S}$ are, respectively, the longitudinal, transverse, and surface wave velocities in the lower (here solid) half space. ***Bottom:*** In the case of Mach reflection, a second family of SHWs is generated: at the transition from regular reflection into Mach reflection, a disturbance is produced that propagates along the interface of the two media, thereby according to HUYGENS' principle sending secondary waves into the upper half space and additionally generating a second family of SHWs under angles β_L, β_T, and β_S, which all run into the triple point. However, in the case of water as the upper medium (u_W = 1,483 m/s at 20 °C) and lead (longitudinal velocity u_L = 1,960 m/s, u_T = 690 m/s) as the lower medium, only the longitudinal Schmidt head waves of both families can arise. [P. KREHL ET AL.: *Erzeugung von Mach-Reflexion bei schwachen Stoßwellen in Wasser*. Frühjahrstagung "Kurzzeitphysik," Verhandl. Dt. Phys. Gesellsch., Hannover (1976)]

4.13 **MACH EFFECT** – Shock Interactions in Solids

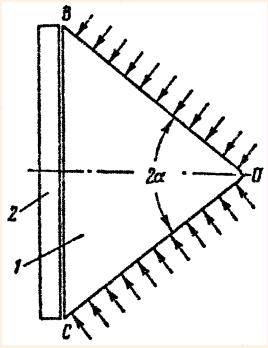

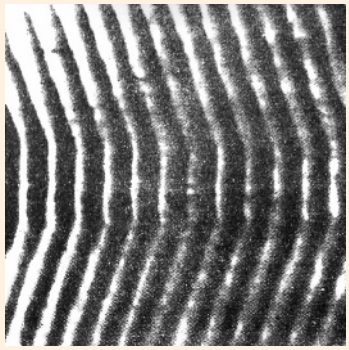

4.13–K In the former Soviet Union, E.A. FEOKTISTOVA first visualized Mach reflection in a detonating solid explosive. ***Left:*** The schematic shows the interaction of detonation waves emerging from the lateral prism faces *OB* and *OC* of a solid explosive *1* and being recorded through a Plexiglas window *2* in the plane of the prism base *BC* by a high-speed photochronograph. A series of slits, located at the focus of the chronograph optical system, were arranged perpendicular to the direction of the development of the interaction process. ***Right:*** The photochronogram, taken along the axis of symmetry, clearly shows the Mach reflection regime. [Sov. Phys. Dokl. **6**, 162 (1961)]

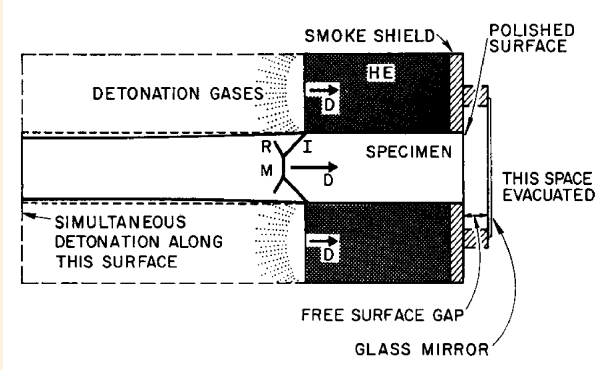

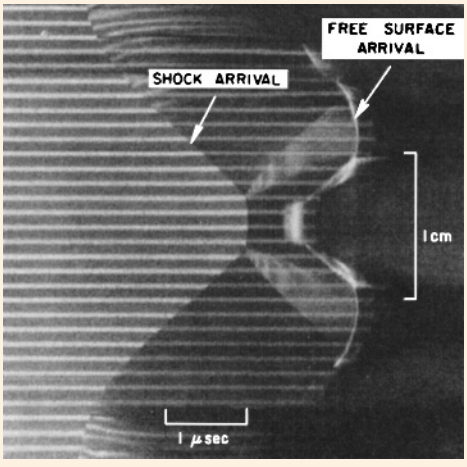

4.13–L In the mid-1960s, George R. FOWLES and William M. ISBELL at Pouter Laboratory of Stanford Research Institute (Menlo Park, CA) carried out optical studies on the interaction of shock waves in non-transparent solids. ***Top:*** At the example of a cylindrical copper sample, compressed up to 1.9 Mbar by a surrounding hollow cylinder of a high explosive, they visualized the shock interaction phenomena by a partially reflecting glass plate supported at a known distance from the surface. ***Bottom:*** Using an ultrahigh-speed streak camera, they recorded images of point light sources reflected in the glass and in the polished metal surface. A record of the shock and free-surface arrival shows a distinct region of Mach reflection that is accessible to Hugoniot equation-of-state measurements. The size of the Mach disk depends on the type of explosive employed and the specimen material. [J. Appl. Phys. **36**, 1377 (1965)]

4.13 **MACH EFFECT** – Shock Interactions in Solids *(cont'd)*

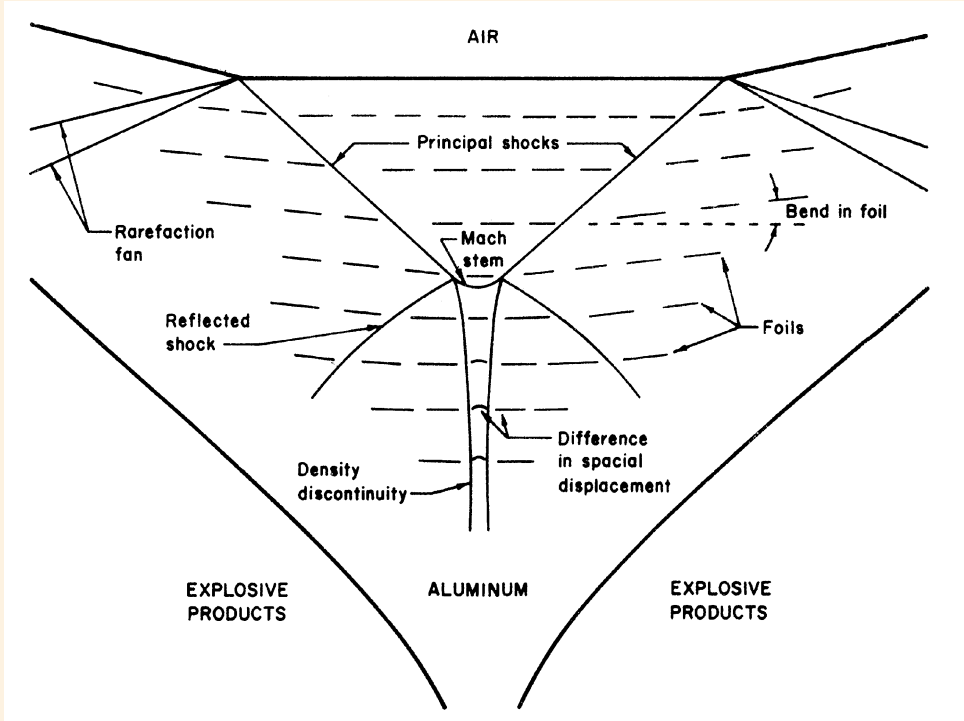

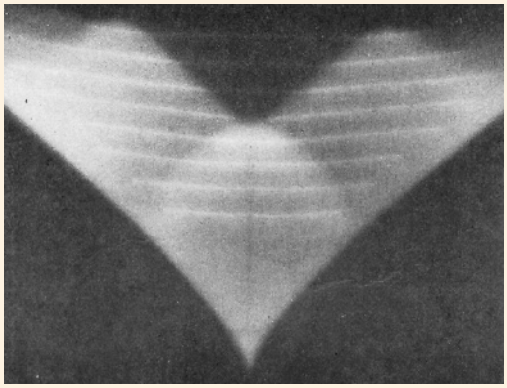

4.13–M Timothy R. NEAL at LASL (Los Alamos, NM) studied Mach reflection in shock-compressed aluminum using flash radiography. ***Top:*** To monitor the material flow and to provide a high radiographic contrast, he used a parallel, equidistant arrangement of 0.0127-mm-thick tantalum foils embedded in the aluminum test sample. By measuring the bents in the foils he determined the density behind the principal shocks from which he calculated a shock pressure of 277 kbar. From his Mach reflection model, which closely follows John VON NEUMANN's first proposed three-shock model (1943), he estimated a shock pressure behind the Mach disk of 887 kbar. ***Bottom:*** Example of a flash radiograph of two interacting shock waves. Driven by the explosive products of two columns of solid explosive (Composition B3), they obliquely interfere and produce Mach reflection. Note that the two reflected shocks and the slip lines, separating regions of the same pressure but different densities, are clearly visible. [J. Appl. Phys. **46**, 2521 (1975)]

4.14 SHOCK WAVE EFFECTS – Shock-Induced Creation of Prebiotic Substances

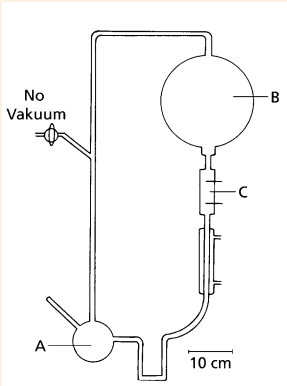

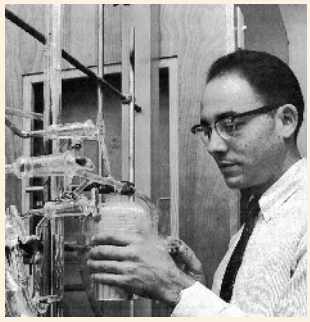

4.14–A In 1953, Stanley L. MILLER, a chemistry student of Prof. Harold UREY at the University of Chicago, devised a spectacular experiment producing amino acids by repetitively generating a spark discharge in a gaseous "atmosphere" of hydrogen, methane, ammonia, and purified water, thus simulating the influence of heat and shock on a primitive Earth atmosphere such as generated by lightning and thunder. ***Left:*** Schematic of his experimental setup. A steady stream of steam, generated in boiling flask *A* and mixed with the gases in flask *B*, passed the spark gap *C* fed by an induction coil, and returned to *A*. After about 1 week of operation, amino acids – essential building blocks of organic life – accumulated in the small flask *A*. [Science **117**, 528 (1953)] ***Right:*** This photo shows MILLER together with his famous so-called "Miller-Urey spark-discharge apparatus." [http://www.astro.virginia.edu/~eww6n/bios/Miller.html]

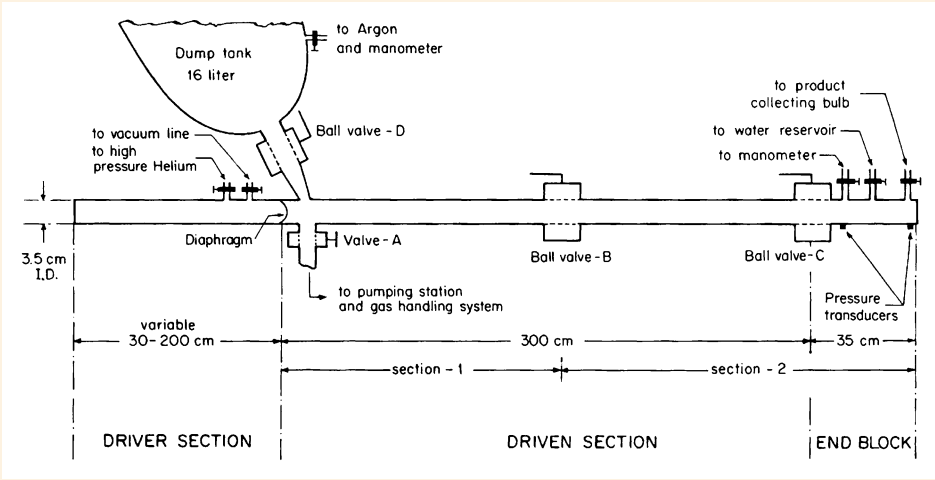

← Two different shock tubes of similar design were used: a 50-mm-inner-dia. Pyrex tube and a 35-mm-inner-dia. stain-less steel tube as shown here. Both driven sections, which could be heated to 80 °C, were pumped to $< 10^{-4}$ Torr, and water vapor and the reaction mixture were introduced into the entire driven section. The dwell times at the high temperature ranged from 200 to 500 μs.

4.14–B Akiva BAR-NUN at Hebrew University in Jerusalem synthesized amino acids behind high-temperature shock waves in methane, ethane, ammonia, and water. Aldehydes and HCN were formed separately during the short-duration high-temperature period, which recombined with ammonia to form α-amino nitriles. ***Left:*** Schematic of his single-pulse shock-tube technique. ***Right:*** His results obtained on the 50-mm-dia. shock tube. The reaction products were analyzed using paper, column, and gas chromatography. He concluded that thunder shock waves might be a suitable source of energy for the production of amino acids. [Origins Life **6**, 109 (1975)]

TABLE II

Summary of products analysis, μmoles amino acid[a]

Run	Glycine	Alanine	Valine	Leucine	Isoleucine[b]
2	0.98	0.08	0.06	0.22	–
3	50.50	27.50	10.20	9.50	< 0.01
5	121.30	60.10	4.40	12.60	0.30

[a] Calculated from the results of column chromatography and gas chromatography.

[b] Isoleucine was identified only by its elution time in column chromatography. In the gas chromatography and paper chromatography it was not separated from the leucine.

4.4 SHOCK WAVE EFFECTS – Cavitation

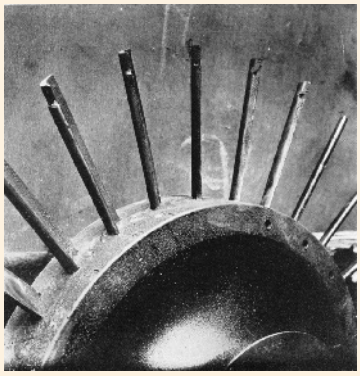

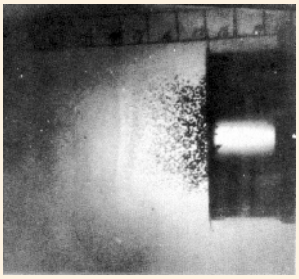

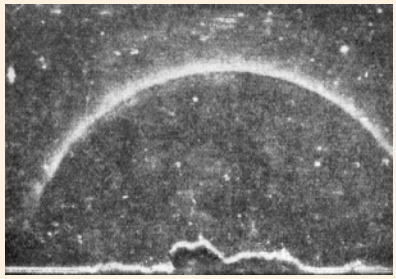

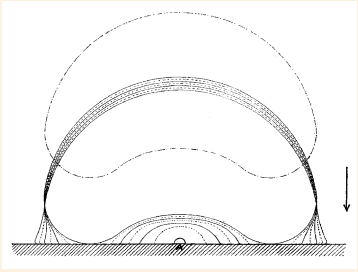

4.14–C ***Left:*** Stanley S. COOK (Brit. Committee of Erosion Research) observed that erosion at steel blade tips (*top*) of a turbine wheel only occurred at the moving blades, which he attributed to water hammer: drops of water, swept off the fixed blades into the path of the moving blades, impacted the blade (*bottom*). [Proc. Roy. Soc. Lond. **A119**, 481 (1928)] ***Center:*** In 1946, John E. ELDRIDGE and collaborators at the U.S. Navy Bureau of Ordnance (Washington, DC) observed that an underwater shock wave, reflected at a model hull (a plate immersed in water and backed by air), caused tension in the water, thus producing a zone of cavitation bubbles near the surface of the plate. The large amount of shock wave energy, trapped in this way in the cavitated water, could later expand in considerable plastic work of deformation. [R.H. COLE: *Underwater explosions*. Dover Publ., New York (1965), plate XII] ***Right:*** Wernfried GÜTH (Dept. of Physics, University of Göttingen), using the schlieren method and snapshot reflected-light photography, recorded the shock wave emerging from the collapse of a single cavitation bubble. Cavitation was generated at the surface of a metal piece – here located at the bottom of the picture – which, excited by a violent blow, was set into strong oscillations. [Acustica **6**, 526 (1956)]

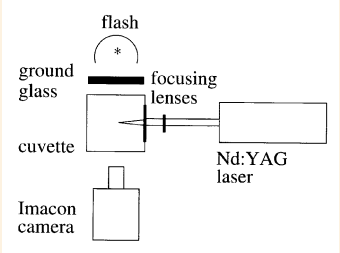

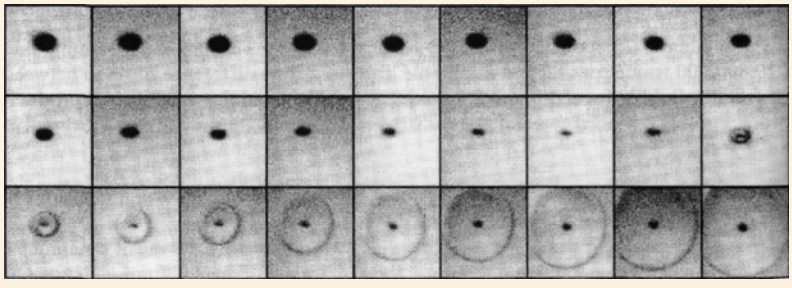

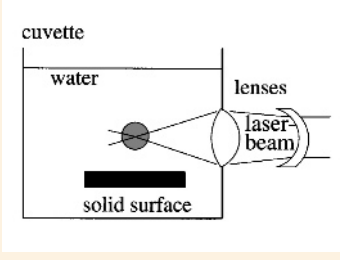

4.14–D ***Left, top:*** Claus-Dieter OHL and collaborators (Institute of Applied Physics, TH Darmstadt) studied the collapse of laser-generated cavitation bubbles using high-speed cinematography. ***Right:*** Example of bubble collapse in a free liquid photographed at 20.8 million frames/s. The maximum bubble diameter before collapse was 2.2 mm. Approaching the very moment of collapse (frame 16), the bubble reveals an ellipsoidal shape. Therefore, the shape of the subsequently rebounding bubble is not spherical, either. The emitted shock wave is first clearly visible in frame 19. ***Bottom:*** When the bubble collapses and rebounds in close proximity to a solid boundary, a jet inside the bubble is created. An additional shock wave, somewhat delayed after the first shock wave due to bubble collapse, is generated, which the researchers sucessfully resolved by cinematography as well. [Ann. Phys. **4** (8), 26 (1995)]

4.14 SHOCK WAVE EFFECTS – Supercavitation

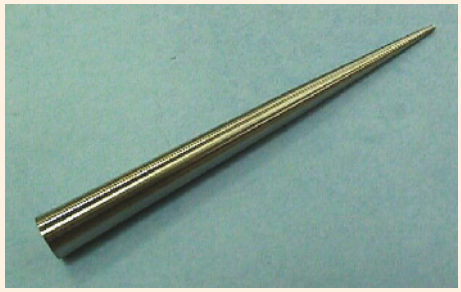

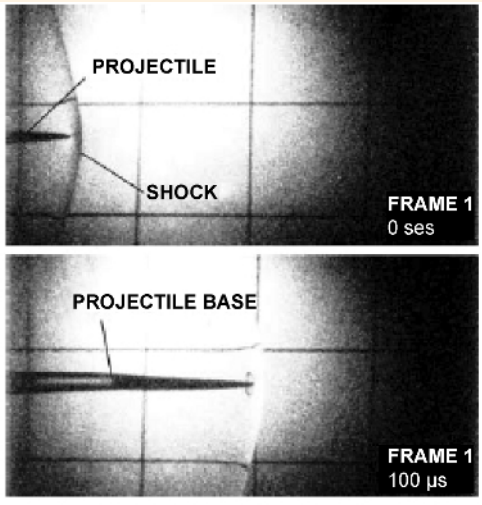

4.14–E ***Left:*** James D. HRUBES at NUWC used slender, 131-mm-long projectiles with a blunt nose to generate a single bubble entirely surrounding the projectile when shot into water. This effect, called "supercavitation," considerably reduces hydrodynamic drag and even allows supersonic projectile velocities under water. ***Right:*** Note the formation of the Mach head wave (M = 1.03). Supersonic velocities could be sustained up to a maximum distance of 2.5 m. [Courtesy Dr. J.D. HRUBES, U.S. Naval Undersea Warfare Center (NUWC), Newport, RI; Exp. Fluids **30**, 57 (2001)]

4.14 SHOCK WAVE EFFECTS – Condensation

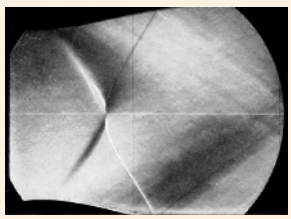

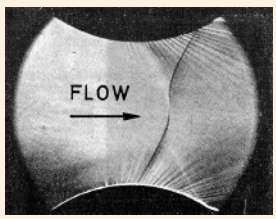

4.14–F ***Top, left:*** Formation of a "condensation shock" in a Laval nozzle, also called "X-shock" or "ghost." This phenomenon, first observed in the 1930s by Carl WIESELSBERGER (TH Aachen) in wind tunnels operated at high Mach numbers, occurs when atmospheric (*i.e.*, moist) air is used. [*50 Jahre Aerodynamisches Institut RWTH Aachen* Abhandl. Aerodyn. Inst. RWTH Aachen, Heft 17 (1963)] ***Top, right:*** Another schlieren picture of a condensation shock in a supersonic nozzle that L. PRANDTL (University of Göttingen) showed in 1935 at the 5th Volta Congress on High Velocity in Aviation. [Acta Mechanica **21**, 77 (1975)] ***Bottom:*** Snapshot of shock condensation effect around the jet fighter Boeing F-18 ("Hornet") at transonic flight in humid air. It apparently arises during acceleration when the air flow at some parts of the fuselage reaches supersonic speeds. When the resulting shock wave detaches, it builds up a sudden rarefaction that, lowering the temperature, causes condensation of the ambient water vapor. This unique picture was published in many journals. [Courtesy J. GAY, U.S. Navy] A similar picture was recently taken from an F-4 ("Phantom II") during an air show at Point Magu Naval Air Station, CA. [*The Military Aircraft Archive*, http://www.milair.simplenet.com/]

4.14 SHOCK WAVE EFFECTS – Aerodynamic Shock Heating

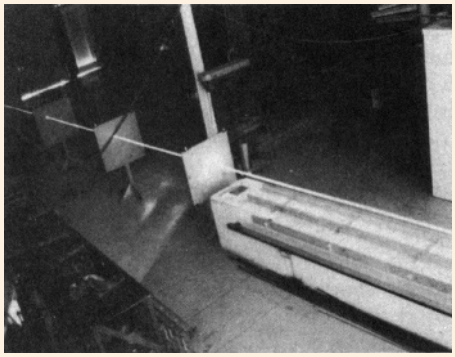

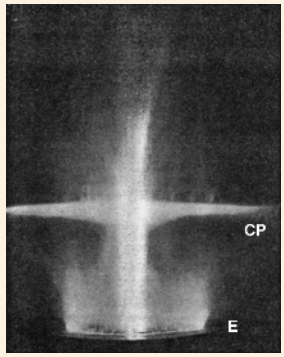

4.14–G ***Left:*** A meteoroid entering the Earth's atmosphere at hypervelocity produces a brilliantly luminous cap of ionized air at its nose, leaving a luminous streak or train of light along its path. Most stony meteorites break up explosively in flight. This photograph of an exploding meteorite was taken by Charles P. BUTLER on November 23, 1895. [Courtesy Science Museum Pictorial, U.K. Image-No. 1901-0146] ***Center:*** This is not a laser beam, but rather a time-exposure photograph of a small cubic polycarbonate (Lexan) projectile fired from an inductively driven rail-gun accelerator and flying at hypervelocity ($M \approx 17$) down the laboratory in the open air. Note the meteorite-like streak that, using a still camera, was taken by Scott C. RASHLEIGH and Richard A. MARSHALL at the University of Canberra. [J. Appl. Phys. **49**, 2540 (1978)] ***Right:*** This unique example of shock heating, caused by shock wave interaction, was taken by Henri MURAOUR in France. It shows the detonation of a bloc of explosive *E* fired at the bottom. About 40 mm above the surface of the explosive a sheet of cigarette paper *CP* was positioned at which the shock wave was reflected, thus creating a strong luminous zone. Initially withstanding the shock by its inertia, the paper was pulverized very shortly afterwards. [L'Astronomie **50**, 153 (1936)]

4.14 SHOCK WAVE EFFECTS – λ-Shock Configuration

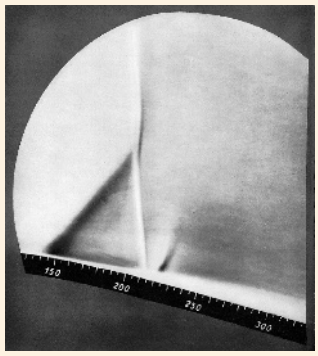

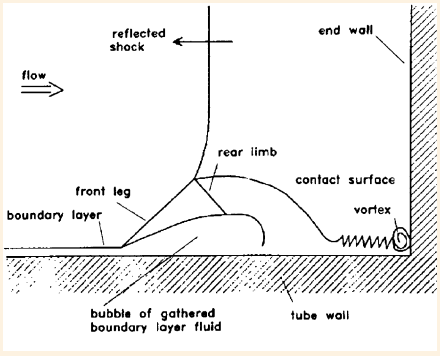

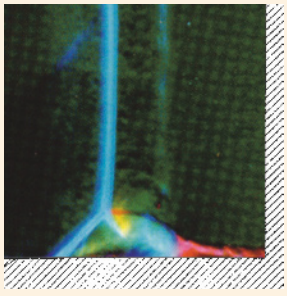

↑ λ-shock in CO_2, incident shock Mach number $M_{SI} = 2.45$.

4.14–H ***Left:*** Jakob ACKERET and Fritz FELDMANN (ETH Zurich) observed that the interaction of a shock wave with a boundary layer results in a new wave configuration, which they called "λ-shock" because of its striking similarity with the Greek letter λ. This schlieren picture shows a λ-shock formed above the surface of an airfoil resulting from an oblique interaction of an incident shock ($M = 1.225$) with a laminar boundary layer. Note that the flow direction is here from left to right. [Interavia **1**, 1 (1946)] In 1958, Hans MARK (NACA's Flight Propulsion Research Laboratory, Cleveland, OH) observed that the interaction of a reflected shock wave with a boundary layer produces a bifurcation. [NACA-TM1418 (1958)] ***Center & right:*** Harald KLEINE (RWTH Aachen) used color schlieren photography to resolve this characteristic wave pattern – a corkscrew-like vortex structure emerging from the corner. [Proc. 18th Int. Symp. on Shock Waves, Sendai (1991). Springer, Berlin (1992), p. 261]

4.14 SHOCK WAVE EFFECTS – Shock Focusing

(a)

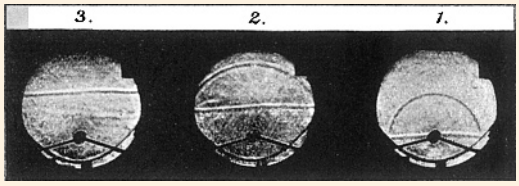

(b)

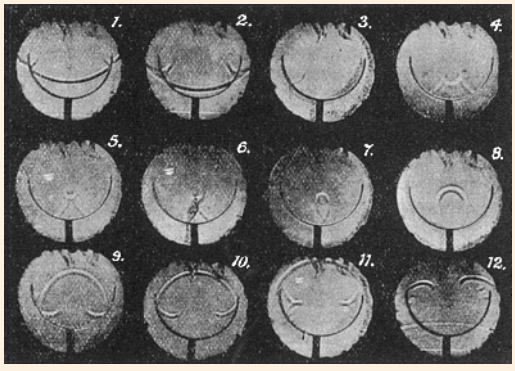

(c)

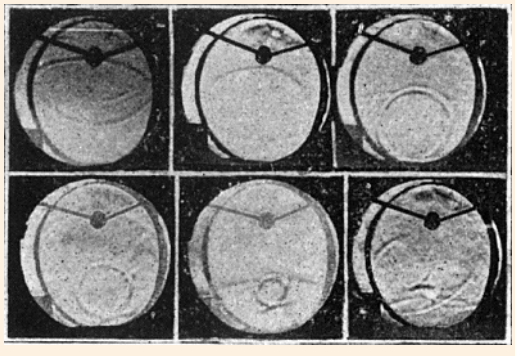

(d)

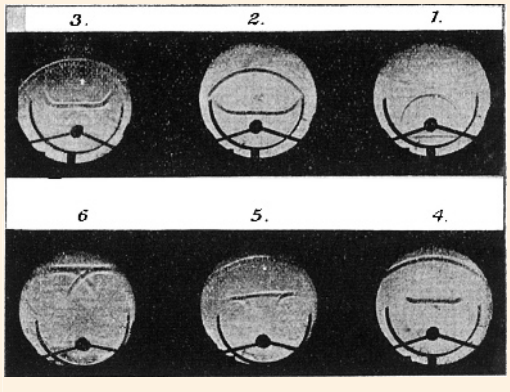

(e)

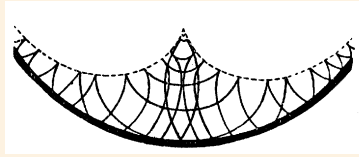

(f)

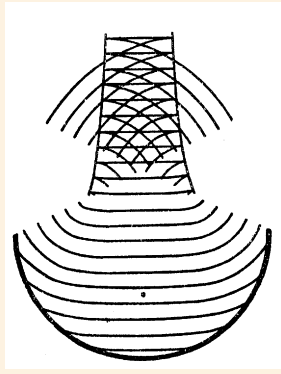

4.14–I In the late 1890s, the U.S. physics professor Robert W. WOOD (University of Wisconsin) resumed the pioneering schlieren studies of August TOEPLER, who in the mid-1860s was the first to visualize stroboscopically the propagation and reflection of weak shock waves emerging from electric sparks {⇨Figs. 4.5–A, B}. WOOD's original motivation was to illustrate in his lectures wave phenomena, in particular certain optical wave phenomena, by the "wave-front method" rather than by the "ray method" – today a standard technique in shock wave physics of interpreting wave phenomena. ***Left:*** He photographed a number of unusual wave focusing phenomena. *(a)* Transformation of a spherical into a plane wave by a parabolic mirror. *(b)* Generation of a cusp that always lies on the caustic surface when a plane wave enters a hemispherical mirror. *(c)* Demonstration of conjugated foci of an elliptical mirror that transforms by reflection a spherical wave diverging from one focus into a converging sphere, shrinking to a point at the other focus. *(d)* Transformation of a wave, starting at the principal focus of a hemispherical mirror and being reflected, into a nearly plane wave front in the vicinity of the axis, which curls up at the edges. ***Right:*** From some of the photographed wave focusing phenomena he drew schematics *(e)* and *(f)* to better illustrate their temporal evolution. [Proc. Roy. Soc. Lond. 66, 283 (1900); Nature 62, 342 (1900)]

4.14 SHOCK WAVE EFFECTS – Shock Focusing *(cont'd)*

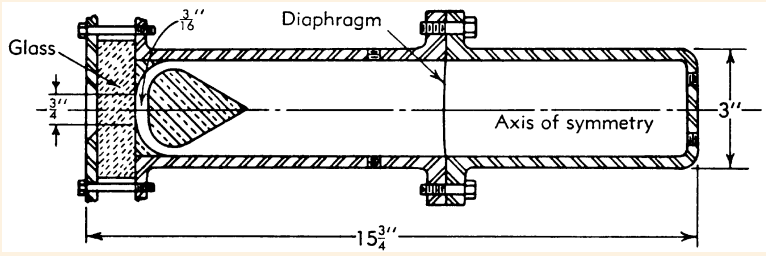

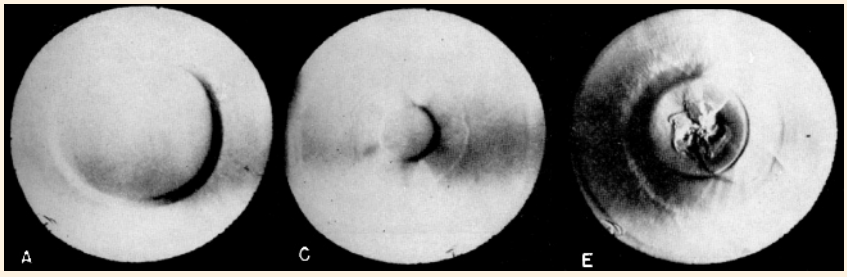

4.14–J ***Top:*** Robert W. PERRY and Anton KANTROWITZ (Cornell University, Ithaca, NY) used a special shock-tube geometry for producing converging cylindrical shock waves. They studied the implosion process through a glass plate "end-on." ***Bottom:*** High-speed cinematography revealed in more detail the conversion process of plane air shock waves with M = 1.8 into convergent cylindrical shock waves. The sequence of shadowgraphs was taken at increasing time instants (A → C → E). They noticed that the convergence stability became poorer with increasing shock strength. [J. Appl. Phys. **22**, 878 (1951)]

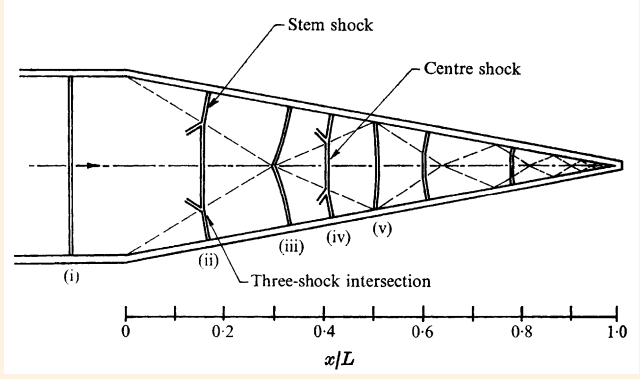

4.14–K ***Left:*** Robert E. SETCHELL, Erik STORM, and Bradford STURTEVANT (CalTech's Aeronautical Laboratory, Pasadena, CA) generated in a shock tube in argon at 1.5 Torr plane shock waves with high initial Mach numbers (M = 6–10.2) and investigated shock strengthening in a 10° half-angle conical convergent channel. ***Right:*** The profile of the shock wave velocity along the cone center line, measured with a new piezoelectric shock velocity probe, revealed that the shock velocity does not display the gradual monotonic increase as predicted by the 1-D Chester-Chisnell-Whitham theory, but rather shows a number of short intervals with sudden jumps. [J. Fluid Mech. **56**, 505 (1972)]

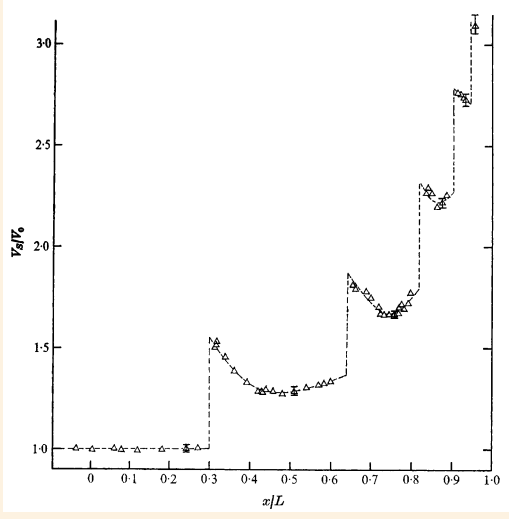

↑ The repeated cycles of Mach reflection on the cone wall, followed by Mach reflection of the stem shock on the cone axis, produce velocity jumps of the shock front along the cone center line, each jump being followed by a rapid decline and a gradual acceleration.

4.14 **SHOCK WAVE EFFECTS** – Transonic Shock Phenomena

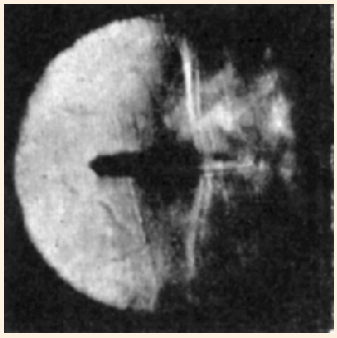

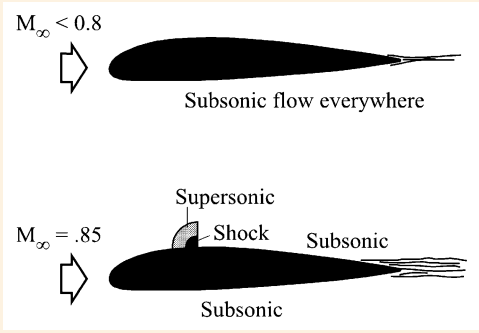

4.14–L When an aircraft approaches the speed of sound, the airflow over the wing reaches supersonic speed before the airplane itself does, and a shock wave forms on the wing. ***Top, left & center:*** In 1935, the U.S. aerodynamicist Eastman N. JACOBS showed pictures taken in NACA's wind tunnel from a transonic flow over a model wing, a NACA airfoil No. 0012-63. For $M < 0.79$ no shock has formed (*left*), but at reaching a so-called "critical Mach number," here $M_c = 0.79$, a shock is created (*center*) at the upper surface of the wing. [Proc. V. Convegno Volta, Rome (1935). Reale Accademia d'Italia, Rome (1936), pp. 383] ***Top, right:*** Schematic of shock wave formation in the transonic regime, when the Mach stream number M_∞ is increased from < 0.8 (subsonic flow above the wing) to 0.85 (supersonic flow). This leads to a sharp rise in drag and a loss of lift – so-called "shock stall." [Courtesy NASA] ***Bottom:*** Two examples of wing compression shock shadowgraphs taken during banked turns of a Lockheed L-1011 at $M = 0.85$ and an altitude of 10,700 m. Note that the left photo was taken looking toward the Sun. The right photo shows the wing-tip shock, which appears to be approx. 2 m high. [Courtesy Carla THOMAS, NASA Dryden Flight Research Center; Proc. 8th Int. Symp. on Flow Visualization, Sorrento (1998). IOS, Amsterdam (1999), p. 17.1]

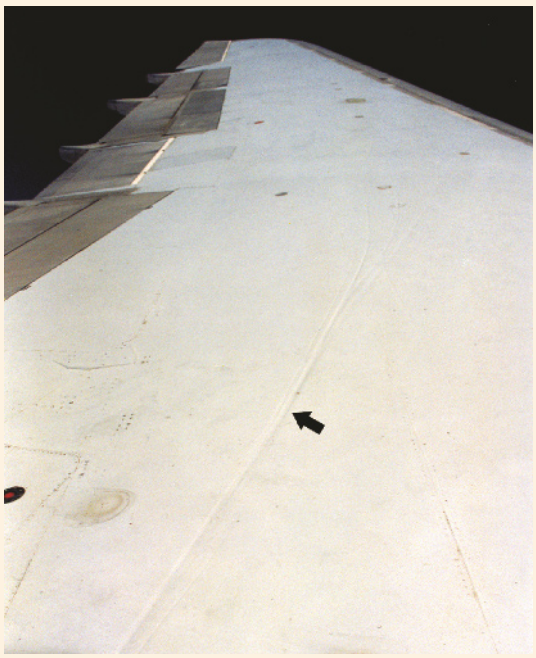

4.14 SHOCK WAVE EFFECTS – Aerodynamic Drag

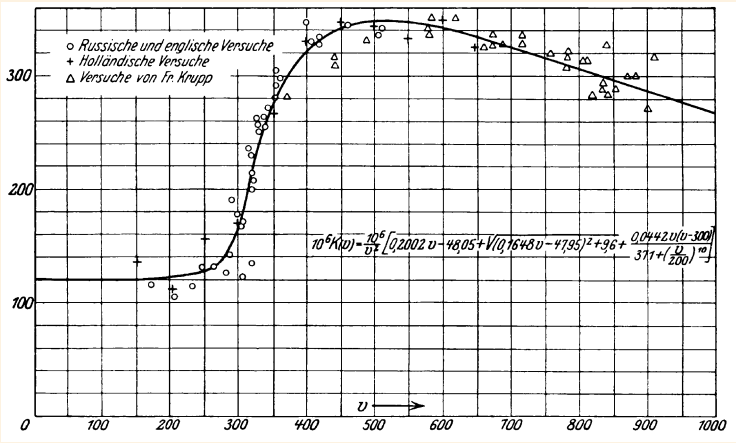

4.14–M This diagram is a result of numerous ballistic tests performed in Russia (MAIYEVSKII 1869), England (BASHFORTH 1866–1870), The Netherlands (HOJEL 1884), and Germany (Krupp Co. 1912). It shows that aerodynamic drag, also called "wave drag," decreases after passing the sound barrier {⇨Fig. 4.19–J}. From these data the Italian ballistician Francesco SIACCI derived in 1896 a standardized law of drag at high velocities. The projectile velocities v are in (m/s). [C. CRANZ: *Lehrbuch der Ballistik*. Springer, Berlin (1925), vol. 1, p. 65; Rivista di Artiglieria e Genio (Rome), vol. 1 (1896)]

4.14 SHOCK WAVE EFFECTS – WHITCOMB's Area Rule

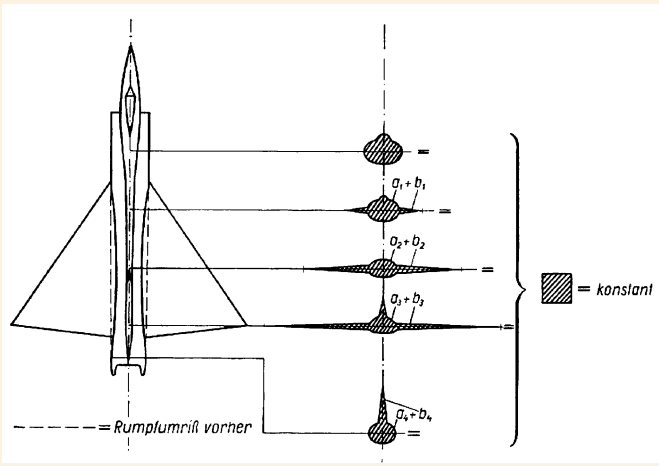

4.14–N ***Left:*** In 1951, Richard T. WHITCOMB at NACA discovered the "area rule," which postulates that, in order to avoid detaching of shock waves at transonic flight, all stepwise changes in cross sections of wings and the fuselage should be avoided and their total areas be kept constant along the plane's axis. In the case of delta wings, this results in a "coke-bottle" (or "Marilyn Monroe") shaped design of the fuselage (*broken lines*). Favorably, this reduces drag – thus allowing higher flight velocities and saving fuel. [Orion **11**, 974 (1956)] ***Right:*** The Convair F-102 ("Delta Dagger") was the first aircraft constructed after the area rule such that the total cross-sectional area of wings, fuselage, and tail should be that of an ideal streamlined body, *i.e.*, with a wasplike waist and a bulging tail. It was the world's first supersonic single-seat all-weather jet interceptor and the USAF's first operational (knife edge) delta-wing aircraft. The F-102 made its initial flight on October 24, 1953; the maximum flight velocity was 810 mph (1,303 km/h). [Courtesy USAF Museum Photo Archives]

4.14 SHOCK WAVE EFFECTS – Pseudo Supersonic Wave Effects

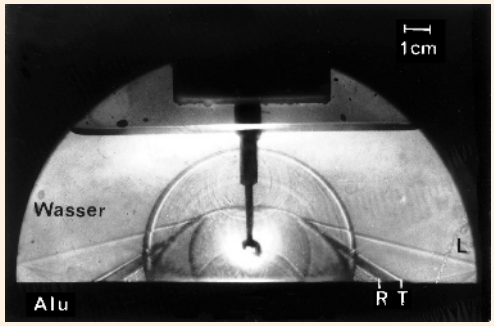

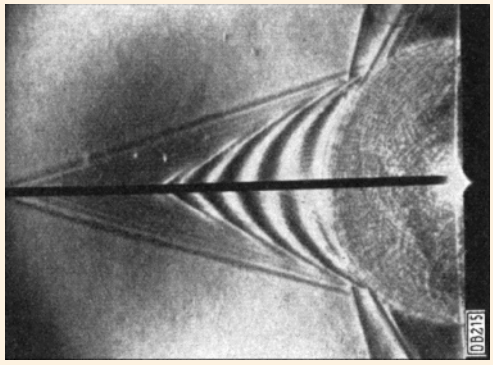

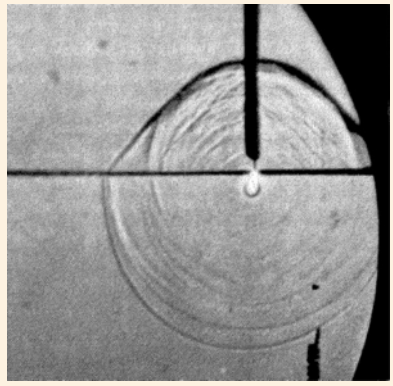

4.14–O Oswald VON SCHMIDT, a physicist at Humboldt University in Berlin, showed that any disturbance produced at the boundary of two media with different sound velocities generates a head wave similar to that of a supersonic projectile – actually a pseudo supersonic wave phenomenon that occurs for both acoustic and shock waves. ***Right:*** An electric spark generated at the interface of two liquids (*above*: an aqueous NaCl solution, sound speed 1,600 m/s; *below*: xylol with 1,175 m/s) produces two hemispherical waves. Waves, traveling some horizontal distance along the interface with 1,600 m/s, return to the upper half space, thereby according to HUYGENS' principle producing a straight "Schmidt head wave" (SHW). [Physik. Z. **39**, 868 (1938)] ***Left, top***: A thin copper wire, exploding in water (sound speed u_1) above an aluminum surface (sound speed u_2), generates the three main types of SHWs, which emerge under different angles α_L, α_T, and α_S according to the relation

$$\alpha_{L,\,T,\,S} = \arcsin u_1/(u_2)_{L,\,T,\,S}.$$

Here $(u_2)_{L,\,T,\,S}$ are the longitudinal, transverse, and surface wave speeds in the lower half space, respectively [Photo by author]. ***Left, bottom:*** At Göttingen University, Erwin MEYER showed that flexural waves also generate SHWs. [Z. Tech. Phys. **19**, 554 (1938)]

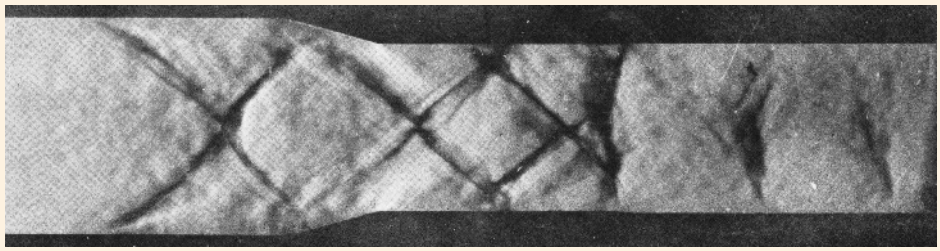

4.14–P E.P. NEUMANN and F. LUSTWERK at MIT (Cambridge, MA) observed the development of a pseudoshock in the presence of thick boundary layers. The pseudoshock taken in the throat of a diffuser actually begins for $M = 2.55$ at the entrance of the convergent portion (*left*). [J. Appl. Mech. **17**, 195 (1949)]

4.14 SHOCK WAVE EFFECTS – Gasdynamic Laser

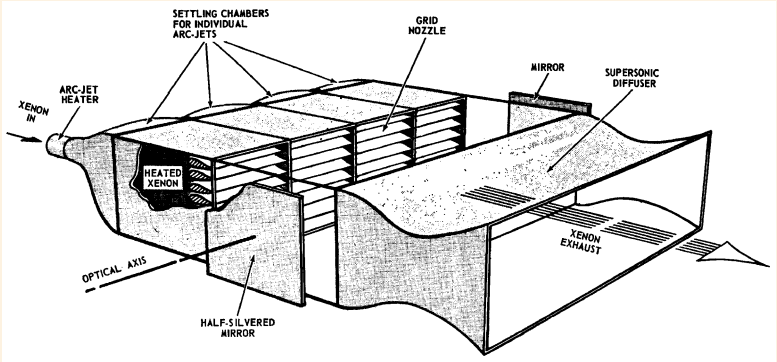

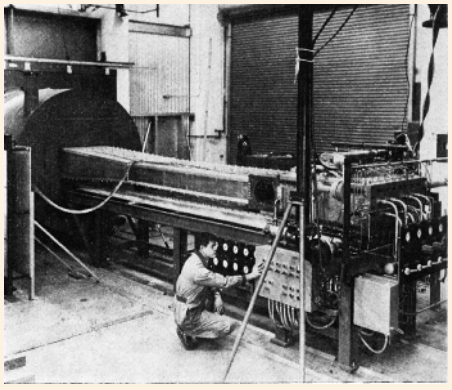

4.14–Q To realize a gasdynamic laser, Ian R. HURLE and Abraham HERTZBERG at Cornell Aeronautical Laboratory (Buffalo, NY) suggested various fluid-mechanical techniques of population inversion. ***Top:*** To create a highly nonequilibrium region where a strong population inversion can take place, they proposed the rapid expansion of a highly excited gas by a system of grid nozzles. However, the immediate experimental proof failed. [Phys. Fluids **8**, 1601 (1965)] In 1966, the first gasdynamic laser, using a hot gas mixture of $CO_2/N_2/H_2O$ expanding through a supersonic nozzle, was successfully operated at AVCO Everett Research Laboratory (Everett, MA). ***Bottom:*** This large-scale gasdynamic laser, developed there and operated with CO as the fuel, was among the very first high-power lasers. It produced 60 kW of multimode power. [IEEE Spectrum **7**, No. 11, 51 (1970)]

4.14 SHOCK WAVE EFFECTS – Shock-On-Shock Problem

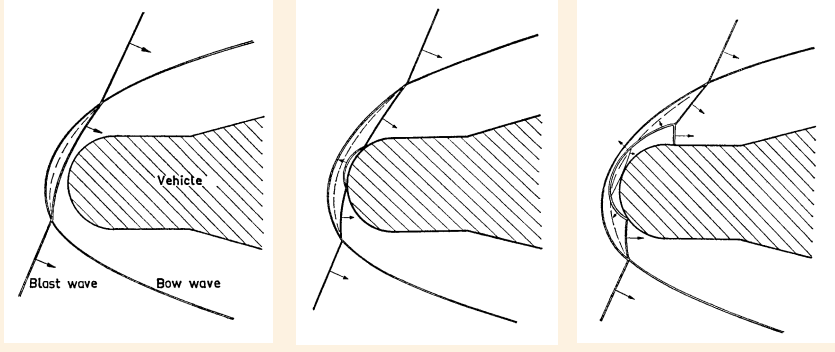

4.14–R Schematic of a "shock-on-shock" (SOS) interaction, illustrated here by Bo LEMBCKE, a Swedish mechanical engineer, at the example of a supersonic body hit obliquely by a plane blast wave (time proceeds from *left* to *right*). A complex wave pattern of reflecting and interacting shocks is produced, including Mach reflection. [FFA-Rep. 109, Aeronaut. Res. Inst. of Sweden, Stockholm (1967)] 2-D and 3-D SOS interactions stimulated many numerical studies.

4.14 **SHOCK WAVE EFFECTS** – Shock Wave Interactions in Metals

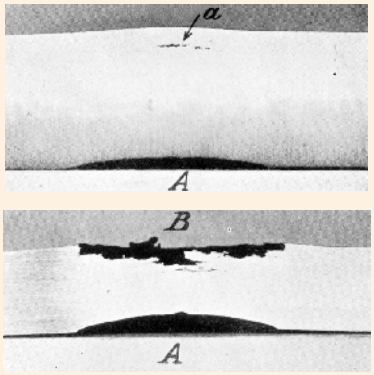

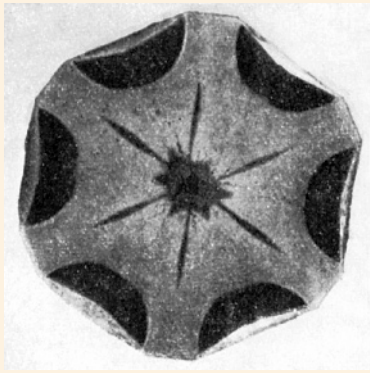

← In 1962, Lev V. AL'TSHULER in the Soviet Union studied the interaction of colliding shock waves in metals subjected to the explosive action of several charges. The dark etched zones of the polished sample, stretching along the radii, are the results of oblique collision of two neighboring shock waves, which produce phase transformation induced by pressures > 130 kbar. The central spot is the result of a superposition of six waves. [Sov. Phys. Uspekhi **8**, No. 1, 72 (1965)]

4.14–S ***Left:*** In the early 1900s, Bertram HOPKINSON at Cambridge University observed that mild steel plates, being exposed to detonating guncotton at their bottom side *A*, revealed either a crack *a* in the case of a 1.25-in. (31.8-mm)-thick plate (*top*) or a scab torn off from *B* in the case of an only 0.75-in. (19-mm)-thick plate (*bottom*). He correctly interpreted that this "spalling effect" is caused by the reflected stress wave, leading to tension and fracture in the shocked material. [*Scientific Papers of B. HOPKINSON.* Cambridge University Press, Cambridge (1921)] ***Right:*** Macrostructure of a steel cylinder in the cross section when six charges are blasted simultaneously

4.14 **SHOCK WAVE EFFECTS** – Shock-Induced Solidification

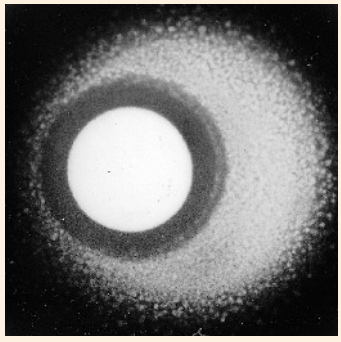

τ = 77 μs; d = 0.15 mm

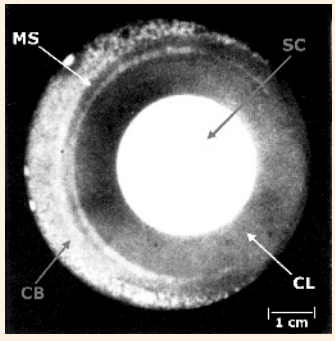

τ = 243 μs; d = 2.0 mm

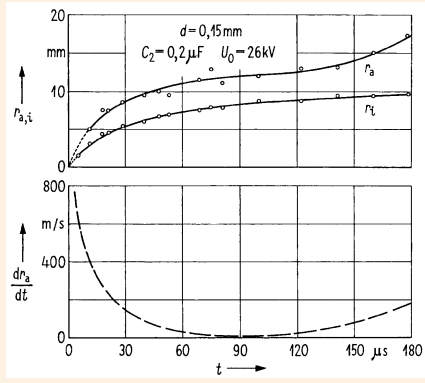

4.14–T ***Left & center:*** Flash radiographs taken at different time instants τ after the onset of discharge of a melting shock wave *MS*, propagating by stepwisely melting from the periphery of a shock-solidified organic liquid (bromobenzene, C_6H_5Br). This phenomenon, predicted by Werner SCHAAFFS at TU Berlin in 1948 and first photographed by Peter KREHL in 1968, was generated in a thin liquid layer of thickness *d* by an expanding plasma *SC* from a capacitor discharge between two plane electrodes. The surrounding compressed liquid *CL* contains numerous cavitation bubbles *CB* initiated by electrode vibrations during discharge. ***Right:*** Diagrams showing the radial expansion of the plasma channel, $r_i(t)$, and of the compression ring, $r_a(t)$. For a 0.15-mm-thick liquid layer, the expansion velocity of the compression ring, dr_a/dt, reaches at about 90 μs a minimum of only a few meters per second, apparently due to the shock-induced solidification of the liquid that solidifies at room temperature under static pressures already at about 3 kbar. [Acustica **23**, 99 (1970)]

4.14 SHOCK WAVE EFFECTS – Other Phenomena

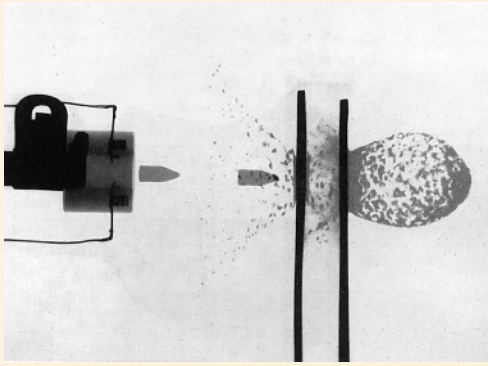

4.14–U Superposition of three flash radiographs showing a sequence of a 30-06 bullet in air penetrating a so-called "Whipple shield" – a configuration invented in 1946 by the astronomer Fred L. WHIPPLE. It is based on the principle that small meteoroids and orbital debris explode when they strike a solid surface; therefore if a spacecraft is protected by an outer skin about a tenth of the thickness of its main skin, an impinging body will be destroyed before it can cause any real damage. The simplest kind of Whipple shield consists of a bumper, such as a thin sheet of aluminum, and a standoff, or open space, between the bumper and the wall of the spacecraft to allow any remaining fragments that make it past the bumper to spread out. Here the shield consists of two $^1/_8$-in. (3.2-mm) lead plates, arranged in parallel at a small distance. [Picture taken by John P. BARBOUR and associates at Field Emission Corporation in McMinnville, OR. *See* Proc. 7th Int. Congr. on High-Speed Photography, Zurich (1965). Helwich, Darmstadt (1967), p. 292]

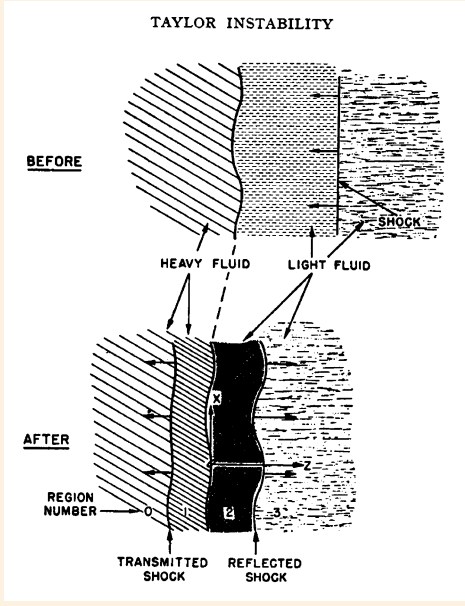

4.14–V The British physicist Geoffrey I. TAYLOR at Cambridge University developed a theory of the growth of irregularities on the interface between two fluids of different densities when they are in accelerated motion, such as illustrated by him in the case of a shock wave striking a boundary. This leads to damped oscillations in the shock wave, which influence the motion of the interface – a phenomenon called "Taylor instability." [Comm. Pure Appl. Math. **13**, 299 (1960)]

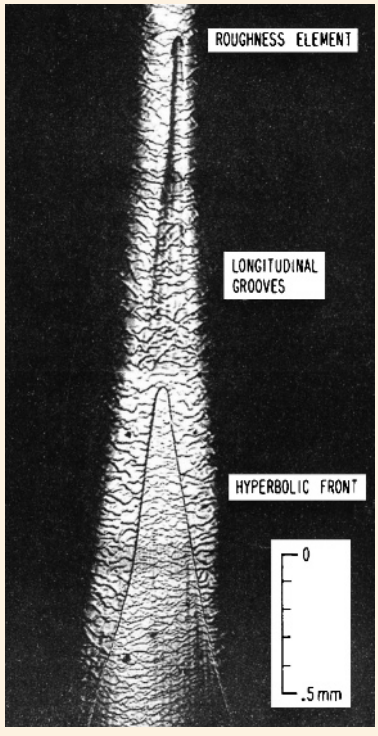

← CANNING and collaborators observed that "longitudinal grooves" and a "hyperbolic front" were superimposed on a pattern of "long- and short-wavelength ripples," overlying the entire surface. The origin of these grooves, etched in the surface within the wedge area, were later interpreted as a by-product of longitudinal vortices caused by Taylor-Görtler vortices in the boundary layer.

4.14–W In the 1960s, Thomas N. CANNING and collaborators at NASA's Ames Research Center (Moffet Field, CA) studied ablation patterns on cones of 1-cm-dia. plastic (Lexan or Delrin) models at hypersonic velocities up to 7 km/s and noticed curious patterns on the cone surface [AIAA J. **6**, 174 (1968)]

4.15 SHOCK WAVE APPLICATIONS – Miscellaneous

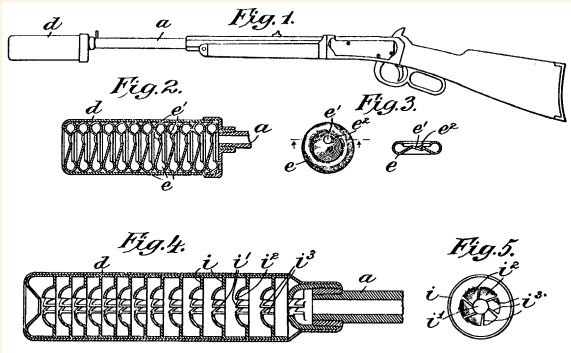

4.15–A The silencer for firearms was invented in New York around 1905 by Hiram Percy MAXIM (son of Sir Hiram Stevens MAXIM – who in 1889 developed the first fully automatic machine gun). ***Top:*** He already used the modern concept of a multiple-baffle system. This drawing was reproduced from one of his early patents granted to him in 1910 by the German Patent Office. [K.R. PAWLAS: *Waffengeschichte.* Chronica-Reihe, Folge **W 123**, Publ. Archiv, Nürnberg (1983); DRP Nr. 220,470 (1910)] ***Bottom:*** View of his perforated deflector system, which reversed the gases stepwise, from diaphragm to diaphragm.

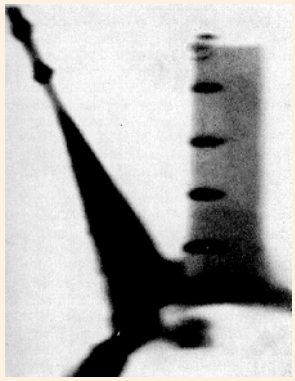

4.15–B Rudi SCHALL and Gustav THOMER, two German physicists at ISL (Saint-Louis, France), proposed a simple method to derive Hugoniot data from flash radiographs of shock-compressed materials. Flash radiograph of a shock wave generated from a solid explosive at the bottom of a water column (*right*) moving upwards. Lead marks positioned along the water column are used for distance calibration. The shock velocity in the water was determined by comparison with a detonating fulminate fuse (*left*) of known detonation velocity and the shock compression ratio ρ/ρ_0 at the shock front from X-ray densitometry data. [Z. angew. Phys. **2**, 252 (1950)]

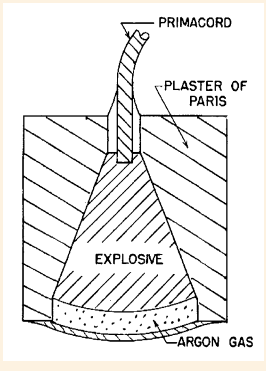

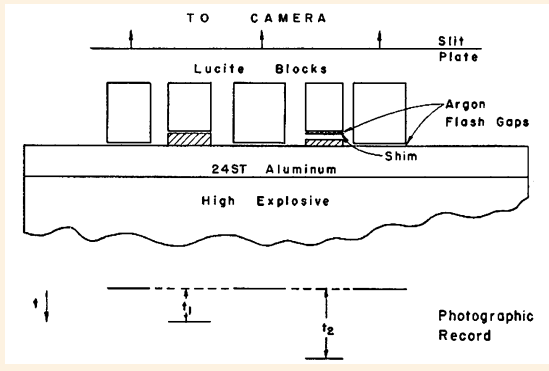

4.15–C A brilliant flash of light is generated when a strong shock wave strikes a layer of a noble gas. The duration of intensity can be made very short by decreasing the thickness of the gas layer. ***Left:*** Example of an "explosive flash charge" designed as a flash light for underwater photography using a thin layer of argon. [R.H. COLE: *Underwater explosions.* Dover, New York (1965), p. 214] ***Right:*** This phenomenon was also applied in the so-called "flash gap technique" developed in the late 1950s by John M. WALSH and Russell H. CHRISTIAN at LASL (Los Alamos, NM) in order to determine the shock-wave and free-surface velocities from measured flash time arrivals, known specimen thickness, and free-run distance. [F. SEITZ and D. TURNBULL (eds.): *Solid state physics.* Academic Press, New York (1958), vol. 6, p. 21]

4.15 SHOCK WAVE APPLICATIONS – Determination of Seismic Wave Velocities

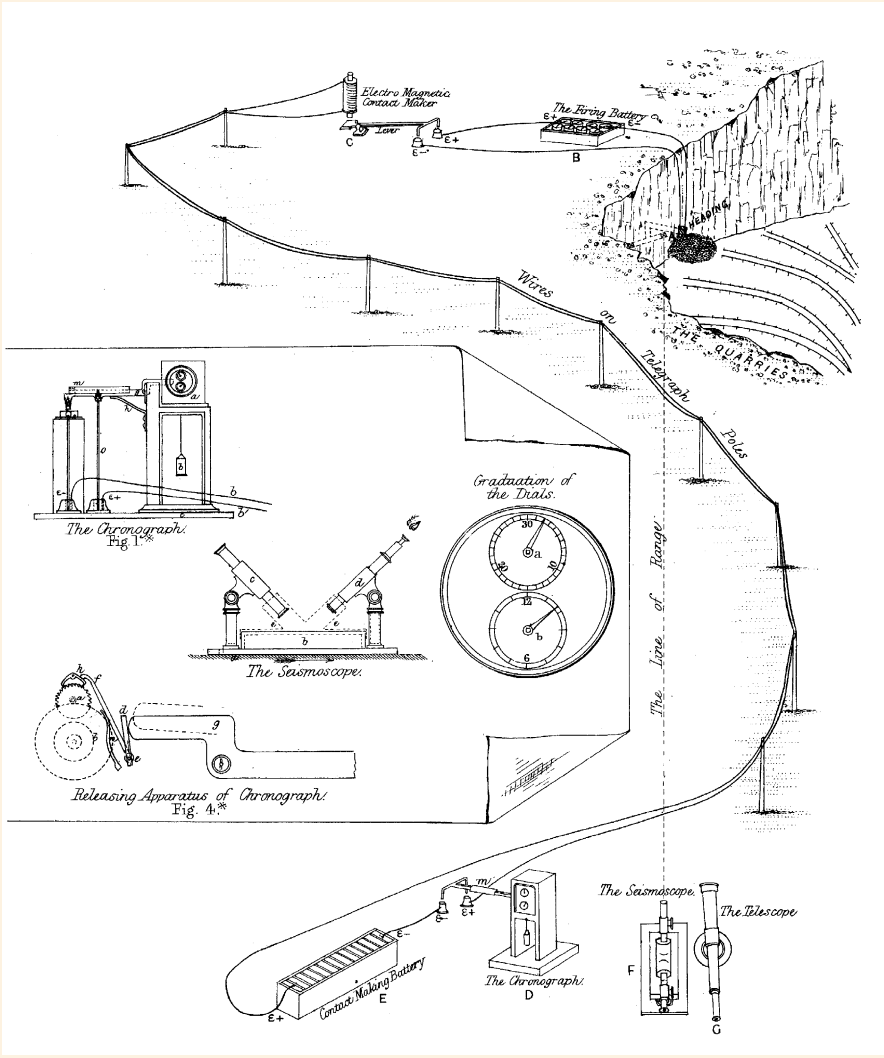

←
MALLET made his seismic experiments at Holyhead in North Wales in order to ascertain the transit velocity of waves, analogous to earthquake waves, through the local rock formations. Supported in his study by Charles WHEATSTONE and Thomas R. ROBINSON, he generated artificial earthquakes by applying black powder, a low explosive not very appropriate for this purpose; however, dynamite had not yet been invented. He positioned a mercury horizontal seismometer at a large distance from the explosion and observed the arrival of the seismic wave that he assumed would show up based on the sudden appearance of ripples at the mercury surface. Note that he used the Hipp-Wheatstone chronometer {⇨Fig. 4.19–A} to measure the delay between triggering the charge and arrival of the longitudinal (P-) wave.

4.15–D In the period 1856–1857, the Irish engineer Robert MALLET performed seismic experiments to study the propagation and velocity of elastic waves in geologic layers, thus hoping to get information on the geologic nature of subterraneous layers. He correctly assumed that the longitudinal (elastic) waves precede the slower transversal waves; however, he did not assume any surface waves. Although he used huge single charges of black powder up to 5,000 kg, he was unable to detect the precursor in a distance beyond 2 km from the origin of explosion. MALLET's pioneering experiments, albeit unsuccessful, were a milestone toward geophysical prospecting. In 1876, the U.S. military engineer Henry L. ABBOT, on the occasion of blowing off the gneiss river bed of the East River at Hallet's Point, NY by using huge charges of high explosives (up to 22,000 kg of dynamite), was able to clearly resolve the arrival of the longitudinal wave at a distance of up to 220 km. [Phil. Trans. Roy. Soc. Lond. **150**, 655 (1860), plate XXIII]

4.15 **SHOCK WAVE APPLICATIONS** – Explosion Seismology: the "Mintrop Wave"

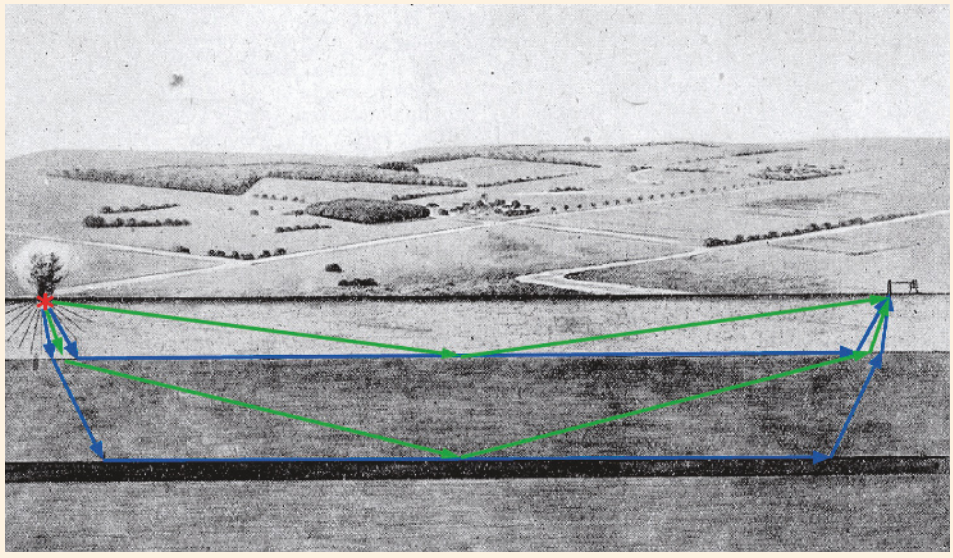

← The two principal seismic survey techniques in simplified form: in the *reflection method* the seismic waves take the green paths; in MINTROP's *refraction method* they take the blue paths. At greater distances the seismic pulse travels faster by the refraction path because its velocity is greater along the boundary than it is through the upper layer, a pseudo-supersonic effect.

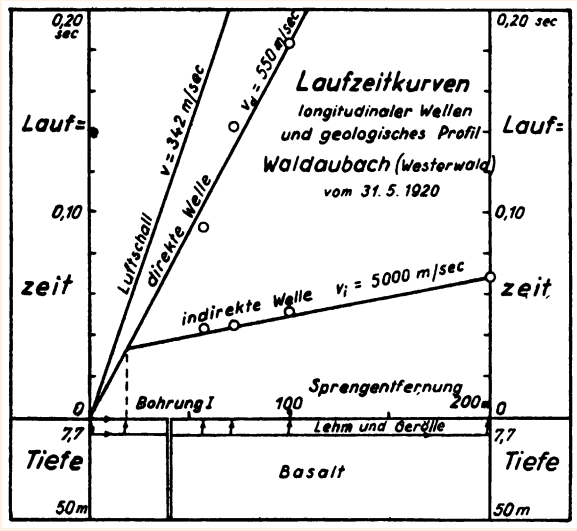

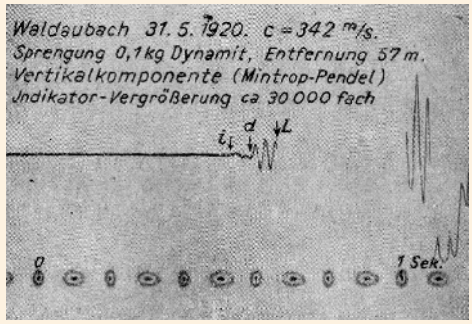

← The arrival times of the direct wave and the indirect wave plotted in a time-distance diagram are located at two straight lines of different slopes that intersect at the so-called "bent distance" from which the unknown depth of the lower stratum can easily be inferred. In the illustrated example, the upper layer consisted of a 7.7-m-thick clay stratum, followed by a thick basalt stratum.

4.15–E ***Top:*** Schematic of the generation, propagation, and recording of elastic seismic waves using MINTROP's refraction or "boundary wave" method. Generally, the density of rocks near the surface of the Earth increases with depth. An explosion generated at the surface induces elastic seismic waves in the soil. When arriving at the boundary of a deeper layer of higher acoustic impedance, the waves are transmitted along the boundary with the sound velocity of the lower layer, *i.e.*, supersonically with respect to the sound velocity of the upper layer. ***Bottom, left:*** Diagram of seismic wave propagation. ***Bottom, right:*** MINTROP's famous seismogram of an "artificial" earthquake taken on May 31, 1920 in Waldaubach, Germany by detonating 0.1 kg of dynamite. [Die Naturwissenschaften **34**, 257 (1947)]

4.15 **SHOCK WAVE APPLICATIONS** – Medical Therapy

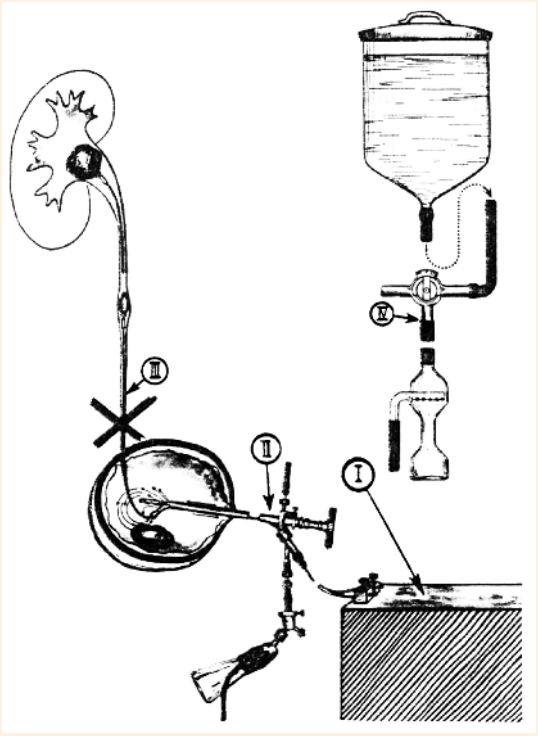

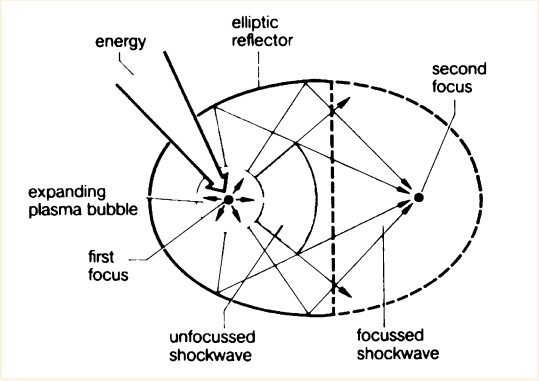

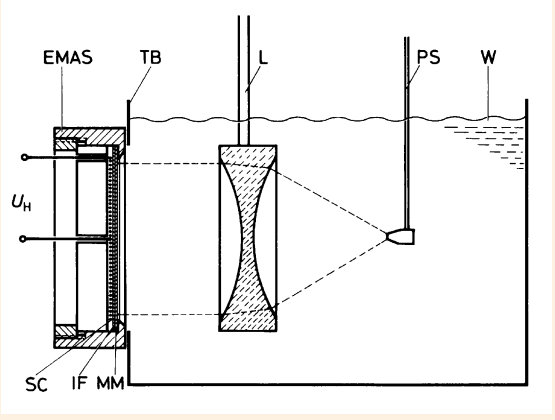

Interframe time 1 ms; Time →

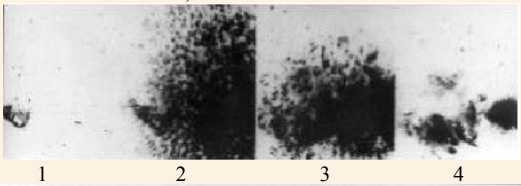

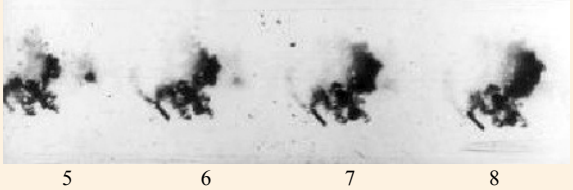

4.15–F ***Left:*** Victor GOLDBERG's "electro-lithotripsy" – the archetype method of modern shock lithotripsy. It was the first successful method of so-called "intracorporeal shock lithotripsy." His first patient was a 58-year-old man. [Der Urologe **B19**, 23 (1979)] ***Right, top:*** So-called "extracorporeal shock lithotripsy," a more advanced method. Developed in Germany by Dornier Medizintechnik, it employs an exploding plasma emitter as a point source together with an elliptical reflector. [Proc. IEEE **76**, 1236 (1988)] ***Right, center:*** Another method, commercialized by Siemens AG, applies an electromagnetic plane shock wave generator with a metallic membrane *MM*, combined with an acoustic lens *L*. [Siemens Forsch.- Entwickl.-Ber. **15**, 187 (1986)] ***Right, bottom:*** The first motion pictures of fragmentation of a kidney stone, taken at 1,000 frames per second by Bernd FORSSMANN and collaborators at Dornier System, NTF Medizintechnik (Friedrichshafen, Germany). The shock wave was generated by a spark discharge and focused by an elliptical reflector. The movie revealed that the stone disintegration was invisible until about 1 to 2 ms after interaction with the shock wave. [BMFT Symp. "Biophysikalische Verfahren zur Diagnose und Therapie von Steinleiden der Harnwege," Meersburg, Germany (Juni 1976). Wiss. Berichte, Dornier System GmbH, Friedrichshafen]

4.15 SHOCK WAVE APPLICATIONS – Materials Research and Metal Working Industry

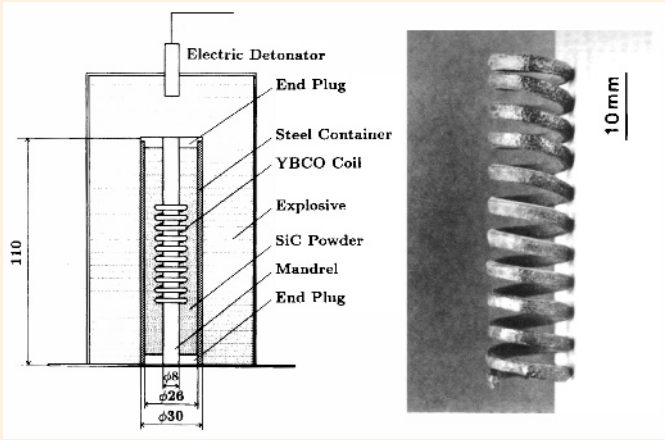

4.15–G Explosive setup used by Kazuki TAKASHIMA and collaborators in Japan for producing a coil of high-density superconductive material from Y-Ba-Cu-oxide powder. [*Proc. 6th APS Topical Conf. on Shock Compression of Condensed Matter*. Albuquerque, NM (1989). North-Holland, Amsterdam (1990), p. 591]

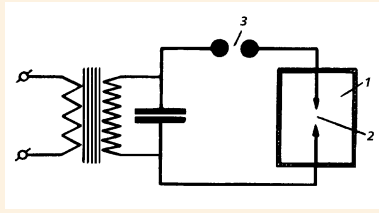

4.15–H Lev A. YUTKIN's circuitry to generate intense shock waves by a spark discharge (*2*) immersed in a non-conducting liquid (*1*). It avoids high-voltage DC potentials by using a pulse transformer. YUTKIN's so-called "electrohydraulic effect" was later applied to industrial metal forming ("hydrospark forming") and intensification of chemical-metallurgical processes, but also appears promising for well-drilling and grinding of materials. The urologist V. GOLDBERG first used this method for disintegrating bladder stones {⇨Fig. 4.15–F}. [L.A. YUTKIN: *Elektrogidrav-liceskij effekt*. Masgiz, Moscow (1955)]

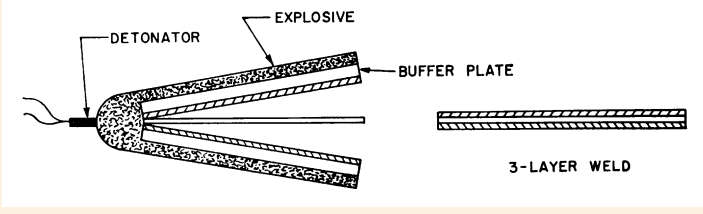

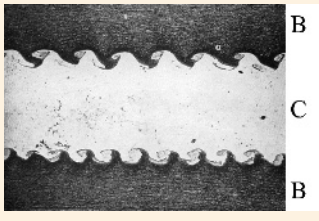

← This photomicrograph shows multiple welds between brass *B* and copper *C*. The surface waves that arose across while the metals were melted have frozen into a pattern of tiny hooks that strengthen the two bonds considerably.

4.15–I The most common explosive metalworking technique is "explosive welding," also known as "explosive bonding." When two dissimilar metal plates are driven together by detonation of a high explosive, they impact with each other at high velocity and may bond along the interface. ***Top:*** Experimental arrangement for a three-layer weld. As the detonation wave propagates along the explosive layers, the upper and lower plate violently collapse against the central plate. ***Bottom:*** The sequential collapse of the plate elements causes the metal close to the interacting surface to participate in the surface jetting effect. [J.S. RINEHART and J. PEARSON: *Explosive working of metals*. Pergamon, Oxford (1963), p. 312]

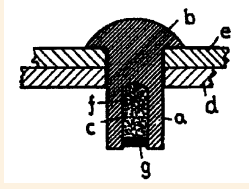

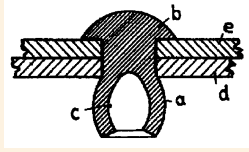

4.15–J The explosive rivet was invented by the German BUTTER Brothers. ***Top:*** Its shank *a* is filled with an explosive compound *c*, and the head of rivet *b* is heated to initiate the explosive. ***Bottom:*** The explosion forces the bottom of the rivet that extends past the edge of the material to expand to be larger than the diameter of the drilled hole. Blind rivets are needed when space limitations make conventional rivets impractical. They were first largely used during World War II in the U.S. aircraft industry. [Germ. Patent Nr. 655,669 (1937)]

4.15 SHOCK WAVE APPLICATIONS – Oil Production Industry

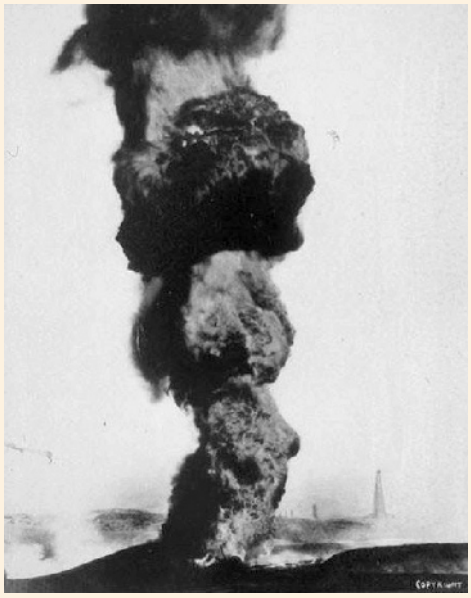

4.15–K ***Left:*** Photo of a burning oil well taken in 1913 at KT&O, Midway Fields (near Taft, CA). It shows smoke and flames ringing straight up in a column over 300 m high. The American Karl KINLEY had the idea of putting out the fire using for the first time nitroglycerin, appropriately calling the blast's action on the flame torch "snuffing it out." ***Right:*** Photo showing KINLEY standing far right, his right hand resting on the box of explosives which he used to put out the fire. [Courtesy Karl KINLEY Jr., Kinley Corp., Houston, TX]

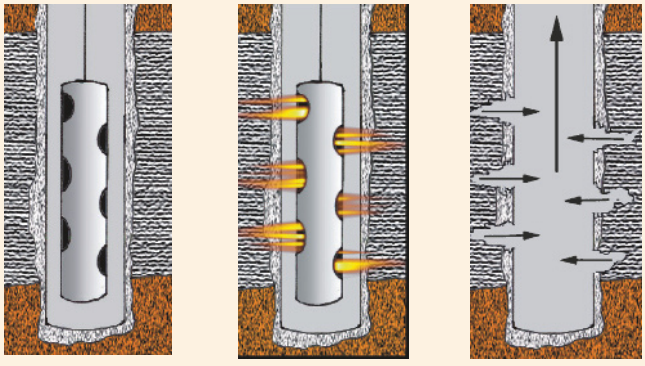

4.15–L Shaped charges accomplish penetration by creating jets of high-pressure, high-velocity gas. When the petroleum industry discovered the outstanding utility of shaped charges, they were used in the perforation of steel casings of well bores at depths thousands of feet below the surface. ***Left:*** The shaped charges, similar to those used in armor-piercing shells, are arranged in a tool, called a "gun," which is lowered into the well on a wire line and positioned opposite the producing zone (*left*). Then the charges are fired by electronic means from the surface (*center*), which produces holes extending some distance into the geologic formation. After the perforations are made, the tool is retrieved (*right*). Oil or gas now flows easier into the well bore. The use of these so-called "shaped-charge perforating guns" became the standard method of completing oil- and gas-producing wells. [Maverick Energy, Robinson, IL, http://www.maverickenergy.com/fundamentals.html] ***Right:*** A close-up of the shaped-charge perforating gun showing a shaped charge with primer belonging to it. A number of shaped charges are connected in a series via a detonation cord which provokes that the shaped charges are fired in a sequence. [Schlumberger Oil Field Glossary; http://www.glossary.oilfield.slb.com/DisplayImage.cfm?ID=474]

4.16 EXPLOSION, IMPLOSION, AND DETONATION – Early Use of Black Powder

← The enlargement shows details of the blasting work: The charge was put in holes, tamped, and triggered via a match set on fire by a lamp. Since remote electric triggering was not yet available, the miner had to flee immediately from the gallery. The miners wore leather jackets with a deeply cut tail, because much work could be done in a lying position only.

4.16–A Black powder for blasting purposes was used in Lower Hungary since 1629. The back side of this Anhalt-Harzgerode "yield medal," coined in 1694 by the Dessau Mint (silver-weight 86 g, dia. 62 mm), illustrates on its left side the blasting method. The translation of the Latin inscription is "Under the protection of God in naught to fear." [Originally kept at Preußische Bergwerks- und Hütten-AG in Hannover, Germany; present location unknown]

4.16 EXPLOSION, IMPLOSION, AND DETONATION – Hollow Charge Effect

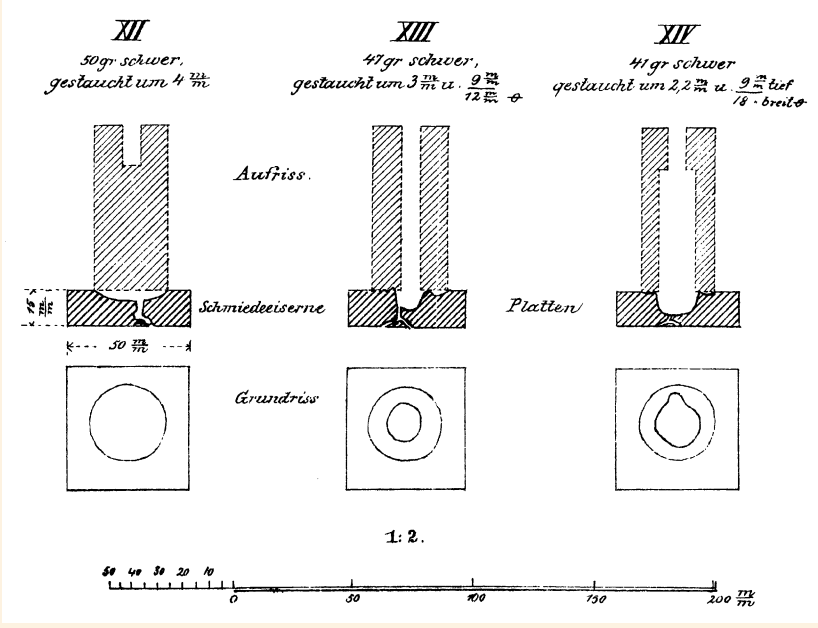

4.16–B In the early 1880s, Max VON FÖRSTER, a German mining engineer, experimented with detonating cartridges filled with guncotton. He systematically studied their mechanical action on a 15-mm-thick wrought-iron plate, the influence of the charge weight, and its geometry on the produced damage. His experiments revealed the surprising result that a hollow cartridge (*XIII*, *XIV*) produced a cavity about twice as deep as a solid cartridge (*XII*) of higher weight. [M. VON FÖRSTER: *Versuche mit comprimirter Schießbaumwolle*. Mittler, Berlin (1883)] Five years later, the U.S. military chemist and inventor Charles MUNROE discovered the same effect ("Munroe effect"). Also known as the "hollow charge effect" or "cavity effect" this discovery is a milestone in the evolution of detonation physics and military technique.

4.16 EXPLOSION, IMPLOSION, AND DETONATION – Underwater Explosions

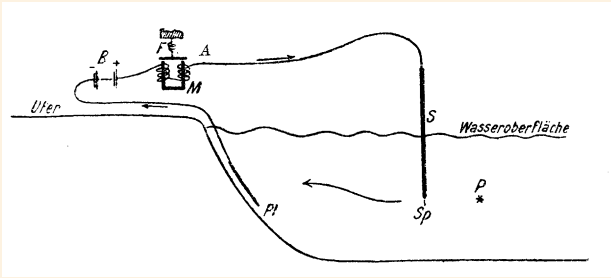

4.16–C Carl W. RAMSAUER, a German physicist at Danzig University, used an electrolytic method to measure the expansion dynamics of the gas sphere ("bubble") of an underwater explosion. Illustrated here on the example of a single-probe circuit, it applies a battery *B*, an electromagnet *M*, an isolated steel rod *S* with a bare tip *Sp*, and a plate electrode *Pl*. The sea water, acting as an electrolyte, forms a conducting circuit and activates *M*. When an explosive is initiated at *P*, the bubble expands and at the arrival of *Sp* interrupts the current, thereby deactivating *M*. Using a chronograph and many such probes arranged at different distances from *P*, it is possible to resolve in time both the growth of the bubble and its upward motion. [Ann. Phys. **72** (IV), 265 (1923)]

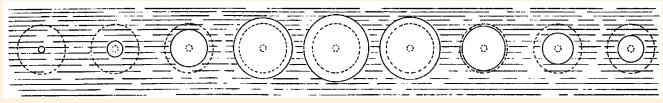

4.16–D In the 1890s, G.F. Rudolph BLOCHMANN, a military engineer at the German Imperial Navy, first studied the gas globe oscillation of an underwater explosion (*top*). To measure the pressure-time profiles in the water he used a "dynamometer" (*center*), a pressure gauge with a spring-loaded piston, and recorded the piston displacement by a rotating-drum chronograph. He produced small-scale underwater explosions by detonating small charges of guncotton (15–60 g) and first observed a train of pressure pulses (*bottom*) which he correctly correlated to the oscillating gas sphere, the so-called "bubble pulsations." Working out a first theory of underwater explosions, he compared the gas globe oscillation with the vibration of a simple spring-mass system. [Marine-Rundschau **9** (1. Teil), 197 (1898)]

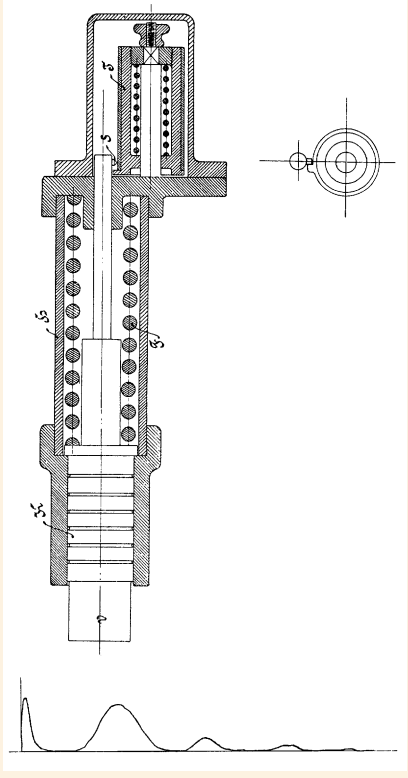

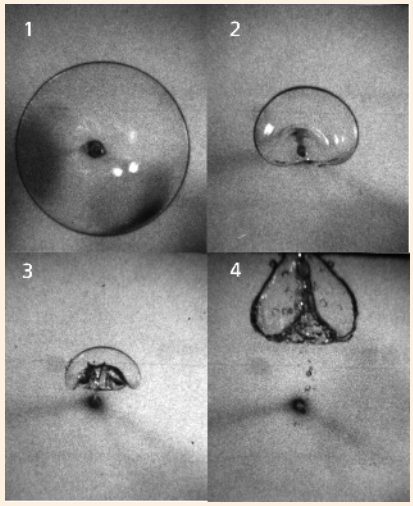

4.16–E Georges L. CHAHINE at Dynaflow and researchers at the Naval Surface Weapons Center used spark-generated bubbles for modeling underwater explosion bubble dynamics. This allows clear observation of reentrant jet formation inside the bubble, because the explosive detonation products generally occlude the view of the interior of the bubble. This series, taken with a Hycam camera at 10,000 frames/s, illustrates bubble dynamics in a gravity field, the reentrant jet dynamics, and the toroidal bubble rebound. [Courtesy Dr. Georges L. CHAHINE, Dynaflow, Fulton, MD. Proc. 66th Shock & Vibration Symp., Biloxi, MS (1995). SAVIAC, Arlington, VA (1995), vol. 2, p. 265]

4.16 EXPLOSION, IMPLOSION, AND DETONATION – Implosion and Explosion in a Gas

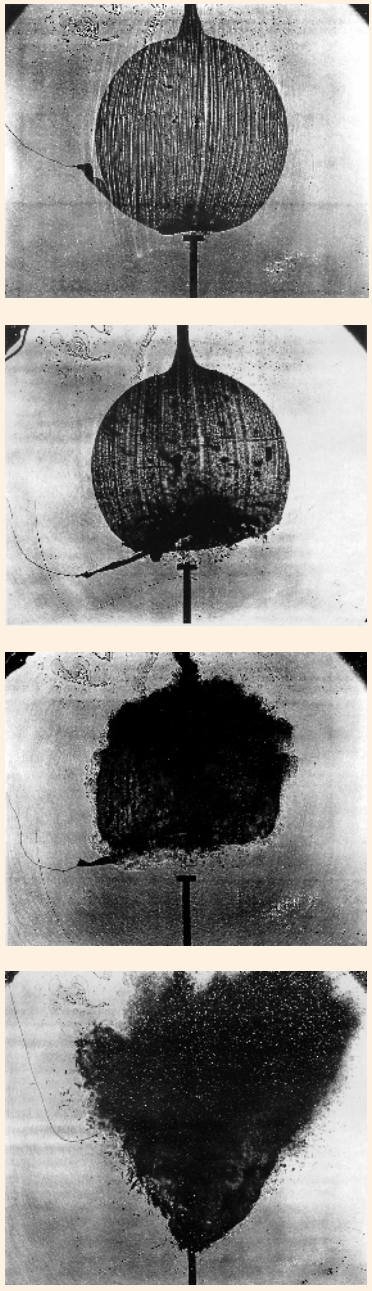

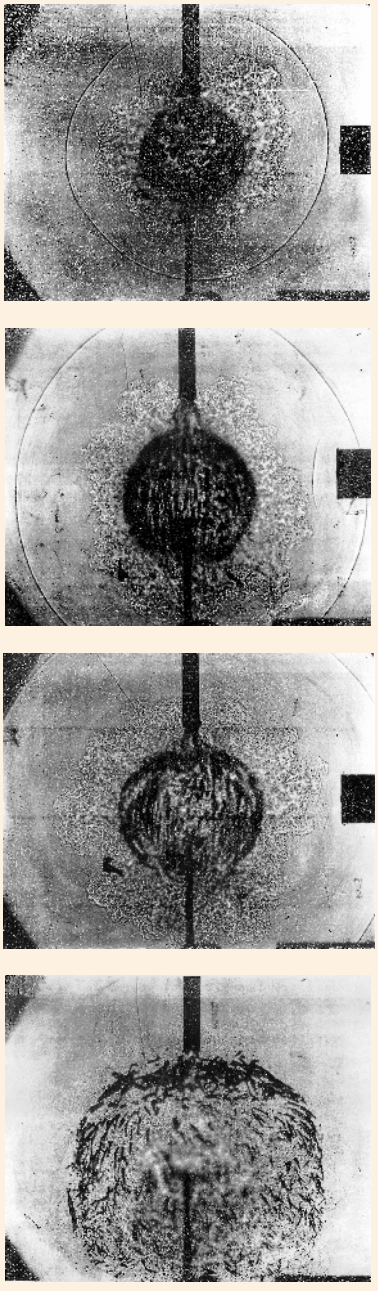

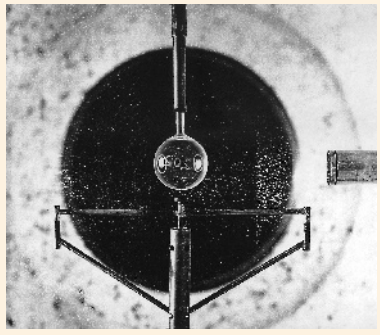

4.16–F ***Right:*** Donald W. BOYER at the University of Toronto Institute of Aerophysics (UTIA) studied the explosion and implosion of thin glass spheres using the schlieren method in conjunction with a rotating-drum camera. ***Left:*** Implosion was provoked by reducing the internal pressure of a 5-in. (12.7-cm)-dia. sphere to about 7 psi (0.48 bar) and increasing the external air pressure to 65 psi (4.5 bar); triggering occurred by using a mallet striking the glass sphere. ***Center:*** Explosion of a 2-in. (5.1-cm)-dia. glass sphere into ambient pressure was provoked by increasing its internal pressure up to 400 psi (27.5 bar). The emitted shock wave is clearly visible and could be measured with a pressure gauge shown on the far right of each frame. At a later time instant, the glass fragments have moved out noticeably, though collectively they still form a rough sphere. [D.W. BOYER: *Spherical explosions and implosions*. UTIA Rept. No. 58 (1959)]

←←
IMPLOSION, taken 0; 1,350; 1,740; and 2,195 μs after triggering

←
EXPLOSION, taken 300, 315, 355, and 750 μs after triggering

4.16 EXPLOSION, IMPLOSION, AND DETONATION – Nuclear Implosion Device: The "Gadget"

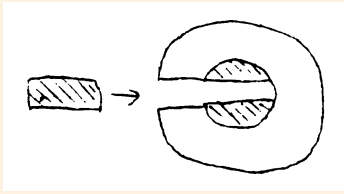

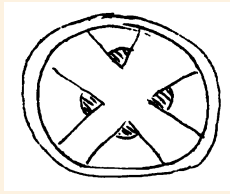

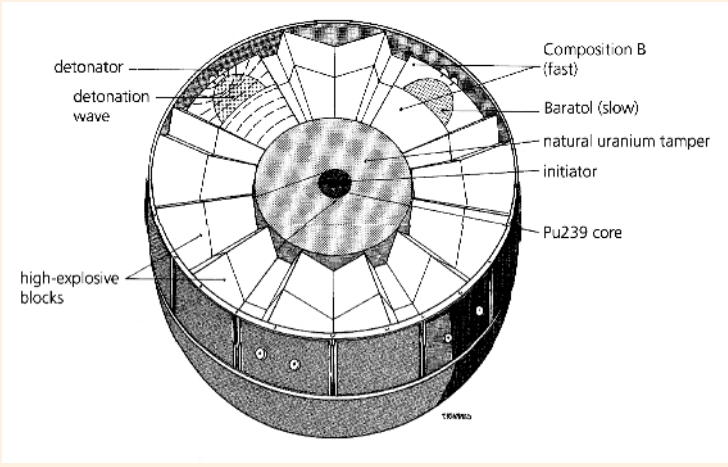

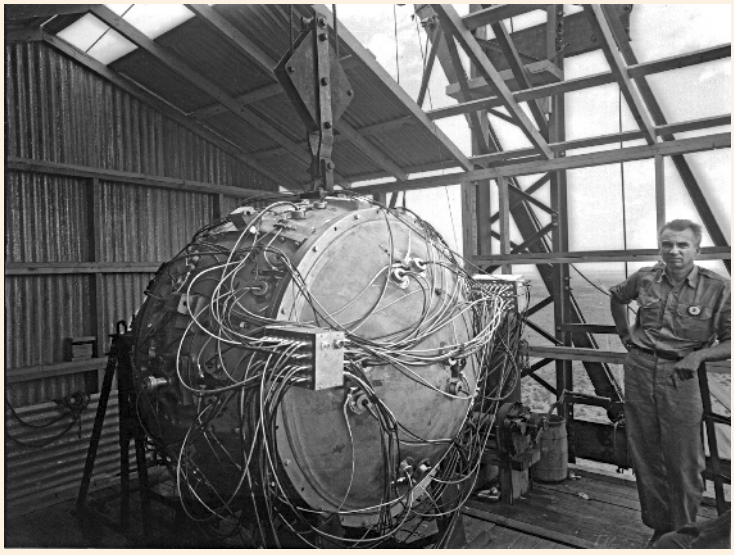

4.16–G ***Top:*** In April 1943, the physicist Robert SERBER delivered five top-secret lectures on how to build an atomic bomb in order to introduce scientists arriving at Los Alamos to the current state of nuclear weapons research. He showed sketches of the gun assembly (*left*) and the implosion-assembly device (*right*), the "Gadget," which became the first atomic bomb. [R. SERBER: *The Los Alamos Primer*. Univ. of Cal. Press, Berkeley 1992)] ***Center:*** Schematic of implosion bomb showing fast and slow explosive lens components and the two subcritical hemispheres of plutonium Pu-239 (diameter approx. 8.1 cm) that were driven inward and compressed to supercriticality by the implosion. In the center of the plutonium sphere, which had approximately the diameter of an orange, an initiator was placed in order to release a burst of neutrons when struck by the pressure wave. The bomb initiator was based on the (α, n)-reaction of Po-210 and Be-9. The arrival of the shock wave caused mechanical mixing that allowed α-particles to impinge on the beryllium and to yield neutrons. One of the greatest problems of any implosion device using high explosives is to ensure a symmetric collapse and to avoid any jet formation and instabilities that, provoking a predetonation, would result in a low energy release (yield). The spherical implosion charge consisted of 96 segments cast from slurries of explosives. Set such that detonation started simultaneously at certain points on the surface of the charge, the individual detonation waves were converted by high explosive lenses into a single convergent wave front compressing the natural uranium tamper with the contained plutonium. The tamper served to reflect neutrons back into the core, thus improving the chain reaction rate. [R. RHODES: *The making of the atomic bomb*. Simon & Schuster, New York (1986), p. 575; A more detailed schematic of "The Gadget" is shown in F.H. SHELTON's book *Reflections of a nuclear weaponeer*. Shelton Enterprise, Colorado Springs, CO (1988), p. **3**-36] ***Bottom:*** View of the completely assembled "gadget" atop the 100-ft tower, with physicist Norris BRADBURY. The photo was taken the day before the Trinity Test, which occurred on July 16, 1945. [From SERBER's book cited above.]

4.16 EXPLOSION, IMPLOSION, AND DETONATION – Examples of Nuclear Explosions

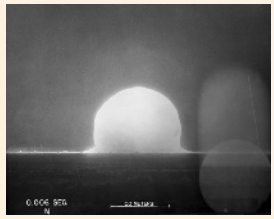

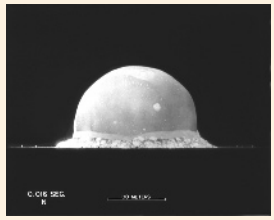

4.16–H ***Left:*** On July 16, 1945 the first atomic explosion, the so-called "Trinity Test," took place at Trinity Site in the Alamogordo Desert of New Mexico. The plutonium bomb, an implosion-type device, detonated on top of a 100-ft (30-m)-high tower and had a yield of about 19 kilotons TNT equivalent. [Courtesy LLNL, Livermore, CA] ***Right:*** These are four pictures from a movie of the explosion taken by LASL staff scientist Berlyn BRIXNER, a professional high-speed photographer and inventor. His Fastax camera was positioned in the North Shelter, at a distance of 10,000 yards (9,144 m) from the explosion. The pictures were taken 6 ms (*top*), 16 ms (*center*), and 10 s (*bottom*) after ignition. A movie of the first nuclear explosion in real time can be viewed on the Internet. [LLNL Archives, Livermore, CA; http://www.cddc.vt.edu/host/atomic/trinity/tr_test.html]

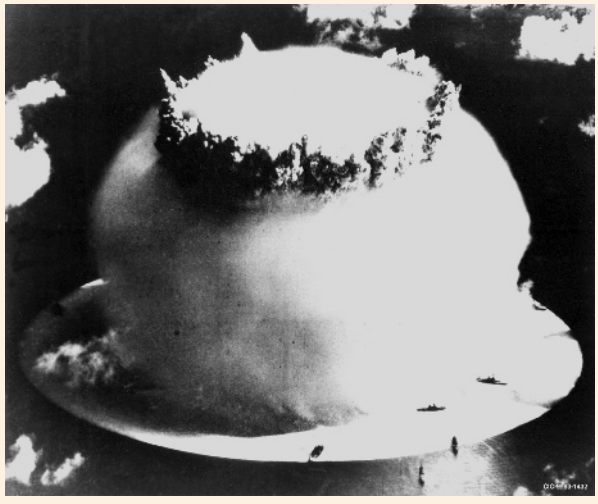

4.16–I The first nuclear underwater explosion – officially called Test "BAKER" of operation "CROSSROADS" – and the fifth nuclear explosion in history took place at Bikini Atoll on July 25, 1946. The weapon was suspended beneath the landing craft LSM-60 (a World War II amphibious assault ship) anchored in the midst of the target fleet and ignited within the atoll 90 ft (27.4 m) beneath the surface of the lagoon. A target armada consisting of nine ships was exposed to the explosion in order to study nuclear vulnerability effects under combat conditions and to determine the hull damage caused by the hydraulic effect of the underwater nuclear detonation. It produced a huge moisture cloud typical for underwater nuclear explosions. Eight ships sunk, the USS *Prinz Eugen* (a captured heavy cruiser of the German Navy), survived the test but was too radioactive to have leaks repaired. [F.H. SHELTON: *Reflections of a nuclear weaponeer*. Shelton Enterprise, Colorado Springs, CO (1988), p. **2**–48]

4.16 EXPLOSION, IMPLOSION, AND DETONATION – Examples of Nuclear Explosions *(cont'd)*




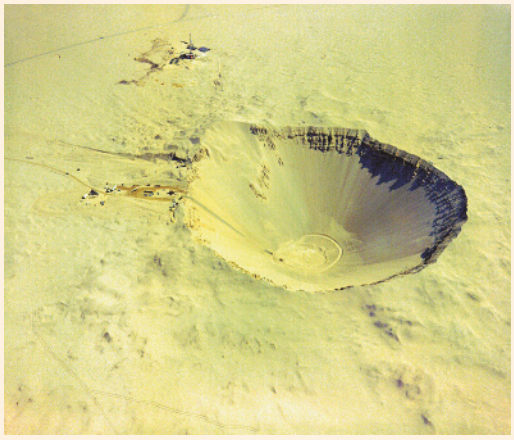

4.16–J Nuclear excavation experiments were conducted by the U.S. Atomic Energy Commission (AEC) in order to develop possible peaceful uses for nuclear explosives. In the so-called "AEC's Plowshare Program," various earth-moving projects were under study. For example, on July 6, 1962, the experiment SEDAN was carried out. The 104-kT nuclear device was detonated at the Nevada Test Site, buried under 635 ft (193 m) of desert alluvium. ***Top:*** Three pictures from a series of the moving earth bubble taken at 1.9 s (*left*), 2.8 s (*center*), and 5 s (*right*) after ignition of the nuclear device. ***Bottom:*** The detonation produced a crater 1,280 ft (390 m) in diameter and 320 ft (97.5 m) deep. [Courtesy LLNL Archives, Livermore, CA]

Open ditches are necessary for farm drainage, mosquito and flood control, pipelines, highway construction, land reclamation, stream corrections, and various other purposes. They can be dug quickly in many types of soil by using dynamite – so-called "blast ditching." In the 1970s, an idea was proposed of using this technique to construct a new, wider, and deeper Atlantic-Pacific canal north of the present Panama Canal, but using nuclear instead of chemical explosives.

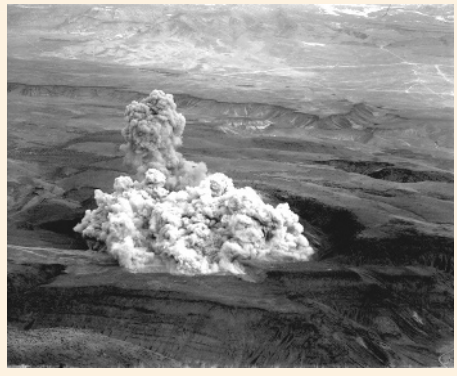

4.16–K ***Left:*** This photo shows a well-executed ditch blast in action, resulting from a chemical explosive. In wet soil, ditches may be blasted by the propagation method, *i.e.*, only one hole is primed, the concussion from the explosion of this one charge being sufficient to propagate the detonation through the soil and set off the whole line of charges. The other method of initiating applies either electric caps or "Primacord" to each hole. [*Blasters' handbook*. E.I. du Pont de Nemours, Wilmington, DE (1967), p. 368] ***Right:*** The "BUGGY" Excavation Test performed in 1968 used five nuclear devices in a row, each about 50 m apart, that were detonated simultaneously. It was part of the U.S. Plowshare Program, an initiative to develop peaceful uses of nuclear weapons. [Courtesy LLNL Archives, Livermore, CA]

4.16 EXPLOSION, IMPLOSION, AND DETONATION – Electric Guns

4.16–L This model "electric gun" was used in the 19th century to demonstrate the action of suddenly heated air by discharging a battery of Leiden jars via two electrodes into a wooden discharge chamber. The expanding hot gases blow out the mortar – here an ivory ball. [G.L.E. TURNER: *19th-century scientific instruments*. Sotheby, London (1983), p. 193]

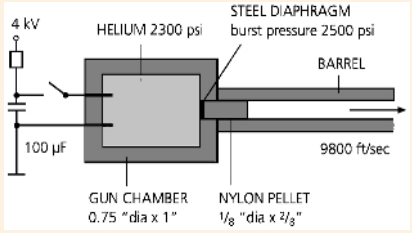

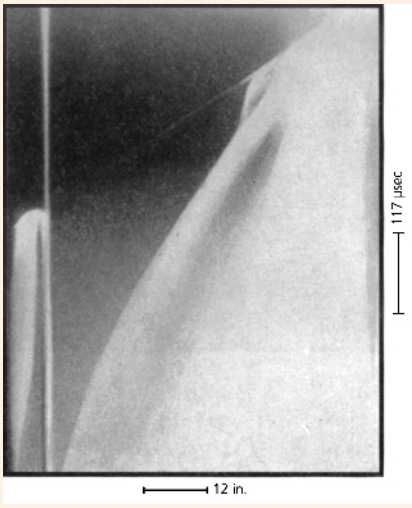

4.16–M The principle of the electric gun, in modern terms an "electrothermal plasma gun," saw a renaissance after World War II. ***Top:*** Daniel E. BLOXSOM JR., a researcher at Rhodes & Bloxsom Co. (Canoga Park, CA), used pressurized helium gas that was suddenly heated in a small gun chamber by a capacitor discharge. Using energies up to 8 kJ, the helium could be heated up to approx. 21,000 K. The high dynamic pressure in the chamber ruptured a thin steel diaphragm, thereby accelerating a small pellet freely moving in a barrel up to hypersonic velocities. ***Bottom:*** Example of an optical streak record – a diagram showing time *vs*. distance – taken from a $^1/_3$-in. (8.47-mm)-dia. nylon pellet fired into laboratory air at 9,800 ft/s (2,987 m/s). The flash on the left shows the nylon pellet disintegrating upon striking a thin aluminum foil. Ablation of the nylon pellet may also be seen in the first 3 in. of flight. [J. Appl. Phys. **29**, 1049 (1958)]

4.16 EXPLOSION, IMPLOSION, AND DETONATION – Exploding Wires

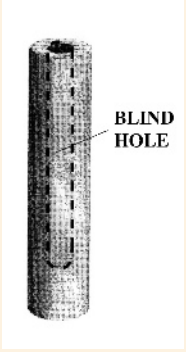

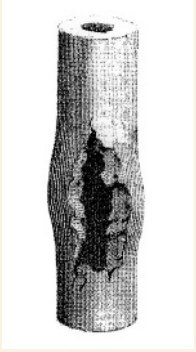

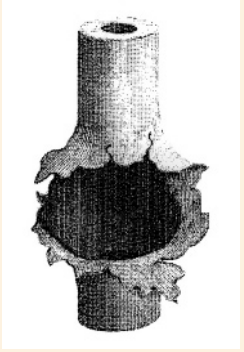

4.16–N ***Left:*** In 1815, the English electricians George J. SINGER and Andrew CROSSE studied the destructive effects of exploding wires by inserting a leaden wire *w* to the lower end of a needle, which was provided with insulating space holders *c* positioned on the axis of a water-filled metallic cylinder, the wire resting with its point on the bottom thereof. ***Center & right:*** The discharge of Leiden jars through the wire *w* provoked ruptures even of thick-walled tubes such as of a musket barrel. [Phil. Mag. **46** (I), 161 (1815)]

4.16 EXPLOSION, IMPLOSION, AND DETONATION – Exploding Wires (cont'd)

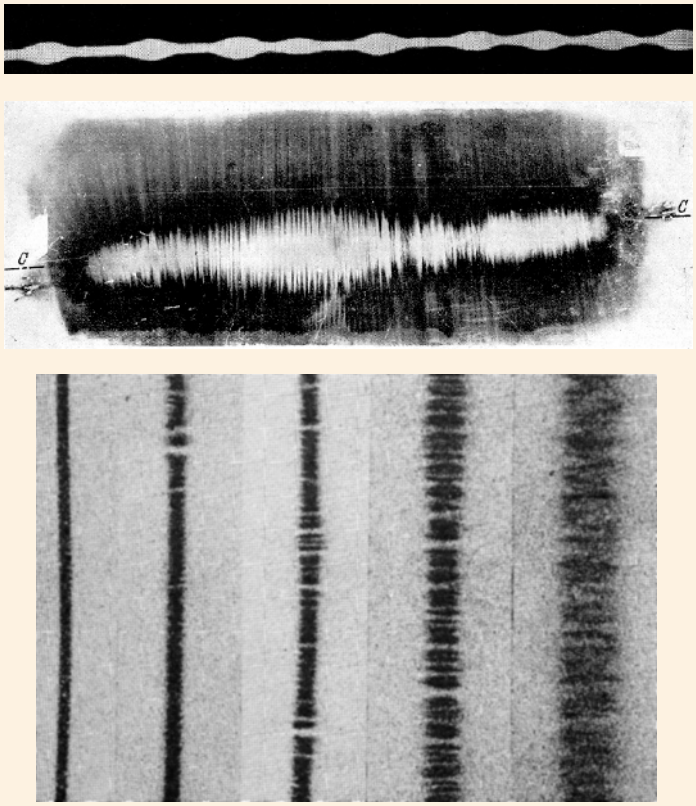

4.16–O ***Top:*** Silhouette of a long copper wire pulsed by a high current. Shortly before the formation of molten wire droplets begins, this curious wire geometry arises, which Henry W. BAXTER, a British researcher, first called "unduloids." He correctly interpreted this curious phenomenon as the result of surface tension. [H.W. BAXTER: *Electric fuses*. Arnold, London (1950), p. 69] ***Center:*** Heinrich ARNOLD and William M. CONN, two German researchers at Würzburg University, placed a glass slide at a short distance from and parallel to an exploding wire and found in the deposits a characteristic "striation" structure. This picture was obtained from a 0.16-mm-dia. silver wire; the distance from wire to glass plate was 3 mm. [W.G. CHACE and H.K. MOORE (eds.) *Exploding wires*. Plenum, New York (1962), vol. II, p. 77] ***Bottom:*** The German physicists Francis JAMET and Gustav THOMER, two research physicists at ISL (Saint-Louis, France), using flash radiography resolved this striation process in time and found that the disintegration of the wire occurs shortly after the current pause. At this characteristic time instant – the so-called "dwell" – the wire material, completely evaporating and becoming non-conducting, expands at high speed in a radial direction. The pictures illustrate (from left to right) the evolution of the explosion process of a 0.1-mm-dia. copper wire, taken at a rate of 10^5 frames/s. [F. JAMET and G. THOMER: *Flash radiography*. Elsevier, Amsterdam (1976), p. 153]

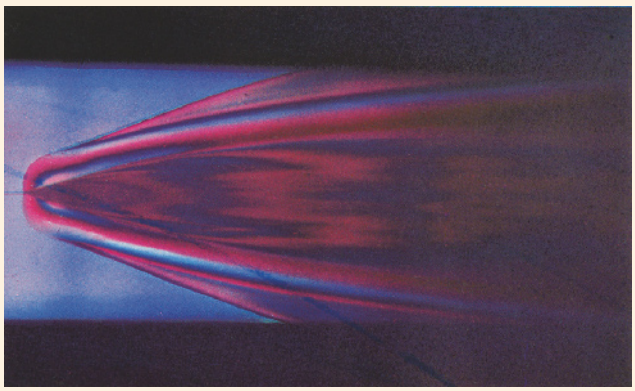

4.16–P Frederick D. BENNETT and D.D. SHEAR at BRL (Aberdeen, MD) investigated the mechanism of shock wave production from exploding wires. They found that shock wave production does not proceed from the expansion of the heated metal vapor alone, but rather depends on a two-stage process in which the early expansion of a plasma created by the peripheral arc plays an important part. This single-fringe, streak interferogram of an exploding 4-mil (0.1-mm) copper wire in argon at $^1/_8$ bar was taken in white light. Note that the complex jagged fringes near the axis attest to a high degree of cylindrical symmetry in the expanding metal. The outermost boundary is the head shock trajectory, while the rounded tip represents the peripheral arc. [W.G. CHACE and H.K. MOORE (eds.) *Exploding wires*. Plenum, New York (1962), vol. II, p. 181]

4.16 EXPLOSION, IMPLOSION, AND DETONATION – Large Yield Surface Detonations

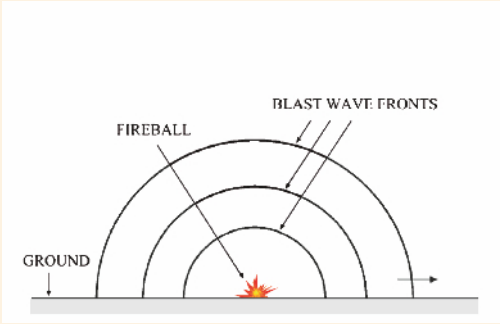

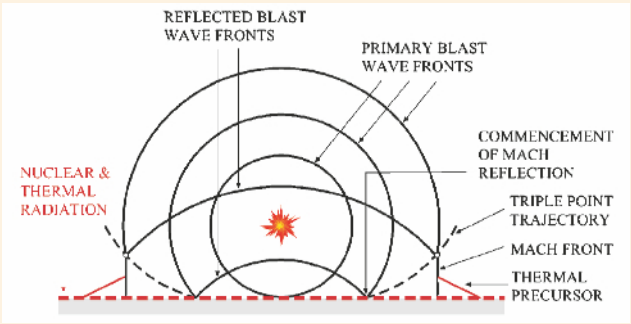

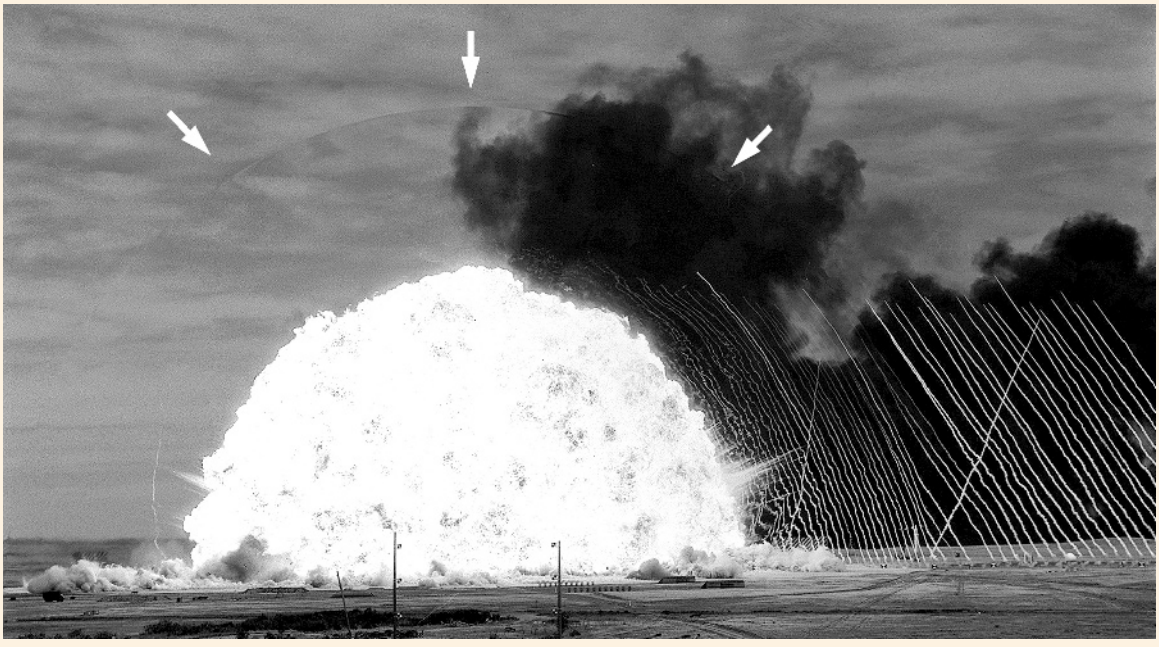

4.16–Q ***Top:*** Schematic of blast wave propagation from a chemical explosive detonated at the surface (*left*) and at a certain altitude above ground (*right*). In the case of a nuclear explosion, a thin layer of high-temperature gas above the ground surface is produced by adsorption of the thermal radiation (*broken red line*), creating ahead of the Mach front a "thermal precursor" – a shock wave (*solid red line*). The rapid expansion of the fireball also initiates seismic shock waves in the ground that generally precede the blast wave. [By author] ***Bottom:*** Refractive photography of the blast wave generated at the surface by detonation of a hemispherical 500-ton TNT charge, taken in July 1964 at the Canadian Defence Research Establishment (CDRE), Suffield, Alberta. The velocity of the blast wave was measured using cinematography, and the particle velocity using the smoke trail displacement technique. The white smoke trails were formed using cylindrical containers filled with titanium tetrachloride, which were projected from simple mortars. To improve the contrast of the photographic records, a black-smoke background was formed by burning crude oil. These data then allowed the determination of all other blast parameters as functions of time and radial distance. [Courtesy Defence R&D Canada, Suffield, Canada] The analysis of data was carried out and described in more detail by J.M. DEWEY in Proc. Roy. Soc. Lond. **A324**, 275 (1964).

4.16 EXPLOSION, IMPLOSION, AND DETONATION – Precursor Detonation Phenomenon

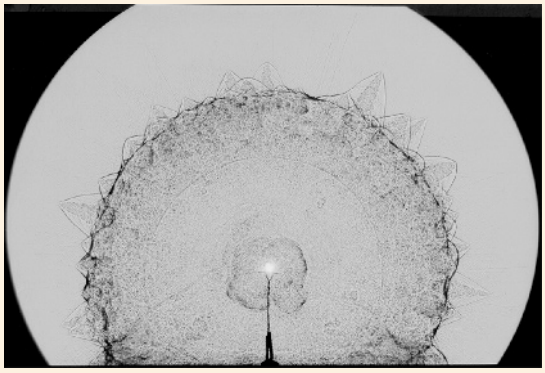

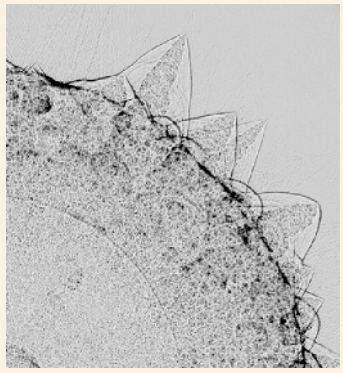

← Magnification of mini precursor shock waves reveals that a conical flow region of turbulent detonation reaction products, following each supersonic particle, is clearly visible. This "head wave" phenomenon is well known from supersonic ballistics and was first observed by Peter SALCHER and Ernst MACH in 1886.

4.16–R Precursor shocks are generated in the early stage of a detonating explosive, shown here for a 1-g nitropenta detonator. Small particles of still detonating explosive or paint particles have separated from the main body and, flying with higher velocity than the blast wave, produce small head waves. [Courtesy Dr. Peter NEUWALD, EMI, Freiburg]

4.16 EXPLOSION, IMPLOSION, AND DETONATION – One-Dimensional Detonation Front Models

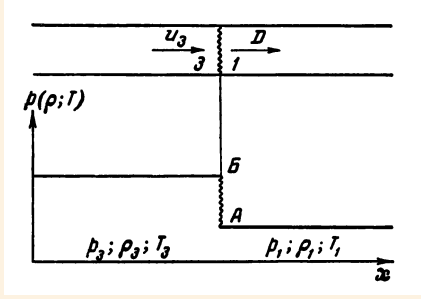

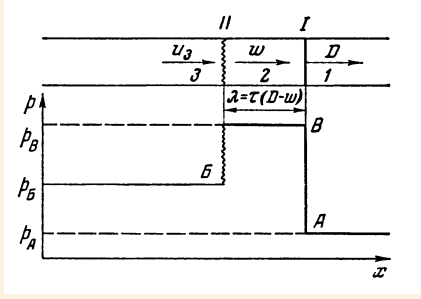

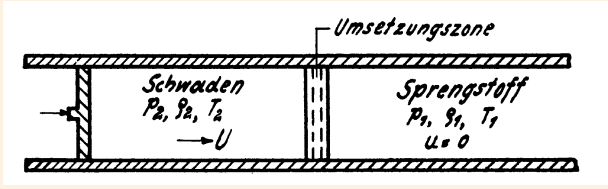

4.16–S ***Left, top:*** MIKHEL'SON (1893), CHAPMAN (1899), and JOUGUET (1904, 1917) assumed that in a detonation the distribution of pressure, density, and temperature occurs instantaneously at the "detonation front." However, combustion is not an instantaneous process, and it takes a certain time until the compressed mixture reacts. ***Left, bottom:*** In the early 1940s, Yakov ZEL'DOVICH in the U.S.S.R., John VON NEUMANN in the United States, and Werner DÖRING in Germany independently introduced a chemical reaction zone, here denoted by I–II, to take into account the kinetics of the chemical reaction in a detonation. Both models proved useful for a large number of applications. However, experimental facts of irregularities in the detonation front – such as spinning detonation {⇨Fig. 4.16–T} and periodic cell structure {⇨Fig. 4.16–U} – contradict both models: instead of a propagating plane detonation front, gas ignition rather occurs at separate centers, and the plane front disintegrates. [K.I. SHCHELKIN and Y.K. TROSHIN: *Gasdynamics of combustion.* Mono, Baltimore (1965), p. 12] ***Right:*** Schematic of DÖRING's detonation model as illustrated in his secret report "Beiträge zur Theorie der Detonation." [Forschungsbericht Nr. 1939, Deutsche Luftfahrtforschung, Berlin-Adlershof (1944)]

4.16 EXPLOSION, IMPLOSION, AND DETONATION – Spinning Detonation

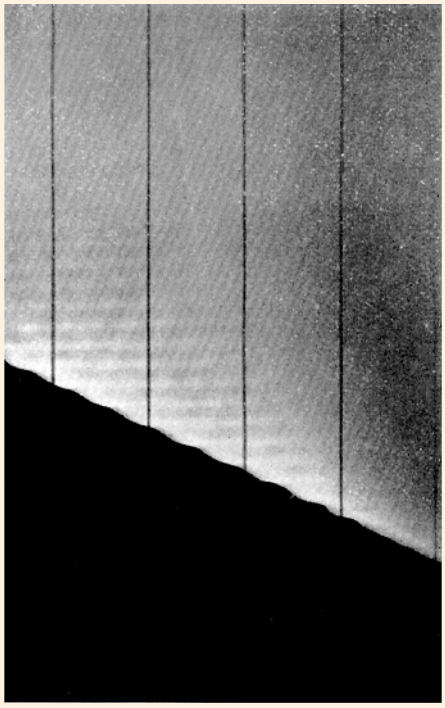

4.16–T In 1926, the British chemists Colin CAMPBELL and Donald W. WOODHEAD at the University of Manchester studied the ignition of explosive gaseous mixtures and measured the velocity of the detonation wave. Their apparatus consisted of a series of metal and glass tubes, forming a continuous horizontal gallery through which the flame passed in front of a drum camera that had a peripheral speed of about 45 m/s. The flame in the test mixture was initiated by the explosion of a hydrogen-oxygen mixture contained in a similar tube in a coaxial position; the complete separation of the two mixtures until shortly before firing was effected by a metal shutter. ***Top:*** This is a "moving-film" or "smear" record, a diagram time *vs*. distance, of the explosion-wave passing through a moist mixture of $2\,CO + O_2$. The *vertical black lines* are for reference purpose and have intervals of 10 cm. The researchers noticed that the burning gases behind the wave front showed marked horizontal bands. In the following year, a more detailed study of this apparently undulatory form of the detonation wave suggested the idea that the detonation wave propagated along a helical path, a unique phenomenon called "spinning detonation." [J. Chem. Soc. **130**, 1573 (1927)]

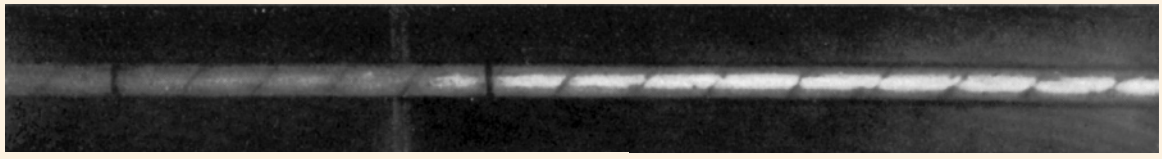

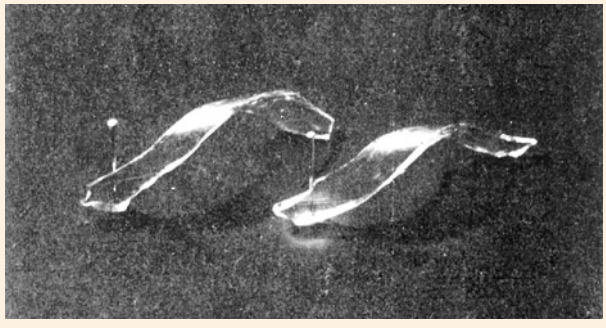

Center: William A. BONE and Reginald P. FRASER, two combustion researchers at Imperial College (London, U.K.), resumed Colin CAMPBELL's studies on spinning detonation. They provoked detonation in a lead tube, followed by a glass tube. They photographed the helical track formed by the "head" of detonation in the glass tube as a thin gray film of lead. [Phil. Trans. Roy. Soc. Lond. **A228** (1929), plate 11] ***Bottom:*** Spiral fragments of a 1.3-cm-inner-dia. glass tube that had been shattered by the detonation of a $C_2N_2 + O_2$ medium in it, as though a spiraling compression wave had passed through the glass and sheared it. [Phil. Trans. Roy. Soc. Lond. **A230** (1932), plate 20]

4.16 EXPLOSION, IMPLOSION, AND DETONATION – Periodic Cell Structure

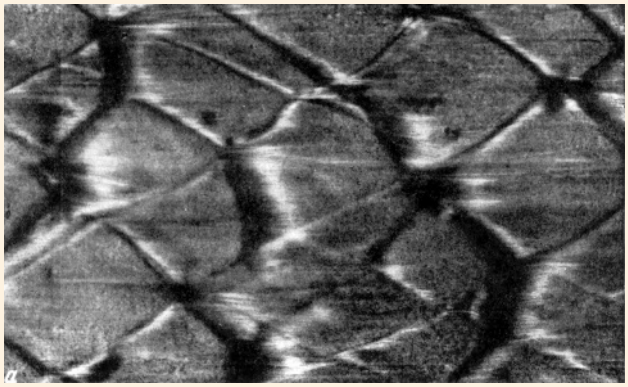

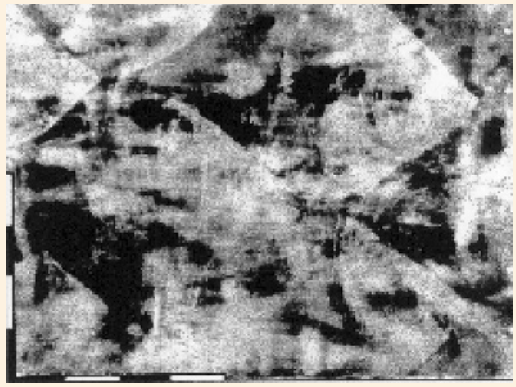

4.16–U ***Left:*** In 1959, the Soviet combustion researchers Yuri N. DENISOV and Yakov K. TROSHIN first reported on the discovery of a cellular structure of detonation waves using smoked foils exposed to the detonation, a recording technique based upon ANTOLIK's soot method {⇨Fig. 4.5–C}. Depending on the ambient pressure and mixing ratio, they observed curious soot patterns of an almost periodic cell structure. [Dokl. Akad. Nauk **125**, 110 (1959)] ***Right:*** More recently, Fuqing ZHANG and collaborators at RWTH Aachen, using the smoked-foil technique, recorded from a dust detonation traces of triple points on the tube wall, thus first showing that cell structures also exist in dust explosions. [Shock Waves **11**, 53 (2001). Courtesy Prof. Hans GRÖNIG, Stoßwellenlabor der RWTH Aachen]

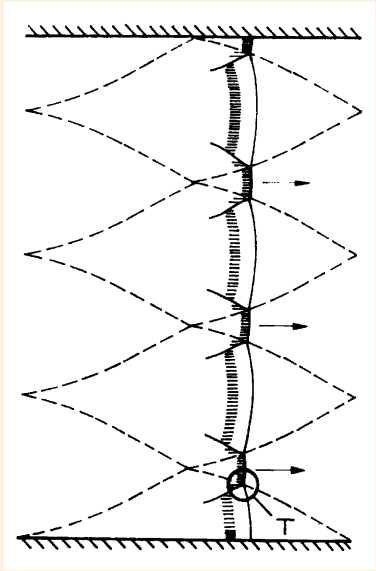

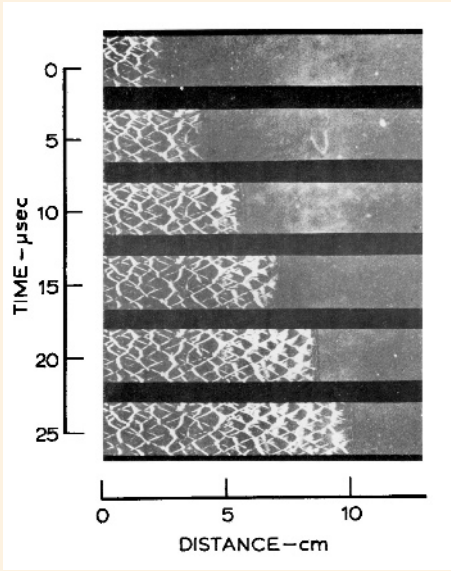

4.16–V Schlieren photography has shown that the detonation front actually consists of a system of intersecting shock fronts that produce Mach reflection. ***Left:*** Schematic diagram of a detonation wave. The *solid lines* represent curved shock fronts, the *shaded regimes* are the combustion zones, and the *broken lines* depict the traces of the wave intersection points. Vortices in the triple points act as rotating styli and generate the diamond-shaped cellular pattern. The *arrows* indicate the positions where the wave system may receive the propulsive drive. ***Right:*** Sequence of stroboscopic laser-shadow photographs of a gaseous detonation in a hydrogen-oxygen mixture. [A.K. OPPENHEIM: *Introduction to gasdynamics.* Springer, Vienna (1970), pp. 27, 31]

4.16 EXPLOSION, IMPLOSION, AND DETONATION – Other Explosion Phenomena *(cont'd)*

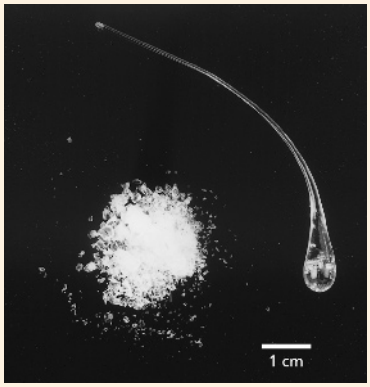

4.16–W So-called "Prince RUPERT's drops" are formed by dropping a small gob of hot, molten glass into cold water. They were used from the 17th century to demonstrate the high internal stress frozen inside of the tadpole-shaped glass. Upon breaking the thin tail, the glass releases the internal stress explosively so that the entire piece shatters into a fine powder. [Courtesy Dr. Heinz REICHENBACH, EMI, Freiburg]

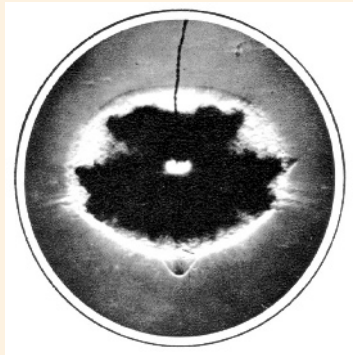

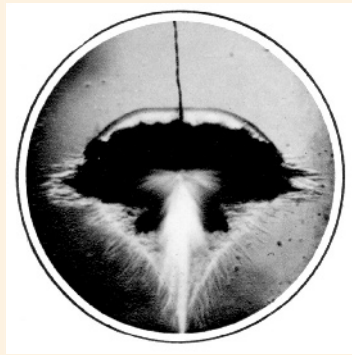

4.16–X In England, William H. PAYMAN and collaborators at the British Safety in Mines Research Establishment (SMRE) studied near-field explosion phenomena of plain No. 6 detonator caps using a schlieren camera and making snapshot spark photographs. The solid particles that appear to play an important part in the initiation of explosion by a detonator may be composed either of metal torn from the case or of unconsumed detonating composition, or of both. ***Left:*** For a copper-cased fulminate-chlorate detonator bursting occurs quicker in the lateral than in the axial direction, leading to an ellipsoidal wave geometry, and no focusing effect happens. ***Right:*** For a compound aluminum-cased lead azide detonator the researchers observed jetting of gases and particles sent out in advance of the main shock. This type of detonator will ignite firedamp-air mixtures, unlike the copper-cased fulminate-chlorate detonator. [Proc. Roy. Soc. Lond. **A148**, 604 (1935)]

4.16–Y In flash X-ray tubes high-velocity electrons impinging as a beam on a metallic surface are scattered, slowed down, and stopped within a short depth below the surface. Most of the kinetic energy of the beam is transformed into heat and only about 1‰ goes into X-rays. Depending on the electron energy and the absorption and melting characteristics of the applied anode material, the impact of fast electrons can be accompanied by subsurface mini explosions. The SEM picture, taken by Reinhard THAM (EMI, Freiburg) in 1984, shows the tip of a conical Mo-anode from a vacuum-discharge flash X-ray tube, after being pulsed several hundred times via a 100-kV low-impedance transmission line. [P. KREHL, Proc. 13th Int. Congr. High-Speed Photography & Photonics, Tokyo (1978). Japan Society of Precision Engineering, Tokyo (1979), p. 409] For a photon energy of 100 keV the penetration depth in molybdenum is in the order of 1 mm and quickly diminishes with decreasing photon energy. The high-velocity bombardment of electrons generates a curious, "banana-split"-type erosion pattern. [EMI Archives, Freiburg, Germany]

4.16 EXPLOSION, IMPLOSION, AND DETONATION – Explosive Ablation of Biological Tissue

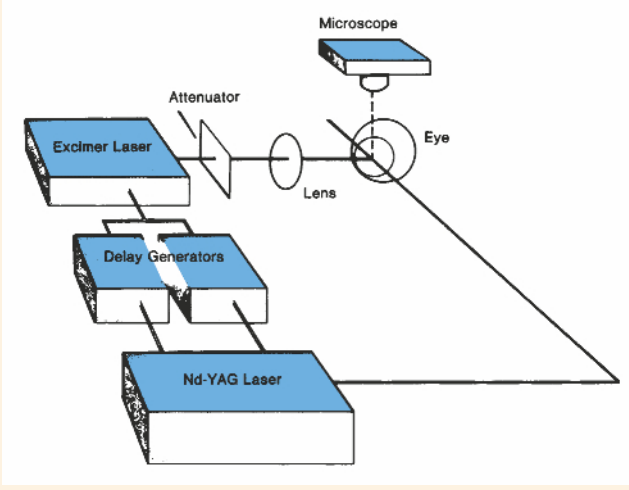

4.16–Z The irradiation of biological tissue by an ultrashort laser pulse is an explosionlike process similar in appearance to other laser-induced explosive phenomena. This so-called "ablative photo decomposition effect" is used in medical therapy, for example in dermatology and ophthalmology. In the mid-1980s, the U.S. ophthalmologist Carmen A. PULIAFITO and collaborators at Boston's Laser Research Laboratory and Harvard's Medical School first studied laser ablation of the cornea using high-speed photography. ***Top:*** They used a 0.9-J/cm^2 15-ns FWHM excimer laser at 193 nm, which was focused on the cornea to a spot size of 0.44 mm in diameter. A second laser, triggered after a variable delay time, was used as a flash light source to illuminate the near environment of the cornea and to visualize the ablation process perpendicularly to the plume propagation. Pictures of the ablation process were recorded using a 35-mm still camera (Nikon) attached to an operating microscope. [Arch. Ophthalmol. **105**, 1255 (1987)]

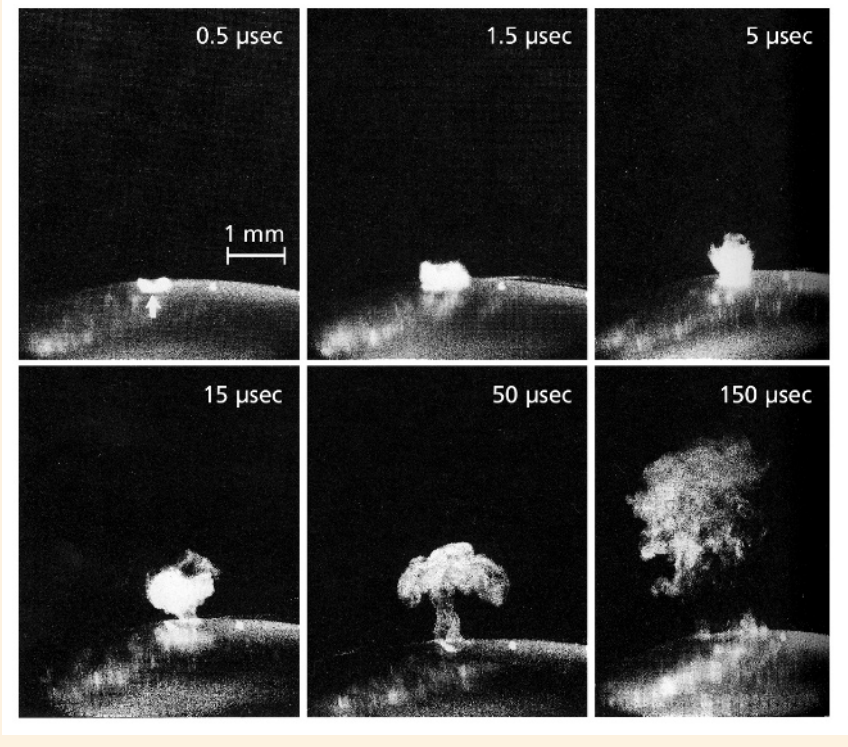

Bottom: This is a series of single-shot shadowgraphs (or pseudo cinematography) of the ablation process taken at six different time instants after firing the excimer laser. The laser beam comes from above the photograph and strikes the cornea near the point indicated by the *white arrow* (*top, left*). At 0.5 µs after firing of the excimer laser pulse the plume of ablated material extends 0.2 mm from the cornea, indicating an initial average supersonic velocity of 400 m/s. The ablation process is essentially completed between 5 and 15 µs after the excimer pulse. Note the formation of a mushroom cloud with a long stem at 50 µs. By 150 µs the effects of diffusion and turbulence have become dominant. Today ultraviolet pulsed radiation from excimer lasers is routinely applied to the surface of the cornea in order to correct low to high levels of nearsightedness, farsightedness, and astigmatism.

4.17 EXPLOSION AND DETONATION DIAGNOSTICS – Maximum Pressure of Fired Gunpowder

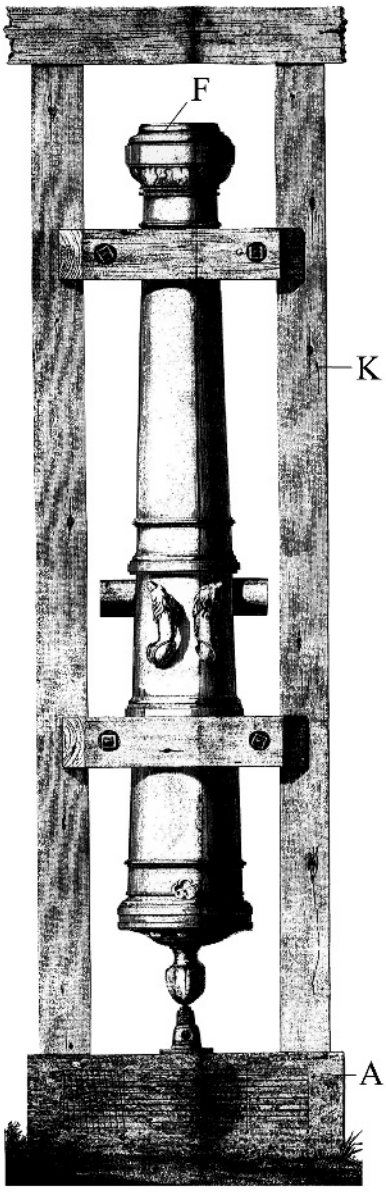

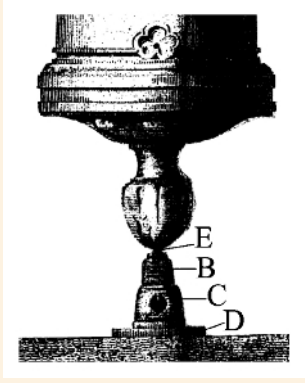

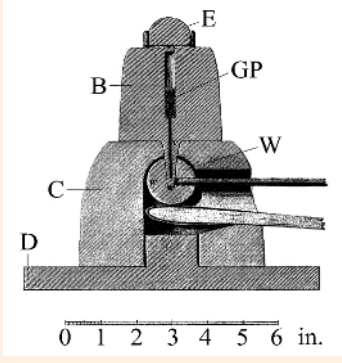

← Cross section of his setup for testing the force of fired gunpowder:
A – solid block of very hard stone
B – barrel of hammered iron
C – support of cast brass
D – circular plate of hammered iron
E – hemisphere of hardened steel
F – 24-pdr cannon, used as a heavy weight
GP – gunpowder test sample
K – wooden frame
W – heated iron ball for igniting GP

4.17–A In the 1790s, Sir Benjamin THOMPSON, Count VON RUMFORD, then Bavarian Minister of War, developed an experimental method to systematically determine the force of fired gunpowder. ***Right:*** His "test bomb" *B*, a short iron gun barrel with thick walls, was closed at the top by a movable hemisphere *E*. ***Left***: To counterbalance the pressure of the generated "elastic fluid" (*i.e.*, of the hot explosion products), he used a heavy 24-pdr cannon *F* that rested on *E* and was movable in a vertical position within a wooden frame *K*. The bottom of *B* rested on a solid block *A* via a steel disk *D*. In order to avoid erosion of the vent and a loss of elastic fluid, he ignited the gunpowder *GP* inside *B* by bringing a red-hot ball *W* in contact with the bottom of *B*. When the force of the generated elastic vapor was just sufficient to raise the weight, the explosion was attended by a very sharp report. In the special case that the chamber was completely filled, which required 1.8 g of powder, he estimated a force of fired gunpowder of about 29,000 at. However, he observed that the force of fired gunpowder also depended on its moisture content. From an experiment resulting in a destroyed chamber he (erroneously) estimated the enormous pressure of 101,021 atm – a value very different from 5,500 atm as later determined by Sir Frederick A. ABEL and Sir Andrew NOBLE in careful measurements. [Phil. Trans. Roy. Soc. Lond. **87**, 222 (1797)]

4.17 EXPLOSION AND DETONATION DIAGNOSTICS – Maximum Pressure and Temperature

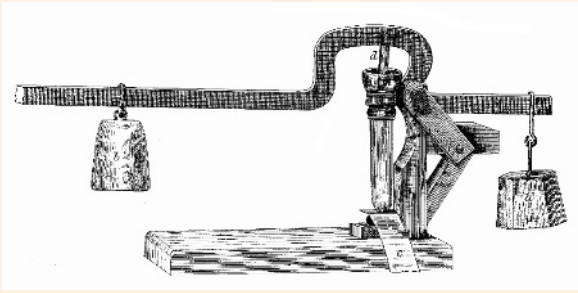

4.17–B View of Robert W. BUNSEN's exploding vessel, which he used in his laboratory at the University of Heidelberg in an attempt to measure the maximum pressure caused by the detonation of explosive gaseous mixtures. His handy instrument consisted of a closed air-tight tube with a weight-loaded valve and allowed one to determine the temperature of detonation. The ignition of the test gas occurred by an electric spark via electrodes *c* and *d* through the entire length of the tube. He observed which weight *b* could still be raised by the detonating gases. [Phil. Mag. **34** (IV), 489 (1867)]

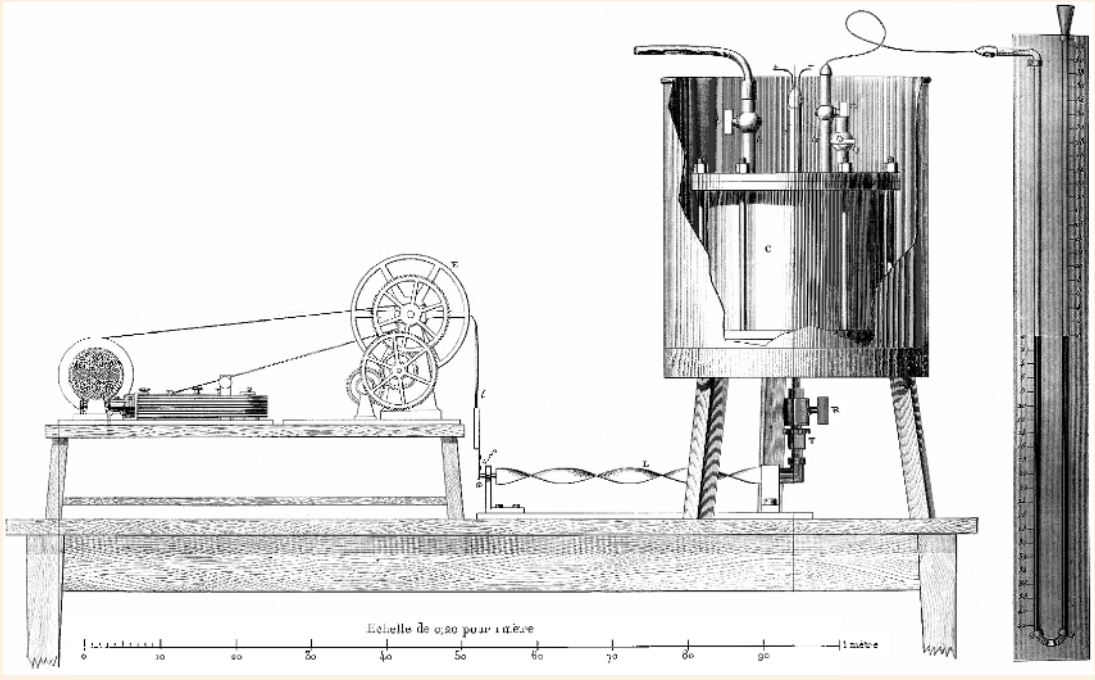

4.17–C François E. MALLARD and Henry L. LE CHÂTELIER at the Ecole des Mines in Paris determined the temperature of detonation of firedamp and other combustible gaseous mixtures indirectly by measuring the explosion pressure in a closed reaction vessel. They used a calibrated Bourdon gauge connected via a stiff axle *L* to a Deprez chronograph, which was provided with a needle *l* at its end, and registered the pressure on a revolving cylinder covered with black paper. The gaseous mixture was fed to the reaction vessel *C* via a pipe t_1. Another pipe *t* was a feed-through for two electric wires, which ignited the test gaseous mixture via an electric spark. While studying the specific heat and dissociation of gases at elevated temperatures, they made the curious observation that ignition of firedamp only occurs when the gaseous mixture is kept a certain time above its ignition temperature, which is approx. 650 °C for firedamp. This delay of ignition allows the application of special explosives of even high combustion temperatures for shooting purposes in the coal-mining industry, such as ammonium nitrate. Although its combustion temperature is about 1,100°C – *i.e.*, well above the ignition temperature of firedamp – it cannot ignite, because the duration of this high combustion temperature is too short. [Ann. des Mines **4** (IV), 274 (1883)]

4.17 EXPLOSION AND DETONATION DIAGNOSTICS – Chamber Pressure of a Detonating Explosive

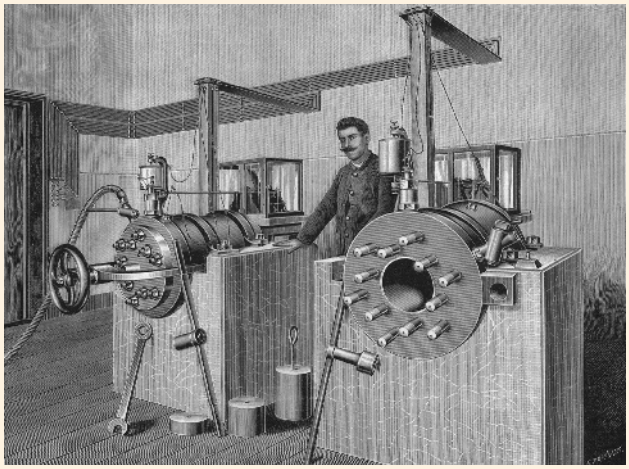

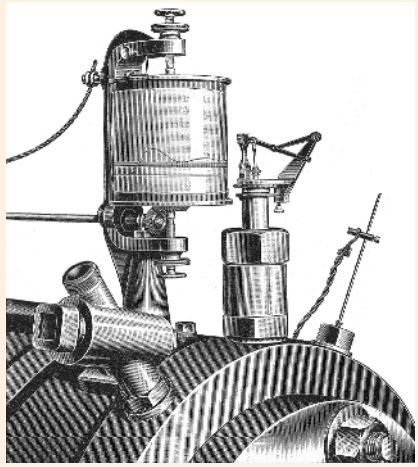

4.17–D ***Left:*** At the Sprengstoff-AG Carbonit (Schlebusch/Köln), Christian E. BICHEL, a German combustion researcher, determined the pressure in a closed chamber generated by the detonation of various explosives. ***Right:*** His mechanical "brisance gauge," a steam-engine indicator coupled with a rotating drum, provided crude pressure-time profiles from which he tried to determine the maximum pressure and the performed work. From the rise of pressure he estimated the brisance of an explosive. [C.E. BICHEL: *Experimentelle Untersuchung von Sprengstoffen*. Mittler, Berlin (1898), plates V and VI]

4.17 EXPLOSION AND DETONATION DIAGNOSTICS – Brisance Test of Gunpowder

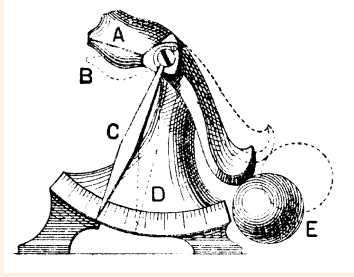

4.17–E ***Left & center:*** A 19th-century éprouvette, probably of British origin, in the form of a small pistol (overall length about 15 cm). Upon firing, the force of gunpowder turns a friction-restrained wheel numbered 1,2…,8 for calibration purposes [Courtesy R. WATSON, Manitou, Manitoba, Canada] ***Right:*** The éprouvette was used for quickly testing the brisance quality of gunpowder for use in cannons. It consists of a lever that carries on one end a lid *B* covering a small explosion chamber *A* and at the opposite end a counterweight *E*. The explosion of a test quantity of gunpowder in *A* moves lever *B* and the trailing pointer *C* into the *dotted position*. The amount of shift read at scale *D* was a measure of the brisance of the tested gunpowder. [*Larousse du XX^e Siècle.* Larousse, Paris (1930), vol. 3, p. 231] However, the efficiency of gunpowder applied in firearms depends on a variety of firearm parameters and cannot simply be determined by these primitive testing methods. For example, Carl CRANZ appropriately wrote, "The term 'brisance' is not an established one. For one firearm a powder may be too explosive, while for another it may be too sluggish…" [C. CRANZ: *Lehrbuch der Ballistik.* Springer, Berlin (1927), vol. 2, p.116]

4.17 EXPLOSION AND DETONATION DIAGNOSTICS – Brisance Test of a High Explosive

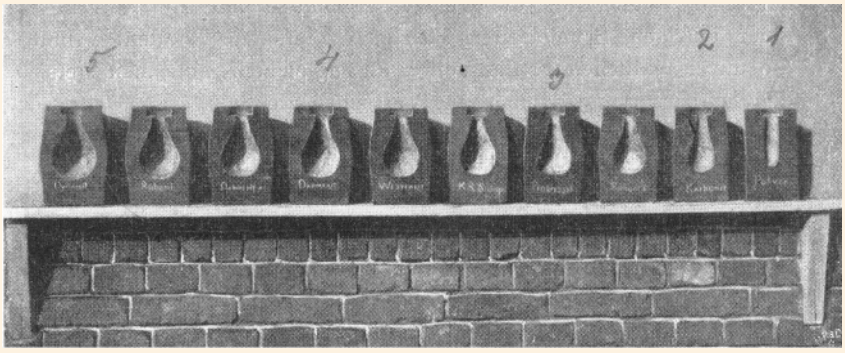

← View of ten cut-open Trauzl probes of different high explosives but of the same weight. *Left* to *right*: Nine explosives of German production (Dynamit, Roburit, Dahmenit, Dahmenit A, Westfalit, Köln-Rottweiler Sicherheitssprengpulver, Progressit, Roburit I, Kohlenkarbonit), followed by conventional gunpowder (*far right*). All high explosives produce a pear-shaped bulge, while only gunpowder produces a cylindrical cavity.

4.17–F In the 1880s, Isidor TRAUZL, an Austrian blasting engineer, devised a simple brisance test, the so-called "Trauzl lead block test." First introduced in Germany in 1903 as a standard test method, it allowed one to compare the brisance of new explosives in a simple manner. For the standard test, the blocks are cast from pure lead, 20 cm in height and 20 cm in diameter, with a central hole made by the mold, 12.5 cm deep and 2.5 cm in diameter. The Trauzl lead block test was later adopted worldwide and is still in use today. [F. HEISE: *Sprengstoffe und Zündung der Sprengschüsse*. Springer, Berlin (1904), p. 36]

4.17 EXPLOSION AND DETONATION DIAGNOSTICS – Test of Explosives Used in Mining

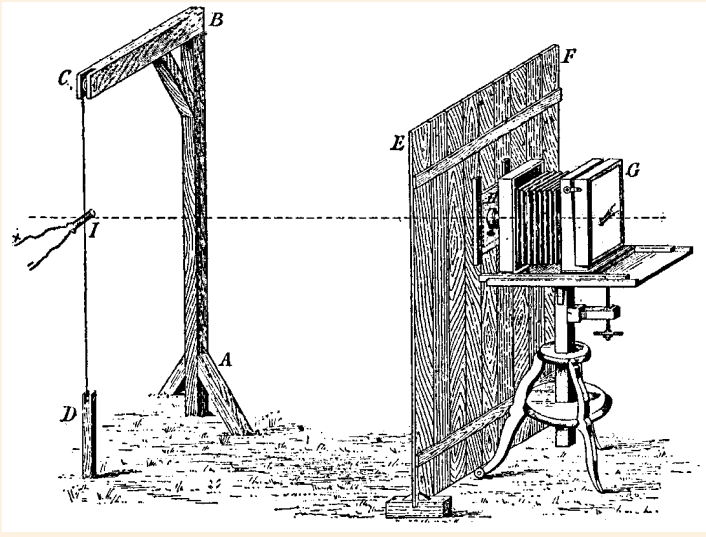

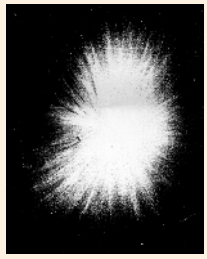

← SIERSCH at Dynamit AG in Vienna tested a large number of explosives with his photographic method. For example, he observed that a 100-g charge of Guhr Dynamite (*top*), housed in a freely suspended cartridge, produces a brilliant light flash that might ignite firedamp or coal dust in a mine, while the explosion of the same amount of nitroglycerine (*bottom*) is only accompanied by a faint flash of light.

4.17–G The Austrian explosives specialist Alfred SIERSCH used photography as a tool to classify "safe" explosives for use in mining. ***Left:*** He photographed the test explosive *I* in its own light with a still camera *G* through a shield *E–F*. Since he worked with an open shutter *H*, he had to conduct his studies at night. ***Right:*** According to his classification, safe explosives were those that emitted only a little light and, therefore, only a little heat to provoke firedamp and/or coal dust explosions. [Trans. Fed. Inst. Min. Eng. **11**, 2 (1896)]

4.17 EXPLOSION AND DETONATION DIAGNOSTICS – Dust Explosion Tester

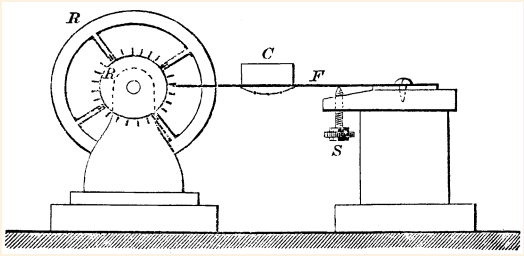

4.17–H Rudolph WEBER at the Polytechnic Institute in Berlin studied the causes of flour-dust explosions. To generate a steady stream of dust for experimentation with an open flame or an electric spark, he invented a simple dust generator. It consisted of a wheel *R* provided with 24 spikes that successively struck a leaf spring *F* carrying a cylinder *C*. This cylinder contained the flour dust sample to be tested and was provided at its bottom with a fine grid. Upon rotation of *R*, the spikes shook the cylinder, thus producing a constant flow of flour dust. A screw *S* allowed one to adjust the dust intensity. WEBER tested the trigger ability of a flour-dust explosion by positioning the heat source close to the generator and found that explosions occurred at concentrations of 20–30 mg dust in 1 liter of air. [Z. Tech. Hochschulen **3**, 51 (1878)]

4.17 EXPLOSION AND DETONATION DIAGNOSTICS – Detonation Velocity of a High Explosive

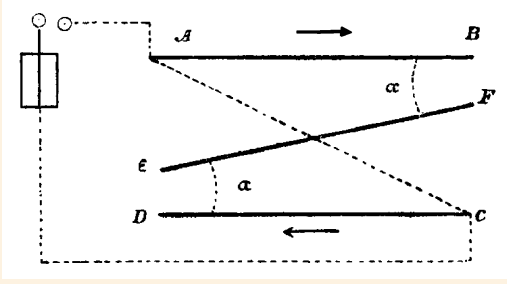

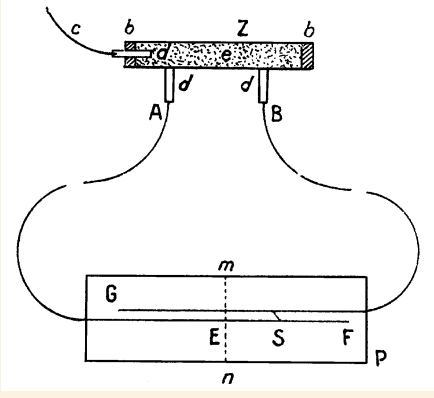

4.17–I Illustration of two examples of "antiparallel" testing methods as used in early detonation diagnostics: ***Top:*** Ernst MACH and Josef WENTZEL at the German Charles University in Prague used an ingenious setup to determine the detonation velocity of silver fulminate: two parallel line charges, *AB* and *CD*, triggered simultaneously by discharging a Leiden jar, produce an interference line *EF*, which is recorded on a fixed soot-covered plate positioned in the center. They determined the detonation velocity *D* from the inclination of the line *EF* by $\sin\alpha = c/D$, with *c* as the sound velocity in air. [Sitzungsber. Akad. Wiss. Wien **92** (II), 625 (1885)] ***Bottom:*** The Frenchman Henri J. DAUTRICHE also invented an antiparallel method of determining the detonation velocity that, like MACH and WENTZEL's setup does not require the use of a chronograph. However, his method depends upon a comparison of the velocities of the unknown explosive *Z* with a standard explosive of known velocity of detonation, here given in the form of a cordeau of length *A*–*B*. The point *S* where the two explosive waves in the cordeau meet is marked on the surface of a lead plate upon which the cordeau is resting. The shift *E*–*S* of this mark from the midpoint of cordeau allows one to determine the detonation velocity by a simple formula. [Mém. Poudres Salpêtres **14**, 216 (1906–1907)]

4.17 EXPLOSION AND DETONATION DIAGNOSTICS – Detonation Velocity of a Gaseous Explosion

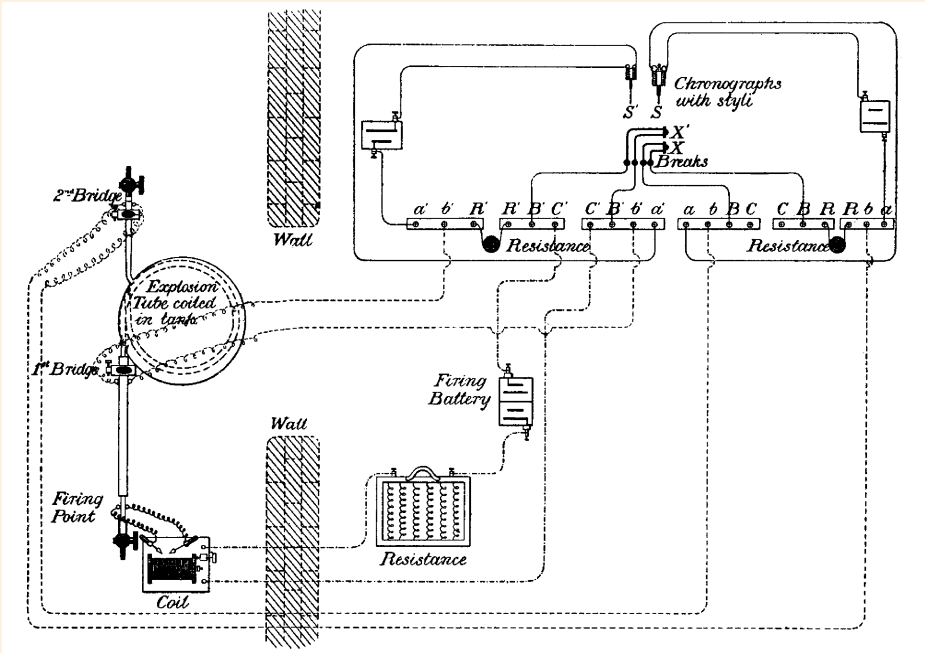

← Two styli, *S* and *S'*, were put in a circuit through resistances *RR* and *R'R'* and the breaks *X* and *X'*, respectively. The explosion wave traveling down the tube first breaks the bridge wire at the entrance of the coil and then breaks a second wire upon reaching the coil exit. The time difference between these activations of the two styli, a measure of the flame needed to propagate through the coiled tube, was recorded with an Elliot chronograph – a heavy pendulum carrying a smoked-glass plate. On letting the pendulum fall, the two styli were released, thus registering their marks on the moving glass plate.

4.17–J Schematic of a setup used by the British physicist Harold B. DIXON to measure the detonation velocity of gaseous mixtures. He used a long leaded tube, mostly 100 m long and 9 mm in diameter. Wound up to a coil and filled with the electrolytic gas, it was fired at the fixing point by interrupting the current flowing through an ignition coil via the break contact *X'*. For an oxyhydrogen detonation he found a detonation velocity of 2,821 m/s. [Phil. Trans. Roy. Soc. Lond. **A184**, 97 (1893)]

4.17 EXPLOSION AND DETONATION DIAGNOSTICS – Interior Ballistic Studies

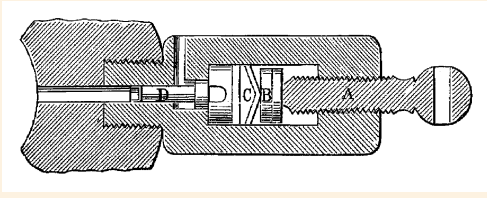

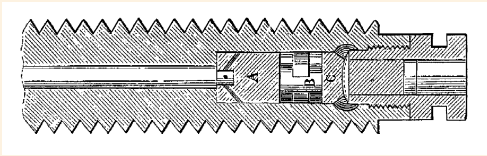

4.17–K ***Top:*** In 1857, Captain Thomas J. RODMAN of the U.S. Army (Allegheny Arsenal, PA) used an indentation gauge to measure the maximum gas pressure in the bore of a gun, the so-called "Rodman gauge." He observed that the pressure diminishes with increasing grain size of the gunpowder, which is particularly advantageous for the operation of large-caliber guns. ***Bottom:*** For the same purpose, Sir Andrew NOBLE at W.G. Armstrong & Co. (Elswick, U.K) invented in 1862 a crusher gauge, the so-called "Noble gauge." Based on the analysis of the deformation of a metal cylinder, it provides more precise pressure data than the Rodman gauge. Both gauges were calibrated using a static pressure loading. [*Meyers Konversations-Lexikon*, Bibliographisches Institut, Leipzig (1897), vol. 15, p. 434] NOBLE, measuring the "elastic force of fired gunpowder" by using his crusher gauge, noticed that RODMAN had measured erroneously a too high pressure of 12,400 atmospheres, a value almost twice as much as he obtained.

4.17 EXPLOSION AND DETONATION DIAGNOSTICS – Interior Ballistic Studies *(cont'd)*

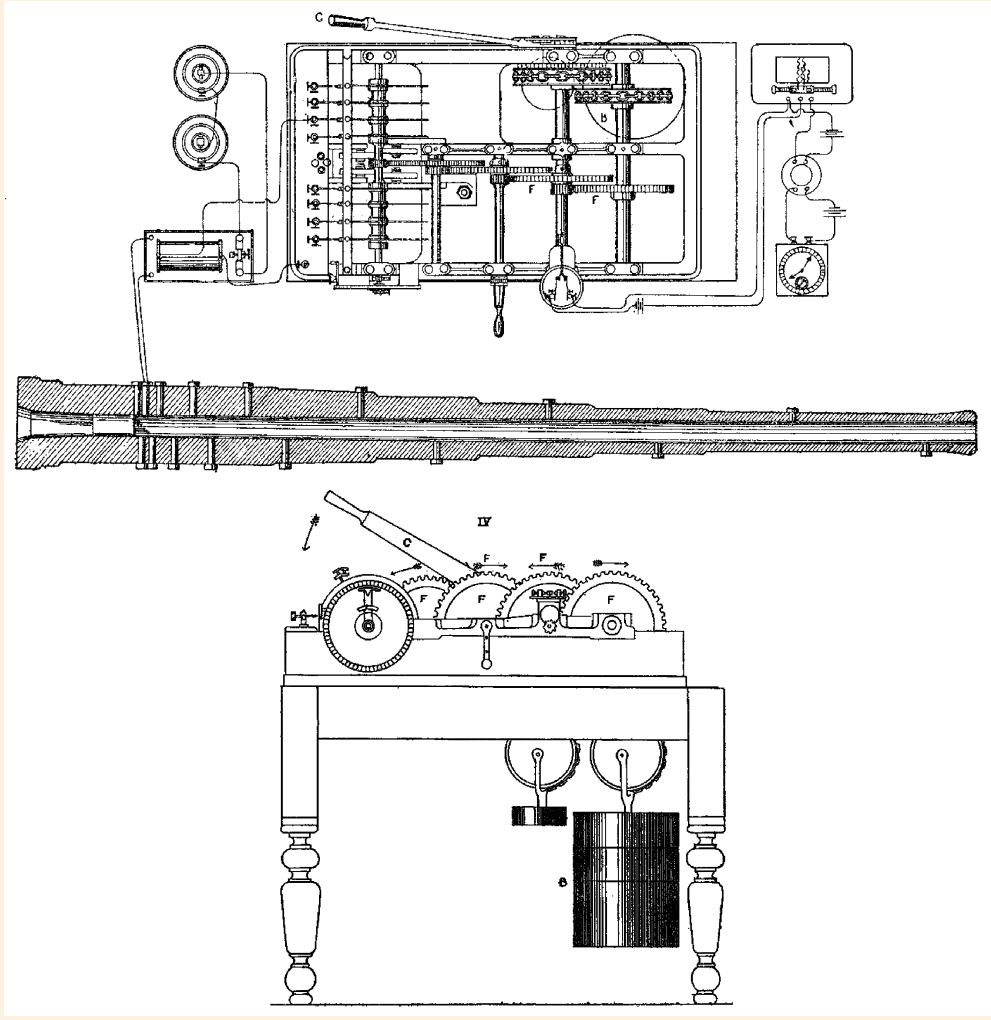

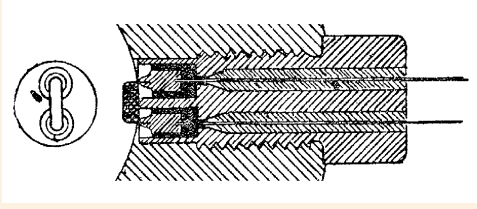

4.17–L ***Top:*** The Noble chronograph allowed one to measure the times at which a projectile passes certain fixed points in the bore of a gun and to record time differences of about 1 μs. The derived kinematic data were correlated with pressure data obtained by crusher gauges {⇨Fig. 4.17–K}. ***Bottom:*** Sir Andrew NOBLE used an apparatus for cutting wire by moving shot, his so-called "cutting-wire gauge." It was used in the bore of a gun to reliably trigger his chronograph at the moment of arrival of the projectile During passage of the projectile, the gauge interrupted an electric current in an induction coil which provoked a slight spark between a stylus and a sheet of paper fixed on a rotating drum. [Brit. Assoc. Rept. **64**, 523 (1894)]

4.17 EXPLOSION AND DETONATION DIAGNOSTICS – Blast Wave Recording

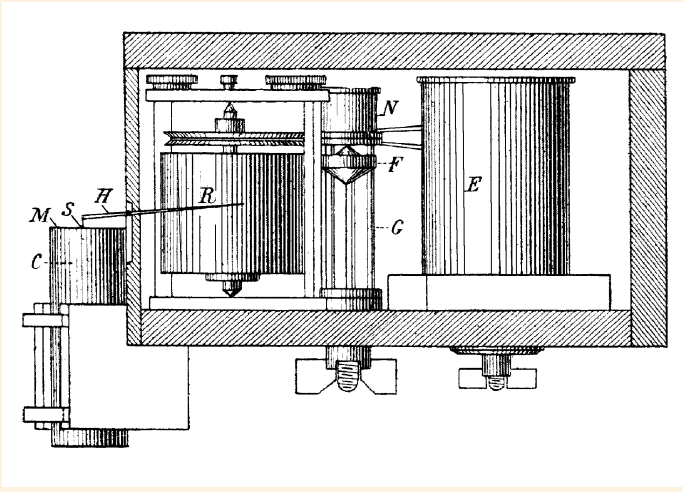

↑ *C* – brass cylinder, *E* – small electric motor, *F* – dropping weight, *G* – gliding bars, *H* – lever, *M* – caoutchouc membrane, *N* – electromagnet, *R* – recording drum, *S* – stylus

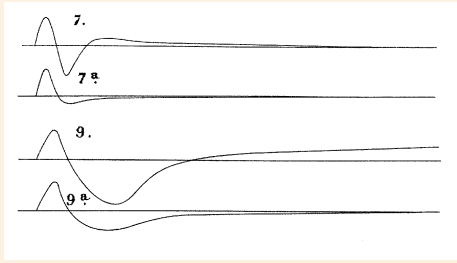

4.17–M W. WOLFF, a military engineer at the German Army Ballistic Test Site in Berlin-Cummersdorf, used a mechanical membrane-type pressure gauge and a rotating-drum chronograph to record free-field pressure-time profiles of large-scale chemical explosions in air. He compared blast effects of charges up to weights of 1,500 kg using two different explosives, black powder and trinitrophenol. Note that the typical negative pressure phase of a blast wave is correctly reproduced. [Ann. Phys. Chem. **69** (III), 329 (1899)]

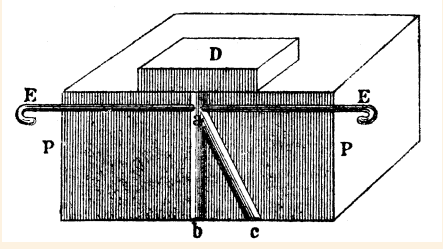

4.17–N Schematic of Ernst MACH's ingenious arrangement for measuring the propagation velocity of a blast wave, which he generated by an electric spark *a* between two electrodes *E*–*E*. The blast wave, split into two shock waves and propagating in the two bores *a*–*b* and *a*–*c* of different lengths arranged in a wooden block *P*–*P*, arrived at two different time instants at openings *b* and *c*. Here their arrivals were recorded as angular marks on a soot-coated, fast-revolving disk. Using blocks *P*-*P* of different thickness that provided different channel lengths *a*–*b* and *a*–*c*, MACH also applied this simple method to determine point-by-point how the shock-front velocity decays with distance from the explosion source. [Sitzungsber. Akad. Wiss. Wien **77** (II), 819 (1878)]

4.17–O Wolfgang PARR and collaborators at EMI developed a ballistic "roller pendulum" to measure the combined blast and fragment loading on a vertical surface near the ground. The instrument had a target area of 0.2 m^2 and allowed one to measure with sufficient accuracy impulsive loads ranging from 0.2 to 200 kg m/s. The picture shows a setup of four roller pendulums positioned in the near-field around a detonating model shell consisting of 1 kg Composition B and a 2-kg steel jacket. In order to avoid gliding, the center of percussion in this pendulum type must be located close to the point of contact. [Bericht E20 (1983), EMI, Freiburg]

4.17 EXPLOSION AND DETONATION DIAGNOSTICS – Streak Photography in Detonics

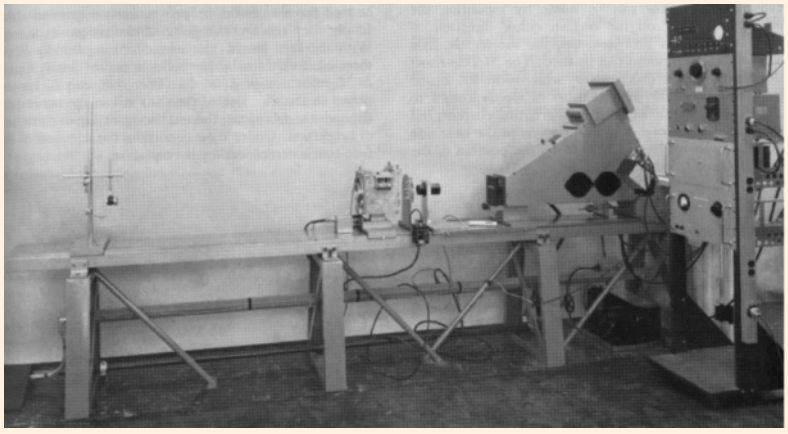

4.17–P Berlyn BRIXNER, a high-speed photographer at LASL (Los Alamos, NM), developed a high-speed sweeping image camera for routine explosive testing. The rotating mirror, revolving at 2,000 rps, sweeps the image of a 3-in. (76-mm) long slit at a velocity of 13 mm/μs. The photo shows a general view of his camera assembly used for studying miniature explosive events such as sparks, exploding wires, detonators, and other miniature explosive charges contained in the box shown at the center; a welded-steel construction provided with Lucite windows as viewing ports on two sides was also used to permit use of backlighting when desired. [J. SMPTE **70**, 180 (1961)]

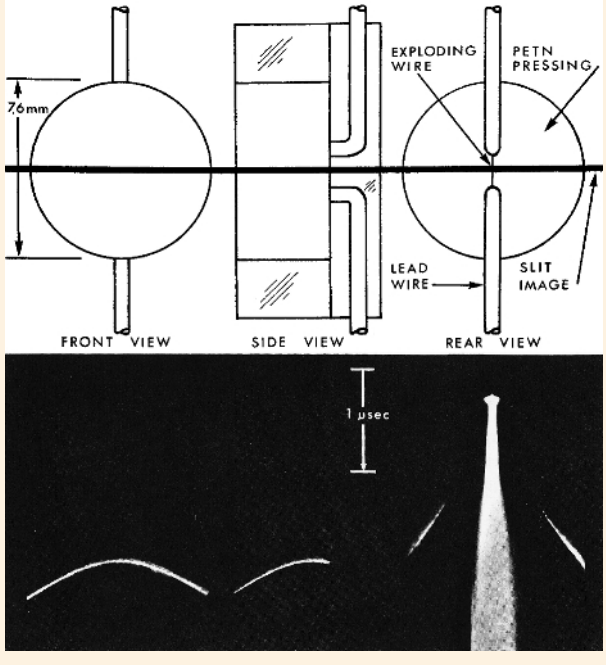

4.17–Q In the 1960s, James H. BLACKBURN and Robert J. REITHEL, two detonation researchers at LASL, used BRIXNER's high-speed sweeping image camera to study the initiation of detonation in PETN by an exploding wire. They took photographs through a modified, transparent head of a detonator. ***Top:*** Schematic of their test setup showing three views of a modified exploding wire detonator with two 0.8-mm-dia. lead wires embedded in a Lucite insulator. ***Bottom:*** Streak photographs taken in front, side, and rear view. The first light recorded has the image of an arrowhead, the tip designated as the wire light and the blade as the flare light. The two traces proceeding outward to the sides denote the initiated detonation wave. Note that detonation does not occur immediately after wire explosion begins, but rather that a buildup phase with a duration of about 1 μs is required. [W.G. CHACE and H.K. MOORE (eds.) *Exploding wires*. Plenum, New York (1964), vol. 3, p. 153]

4.17 EXPLOSION AND DETONATION DIAGNOSTICS – Reflected-Light Photography in Detonics

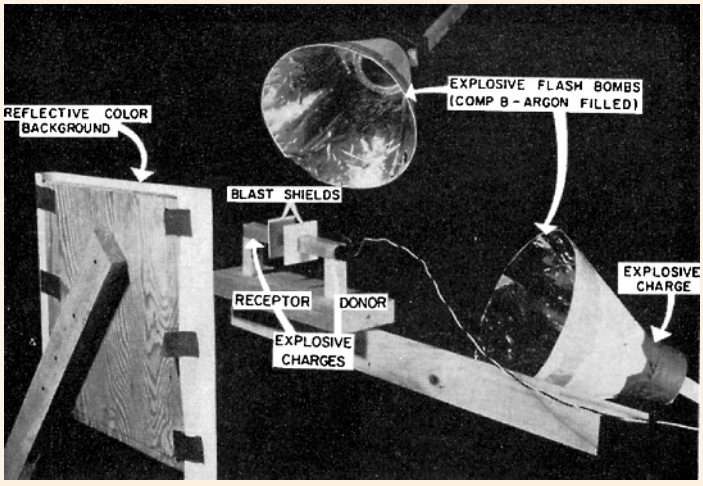

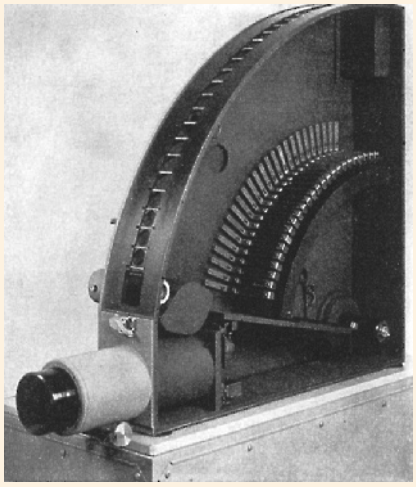

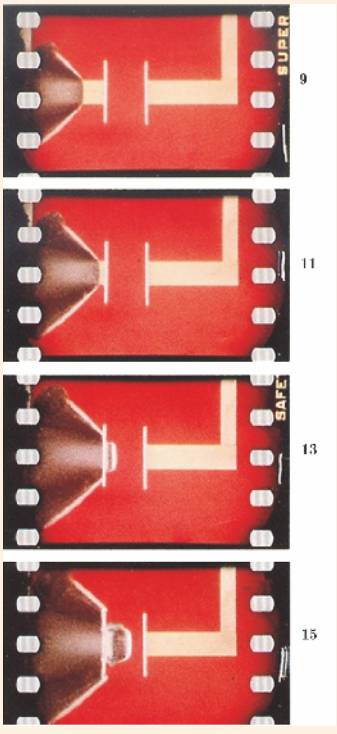

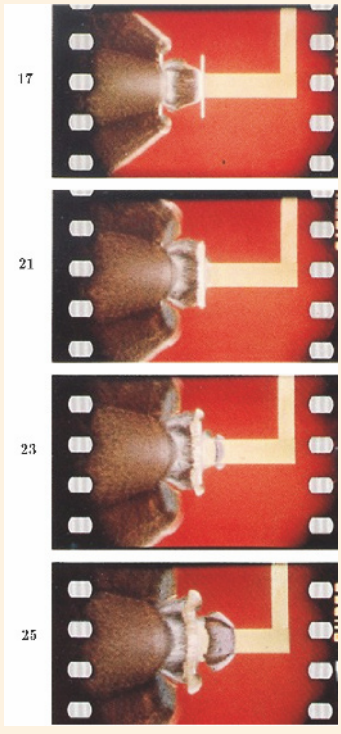

4.17–R Morton SULTANOFF and Robert L. JAMESON at BRL (Aberdeen, MD) used submicrosecond color cinematography to investigate the influence of the air shock sent out from the end face of a detonating explosive on a second high explosive positioned close by. This strong blast interaction did not cause immediate reaction in the receptor explosive, but rather produced a discontinuity to the detonation of the receptor charge. ***Top, left:*** View of experimental setup. Lighting was provided by two argon flash bombs positioned at 45° from the event (flash duration ca. 30 μs). Both end faces were provided with "blast shields" to prevent the detonation gases from spilling over and obscuring the receptor stick until the appearance of the detonation in the receptor stick. ***Top, right:*** View of the Beckman & Whitley camera model 189, a 25-frame reimaging high-speed camera. Operated at a rate of up to 1.2 million frames/s, this resulted in a full recording time of 20 μs and an exposure time of 0.1 μs. [W.G. HYZER: *Engineering and scientific high-speed photography*. Macmillan, New York (1962), p. 127] ***Bottom:*** The receptor charge (*right*) was separated from the donor charge (*left*) by a 5-mm air gap. Using 35-mm film Super Anscochrome, they recorded the detonation events in reflected light. The obvious preliminary shock in the receptor explosive stick, which explains the heretofore incompatible physical discontinuity to detonation, can be seen in the selected frames. [J. SMPTE **69**, 113 (1960)]

4.18 OPTICAL METHODS FOR FLOW VISUALIZATION – Schlieren Photography

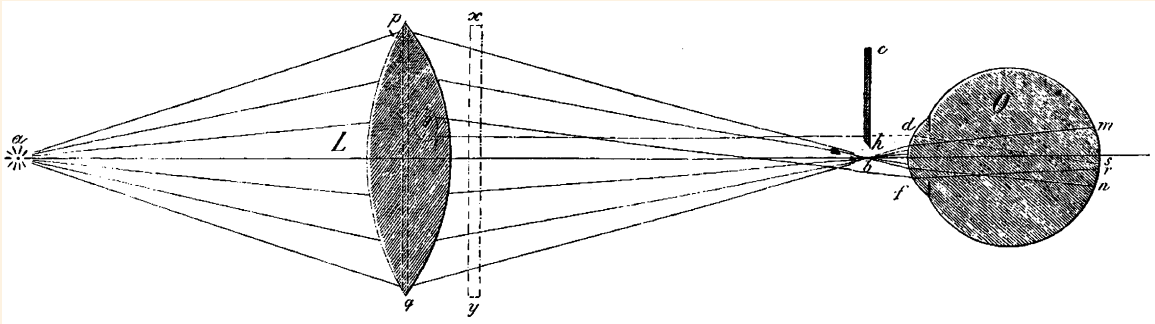

4.18–A Schematic of August TOEPLER's schlieren method. It essentially consists of an electric spark *a* acting as a high-intensity short-duration flash point light source, a lens *L*, and a knife edge *c*–*h*. TOEPLER positioned the object *x*–*y* to be studied behind *L* and used the edge *c*–*h* close to the eye *O* such that the central beam was cut off. The object, for example the density jump at the front of an aerial shock wave, is then visible on a dark background. [A. TOEPLER: *Beobachtungen nach einer neuen optischen Methode*. Cohen, Bonn (1864), plate I, fig. 1]

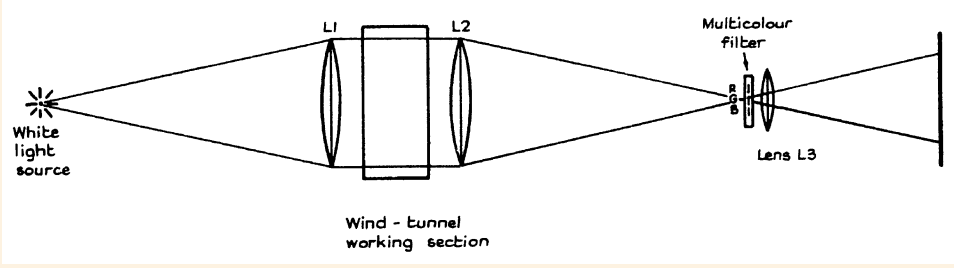

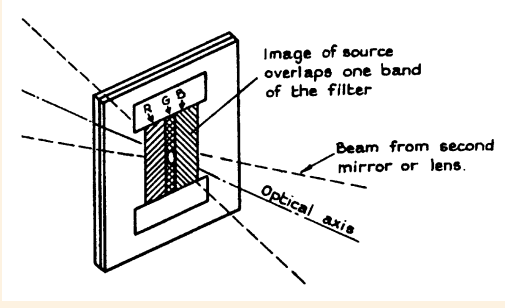

Bottom: A tricolor filter can consist of a simple arrangement of narrow strips of colored gelatin film laid side by side and clamped between two thin glass plates. Schematic showing position and orientation of color filter: *R* – red, *G* – green, and *B* – blue.

4.18–B Color schlieren methods are derivatives of TOEPLER's classic schlieren method and have been known since the end of the 19th century. Not only are hue, saturation, and color intensity useful as aids in a quantitative analysis, but color schlieren pictures also result in more aesthetic pictures than black-and-white images. There exists a wealth of methods for color coding of the refraction magnitude and direction, *e.g.*, by using prisms, diffraction gratings, interference filters, and chromatic aberration. ***Top:*** The color schlieren method shown here schematically was devised by the British researchers R. John NORTH and Douglas W. HOLDER at the former Aerodynamics Division of the NPL (Teddington, U.K.). He applied a white light source (such as an electric spark or a xenon flash tube) in the source plane and a multicolor filter in the cutoff plane (instead of the classic knife edge). Today 1- and 2-D color schlieren techniques are widely applied in high-speed flow visualization studies, using colored filter masks of different designs and gradient directions especially tailored to a certain problem. [NPL Aero Rep. No. 266 (1954). Courtesy British Marine Technology, Teddington, U.K.]

4.18 OPTICAL METHODS FOR FLOW VISUALIZATION – Shadowgraphy

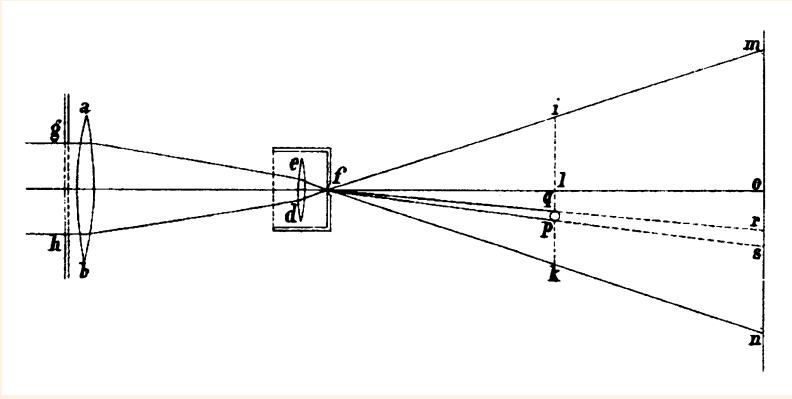

4.18–C The shadow method was invented in the late 1870s by Vincent DVOŘÁK at Agram University. It only requires a point light source and a white screen for projection purposes. The light, passing the test object *p–q* (*e.g.*, a small inhomogeneity in glass or a "schliere" in air), is deviated and produces its image *r–s* on the screen. The aperture *i–k* determines the field of view *m–n* on the screen. DVOŘÁK realized a point light source by using a heliostat (*i.e.*, using sunlight) and focusing the light onto a pinhole *f*. [Ann. Phys. Chem. **9** (III), 502 (1880)]

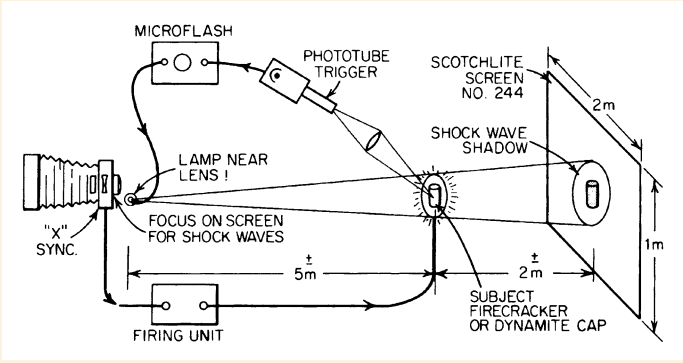

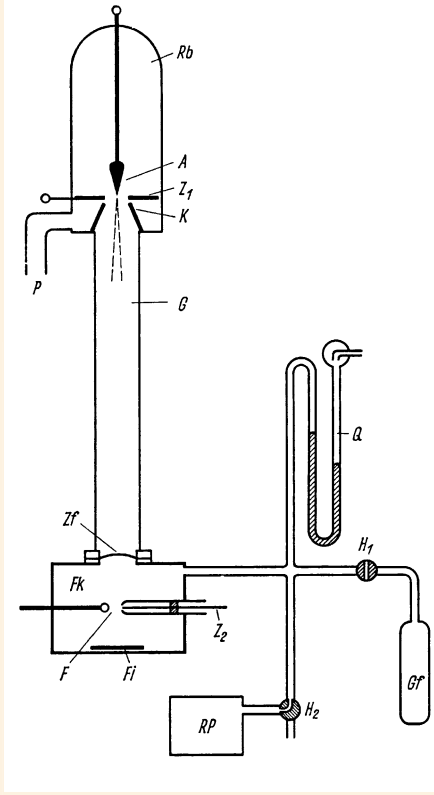

4.18–D The shadow method is most useful for visualizing shock waves and can be modified in a manifold manner. ***Left:*** Harold E. EDGERTON at MIT (Cambridge, MA) used an arrangement that employs a retroreflective screen (*e.g.*, Scotchlite, a 3M product) to photograph shock waves in large-scale experiments. The point light source should be placed as close to the lens as practical, but with a shield to keep the direct light from the camera lens. [H.E. EDGERTON: *Electronic flash, strobe*. MIT Press, Cambridge, MA (1970), p. 344] ***Right:*** Radiography is also a shadow method but uses X-rays instead of visible light. Karl-Heinz HERRMANN at the Freie Universität Berlin was the first to make a radiograph of a propagating shock wave in air and other gases without using any high-atomic-number additives in the test gas {⇨Fig. 4.5–H}. In order to get a sufficient contrast, he applied a flash soft X-ray tube *Rb* pulsed from a low-voltage high-current capacitor discharge, and included a vacuum tube *G* between *Rb* and object *F* to minimize the absorption of soft X-rays. The shock wave emerging from a spark gap *F* was recorded on film *Fi*. Photo densitometry of the radiograph first allowed for the determination of the density jump and the steepening process at the shock front. [Z. angew. Phys. **10**, 349 (1958)]

4.18 OPTICAL METHODS FOR FLOW VISUALIZATION – Interferometry

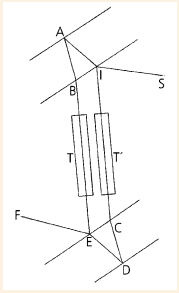

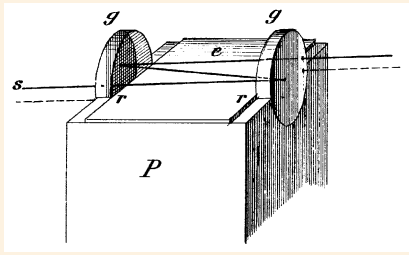

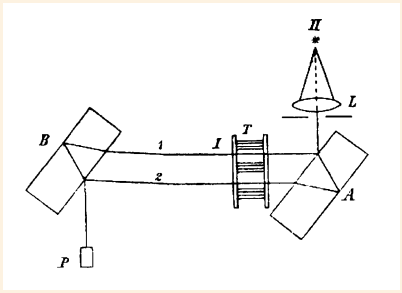

4.18–E The archetype of most interferometer constructions currently used in fluid and gas dynamics is the "Jamin interferometer." ***Left:*** Invented in 1856 in France by Jules C. JAMIN, it consists of two equally-thick plane parallel glass plates of the same refractive index, opaquely silvered on their back surfaces, thus combining mirror and beam splitter into one element. A beam of light $S \rightarrow I$, incident on the upper shown plate at about 45°, gives rise to two beams: one reflected from the front surface and the rear surface of the second plate ($I \rightarrow C \rightarrow D \rightarrow E$), the other reflected from the rear surface of the first plate and the front surface of the second plate ($I \rightarrow A \rightarrow B \rightarrow E$). Both beams are recombined to give an interference pattern in the axis $E \rightarrow F$ of a telescope. JAMIN positioned two tubular gas chambers, T and T', in the two beams in order to measure the difference in the refractive index. The instrument, however, only allows a small distance between the two beams, normally not exceeding a few centimeters. [Ann. Phys. **98** (II) 345 (1856)] ***Center:*** August TOEPLER and Ludwig E. BOLTZMANN used the Jamin interferometer to measure the amplitude of sound at the threshold of hearing. They closely attached two circular parallel glass plates g–g at the side walls of a covered wooden pipe P such that they touched the two side walls r–r of an iron plate e and parallel faced each other, thus forming a Jamin interferometer. One light beam (*solid line*) ran outside of the pipe, the other (*broken line*) inside, being exposed to the periodic changes in refractive index. A stroboscopic illumination allowed one to observe the fringes as a stationary picture. [Ann. Phys. **141** (II), 321 (1870)] ***Right:*** Ernst MACH and J. VON WELTRUBSKY first visualized the local density profile through the front of an aerial shock wave. A and B denote the two Jamin plates. The shock wave was generated by an electric spark I in a cuvette T and interacted with the light beam 1; beam 2 was shielded from the shock wave. A second spark II, serving as a flash light source, was triggered in delay to spark I. Observation of the fringes occurred through a prism P such that the eye rested on T as well as on a slit positioned behind the condenser L. [Sitzungsber. Akad. Wiss. Wien **78**, 551 (1878)]

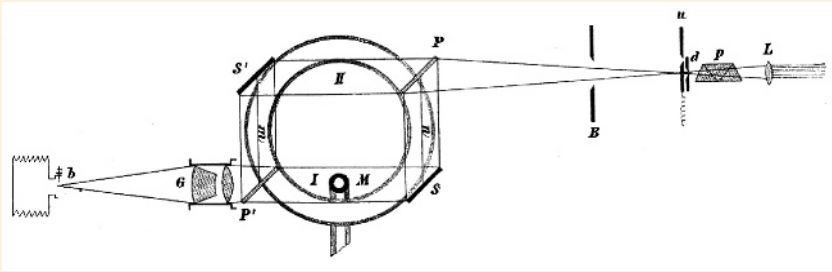

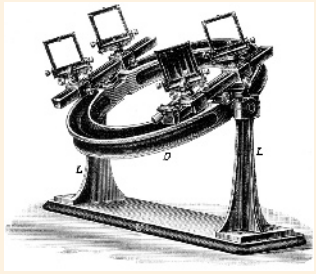

4.18–F ***Left:*** In 1891, Ludwig MACH at the German Charles University in Prague and, independently, Ludwig ZEHNDER at the University of Würzburg invented the so-called "Mach-Zehnder interferometer." It differs from JAMIN's interferometer in that the two beams I and II are widely separated so that one beam can be exposed to a violent environment, such as the trajectory of a projectile, and the other beam can be shielded from any aerial disturbances. [Sitzungsber. Akad. Wiss. Wien **106** (Abt. IIa), 1057 (1897)] ***Right:*** L. MACH applied his interferometer construction in nonstationary gas dynamics. The two plane mirrors and the two beam splitters, both 10×10 cm^2 in size, are altogether mounted on a heavy annular support of about 40 cm in diameter, which provides a central area between these four optical elements free of any mechanical support. This allowed L. MACH to position the interferometer along the trajectory of a flying projectile {⇨Fig. 4.6–L}. [Z. für Instrumentenkunde **12**, 89 (1892)]

4.18 OPTICAL METHODS FOR FLOW VISUALIZATION – Holography

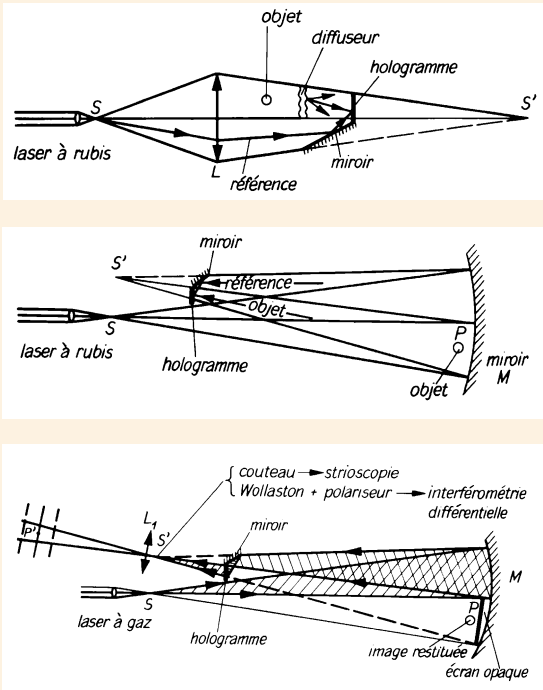

4.18–G In 1948, the Hungarian-born British engineer Dennis GABOR invented holography, which was extended in the 1960s to the recording of fast transient events. So-called "high-speed holography" allows a 3-D reconstruction of a fast moving object, *e.g.*, a propagating shock wave or a fast-flying projectile and its aerodynamic flow environment. When a flash hologram of a high-speed event has been taken at a desired time instant, it can be submitted successively to various standard optical methods such as to shadowgraphy, schlieren, and differential interferometry. This allows one to solve a variety of problems with a single shot only. The schematics given here illustrate the high-speed holographic technique in more detail. ***Top:*** Schematic arrangements for taking holograms in diffuse light as used by Paul SMIGIELSKI and Henri ROYER at ISL (Saint-Louis, France). The light source is a pulsed laser of high coherence and high energy per pulse, such as a ruby laser. ***Center:*** Arrangement for taking holograms in reflected light. ***Bottom:*** For reconstruction purposes, the same arrangement as sketched above is used but with a continuously operated laser instead of a pulsed laser. Furthermore, the object beam is screened. An example of a holographic image of a head wave is shown in Fig. 4.6–I. Using a repetitive Q-switched ruby laser and a rotating photographic plate – or different lasers pulsed at different times and a steady plate – they were able to realize cine-holography, which significantly extends holography for the study of high-speed events. [Courtesy ISL; Proc. 8th Int. Congr. on High-Speed Photography, Stockholm (1968). Almquist & Wiksell, Stockholm (1968), p. 324].

4.18 OPTICAL METHODS FOR FLOW VISUALIZATION – Surface Thermography

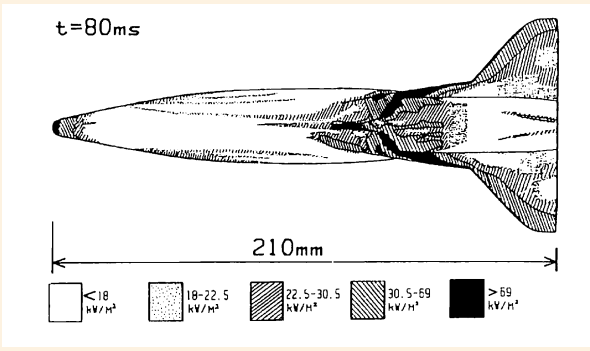

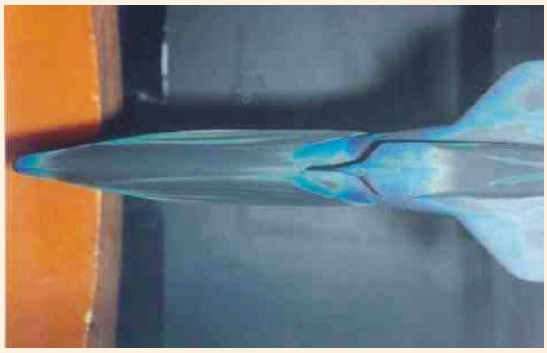

4.18–H Robin A. EAST at the Dept. of Aeronautics and Astronautics (University of Southampton, U.K.) applied "liquid crystal surface thermography" to the study of hypersonic flow with heat transfer rates ranging from 1 to 500 kW/m^2. Using a coating of microencapsulated liquid crystals he obtained quantitative heat transfer data for an aerospace plane model at $M = 6.85$ and $Re_\infty = 3 \times 10^7$/m in running times as short as 20 ms. [Courtesy Prof. R.A. East; Proc. 18th Int. Symp. on Shock Waves, Sendai, Japan (1991). Springer, Berlin (1992), p. 643]

4.19 HIGH-SPEED DIAGNOSTICS – Chronoscopes and Chronographs

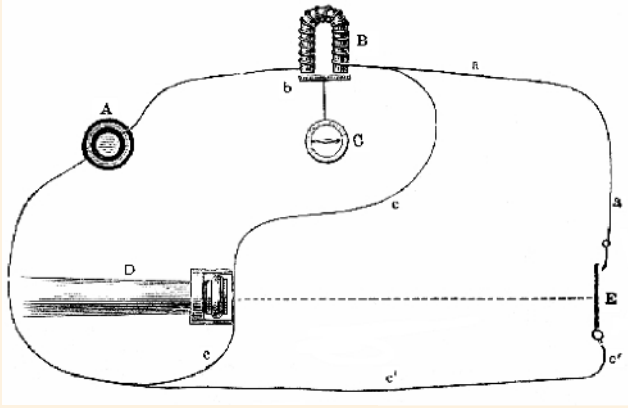

← Matthias HIPP, a German-born Swiss watchmaker, improved the accuracy of the Wheatstone chronoscope by using a clock with two faces, each moving over a scale divided into intervals of 10 ms and 1 ms.

4.19–A ***Top:*** In 1840, the English physicist Charles WHEATSTONE devised the so-called "Wheatstone chronoscope," an electrically activated stopwatch. The principle is illustrated here on the example of measuring the muzzle velocity of a gun *D*. The projectile first deactivates a magnetic clutch *B*, which starts a watch *C*. After traveling a known distance in free flight, it closes a contact *E*, which activates a magnet *B*, stopping the watch. [*Meyers Konversations-Lexikon*. Bibliogr. Inst., Leipzig (1894), vol. 4, p. 154] ***Bottom:*** View of a "Hipp-Wheatstone clock" made around 1900 by the renowned German instrument maker Ernst ZIMMERMANN at Leipzig. [Courtesy Institut für Psychologie, Karl-Franzens-Universität,Graz, Austria]

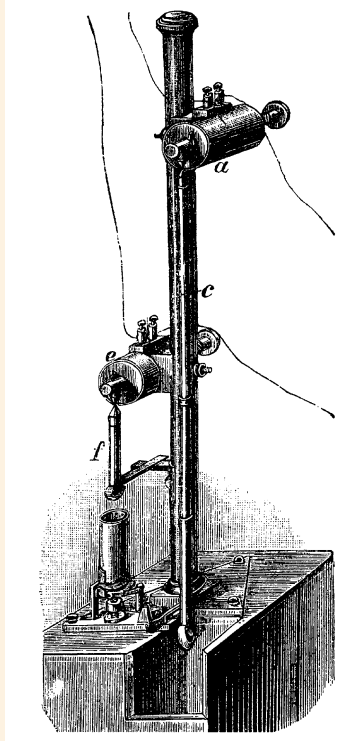

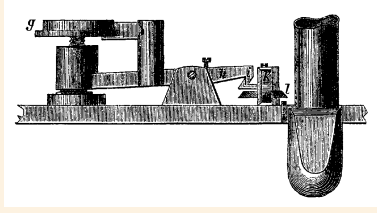

4.19–B In the early 1860s, the Belgian artillerist Paul LE BOULENGÉ devised the electrically triggerable so-called "Le-Boulengé chronograph," which became the standard instrument in ballistics for measuring muzzle velocities. Using two wire screens along the trajectory, the bullet, interrupting the first screen, deactivated a magnet, thus starting the free-fall dropping of a first rod *c*. Upon passage of the second screen another suspended rod *f* fell, thereby releasing a spring-loaded knife (*bottom*) marking rod *c*. Thus, the height of fall is known, and, likewise, the time of fall. [*Brockhaus' Konversations-Lexikon*. Brockhaus, Leipzig (1908), vol. 4, p. 241]

4.19 HIGH-SPEED DIAGNOSTICS – Cathode-Ray Oscilloscopes

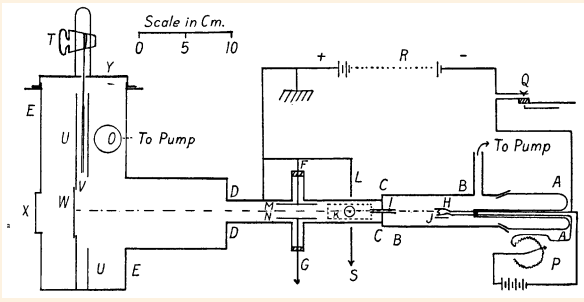

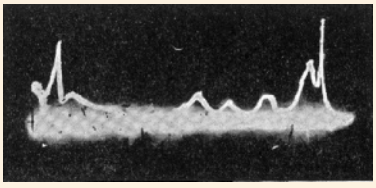

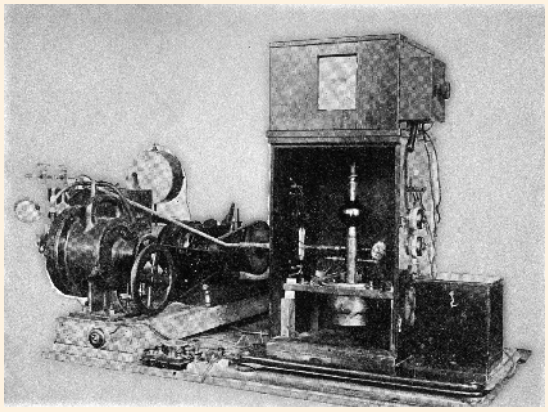

↑ The Wood oscillograph, devised by the British physicist Joseph J. THOMSON, used a cathode-ray tube (or Braun tube) with a hot cathode and two pairs of deflection plates.

4.19–C In 1921, the British physicist David A. KEYS at McGill University (Montreal, Canada) applied the so-called "Wood oscillograph" to record pressure-time profiles of underwater explosions. ***Left:*** Schematic (*top*) of his experimental setup and a pressure-time profile (*bottom*) of an explosion of guncotton in water, recorded with a tourmaline gauge. ***Right:*** View of the Wood oscillograph constructed and tested by the British physicist Albert B. WOOD at the Admiralty Research Laboratory (Teddington, U.K.). The film plate, placed inside the vacuum, was directly exposed by the 3-kV cathode ray. [J. Franklin Inst. **196**, 576 (1923)]

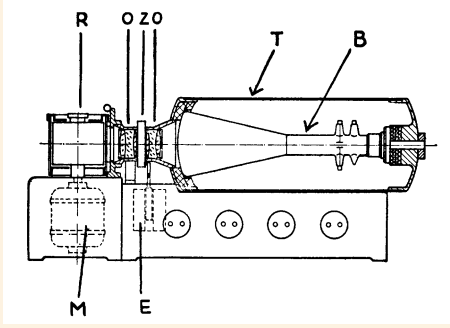

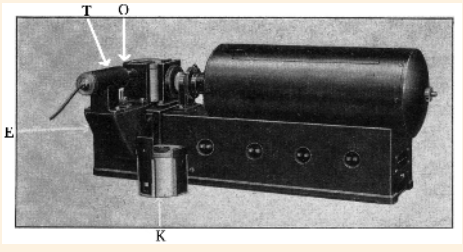

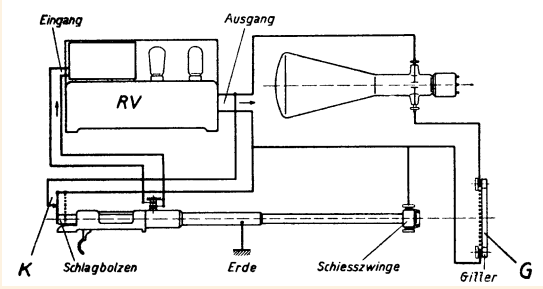

4.19–D In 1932, the physicists Hans JOACHIM and Hans ILLGEN at Zeiss-Ikon AG (Dresden, Germany) measured the dynamic gas pressure in firearms using a quartz gauge. ***Right:*** The signal of the pressure gauge was amplified (*RV*) and via a grid *G* fed to the vertical pair of deflection plates of a Braun tube *T*. Triggering occurred via contact *K*, which opened at the moment the gun was fired. The voltage at the deflection plates was interrupted when the bullet destroyed *G*. ***Left:*** Schematic (*top*) and view (*bottom*) of their electronic-mechanical oscillograph: time display was achieved mechanically by sweeping the image of *T* via lenses *O* and a mechanical shutter *Z* onto a film fixed on a rotating drum *R* driven by a synchronous motor *M* at 3,000 rpm. They found that gas pressures in gun barrels typically range between 3 and 4 kbar, which, however, only last about 1 ms FWHM. [Z. ges. Schieß- & Sprengstoffwesen **27**, 121 (1932)]

4.19 HIGH-SPEED DIAGNOSTICS – Time-Delay Generators

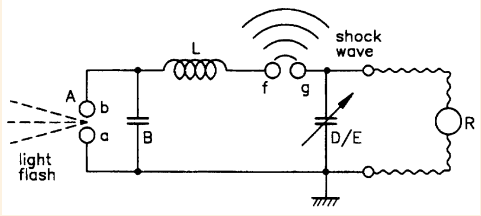

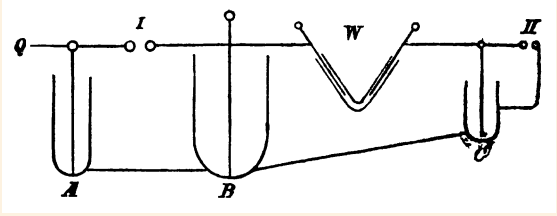

4.19–E In 1858, Karl-Wilhelm KNOCHENHAUER, a high-school teacher (Meiningen, Thuringia, Germany) devised a high-voltage delay circuit based on the coupling of two capacitor discharges. ***Left:*** The so-called "Knochenhauer circuit" was used in 1864 by August TOEPLER {⇨Fig. 4.5–A} to generate a shock wave by a first spark *f–g* and a light flash by a second, delayed spark *a–b* for visualizing the propagating shock wave at different time instants, which were varied by trimming the capacitor *D/E*. ***Right:*** In 1878, this circuit was improved by Ernst MACH, the so-called "Mach circuit." The spark generating the shock wave is designated by *I* and the illumination spark, fired delayed, by *II*. [Shock Waves **5**, 1 (1995)]

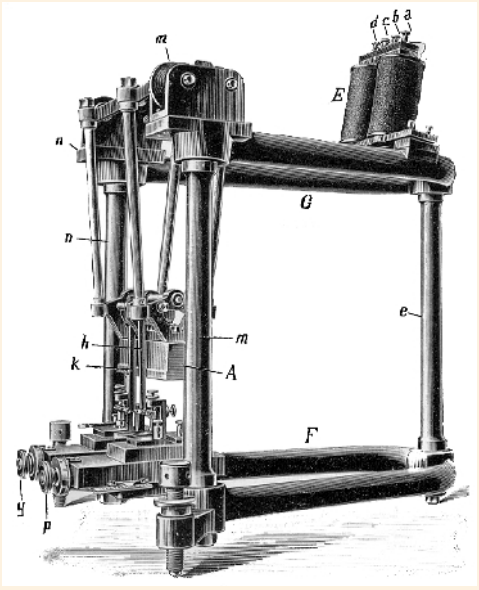

4.19–F The "Helmholtz pendulum," a precise contact breaker, was originally constructed for physiological studies by the German professor Max T. EDELMANN. But it was also used in ballistics and detonics for triggering purposes to derive a delayed electric pulse from the high-speed event to be studied. Provided with two pairs of contacts for opening and closing actions and adjustable against each other via micrometric screws, it allowed the generation of current pulses of variable duration. One full turn of the micrometric screw corresponded to a time difference of 156 µs. [Z. f. Instumentenkunde **21**, 124 (1901)]

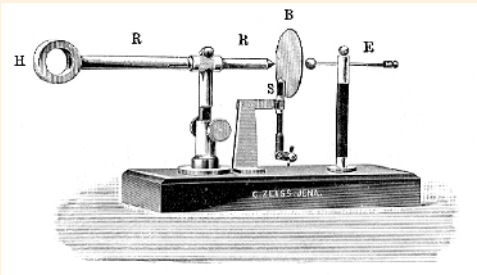

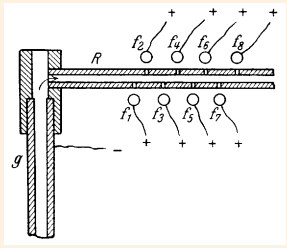

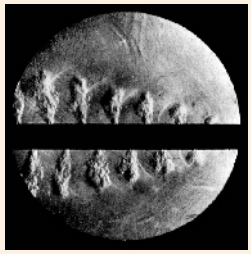

4.19–G ***Top:*** Ludwig MACH (German Charles University, Prague) applied the head wave to trigger a spark outside of his interferometer such that the head wave upon entering the interferometer was illuminated by a spark flash after a certain delay time. Using a ring *H* connected to a tube *R*, the head wave, generated by the projectile flying through *H*, coupled a shock wave to *R*, which, arriving at the end and passing a hole in an aperture *B*, triggered a spark gap *S–E*. [Sitzungsber. Akad. Wiss. Wien **105** (IIa), 605 (1896)] ***Bottom:*** Carl CRANZ and Hubert SCHARDIN (Institut für Technische Physik, Berlin) taking up this method in their multiple-spark camera, generated a series of eight flashes up to a rate of 50,000/s. They used a gun barrel *G* connected to a pipe *R* along which eight trigger spark gaps, $f_1 \ldots f_8$, were arranged (*left*). Illustration of the successive escape of hot gases from the holes after passage of the shock wave (*right*). [Z. Phys. **56**, 147 (1929)]

4.19 HIGH-SPEED DIAGNOSTICS – Triggered Snapshot Photography

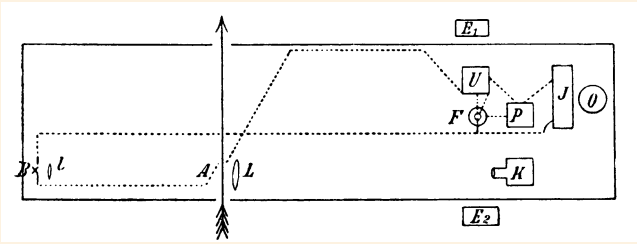

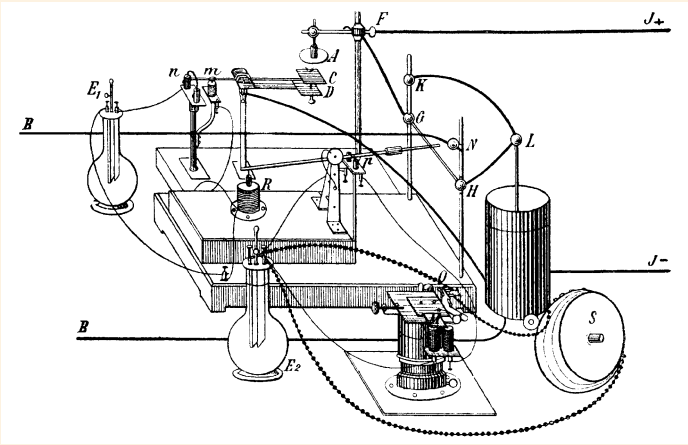

4.19–H The "snapshot" or "single-shot" photography was first used in 1851 by the Englishman W.H. Fox TALBOT. It required the least expenditure of equipment but only provided a single picture at a preselected time instant. With the advent of high-sensitive gelatin dry plates, snapshot photography was increasingly used to freeze high-speed events. ***Top:*** Schematic of an experimental setup that Ernst MACH and Peter SALCHER used in the late 1880s at the Meppen Ballistic Test Site in northern Germany for outdoor photography of large-caliber supersonic projectiles in free flight, about 12 m from the muzzle. Inside a wooden cabin they installed an optical setup (B – spark light source, l and L – schlieren optics, K – camera, an electric circuitry (F – Leiden jar, J – influence machine, P – voltage controller, U – commutator), and an external power supply (E_1 and E_2 – Bunsen batteries). The cabin was heated to minimize any loss of charge caused by corona discharges. The projectile, entering and leaving the cabin through small portholes to minimize detrimental daylight exposure, passed a fluid-dynamic trigger device A {⇨Fig. 4.19–G}. ***Bottom:*** To ensure precise triggering and safe operation it required precise circuitry: When the full potential of the Leiden jar was reached, the circuit automatically activated the camera shutter and a bell S. Upon the bell signal, the gun had to be fired and the camera shutter closed immediately after, both by hand. Precise triggering of the illumination spark B was achieved automatically upon projectile passage of the trigger spark gap A; both spark gaps were connected in series and with the circuitry via lines B. The HV circuitry was charged by the influence machine J via lines J+ and J–. [Sitzungsber. Akad. Wiss. Wien **98** (IIa), 41 (1889)]

4.19 HIGH-SPEED DIAGNOSTICS – Rotating Mirror

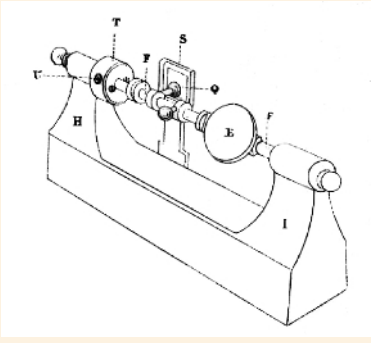

4.19–I In 1834, the English physicist Sir Charles WHEATSTONE first proposed the "rotating mirror" as a diagnostic tool to measure time spans to the millionth of a second. The device that he used to determine the velocity of electricity and light consisted of a brass frame H-I, a plane circular mirror E of polished steel fixed to the horizontal axis F–F such that the axis of rotation was in the plane of the mirror. Motion up to 800/s was communicated to the axis by means of a thread passing to a hand wheel. The arm Q, connected with a discharger S and mounted on F–F, provided a stroboscopic switch for triggering purposes. [Proc. Roy. Soc. Lond. **3**, 583 (1834)]. WHEATSTONE used the rotating mirror in the first measurement of the velocity of an electrical current passing through a wire. He later suggested that the same device could be used to also measure the speed of light. WHEATSTONE, together with the Irish natural philosopher John TYNDALL, also used his rotating mirror to show that Michael FARADAY's hypothesis on the "chemical harmonica" (or "burning harmonica"), a special case of the singing flame, was indeed correct.

4.19 HIGH-SPEED DIAGNOSTICS – Spark Chronography of a Flying Projectile

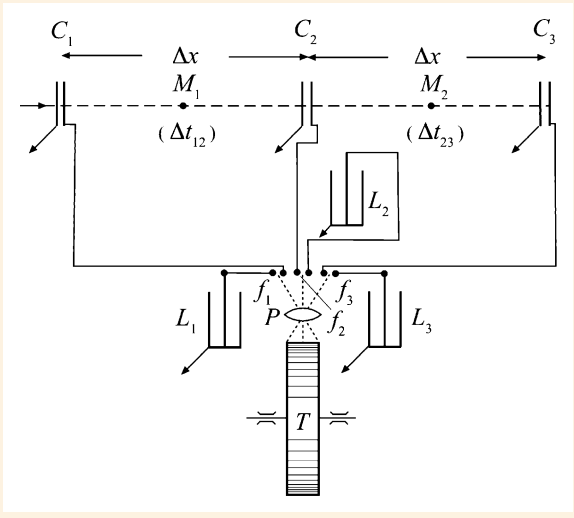

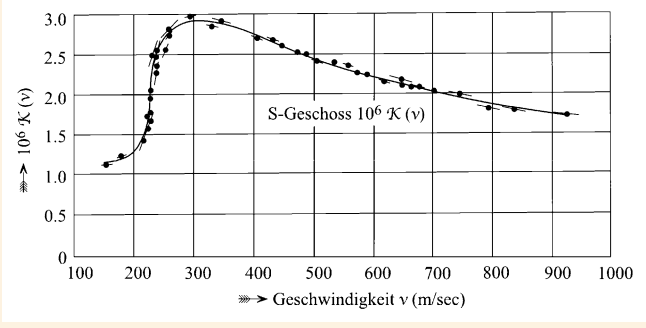

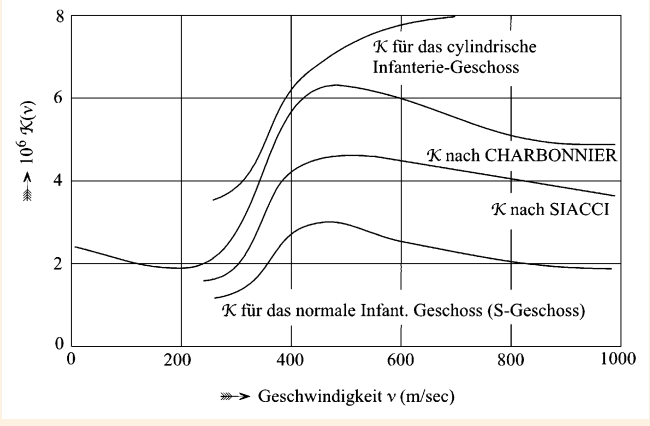

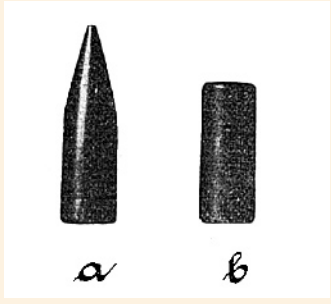

4.19–J In the late 1900s, Karl BECKER and Carl CRANZ, two German ballisticians at the Militärtechnische Akademie Berlin, began to develop a method to measure aerodynamic drag of infantry bullets as a function of the projectile velocity v with an accuracy of ca. 1%. ***Left, top:*** Their electric-spark photochronograph, the so-called "Cranz-Becker chronograph," consisted of a rapidly revolving drum T covered with a photographic film onto which, via a focusing lens P, the light of three spark gaps, f_1, f_2, and f_3, was projected. These spark gaps were triggered subsequently when the projectile had passed the contact plates C_1, C_2, and C_3, thus discharging the Leiden jars L_1, L_2, and L_3 via f_1, f_2, and f_3, respectively. Each contact plate C consisted of two pieces of aluminum foil, closely facing each other, which became conductive upon penetration of the bullet. The distance Δx between C_1 and C_2 and C_2 and C_3 was 20 m. Prior to firing the rifle, the Leiden jars were charged up to a high voltage by an influence machine and then disconnected. ***Left, center***: From the loss of velocity BECKER and CRANZ determined the drag coefficient $K(v)$. ***Left, bottom & right:*** They obtained the remarkable result that, compared to a cylindrical bullet with a flat head, a pointed bullet with an ogival head – the so-called "S-bullet" [Germ. *Spitzgeschoss*] – has a much lower aerodynamic drag. In addition, it was found that S-bullets shoot more accurately than those with round or truncated noses and retain a higher velocity when reaching the remote target. As early as before World War I, most European armies began to replace hitherto used round ammunition by the more efficient pointed one. [Artilleristische Monatshefte **69**, 189 (1912); Ibid. **71**, 333 (1912)]

4.19 HIGH-SPEED DIAGNOSTICS – Rotating Mirror Streak Cameras

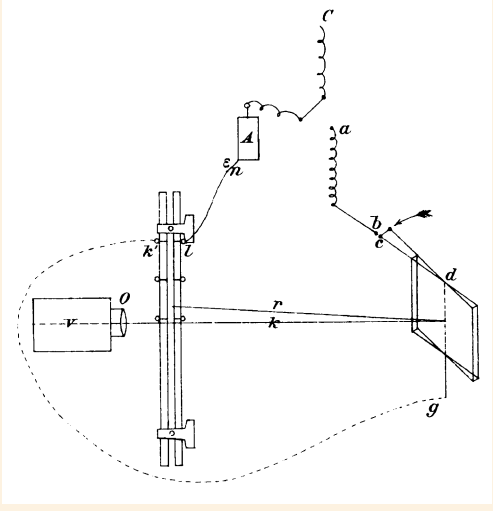

← The propagation of the front of the detonation wave was visualized through a 3-mm-wide slit glued along the tube axis and imaged via the rotating mirror *d* into a conventional still camera *F*. The mirror was provided with a pointer *c* in order to trigger the detonation in the glass tube by discharging a Leiden jar *A* along the electric path *n*–*l*–*k*–*g*–*d*–*c*–*b*–*a*.

→ For oxyhydrogen they determined from the inclinations of the streak records a detonation velocity ranging from approx. 2,200 m/s at the beginning to approx. 850 m/s at the end of the eudiometer tube.

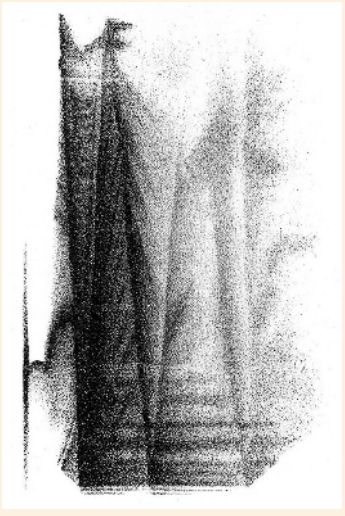

4.19–K ***Left:*** In 1888, Arthur VON OETTINGEN and Arnold VON GERNET, two German physicists at the University of Dorpat (West Russia), studied the propagation and reflection of detonation waves of gaseous explosive mixtures in 400-mm-long glass tubes using a rotating mirror. ***Right:*** Example of a streak record of an oxyhydrogen explosion. The streak record, beginning at the left side with the triggering spark discharge and covering a time span of about 3.7 ms, shows the propagation and three reflection cycles of the detonation front. [Ann. Phys. Chem. **33** (III), 586 (1888)]

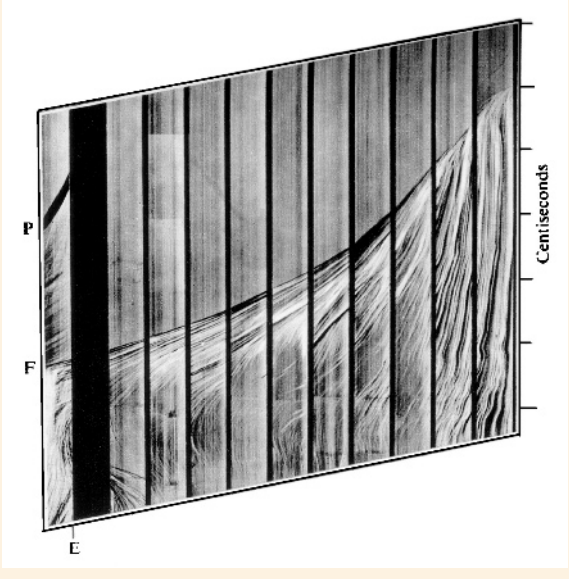

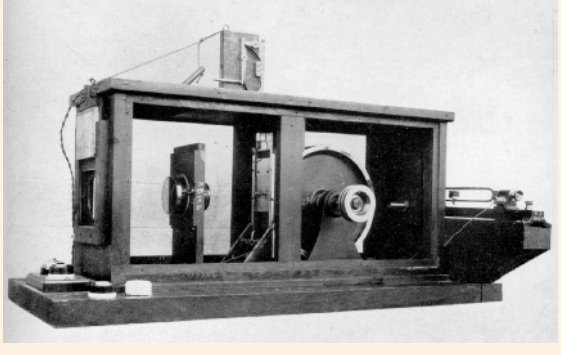

4.19–L ***Right:*** William H. PAYMAN and collaborators at the British Safety in Mines Research Establishment (SMRE) constructed a "wave speed camera," a streak camera, to record detonation phenomena in gaseous mixtures [Proc. Roy. Soc. Lond. **A132**, 200 (1931)] ***Left:*** Example of a typical composite streak record $s(t)$ showing the propagation of the detonation front in an air/methane mixture as a function of time t. From the slope of the streak record PAYMAN could analyze the starting process of detonation. [Proc. Roy. Soc. Lond. **A158**, 348 (1937)]

4.19 HIGH-SPEED DIAGNOSTICS – High-Speed Cinematography

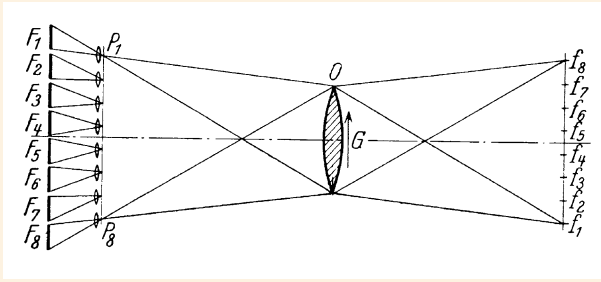

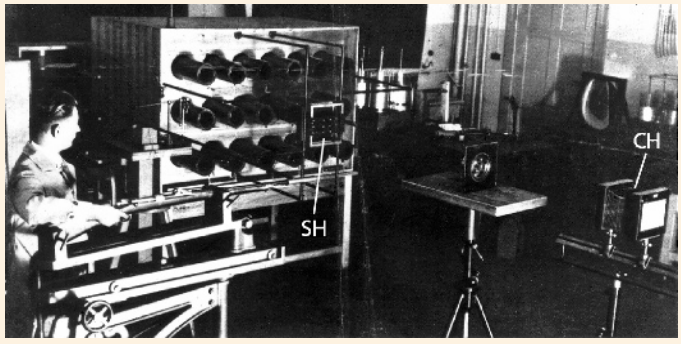

4.19–M ***Top:*** Schematic of the "Cranz-Schardin multiple-spark camera" invented by Carl CRANZ and Hubert SCHARDIN (Institut für Technische Physik, Berlin) in the late 1920s. It consists of a bundle of single-shot spark light source, $f_1 \ldots f_8$, arranged around a common axis and triggerable at any desired time instant. The camera gives from an object, positioned at G and viewed through a common lens O, a limited number of slightly oblique views $F_1 \ldots F_8$, which are imaged via individual lenses as pictures $P_1 \ldots P_8$ on a common film plane. Since the film is stationary, the picture frequency can be very high, and the quality is as good as that from a single flash system. [Z. Phys. **56**, 147 (1929)] ***Bottom:*** This photo shows Hubert SCHARDIN while recording ballistic experiments cinematographically using his multiple-spark camera. The camera prototype, built in the period 1927–1928, had only nine spark/frame units, but in 1936 this was extended to 24 frames. Note the spark head *SH* with the sparks $f_1 \ldots f_9$ and the camera head *CH*. Each spark was fed by a pair of cylindrical, low-inductance capacitors (shown in the background). This camera type was later used at EMI, ISL, MIT, and other laboratories. [Proc. 4th Int. Congr. on High-Speed Photography, Cologne (1958). Helwich, Darmstadt (1959), p. 139. Courtesy EMI-Archives, Freiburg]

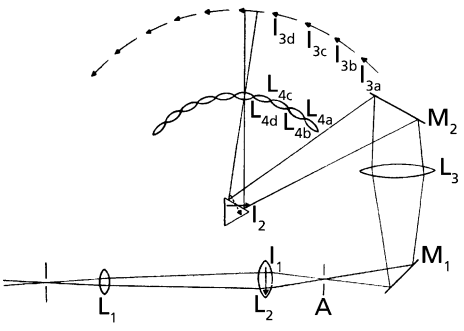

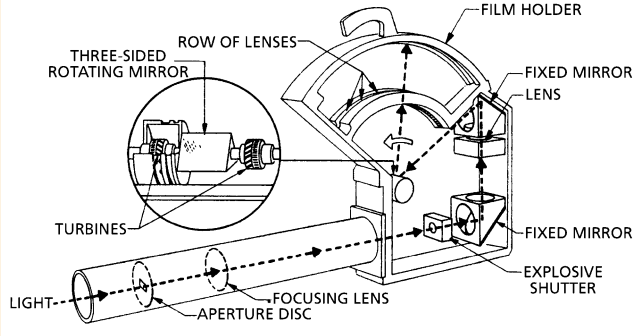

4.19–N Berlyn BRIXNER at LASL (Los Alamos, NM) developed an ultrahigh-speed framing camera capable of taking 96 consecutive motion pictures of explosive phenomena and shock wave actions (particularly of nuclear detonations) at a rate of 15 million frames/s. ***Left:*** The optical system in this camera is based on the use of a rotating mirror and refocused revolving beams as pioneered by Cearcy D. MILLER in the mid-1930s. An image I_1 of the event being studied is formed at field lens L_2 by the objective L_1. This image is relayed to the rotating-mirror surface at I_2 by means of lens L_3. Folding mirrors M_1 and M_2 are used to make a compact camera. As the mirror rotates, the reflected light beam passes through the final framing lenses L_{4a}, L_{4b}, *etc.* to form images I_{3a}, I_{3b}, *etc.* on the film plane. [U.S. Patent No. 2,400,887 (1946)] ***Right:*** Schematic of the Los Alamos camera, showing path of light rays and direction in which the light beam is swept across secondary lenses. [Proc. 2nd Int. Congr. on High-Speed Photography, Paris (1954). Dunod, Paris (1956), p. 108]

4.19 HIGH-SPEED DIAGNOSTICS – High-Speed Cinematography *(cont'd)*

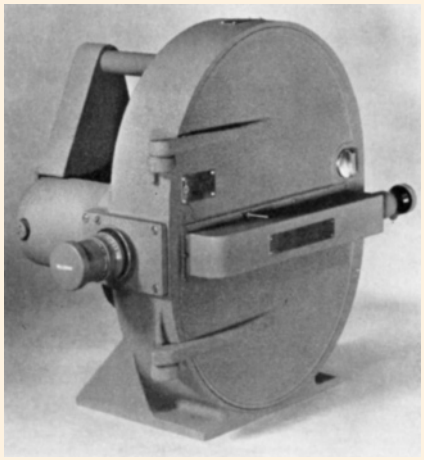

4.19–O ***Top:*** The Fastax, a high-speed rotating-prism camera (max. 16,000 frames/s), was a milestone in photo instrumentation and was also successfully used at Trinity Test (1945) to record minute details of the nuclear fireball growth. Today mechanical cameras at this frame rate are superseded by high-speed video cameras. [R.F. SAXE: *High-speed photography.* Focal Press, London (1966), p. 25] ***Bottom:*** In 1991, Photron Ltd. at Tokyo, Japan designed the world's fastest high-speed video system (max. 40,500 frames/s), which was commercialized by Kodak as model 4540. One important advantage of this digital camera is that it permanently records, and a trigger pulse stops recording. This enables the experimenter to also capture pretrigger events, such as in failure studies, which otherwise would not be accessible to observation. Contrast and illumination can be improved by using a copper vapor laser as a stroboscopic light source: Because of the ultrashort duration of laser flashes, image blurring is practically eliminated, regardless of the speed of the event. [Courtesy Photron Ltd., Tokyo]

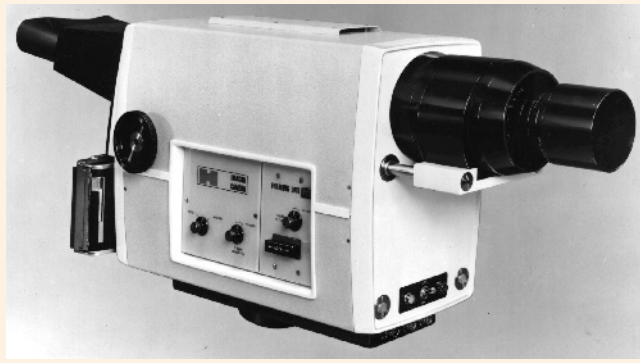

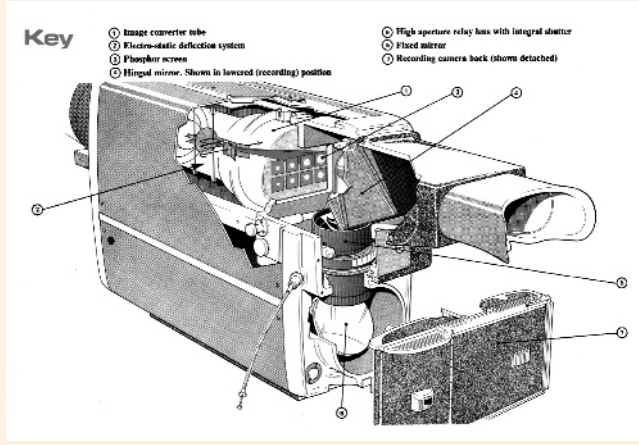

4.19–P A framing operation with image converters is usually achieved by (1) interrupting the electron beam in the tube to effect repetitive shuttering and (2) shifting the interrupted beam to different areas of the screen – thereby producing a pattern of discrete images on screen. ***Top:*** View of the Imacon 700, the first commercial electronic high-speed framing camera, which allowed one to take up to 16 images at a rate ranging from 25,000 to 20,000,000 frames/s. Based on original ideas developed by the Englishman Alec E. HUSTON at AWRE (Aldermaston, U.K.); it was commercialized by John Hadland and first became available in May 1967. ***Bottom:*** Schematic of the camera as seen from the back. The latent picture on the phosphorus screen was recorded on Polaroid film, *i.e.*, recording of a complete scene was available on film only 10 s after the experiment. Lens coupling of the film was later replaced by fiber optic coupling. The camera concept opened the door to a new generation of electronic digital multi-frame cameras, which today considerably facilitates high-speed recording of shock waves, detonation waves, exploding wires, fracture phenomena, and other ultra-high-speed events. [Courtesy B. SPEYER, DRS Hadland, Tring, U.K.]

4.20 **HIGH-SPEED VEHICLES** – Mythologies

4.20–A Covering large distances in a short time has been humanity's dream since time immemorial. High-speed vehicles, in antiquity light two-wheeled chariots drawn by up to four horses, were a privilege and only reserved to deities and high-ranked persons such as emperors, kings, generals, *etc.* In Greek mythology, the Sun-god HELIOS was conceived as driving a glowing chariot daily across the sky from the morning's eastern portals to the evening's western gates and as sailing nightly in a golden boat on the ocean along the Earth's northern border back to his palace. This picture shows a *situla* made of pottery (about 330 B.C.) – a ceremonial bucket-shaped vessel probably used to hold holy water; the total height is 33.5 cm. It was found in a tomb in Apulia, southeastern Italy, then a Greek colony. HELIOS is shown here driving a quadriga and wearing a radiative crown. His "supersonic" vehicle is a delicate chariot drawn by four fiery stallions. [From the Collection W. KROPATSCHECK, Helgoland. Courtesy Museum für Kunst und Gewerbe, Hamburg]

4.20–B ***Left:*** According to legend, a Chinese minor official named WAN-HOO attempted in the early 16th century a flight to the Moon using a large wicker chair to which were fastened 47 large rockets. However, his rocket experiment failed, and he disappeared in a huge cloud of smoke. [http://encyclopedia.thefreedictionary.com/_/viewer.aspx?path=5/5c/&name=Wan_Hu_large.png] ***Right:*** In the 12th century, the Chinese invented rockets and began to use military rockets in the battlefield. This is a drawing of a Chinese soldier launching a fire arrow. [NASA-MSFC; http://history.msfc.nasa.gov/rocketry/03.html]

4.20 HIGH-SPEED VEHICLES – First Supersonic Rocket Flight

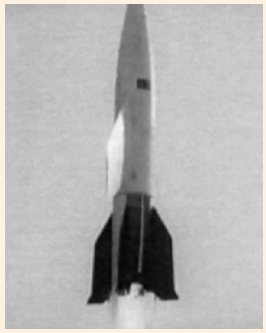

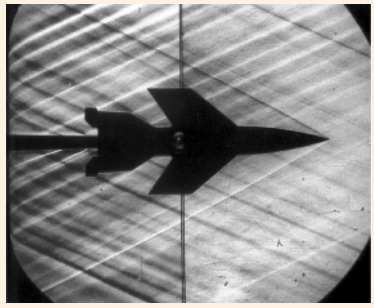

4.20–C ***Left:*** Launch of the German rocket A-4 (in 1944 renamed V2) at the Peenemünde Test Site on October 3, 1942, reaching a record distance of 191 km, a velocity of M > 4, and a height of 84.5 km. It was the first time that a large structure (length 14.3 m, takeoff weight 12.8 tons) broke the sound barrier. ***Center:*** A rare picture of a successful takeoff of an A-4b, the winged long-distance version of the A-4, taken on January 24, 1945. [Courtesy Deutsches Museum, Munich] ***Right:*** Schlieren photo of a model of the A-4b taken at a velocity of about $M = 2.1$ in the Peenemünde wind tunnel. It was anticipated that this so-called "glider" could increase the distance from firing location to the target. Note that up to about $M = 2.6$ the wing tips would still remain within the Mach cone, thus considerably reducing aerodynamic drag. [P.P. WEGENER: *The Peenemünde Wind Tunnels*. Yale University Press, New Haven, CT (1996)]

4.20 HIGH-SPEED VEHICLES – First Hypersonic Rocket Flight

4.20–D ***Left:*** The U.S. WAC-Corporal, a 16-ft (4.88-m)-long rocket with a thrust of 1,500 pounds, was developed by Theodore VON KÁRMÁN's research team at CalTech near the end of World War II. The first WAC-Corporal was launched in October 1945 at White Sands Proving Ground, NM. It reached an altitude of about 45 miles (75 km). The WAC-Corporal, an unguided rocket, was applied for high-altitude research and for providing information and engineering experience to be used in future surface-to-surface missile programs. ***Right:*** On February 24, 1949, a WAC-Corporal, boosted by a captured German V2, reached a record altitude of about 400 km and a hypervelocity of about 2,300 m/s. [National Air and Space Museum, Smithsonian Institution, Washington, DC (NASM, image nos. A-5048-B and SI 76-15531)]

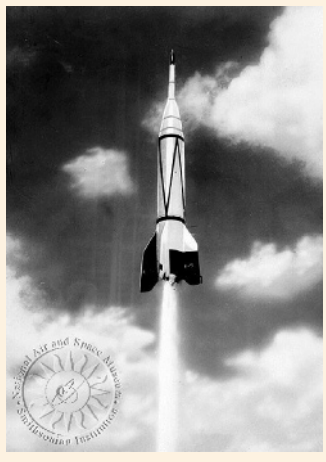

4.20 **HIGH-SPEED VEHICLES** – First Transonic Rocket Plane

4.20–E The Messerschmitt Me 163 or "Komet" was the first rocket plane and the most advanced transonic aircraft of its time. It was designed by the famous German aeronautical engineer Alexander LIPPISCH. Piloted by Heini DITTMAR, it reached on October 2, 1941 a record speed of 1,003 km/h (M = 0.84), thus remaining the fastest jet fighter until the end of World War II. However, it arrived too late to be of any military relevance. ***Left, top:*** A warning lamp was installed at the upper far right side of the cockpit panel. This lamp, labeled *Machwarnung* ("Mach warning"), indicated to the pilot the approach to the sound barrier. Apparently, it was the very first "Mach indicator" ever installed in an airplane. ***Left, center:*** This picture was taken of the Komet during flight. Note the swept-back wings, an idea of the German aerodynamicist Adolf BUSEMANN. First proposed by him at the 5th Volta Conference held in Guidonia/Rome in 1935, this wing concept revolutionized modern high-speed aeronautics. ***Left, bottom:*** View of the small aircraft, which had only a length of 5.7 m and a wing span of 9.3 m. Powered by a 3,300-pound thrust liquid-fuel rocket motor, it was also popularly called *"Kraftei"* – a German word meaning "power egg" – because of its compact fuselage and enormous thrust. [Courtesy Deutsches Museum, Munich] A Messerschmitt Me 163 B-1a (built in 1943) is on display at the Deutsches Museum, Munich.

4.20 HIGH-SPEED VEHICLES – First Supersonic Rocket Plane

4.20–F View of the Bell XS-1 (later designated X-l) with which the U.S.A.F. research pilot Capt. Charles E. YEAGER first broke the sound barrier (M = 1.07) in level flight on October 14, 1947. The little rocket-powered airplane was launched in the air from the bomb-bay of a Boeing B-29 ("Superfortress"), the same kind of airplane that dropped the atomic bombs on Japan in August 1945. The plane, which did not yet have swept-back wings for easing the shock wave problem, measured 31 ft (9.45 m) long with a wingspan of just 28 ft (8.53 m). The maximum speed attained by the X-1 was Mach 1.45 at 40,130 ft (12,232 m) during a flight by YEAGER on March 26, 1948. ***Left:*** Note the stationary, axisymmetric diamondlike shock wave pattern in the jet exhaust of the rocket engine. ***Right:*** The small aircraft is now on display in the Milestones of Flight Hall at the Smithsonian National Air and Space Museum. [Smithsonian NASM, Washington, DC, image nos. SI 97-17485 and SI 2004-50572]

4.20 HIGH-SPEED VEHICLES – Supersonic Propeller

4.20–G The XF-88B (McDonnell 1953) was a turboprop experimental version of the XF-88 ("Voodoo"). Built to conduct propeller research for supersonic planes, the XF-88 was first operated in 1953. At that time, the theory on thin "supersonic" propellers predicted that at low supersonic speeds a specially designed propeller could be more efficient under some circumstances than a jet engine. Until 1956 various propellers were tested at flight speeds up to slightly above Mach 1. At Mach 0.95 a peak efficiency of 80% had been measured. After being kept at Langley Air Force Base in Virginia for several years, the XF-88B was eventually scrapped. [© Boeing, image no. 5212]

4.20 **HIGH-SPEED VEHICLES** – Supersonic Transport (SST)

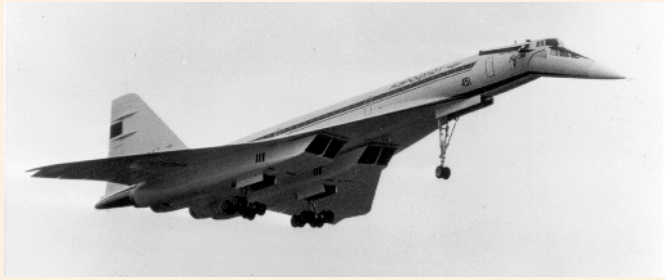

4.20–H In the early 1960s, aeronautical engineers of Great Britain, France, the Soviet Union and the United States developed plans to build a commercial supersonic airliner – so-called "SST" (SuperSonic Transport). All three SST liners were designed to be powered by four turbojet engines and have a fixed delta wing; the concept of using a variable geometry (so-called "swing wing") was abandoned because of weight and complexity. However, the Concorde was designed for lowering its nose during takeoff and landing to improve visibility. Like the Concorde, the Boeing SST had a variable nose geometry to improve flight deck forward views on approach. The primary structural material of SST planes were aluminum alloys, but the leading edges of the nose and wings, where supersonic flight generates high temperatures up to about 150 °C, were manufactured of stainless steel and titanium. ***Top:*** The Soviet Tupolev Tu-144 turboprop airliner was designed for M = 2.4 and 140 passengers. This picture was taken on 3 June 1973 at the Paris Air Show, shortly before the aircraft crashed in Goussainville; the six people on board died. In the 1990s, a modified version of the Tu-144 – named Tu-144LL – was operated as a "flying laboratory" in a joint U.S./Russian research program on supersonic flight. [Photo GettyImages] ***Center:*** The Concorde, a British-French development of BAC and Aerospatiale designed for M = 2 and 144 passengers, was the only operable SST civil airliner and in service until October 2003. [Photo taken by Paul JONGENEELEN, Hoboken, Belgium] ***Bottom:*** Artist's concept of the American SST prototype, the Boeing 2707-300. It was designed for M = 2.7 and 234 passengers. However, governmental funding was withdrawn in 1971 before even the prototype was finished. The original mockup of this unusual aircraft is on display at Hiller Aviation Museum in San Carlos, CA. [© Boeing, image no. 7049]

Both the Tu-144 Machmeter (*left*) and the Concorde Machmeter (*center*) were analog instruments installed on the pilot's control panel. The Concorde also had a 23.5 × 7.3-cm^2 wall-mounted digital Machmeter (*right*) installed in the passenger cabin. [*Left & right:* Courtesy Auto & Technik Museum Sinsheim, Germany; *center:* Photo by British Airways]

4.20 **HIGH-SPEED VEHICLES** – Hypersonic Aircraft

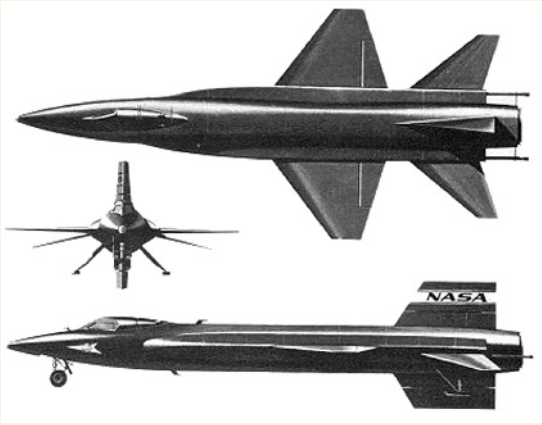

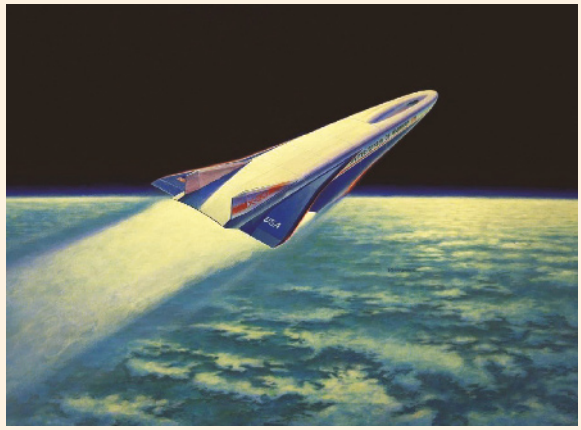

4.20–I ***Left:*** Three views of the North American X-15's original configuration with which it achieved on November 9, 1961 a maximum speed of $M = 6.06$ and a maximum altitude of 354,200 ft (108 km). [W.H. STILLWELL: *X-15. Research results*. NASA Rep. SP-60. NASA Scient. & Tech. Information Office, Washington, DC (1964)] ***Right:*** Artist's concept of the American National Aerospace Plane, X-30 NASP, supposed to take off from a conventional airfield and fly to orbit at a maximum speed of $M = 25$. This unusual aircraft was already planned in the 1980s but never realized. [NASP program, NASA-LRC, image no. EL-2001-00432]

4.20 **HIGH-SPEED VEHICLES –** Manned Spacecraft: Reentry Capsules

← Layers of special "ablative" material (*e.g.*, phenolic epoxy resin) on the shield, varying in thickness from 1.8 to 6.9 cm, were purposely allowed to burn away during reentry to help dissipate the extremely high temperatures caused by atmospheric friction. The blunt-end design for the Command Module was chosen to build upon experience with the similarly shaped Mercury and Gemini spacecraft.

4.20–J ***Left:*** View of the 2.5-m-dia. reentry capsule of the Soviet Vostok-1 mission in which the first man in space, Soviet research pilot Yuri A. GAGARIN, entered space and safely returned to Earth, thereby entering the atmosphere with the so-called "first cosmic velocity" of about 8 km/s, that is, $M > 20$. [Photo by Anatoly ZAK, Moscow; http://www.russianspaceweb.com/spacecraft_manned-first.html] ***Right:*** View of the American Apollo 11 Command Module Columbia, which, carrying on July 16-24, 1969 three astronauts on their historic voyage to the Moon and back, reentered the atmosphere with its protective heat shield facing forward. Since Columbia returned from the Moon to the Earth, the reentry velocity was higher than in the case of Vostok's reentry and amounted to $M > 30$. [Photo by Eric F. LONG, National Air and Space Museum, Smithsonian Institution (SI 98-16042)]

4.20 HIGH-SPEED VEHICLES – Manned Spacecraft: Shuttles

4.20–K The space shuttle Columbia was designed for scientific missions in the fields of space research and exploration as well as for technical and scientific applications. The speed of a space shuttle in low Earth orbit is about 7.8 km/s. An orbiter can fly at various altitudes, from under 300 to about 560 km above sea level, depending on the mission requirements. In 1981, Columbia became the first space shuttle to fly into Earth's orbit. ***Left:*** Launch view of the Columbia on April 12, 1981 at Kennedy Space Center, FL for the first shuttle mission (STS-1). ***Right:*** After 36 orbits during two days in space, Columbia landed at Edwards Air Force Base, CA in a manner similar to that of an aircraft. [NASA-JSC, Digital Image Collection; http://images.jsc.nasa.gov/index.html]

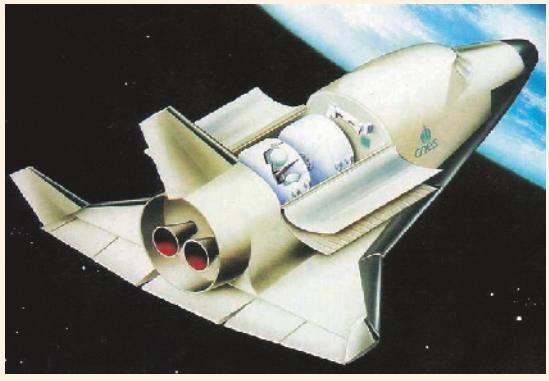

4.20–L ***Left:*** Artist's conception of the Hermes Space Plane (length 19.0 m, weight 23 tons). Designed in the 1980s by the European Space Agency (ESA), it was cancelled in the early 1990s for economic reasons. The purpose of Hermes was for (1) transferring crews and equipment to space stations, (2) servicing unpiloted platforms, (3) repairing satellites in orbit, and (4) putting scientific experiments in orbit during unpiloted flights. [ESA via Marcus LINDROOS at ESA; http://www.astronautix.com/craft/hermes.htm] ***Right:*** Aerodynamic model testing was partly performed at the Hypersonic Shock Tube Facility of the RWTH Aachen. The Hermes model was exposed to various hypersonic flow conditions, here shown at a Mach number of 7.5 and a yaw angle of 30°. Hypersonic flow phenomena were visualized using a color schlieren method. Note that the flow striking the fixed model propagates from right to left. [Courtesy Prof. Hans GRÖNIG, Stoßwellenlabor der RWTH Aachen]

4.20 HIGH-SPEED VEHICLES – Rocket Sleds

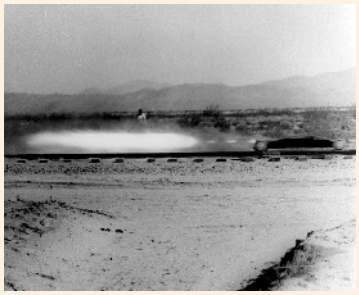

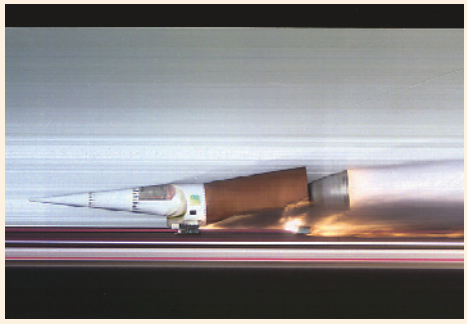

4.20–M Modern supersonic rocket sleds, filling the gap between wind-tunnel and airborne (free-flight) testing, are used to simulate flight conditions and study terminal ballistic phenomena at high speeds. ***Top:*** View of an early wheeled rocket sled during tests performed in 1948 on the Transonic (B-4) Track at the Naval Ordnance Research Track (SNORT), CA. [*China Lake Historical Overview*, http://www.nawcwpns.navy.mil/clmf/oldsled.html] The 50,988-ft (15,541-m)-long Holloman High-Speed Test Track (HHSTT), NM, the largest rocket sled facility in the world, can accelerate test objects from high subsonic speeds to Mach 8. ***Bottom, left:*** An array of head waves, emerging from different parts along the rocket sled, are visible against the background. [By courtesy of Dr. Leonard M. WEINSTEIN, NASA-LRC, Hampton, VA] ***Bottom, right:*** Reflected-light photography of a rocket sled traveling at 4,800 ft/s (M ≈ 4.3). [Photo by A. SEHMER, Sandia National Laboratories, Albuquerque, NM]

4.20 HIGH-SPEED VEHICLES – Supersonic Car

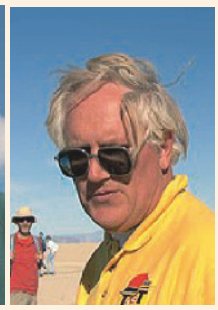

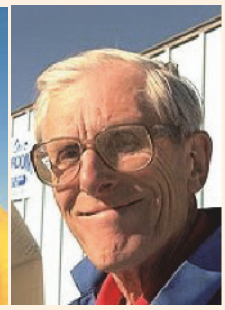

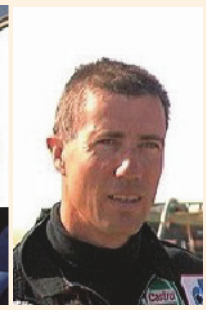

4.20–N ***Left:*** View of the British "ThrustSSC" supersonic car which measures about 16.5 m in length and is powered by a pair of Rolls-Royce jet engines as used in the Phantom fighter, each producing 20,000 pounds of thrust. To avoid lateral deviations from the race track, their individual thrusts are controlled electronically. The wheels consist of forged aluminum discs. ***Right:*** From left to right: The British engineer Richard NOBLE, holder of the 1983 Land Speed Record (1018 km/h), was project director of the ThrustSSC. The car was designed by Glynne BOWSHER. Ron AYERS was chief aerodynamicist of the ThrustSSC project, he only used computational fluid dynamics; no wind tunnel experiments were conducted. The British test pilot Andy GREEN, a member of Richard NOBLE's ThrustSSC team, broke the sound barrier on 17 October 1997 at Black Rock Desert in Nevada {⇨Fig. 4.6–J}: flying mile 763.035 mph (1,227.985 km/h). In setting the record, the sound barrier was broken in both north and south runs. [© Jeremy DAVEY; ThrustSSC team]

4.21 **MAN-MADE DISASTERS** – Steam-Boiler Explosions

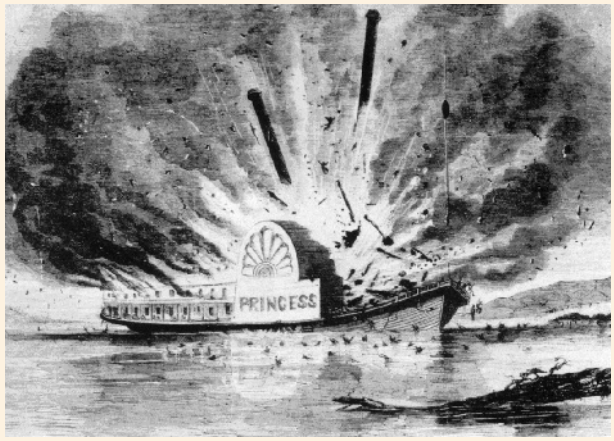

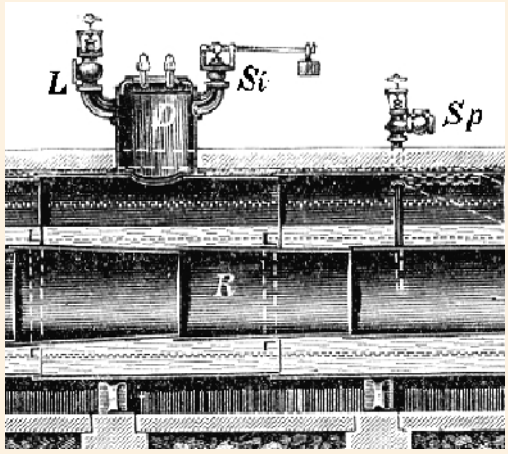

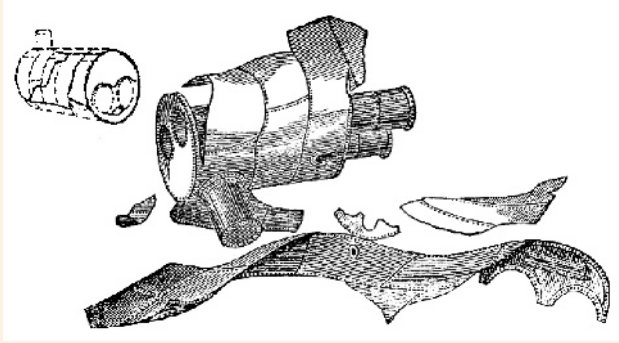

4.21–A In the main era of steam engines, beginning in the early 1700s and reaching its peak at the end of the 19th century, boiler explosions were an omnipresent hazard to man and equipment. They were considered the results of (1) complex thermodynamic phenomena in the steam/water mixture; (2) unfavorable boiler construction, *e.g.*, caused by poor production technology and the use of inappropriate materials; and (3) malfunctions of the safety valve and undue manipulations of it. The numerous accidents not only gave rise to the foundations of the first safety inspection authorities, but also initiated theoretical fluid dynamic studies on the discharge mechanism of a pressurized fluid through a small opening. They revealed that dangerous overpressures in steam boilers could not be reduced immediately, but only with a certain delay. ***Top:*** Contemporary drawing of a steam-boiler explosion on the side-wheeler SS *Princess* with 200 casualties, which occurred in 1859 on the Mississippi River near Baton Rouge, LA. This disaster was typical of many similar tragedies accompanying the use of steam engines in industry and traffic. [F. LESLIE's *Illustrated Newspaper* (March 19, 1859)] ***Center:*** Partial view of a British steam boiler of the Cornwall type, a construction provided with a single fire tube only. The safety valve *Si* was installed on top of the dome *D*; fresh water was supplied via valve *Sp* and the steam taken out via valve *L*. [*Brockhaus' Konversations-Lexikon*, Brockhaus, Leipzig (1908), vol. 4, p. 668] ***Bottom:*** Since high-speed diagnostics was then still in its infancy, it was difficult to uncover the puzzle of boiler explosions. Physical, chemical, and material reasons were likewise discussed. To get insight into possible causes, data from boiler explosions were meticulously collected and published in England in so-called "Boiler Records." From a visual inspection of boiler debris it was hoped that future boiler design could be improved. The picture below shows debris of the exploded boiler of the Bingley-type (1869). [E.B. MARTEN: *Records of steam-boiler explosions*. Stourbridge, London (1869)]

4.21 **MAN-MADE DISASTERS** – Firedamp Explosions

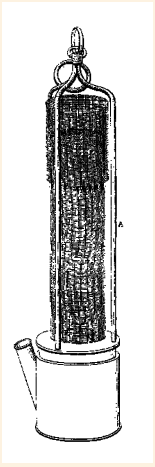

4.21–B ***Left:*** Drawing of a firedamp explosion in the soft-coal mining industry of Bilin [now Bílina, Czechia], killing 3 and seriously injuring 5 miners. Besides fatal blast effects, the sudden deficiency of oxygen often caused death from suffocation. [Das interessante Blatt **8**, No. 9, 1 (1889); courtesy Österreichische Nationalbibliothek, Vienna] ***Center:*** The English chemist Humphry DAVY studied the ignition of firedamp and the propagation of flames in tubes, which led to his invention of a safety mining lamp, the so-called "Davy lamp." A gauze mesh surrounding the flame of the lamp allows light to pass, but not the flame front of ignited firedamp to escape out in the mine atmosphere. [Phil. Trans. R. Soc. Lond. **107**, 84 (1817)] ***Right:*** Early flame safety lamps designed by the railroad engineer George STEPHENSON (*left*), by H. DAVY (*center*), and by the physician William R. CLANNY (*right*). [Courtesy of David S. BARRIE; http://www.thewandofscience.co.uk/]

4.21 **MANMADE DISASTERS** – Gun Barrel Bursts

← View of German heavy 15-cm field howitzers, model 14 (*left*), and model 02 (*right*) which became operational in 1914 and 1902, respectively.

4.21–C Barrel bursts of fire arms are rare phenomena in peacetime but frequently occur in times of war, where they can kill more soldiers and destroy more guns than can enemy fire. In the great battle of Verdun (1916), barrel bursts [Germ. *Rohrkrepierer*] were observed particularly on the German heavy 15-cm field howitzer. [Reprinted with permission from H. SCHIRMER: *Das Gerät der schweren Artillerie vor, in und nach dem Weltkrieg. Bilderband*. Bernhard & Graefe, Berlin (1937)]

4.21 **MANMADE DISASTERS** – Grain Dust Explosions

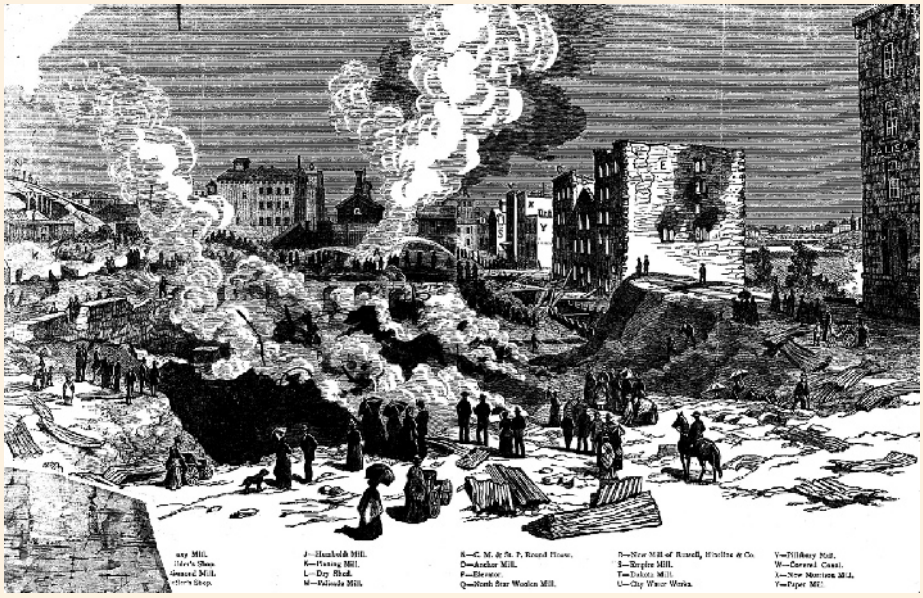

4.21–D Fine dust, in particular grain dust, caused many accidents in the past. It becomes extremely explosive when the dust gets in with the right mixture of oxygen and then comes in contact with a spark or another source of heat. This pen-and-ink drawing shows the mills at Minneapolis after the great flour dust explosion on May 2, 1878. Similar accidents happened there quite frequently in the 1870s, when the center of wheat production moved to Minnesota and Dakota Territory. [Courtesy Minnesota Historical Society, St. Paul, MN]

4.21–E Despite various countermeasures, dust explosions are still an omnipresent hazard to modern grain industry. They often have complex causes and are still a matter of present-day investigations. ***Left:*** In June 1998, a serious grain dust explosion happened at the half-mile-long grain elevator complex of DeBruce Inc., near Wichita, KS. The accident caused a series of explosions throughout the world's largest grain elevator, killing 7 workers and injuring 10 others. The facility mainly consisted of 246 circular grain silos and a central headhouse containing 4 elevator legs. Elevated grain was carried horizontally by belt from the headhouse to a selected silo. The accident was probably caused by a locked roller of a belt, which raised its temperature well beyond the ignition temperature of layered grain dust, which is only around 220 °C. ***Right:*** Aerial view of a part of the elevator complex taken within 1 h after the explosion. [Courtesy U.S. Department of Labor, Occupational Safety and Health Administration (OSHA); http://www.osha.gov/as/opa/foia/hot_6.html]

4.21 **MAN-MADE DISASTERS** – Nuclear Reactor Explosion

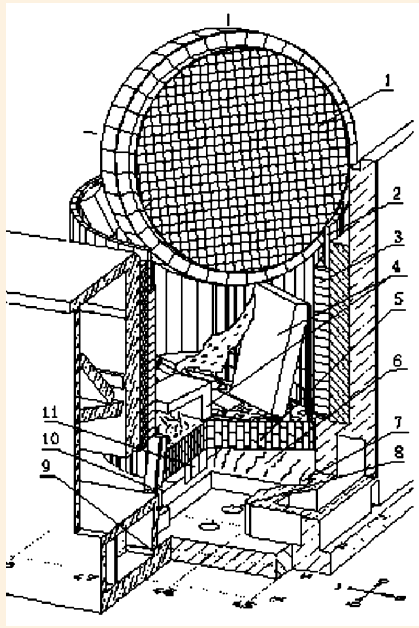

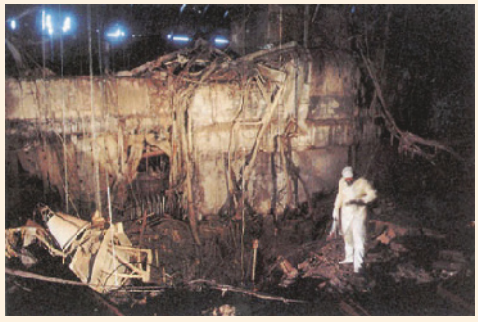

4.21–F On April 26, 1986, the nuclear power plant at Chernobyl (northern Ukraine) in the former Soviet Union was largely destroyed by a huge steam explosion, thereby setting free large quantities of radioactive matter. Ironically, the accident – the most severe ever to have occurred in the nuclear industry – was triggered by a safety test that got out of control. Actions taken during this exercise resulted in a rapid increase in the power level of the reactor, causing a destructive shock wave in the cooling water. Access to the reactor well allowed researchers to switch themselves from hypothetical models describing postaccident reactor state to studying a real state of reactor core, metal structures, and systems of the reactor. There was no core found in the reactor well. Core portions, such as graphite blocks, fragments of fuel channels, and assemblies, were found on the roof of nearby buildings, and individual graphite blocks and fragments of fuel assemblies and fuel rods were found close by, up to 150 m away. ***Left:*** Aerial view of the destroyed Block IV of the nuclear power plant. [From Wikipedia: *Chernobyl disaster*, source unknown] ***Right, top:*** Schematic of the reactor section of Unit IV after the accident, showing the empty core region. [Reprinted from Y.M. Cherkashov et al.: *Post-accident state of Chernobyl-4*. In: "Chernobyl Lessons – Technical Aspects." Int. Seminar held at Desnogorsk, Russia (April 1996); http://www.ignph.kiae.ru/ins/osrez/osrez.htm] ***Right, center & bottom:*** Partial views of destructions in the turbine hall *(center)* and adjacent reactor building *(bottom)*. [From Ogonyok (Moscow), No. 15 (April 2000); http://www.ropnet.ru/ogonyok/win/200015/15-30-33.html]

4.21 MAN-MADE DISASTERS – World Trade Center, NY: Terrorist Bomb Attack

4.21–G ***Left, top:*** On February 26, 1993 a massive explosion occurred in a subterranean garage below the World Trade Center (WTC) Plaza. The bomb, placed by terrorists in a truck parked on level 2, had an estimated yield equivalent to approx. 1,200 lb (544 kg) TNT, blowing a hole half the size of a football field in the basement. The explosions and subsequent fires caused extensive structural damage on several basement levels. Six people were killed and more than 1,000 injured, mostly from smoke inhalation, but the building did not collapse as the terrorists had hoped. The explosion caused nearly $600 million in property damage. Analysts later determined that, had the terrorists not made a minor error in the placement of the bomb, both towers could have fallen. [Courtesy U.S. Bureau of Alcohol, Tobacco, and Firearms; http://www.nycop.com/Stories/Dec_00/World_Trade_Center_Bombing/body_world_trade_center_bombing.html]

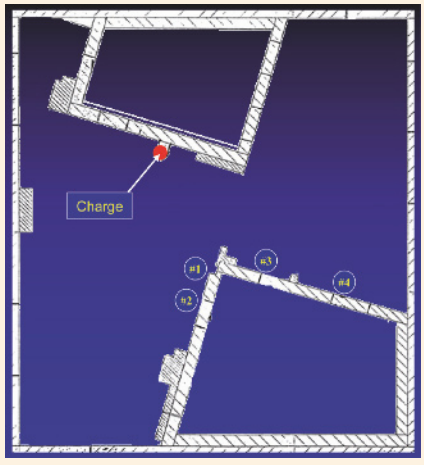

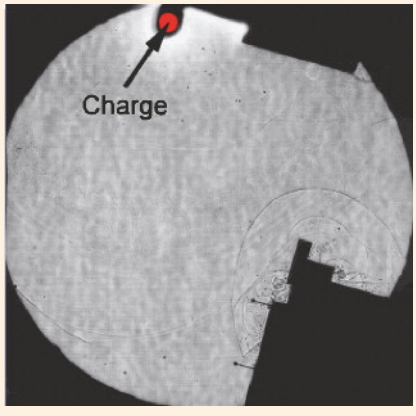

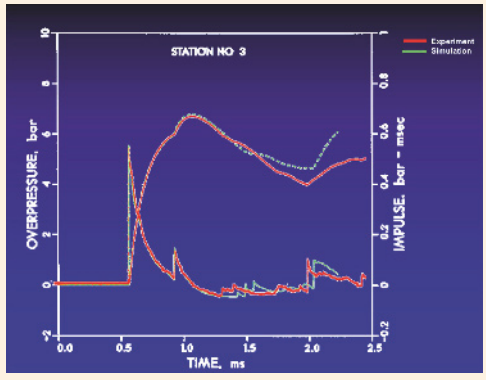

Left, center: Schematic of the floor plan of level 2 of the parking garage. The position where the truck with the bomb was parked is indicated by a *red dot*. ***Left, bottom:*** Heinz REICHENBACH and collaborators at EMI, Freiburg performed 2-D model blast propagation and reflection studies using small explosive charges and optical shadowgraphy. Pressure-time profiles were recorded at various distances from the model explosion center using Kistler pressure gauges. The blast wave, emerging from the charge (*top*), is reflected at the opposite walls and focused in corners (*bottom*), leading at those locations to significant increases in peak pressures. In such areas, the observed damage to parked cars was even greater than in the close environment of the explosion center. [Rept. E2/94 (1994), EMI, Freiburg] ***Right:*** Joseph D. BAUM at Science Applications Int. performed a numerical simulation of the blast wave propagation. A comparison between EMI's measured pressure-time profiles and calculated ones at different locations showed a fairly good agreement. Based on these promising results, BAUM and colleagues at George Mason University, Fairfax, VA, initiated a 3-D numerical modeling of the blast wave propagating in the parking deck. They used the FEFLO96 code, which is based on a 3-D finite-element, shock-capturing methodology. [Courtesy Dr. J.D. BAUM, Science Applications International Corporation, McLean, VA; Proc. 33rd Aerospace Sciences Meeting & Exhibit, Reno, NV (Jan. 1995)]

4.21 **MAN-MADE DISASTERS** – World Trade Center, NY: Terrorist Aircraft Attack

4.21–H On September 11, 2001, two Boeing 757s hijacked by terrorists crashed into the two 417-m-high towers of the World Trade Center. It was the worst disaster in recorded history, killing some 2,800 people. The North Tower and the South Tower collapsed 105 and 62 min after impact, respectively. The Twin Towers were designed to withstand as a whole the forces caused by a horizontal impact of a large aircraft and strong winds. Unfortunately, however, the towers were vulnerable to fire damage due to their primarily steel construction. In the floors impacted by the aircraft the tens of thousands of gallons of aviation fuel that spilled from the doomed airliners caused such intense heat that the supporting steel structures were weakened. This eventually resulted in a collapse of these floors. When the mass of the upper part of the building began to fall, it gained momentum that exceeded the force that the structure below could resist. The resulting collapse then continued down the building as an unstoppable chain reaction borne along by the force of gravity.

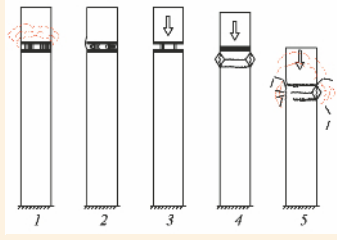

← Photographs showing the collapse of the South Tower at about 5, 5.9, and 7.5 seconds after initiation.

Top: This unique picture was taken shortly before the second plane crashed into the WTC's North Tower. [Reprinted with permission of Robert CLARK, New York City; who took the photo] ***Bottom, left & center:*** View of the South Tower collapsing in a plume of ash and debris. [Images taken from *9-11 Research: South Tower Collapse*: http://911research.wtc7.net/wtc/evidence/photos/wtc2exp9.html; image source unknown] ***Bottom, right:*** Prof. Zdeněk P. BAŽANT and collaborators at the Dept. of Civil Engineering, Northwestern University in Evanston, IL, suggested that the gravitational collapse was the dynamic consequence of the prolonged heating of the steel columns to very high temperatures, thus causing creep buckling and a loss of strength. This is a schematic showing five stages of their failure scenario. The vertical impact of the mass of the upper part onto the lower part produced an enormous vertical dynamic load on the underlying structure. This caused buckling and plastic deformation of the steel structure elements. The collapse of the tower was an almost free fall because the observed duration of 9 s was pretty close to the free fall time of 8.93 s from the tower top (416 m) to the top of the final heap (ca. 25 m above ground). [Reprinted from J. Eng. Mech. ASCE **128**, 2, 369 (2002). With permission of Prof. Z.P. BAŽANT, Northwestern University, Evanston, IL]